Design of Novel Bases for Recognition of GC Base Pairs by Oligonucleotide-Directed Triple Helix Formation

Thesis by

Jong Sung Koh

In Partial Fulfillment of the Requirements

for the Degree of Doctor of Philosophy

California Institute of Technology

Pasadena, California

1991

(Submitted July 9, 1990)

To my Parents and Heryun

Acknowledgements

I wish to thank my advisor, Peter Dervan, for his advice and enthusiastic support during the course of my Ph.D. studies and beyond. Thanks are also due the alumni of the Dervan group, especially John Griffin, Linda Griffin, Warren Wade, and Brent Iverson for their scientific advice, technical assistance and most of all their friendship. I would also like to thank Tom Povsic, Jumi Shin, Hogyu Han, Ken Graham, Laura Kiessling, Kevin Leubke and David Horne for proofreading this thesis and contributing constructive comments.

A word of thanks to my thesis committee, Drs. Harry Gray, Barbara Imperiali, and Douglas Rees for taking the time to read and critique my work. I would like to thank some very, very special people without whose behind-the-scenes support this work would not have been possible. To my parents, many thanks for nurturing my early interest in science, for their never ending support and encouragement over the years. I also give special thanks to Professor Sang Chul Shim at Korea Advanced Institute of Technology who inspired me to continue my education and scientific growth through graduate studies at Caltech.

And finally to that most special, and most wonderful person of all, my dear wife Heryun: how can I thank her enough for her unfailing support, encouragement, and love during what has been the most trying time of our lives together? From the bottom of my heart I extend to her my very deepest gratitute and love.

To my son Sangsoon and daughter Yeji: may you come to discover, as I have, that chemistry is a whole lot of fun. Thank you all for making this possible.

Abstract

Part I

Triple Helix Formation by Oligonucleotide Analogs on Double-Stranded DNA

Chapter 1: Design of Novel Bases for pH-Independent Recognition of GC Base Pairs by Triple Helix Formation

The ability to design synthetic molecules that bind sequence-specifically to unique sites on human DNA could have major applications in the treatment of genetic, neoplastic, and viral diseases. One powerful approach to sequence-specific binding of double helical DNA is oligonucleotide-directed triple helix formation. Specificity arises from the base triplets (T•AT and C+GC) formed by Hoogsteen base pairing of the second pyrimidine strand with the purine strand of the double helix. Because protonation of the N3 is required for cytosine, triple helix formation at G-rich sequences is limited to a narrow pH range. The novel base 3-methyl-5-amino-7H-pyrazolo(4, 3-d)pyrimidine-7-one (**P1**) specifically recognizes GC base pairs as selectively and strongly as C+, but with greater affinity and over an extended pH range. Such selectivities allow binding at a 15 base pair site in pDMAG10 DNA (pH 7.8) containing $dA_5(GA)_5$ and at a 16 base pair site in pHIV-CAT DNA (pH 7.4, 37°C) containing $dA_4GA_4G_6A$.

Abstract

Part I

Triple Helix Formation by Oligonucleotide Analogs on Double-Stranded DNA

Chapter 2: Extension of Triple Helix Formation. Design of Novel Bases for Recognition of CG Base Pairs

Oligonucleotide recognition offers a powerful chemical approach for the sequence-specific binding of double-helical DNA. Because pyrimidine oligonucleotides limit triple helix formation to homopurine tracts containing AT and GC base pairs, it is desirable to study whether oligonucleotides can be designed to bind to all four base pairs. A general solution would allow targeting of oligonucleotides to any sequence. The novel base 3-methyl-5-amino-7H-pyrazolo(4, 3-d)pyrimidine-7-one (**P1**) and cytosine (**C**) moderately recognize CG base pairs. Such specificities allow binding at an 18 base pair site in SV 40 (pH 7.0, 37°C) DNA containing all four base pairs.

Abstract

Part II

Design of DNA Cleaving Groups

Chapter 3: Design of New DNA Cleaving Fuctional Groups and Studies of Their DNA Cleaving Mechanisms

The utility of the DNA cleaving molecules is enormous, ranging from the creation of synthetic restriction enzymes for use by molecular biologists to the development of chemotherapeutic agents which may be effective against a variety of neoplastic diseases. We synthesized three compounds: **12** (P3-Ga-His), **19** (P3-Ga-PYML), and **23** (P3-Ga-Phe). Compound **12** shows sequence-specific cleavage in the presence of Cu(II) and dioxygen, while compound **19** shows sequence-specific cleavage in the presence of dithiothreitol and dioxygen. Interestingly, compound **23** shows strong cleavage at a single site in 167 base pair fragment (EcoRI/RsaI) from plasmid pBR322 in the presence of UV light and β-carbonato(trien)cobalt(III)perchlorate complex. The end product analysis of the cleaved oligonucleotide shows 5'-phosphate, 3'-phosphate, and an unknown 3'-product.

Table of Contents

List of Figures

Part I

Overview:

Chapter 1:

Appendix chapter 1:

Chapter 2:

PART I

Triple Helix Formation by Oligonucleotide Analogs on Double-Stranded DNA

Overview

The sequence-specific cleavage of double helical DNA by restriction endonucleases is essential for many applications in molecular biology, including gene isolation, DNA sequencing, and recombinant DNA manipulations (1,2). With the advent of pulsed-field gel electrophoresis, the separation of large segments of DNA is now possible (3,4). However, the recognition sequences of naturally occurring restriction enzymes are in the range of 4-8 base pairs, and hence their sequence specificities may be inadequate for isolating genes from large chromosomes (10^8 base pairs in size) or mapping genomic DNA. The design of sequence-specific DNA cleaving molecules that go beyond the specificities of the natural enzymes depends on a detailed understanding of the chemical principles underlying two functions: sequence-specific recognition and cleavage of DNA.

The design of DNA-cleaving molecules is generally based on the attachment of a cleaving function to a DNA-binding molecule. The synthetic sequence-specific binding moieties for double helical DNA that have been studied are coupled analogs of natural products (5-7), transition metal complexes (8), and peptide fragments derived from DNA-binding proteins (9). One DNA-cleaving function used in our laboratories is EDTA•Fe(II), which cleaves the DNA backbone by oxidation of the deoxyribose with a short-lived diffusible hydroxyl radical (10). The fact that a hydroxyl radical is a relatively nonspecific cleaving species is useful when studying recognition: the cleavage specificity is due to the binding moiety alone, not the combination of cleavage specificity superimposed on binding specificity. The sequence-specific molecule best characterized so far, with regard to the natural product analog approach, is bis(EDTA-

distamycin)fumaramide, which binds in the minor groove and cleaves at sites containing 9 bp of contiguous A, T DNA (11). A synthetic peptide containing 52 residues from the DNA-binding domain of Hin protein with EDTA at the amino terminus binds and cleaves at the 13-bp Hin site (9). DNA-cleaving is illustrated in the attachment of EDTA•Fe(II) to oligonucleotides (12).

Triple helix formation. One approach to sequence-specific recognition of double helical DNA is the use of an oligodeoxyribonucleotide that can bind in the major groove to a complementary sequence of DNA forming a triple-stranded structure.

The first nucleic acid triplex was described by A. Rich and coworkers three decades ago (13). Poly(U) and poly(A) were found to form a stable 2:1 complex in the presence of $MgCl_2$ (12 mM). After this, several triple-stranded structures were discovered (14,15). One case is of particular interest: at pH 6.2 and moderately high salt conditions, 2 poly(C) can form a triple helical complex with a single equivalent (with respect to bases) of short guanine ribonucleotides. This complex contains one of the pyrimidine strands in the protonated form (16-18). In principle, isomorphous base triplets (T•AT and C+GC) can be formed between any homopurine-homopyrimidine duplex and a corresponding homopyrimidine strand (19) (Figure 1). The DNA duplex poly(dT-dC)•poly(dG-dA) associates with poly(U-C) or poly (dT-dC) below pH 6.0 in the presence of $MgCl_2$ to form a triple-stranded complex (20,21). Several investigators proposed an anti-parallel orientation for the two polypyrimidine strands on the basis of an *anti* conformation of the bases (19-21).

The first X-ray data of triple-stranded fibers (poly(A)•2 poly(U) and poly(dA)•2 poly(dT)) supported this hypothesis and provided additional information about triple helical structures (22-24). The best agreement be-

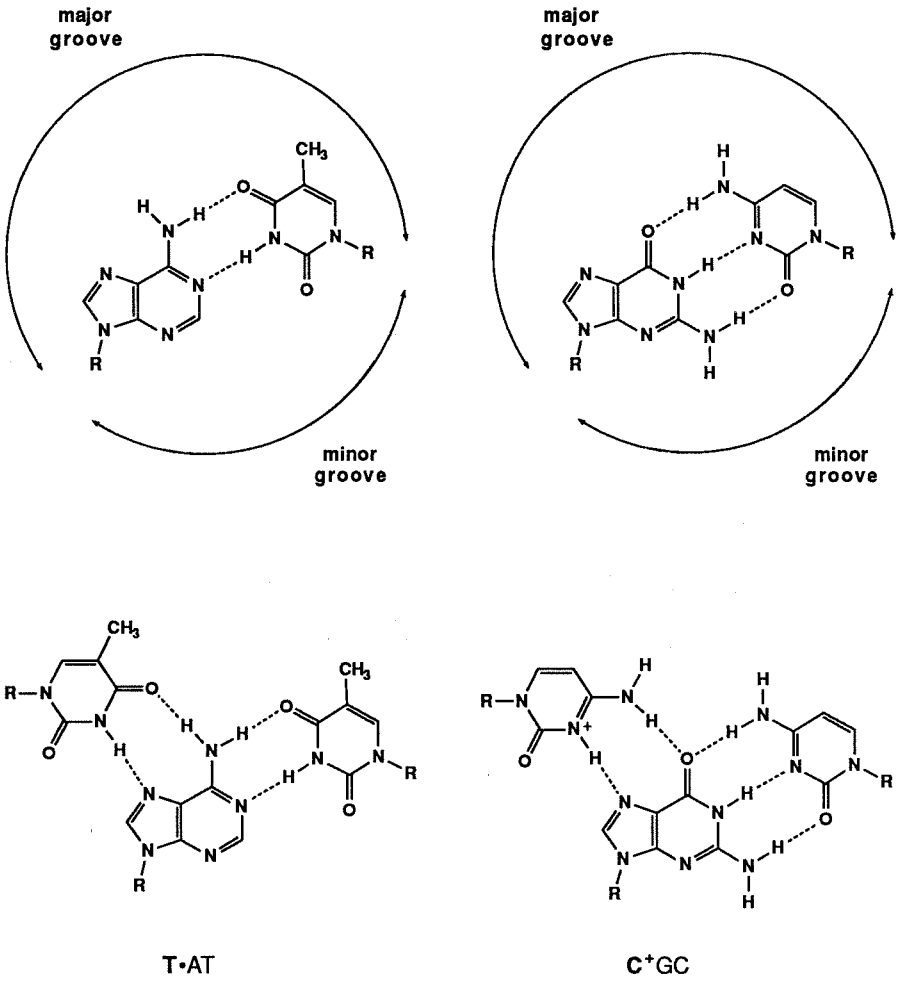

Figure 1. (**Top**) Watson-crick base pairs. (**Bottom**) Isomorphous base triplets T•AT and C+GC. The additional pyrimidine base is bound in the major groove by Hoogsteen hydrogen bonds to the purine base in the Watson-Crick duplex. Protonation of the Hoogsteen bound cytosine is required.

tween experimental and calculated diffraction patterns was obtained with an A'-RNA-like conformation of the two Watson-Crick base paired strands (12-fold helical symmetry, dislocation of axis almost 3Å, C3'-endo sugar puckering and small base-tilts providing a large and deep major groove

that accomodates the additional strand). The third strand has a similar backbone conformation (C3'-endo), and is bound parallel to the homopurine strand of the duplex by Hoogsteen-hydrogen bonds (25,26) (Figure 2). CPK-models support this structure; however, a high resolution X-ray crystal structure of a triple helical DNA or RNA molecule has not been reported so far.

Long stretches of homopurine-homopyrimidine sequences are often found in eukaryotic genomes (27-30). These DNA regions appear to be hypersensitive to S1 nucleases (known to recognize single-stranded DNA). S1 nuclease has an optimum pH of 4.5 for activity that could favor cytosine protonation (27-30). It has been suggested that under superhelical stress and acidic pH any mirror-repeated sequence of purines in one strand can adopt the H-form (31-33). The major element of this structure is a triple helix associated with a homopyrimidine loop through Hoogsteen base pairs. It has been suggested that an acidic pH is important to facilitate protonation of cytosine required for GC Hoogsteen base pairing. It is believed that formation of secondary structures in promoter regions of genes might be important in control of transcription (27-30).

Oligonucleotide-EDTA probes. Oligonucleotides equipped with a DNA cleaving moiety have been described, and these can produce sequence-specific cleavage of single-stranded DNA (34-35). An example of this is oligonucleotide-EDTA•Fe(II) hybridization probes which cleave the complementary single strand sequence. Moser and Dervan have reported that homopyrimidine oligodeoxyribonucleotides with EDTA•Fe attached at a single position bind the corresponding homopyrimidine•homopurine

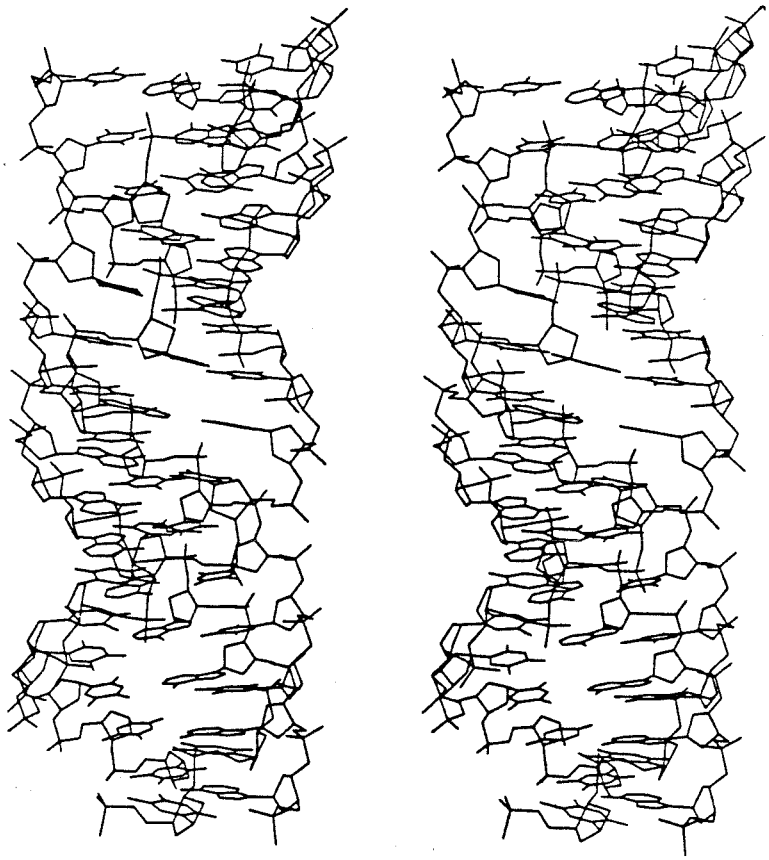

Helix type:	A'
Helix symmetry:	12_1
Pitch height:	39.1 Å
Axial rise per residue:	3.26 Å
Rotation per residue:	30.0°
Dislocation from helix axis:	2.80 Å (Watson-Crick bp)
Base tilt:	8.5°
Sugar puckering:	$C_{3'}$-*endo* (all strands)
conformation at glycosidic links:	anti
orientation of strands:	homopyrimidine strands antiparallel

Figure 2. Stereo presentation of a triple-stranded 16-mer (poly(dA)•2poly(dT)) that was constructed by using the coordinates given in ref. 24. The general features as determined by X-ray crystallography of fibers are tabulated.

tracts within large double-stranded DNA by triple helix formation and cleave at that site (12) (Figure 3).

Oligodeoxyriboucleotides with EDTA•Fe at the 5' end cause a sequence-specific double strand break. The location and asymmetry of the cleavage pattern reveal that the homopyrimidine-EDTA probes bind in the major groove parallel to the homopurine strand of Watson-Crick double helical DNA. Cleavage is not observed in the absence of cations such as spermine or $Co(NH_3)_6^{3+}$, which are presumably required to overcome the repulsion between the two anionic chains of the Watson-Crick duplex and a third negatively charged phosphodiester backbone. The efficiency of oligonucleotide duplex cleavage is increased by a factor of 10 by the addition of ethylene glycol (40% by volume) or other organic solvents that lower the relative humidity. Dehydration of the DNA favors a transition from B form to A form and facilitates formation of a triple helical complex (25). The efficiency of oligonucleotide duplex cleavage by cytidine rich oligonucleotide-EDTA•Fe(II) probes is very sensitive to pH and base composition (37). The oligonucleotide dT*T_4(CT)$_5$•Fe(II) (T*=thymidine-EDTA) does not cleave Watson-Crick DNA above pH 7.0, and the oligonucleotides dT$_4$T*C$_{6-10}$-EDTA•Fe(II) do not cleave Watson-Crick DNA above pH 6.6, and require 30% or more ethanol (37). Cleavage efficiency of oligonucleotides-EDTA•Fe(II) decreases sharply below pH 6.0, most likely the result of partial protonation of the EDTA and the resulting loss of Fe(II) or some pH dependence of the cleavage reaction. Footprinting experiments confirm that the triple helix forms at acidic pH values (38).

Povsic and Dervan recently reported triple helix formation by oligonucleotides on DNA can be extended to the physiological pH range for

the pDMAG10 containing $dA_5(GA)_5$ site (39). The incremental effect on the stability and pH dependence of triple helix formation by substitution at the 5' position of pyrimidines in the Hoogsteen strand was studied. Oligonucleotide-EDTA•Fe probes containing bromouracil and 5-methylcytosine bind and cleave a polypurine sequence in duplex DNA with specificities comparable to those of their thymidine-cytosine analogues, but with greater affinities and over an extended pH range. Oligonucleotides containing uracil bind a polypurine sequence with lower affinity.

Strobel, Moser, and Dervan have reported the double strand cleavage of genomic DNA at a single site by triple helix formation. An oligonucleotide-EDTA•Fe probe equipped with thymidine-EDTA (T*) at the 5' end, 5'-$T^*T_3CT_6CT_4CT$-3', causes double strand cleavage at a single homopurine site 18 base pairs in size (5'-$A_4GA_6GA_4GA$-3') within 48,502 base pairs of bacteriophage λ DNA (40). The double strand cleavage efficiency is 25% (100 mM NaCl, 25 mM tri-acetate, pH 7.0, 1 mM spermine, 24°C). No secondary cleavage sites were detected under these reaction conditions. The oligonucleotide-EDTA•Fe-mediated site-specific double strand cleavage reaction can also be carried out in a low melting point agarose matrix.

Maher, Wold and Dervan have demonstrated the inhibition of DNA binding proteins by oligonucleotide-directed triple helix formation (41). Oligonucleotides that bind to duplex DNA in a sequence specific manner by triple helix formation offer a means for the experimental manipulation of sequence-specific protein binding. Micromolar concentrations of pyrimidine oligodeoxyribonucleotides have been shown to block recognition of double helical DNA by procaryotic modifying enzymes and transcription factors at a homopurine site. Inhibition is sequence specific.

Oligonucleotides containing 5-methylcytosine provide substantially more efficient inhibition than oligonucleotides containing cytosine. These results have implications for gene-specific repression by oligonucleotides or their analogs.

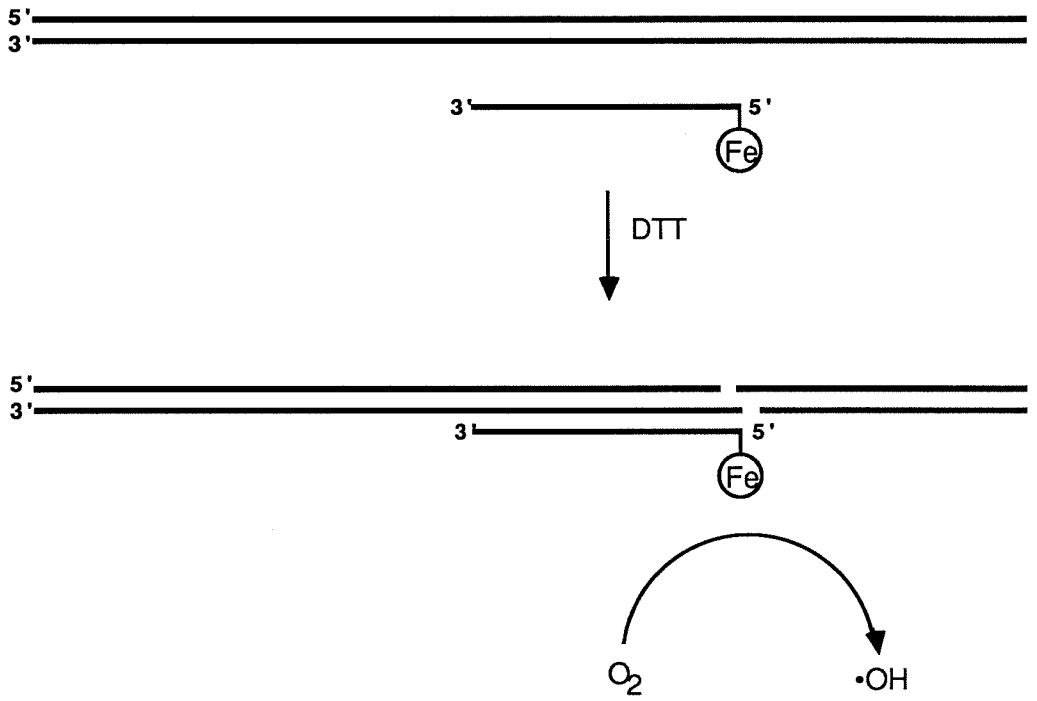

Figure 3. Oligonucleotide-directed cleavage of double helical DNA by a triple helix forming oligonucleotide-EDTA•Fe probe. One thymine has been replaced by thymine with the iron chelator EDTA covalently attached at C-5. Reduction of dioxygen generates localized hydroxyl radical at this position.

Recently, it has been postulated that purine oligonucleotides bind to purines in duplex DNA by triple helix formation (A•AT and G•GC base triplets). Kohwi *et al.* have reported that the G•GC triplex forms in supercoiled DNA in the presence of divalent magnesium ion Mg^{++} (42). Cooney *et al.* have demonstrated *in vitro* gene repression using a G-rich oligonucleotide to bind a G-rich target site (43). However, purine oligonucleotide recognition of double helical DNA is less well understood. α-

Oligonucleotides have also been observed to form triple-stranded structures (44,45).

Studies in the area of oligonucleotide-directed recognition and cleavage of duplex DNA by triple strand formation clearly demonstrate the power and potential of this technique for duplex DNA recognition. However, because triple strand formation is presently limited to homopurine•homopyrimidine tracts of DNA and is sensitive to pH for the C+GC triplet, a general solution to duplex DNA recognition is still lacking. The extension of recognition by triple helix formation to any sequence over a wide range of pH (AT, GC, TA and CG base pairs, Figure 4) is an interesting and challenging problem. Recently, it was demonstrated that guanine in a pyrimidine oligonucleotide specifically recognizes TA base pairs within mixed purine-pyrimidine sites. Although the G•TA triplet within a pyrimidine oligonucleotide extends triple helix specificity to three of the four possible base pairs of double helical DNA, some limitations on sequence composition are likely. It is not clear how far one can deviate from homopurine-homopyrimidine target sequences and still obtain triple helix formation. Rather this result provides structural leads for the design of deoxyribonucleotides (or their analogs) with nonnatural heterocycles directed toward a more general solution. The quest for a general solution will test and refine our understanding of molecular recognition of double stranded DNA. This thesis describes: a) studies of nonnatural bases for pH-independent GC recognition (chapter 1), and b) studies of nonnatural bases for CG recognition (chapter 2).

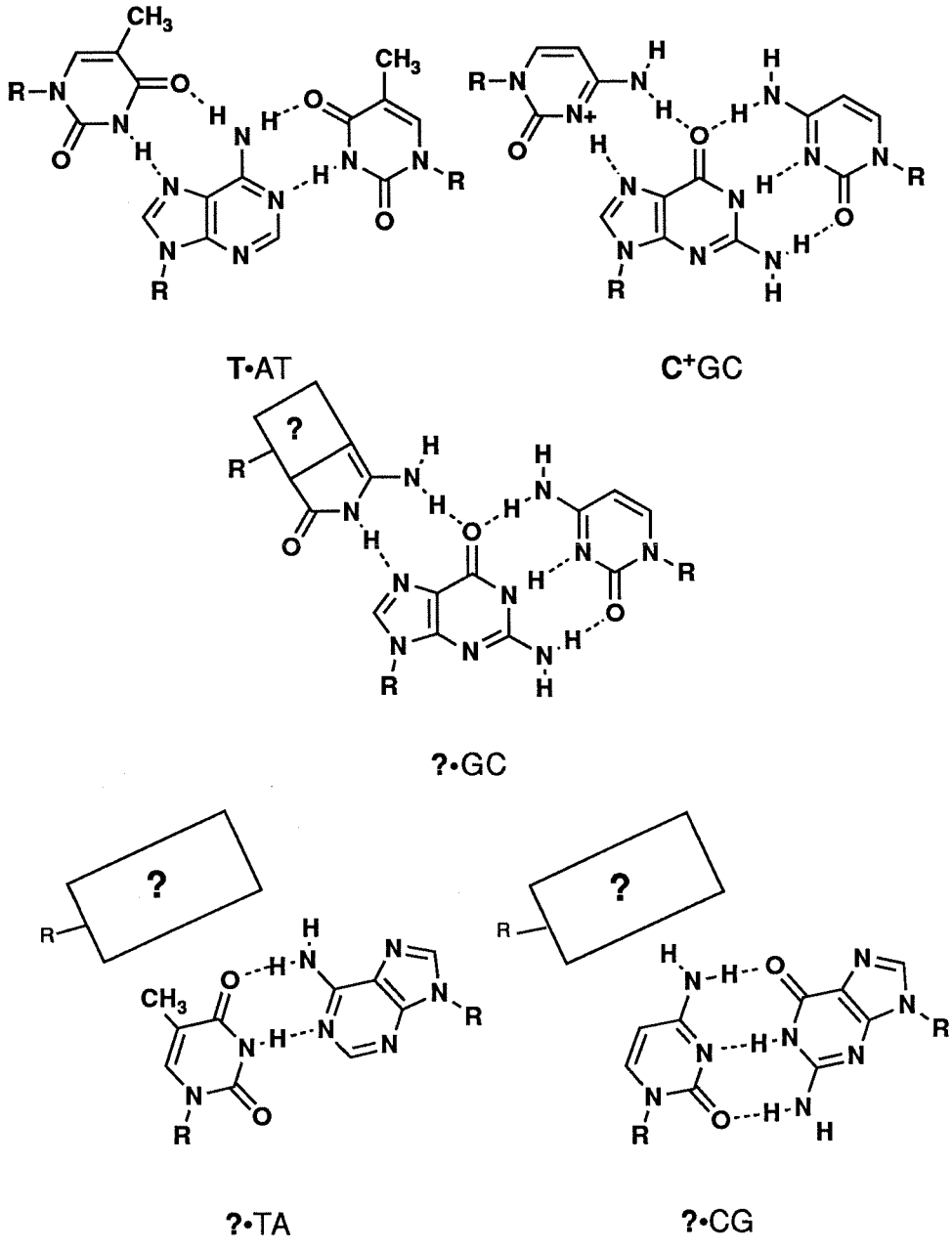

Figure 4. (**Top**) Isomorphous base triplets T•AT and C+GC. (**Middle** and **Bottom**) Unknown new base triplets ?•GC, ?•TA and ?•CG.

References and notes

(1) Smith, H. O. *Science* **1979**, *205*, 455.

(2) Modrich, P. *Crit. Rev. Biochem.* **1982**, *13*, 287.

(3) Schwartz, D.; Cantor, C.R. *Cell* **1984**, *37*, 67.

(4) Carle, C. F; Frank, M.; Olsen, M. V. *Science* **1986**, *232*, 65.

(5) Schultz, P. G.; Dervan, P. B. *J. Amer. Chem. Soc.* **1983**, *105*, 7748.

(6) Schultz, P. G.; Dervan, P. B. *Proc. Natl. Acad. Sci. U. S. A* **1983**, *80*, 6843.

(7) Griffin, J. H.; Dervan, P. B. *J. Amer. Chem. Soc.* **1987**, *109*, 6840.

(8) Barton, J. K.; Raphael, A. L. *J. Amer. Chem. Soc.* **1984**, *106*, 2466.

(9) (a) Sluka, J. P.; Horvath, S. J.; Bruist, M. F.; Simon, M. I.; Dervan, P. B. *Science* **1987**, *238*, 1129. (b) Mack, D. P.; Iverson, B. L.; Dervan, P. B. *J. Amer. Chem. Soc.* **1988**, *110*, 7572. (c) Mack, D. P.; Dervan, P. B. *J. Amer. Chem. Soc.* **1990**, *112*, 4604.

(10) Hertzberg, R. P; Dervan, P. B. *Biochemistry* **1984**, *23*, 3934.

(11) Younquist, R. S; Dervan, P. B. *J. Amer. Chem. Soc.* **1985**, *107*, 5528.

(12) Moser, H. E.; Dervan, P. B. *Science* **1987**, *238*, 645.

(13) Felsenfeld, G.; Davies, D. R.; Rich, A. *J. Amer. Chem. Soc.* **1957**, *79*, 2023.

(14). Michelson, A. M.; Massoulie, J.; Guschlbauer, W. *Prog. Nucl. Acid. Res. Mol. Biol.* **1967**, *6*, 83.

(15) Felsenfeld, G.; Miles, H. T. *Annu. Rev. Biochem.* **1967**, *36*, 407.

(16) Lipsett, M. N. *Biochem. Biophys. Res. Commun.* **1963**, *11*, 224.

(17) Howard, F. B.; Frazier, J.; Lipsett, M. N.; Miles, H. T. *Biochem. Biophys. Res. Commun.* **1964**, *17*, 93.

(18) Lipsett, M. N. *J. Biol. Chem.* **1964**, *239*, 1256.

(19) Miller, J. H.; Sobell, J. M. *Proc. Natl. Acad. Sci. U. S. A.* **1966**, *55*, 1201.

(20) Morgan, A. R.; Wells, R. D. *J. Mol. Biol.* **1968**, *37*, 63.

(21) Lee, J. S.; Johnson, D. A.; Morgan, A. R. *Nucleic Acids. Res.* **1979**, *6*, 3073.

(22) Arnott, S.; Bond, P. J. *Nature New Biology* **1973**, *244*, 99.

(23) Arnott, S.; Selsing, E.*J. Mol. Biol.* **1974**, *88*, 509.

(24) Arnott, S.; Bond, P. J.; Selsing, E.; Smith, P. J. C. *Nucleic Acids Res.* **1976**, *3*, 2459.

(25) Saenger, W. *Principles of Nucleic Acid Structure,* edited by Cantor, C. R.; Springer-Verlag, New York Inc. (**1984**).

(26) Hoogsteen, K. *Acta Crysta.* **1959**, *12*, 822.

(27) Mace, H. A. F.; Pelhan, H. R. B.; Travers, A. *Nature* **1983**, *304*, 555.

(28) Nickol, J. M.; Felsenfeld, G. *Cell* **1982**, *35*, 467.

(29) Larsen, A.; Weintraub, H. *Cell* **1982**, *29*, 609.

(30) Schon, E.; Evans, T.; Welsh, J.; Efstratiadis, A. *Cell* **1983**, *35*, 837.

(31). Hanvey, J. C.; Shimizu, M.; Wells, R. D. *Proc. Natl. Acad. Sci.* **1988**, *85*, 6292.

(32) Mirkin, S. M.; Lyamichev, V. I.; Drushlyak, K. N.; Dobrynin, V. N.; Filippov, S. A.; Frank-Kamenetskii, M. D. *Nature* **1987**, *330*, 495.

(33) Kohwi-Shigematsu, T. ; Kohwi, Y. *Cell* **1985**, *43*, 199.

(34) Dreyer, G. B.; Dervan, P. B. *Proc. Natl. Acad. Sci. U. S. A.* **1985**, *82*, 968.

(35) Chu, C. F.; Orgel, L. E. *Proc. Natl. Acad. Sci.* **1985**, *82*, 963.

(36) Iverson, B. L.; Dervan, P. B. *J. Amer. Chem. Soc.* **1987**, *109*, 1241.

(37) Moser, H. E.; Dervan, P. B., unpublished results.

(38) Povsic, T. J.; Dervan, P. B., unpublished results.

(39). Povsic, T. J.; Dervan, P. B. *J. Amer. Chem. Soc.* **1989**, *111*, 3059.

(40) Strobel, S. A.; Moser, H. E.; Dervan, P. B. *J. Amer. Chem. Soc.* **1988**, *110*, 7927.

(41) Maher III, L. J.; Wold, B.; Dervan, P. B. *Science* **1989**, *245*, 725.

(42) Kohwi, Y.; Kohwi-Shigematzu, T. *Proc. Natl. Acad. Sci. U. S. A.* **1988**, *85*, 3781.

(43) Cooney, M. *et al. Science* **1988**, *241*, 456.

Chapter 1

Design of Novel Bases for pH-Independent Recognition of GC Base Pairs by Oligonucleotide-Directed Triple Helix Formation

Introduction

Pyrimidine oligonucleotides recognize extended purine sequences in the major groove of double helical DNA via triple helix formation (1-7). Specificity is imparted by Hoogsteen base pairing between the pyrimidine oligonucleotide and the purine strand of the Watson-Crick duplex DNA (7-20). Complexes of triple helical nucleic acids containing cytosine (C) and thymine (T) in the Hoogsteen strand are stable in acidic to neutral solutions, but dissociate on increasing pH (4, 5). Sensitivity of triple helix formation to pH also depends on the number and position of the cytosines in the third strand. Oligonucleotides containing contiguous C-rich sequences are most sensitive to pH (21).

Povsic and Dervan have shown that oligonucleotide-EDTA•Fe(II) probes containing 5-bromouracil and 5-methylcytosine bind and cleave the polypurine sequence containing $dA_5(GA)_5$ by triple helix formation with specificity comparable to those of their thymine-cytosine analogs, but with greater affinities and over an extended pH range (5). Substitution of 5-methylcytosine (mC) for C increases the pH range ~0.4 units for triple helix stability in this sequence. However, protonation at N-3 of 5-methylcytosine is still required.

G-rich sequences are often found in eukaryotic genomes. These DNA regions appear to be hypersensitive to S1 nucleases (22-25). It has been suggested that under superhelical stress and acidic pH, any mirror-repeat sequence of purines in one strand can adopt H-form DNA (26-29). The major element of this structure is a triple helix associated with a homopyrimidine loop through Hoogsteen base pairs. Since S1 optimum

activity is observed at pH 4.5, protonation of C could be favored in triple helix formation.

Because oligonucleotide specificity could provide a method for the artificial repression of gene expression, it is desirable to design and synthesize a novel base that could recognize GC base pairs without the requirement of protonation. Oligonucleotides containing such bases could then recognize G-rich sequences over a wide range of pH. From model building studies we chose deoxyriboisoguanosine (G'), 1-(2-deoxy-β-D-erthro-pentofuranosyl)1, 4, 5, 6-tetrahydro-3-methyl-5-amino-7H-pyrazolo(4, 3-d)pyrimidine-7-one (**17a**, P1 nucleoside), and 2-(2-deoxy-β-D-erthro-pentofuranosyl)-2, 4, 5, 6-tetrahydro-3-methyl-5-amino-7H-pyrazolo(4, 3-d)pyrimidine-7-one (**17b,** P2 nucleoside) as initial targets and chose an abasic compound, 1,2-dideoxy-D-ribose as a reference to study the ability of these bases to recognize GC base pairs. Isoguanosine (G'), P1 and P2 bases were designed to form two hydrogen bonds to G in the purine strand with no requirement for protonation (Figure 1).

Base P1 was found to recognize GC base pairs as selectively and strongly as C+ does, while isoguanosine (G') and base P2 were found to recognize GC selectively, but weakly relative to P1 and C+. Although isoguanosine (G') was found to recognize GC selectively, the general usage of G' has limitations due to its instability to the conditions employed in automated synnthesis. ^{1}HNMR, FABMS and enzyme digestion show that the nucleosides P1 and P2 nucleosides are found stable during the automated oligonucleotide synthesis and base deprotection. The utility of P1 is demonstrated for the site-specific binding of the 15 base pair sequence

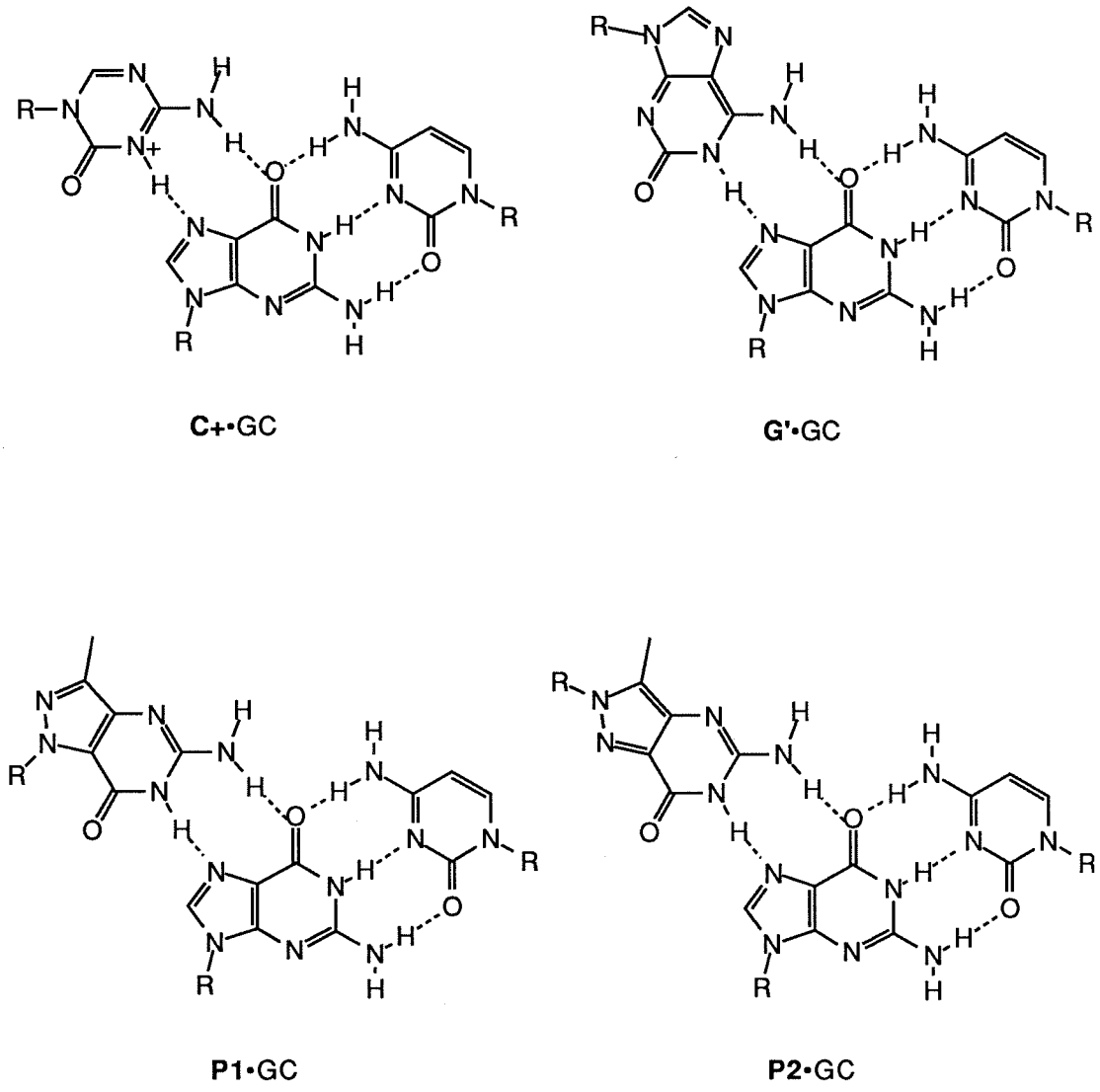

Figure 1. Base triplets C+•GC, G'•GC, P1•GC and P2•GC.

$dA_5(GA)_5$ in the plasmid pDMAG10 and the 16 base pair sequence $dA_4GA_4G_6A$ in the 3' long terminal repeat (LTR) of HIV DNA.

Results and Discussion

Synthesis of Phosphoramidite 10. The synthetic scheme for the nucleoside phosphoramidite **10** is shown in Figure 2. 5-amino-1-β-D-ribofuranosylimidazol-4-carboxamide (AICA-ribose) was reacted with 1,3-dichloro-1,1,3,3-tetraisopropyldisiloxane to give 5-amino-1-[3,5-O-(1,1,3,3-tetraisoproyldisiloxanyl)-β-D-ribofuranosyl]imidazol-4-carboxamide **2**. Reaction of **2** with phenoxythiocarbonylchloride in the presence of N,N-dimethylaminopyridine (DMAP) gave 5-amino-1-[3,5-O-(1,1,3,3-tetraisopropyldisiloxanyl-2-O-phenoxythiocarbonyl)-β-D-ribofuranosyl]-imidazole-4-carboxamide (3), which was reduced with tributyltinhydride to afford a 2'-deoxynucleoside **4** (30). Condensation of 5-amino-1-[3,5-O-(1,1,3,3-tetraisopropylsiloxanyl)-β-D-deoxyribofuranosyl]imidazole-4-carboxamide **4** with benzoylthiocyanate and treatment of the resulting thiourea derivative with DCC furnished 5-(N'-benzoylcarbonyl)amino-imidazole-4-carbonitrile (**5**), which was then annulated with ethanolic ammonia to afford the deoxyriboisoguanosine derivative **6** in a 60% yield (31). **6** was treated with benzoylchloride to give the benzoyl-protected deoxyriboisoguanosine derivative **7**, which was deprotected with tetrabutylammonium fluoride to afford **8**. The 5' hydroxy group of **8** was protected with dimethoxytritylchloride to give **9**. The reaction of **9** with 2-cyanoethyl-N,N-diisopropylchloro-phophoramidite afforded the 5'-DMT-protected phosphoramidite **10**.

Synthesis of P1 and P2. The synthetic scheme for nucleoside phosphoramidites P1 and P2 is shown in Figure 3. Ethyl 3-methyl-4-nitropyrazole-5-carboxylate (**11**) (32) was condensed with 1-chloro-2-deoxy-3, 5-di-o-p-toluoyl-α-D-erthrofuranose (**12**) (33-35) to give the N1 β anomer

13a

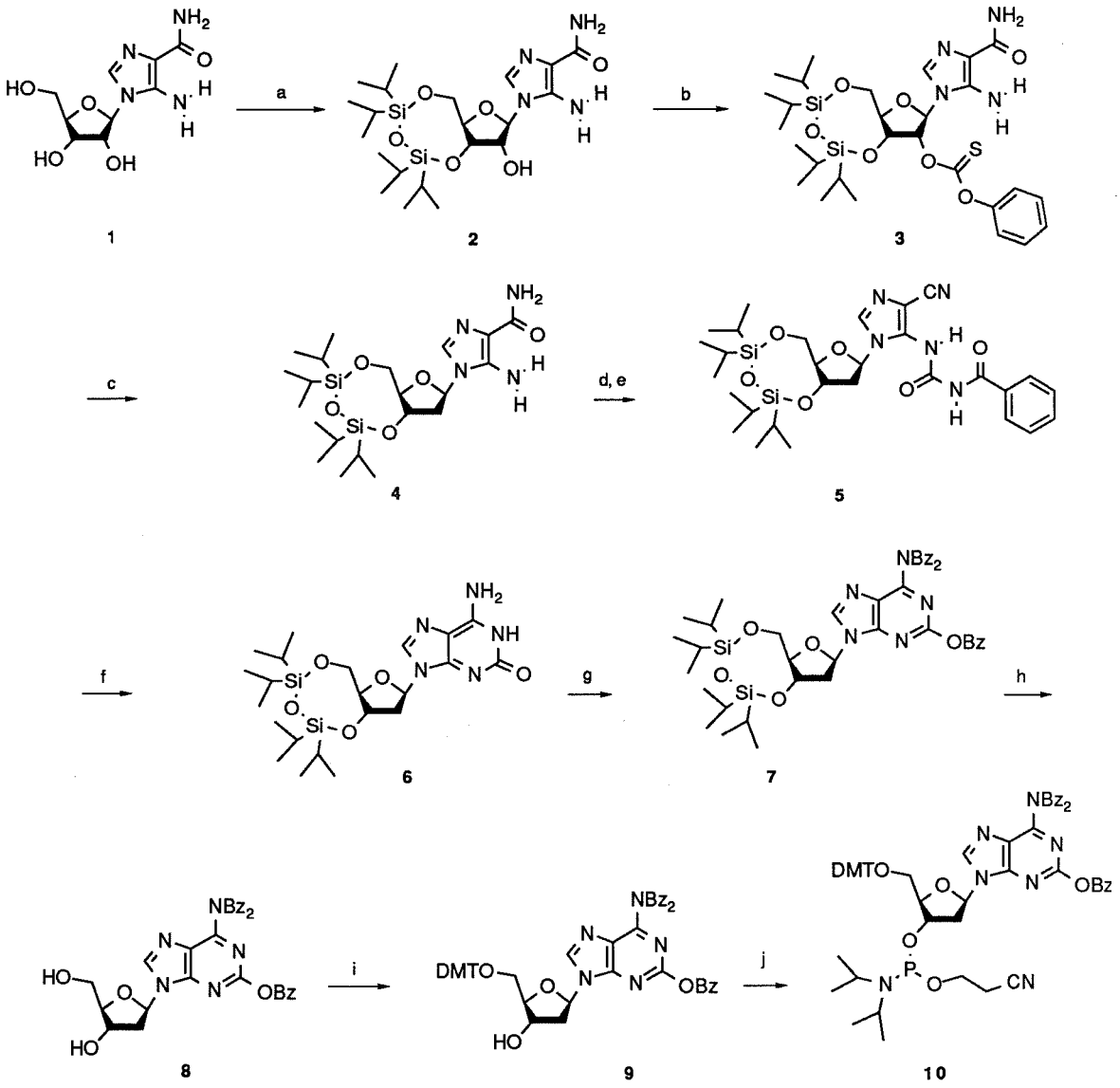

Figure 2. Synthetic scheme of phosphoramidite **10** (**G'**). a) 1, 3-dichloro-1, 1, 3, 3-tetraisopropyldisiloxane, pyridine b) phenoxythiocarbonyl chloride, DMAP, acetonitrile c) 2', 2'-azobis(2-methylpropionitrile), n-Bu_3SnH, toluene d) benzoylisothiocyanate, DMF e) DCC f) NH_4OH (30% in H_2O), ethanol, 10°C g) benzoyl chloride, pyridine, 4°C h) 1N tetrabutylammoniumfluoride in THF, THF i) DMTCl, pyridine j) N, N-diisopropylethylamine, 2-cyanoethyl-N, N-diisopropylamino-chlorophosphoramidite, methylene chloride.

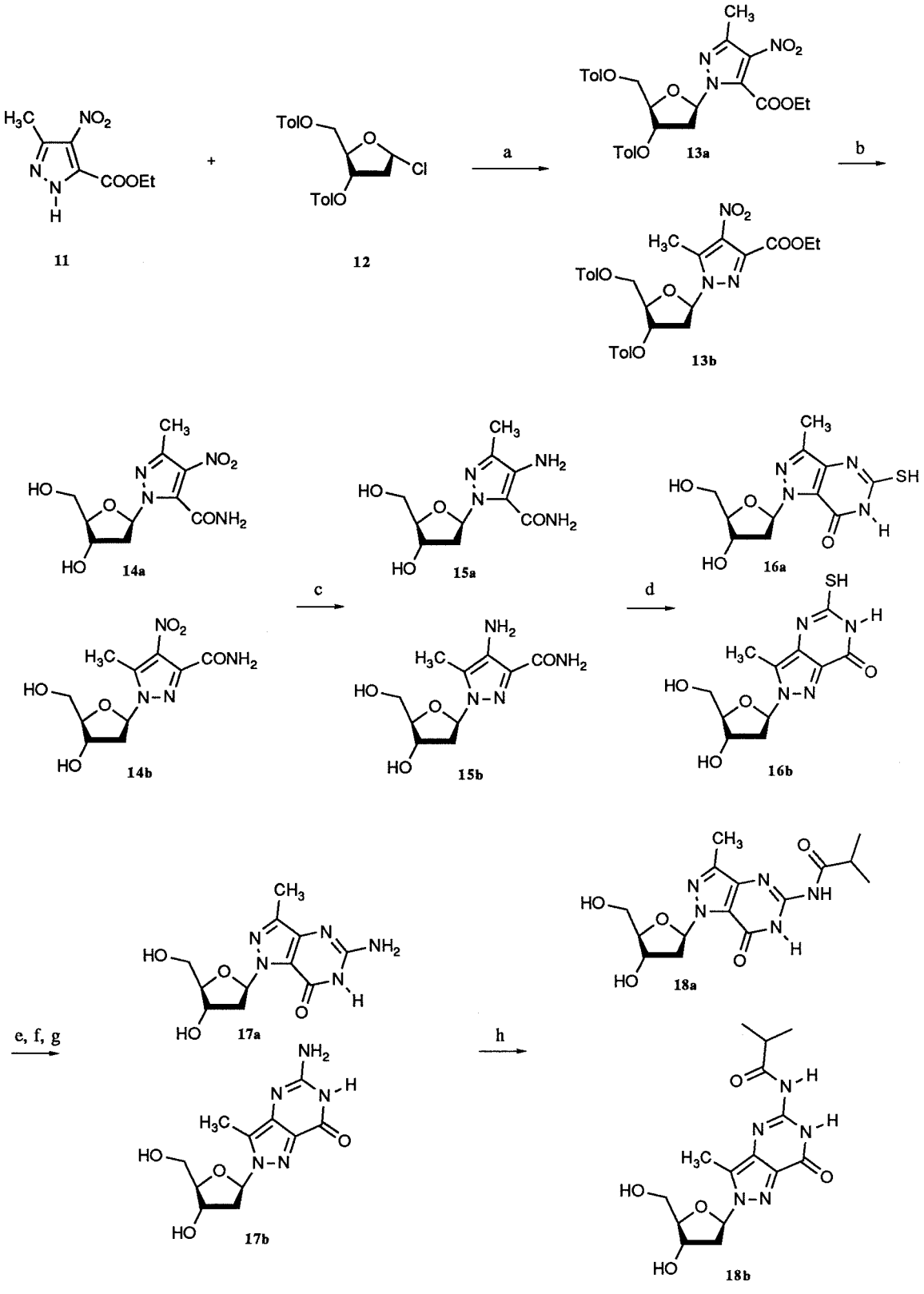
11
12
a
13a
13b
b
14a
14b
c
15a
15b
d
16a
16b
e, f, g
17a
17b
h
18a
18b

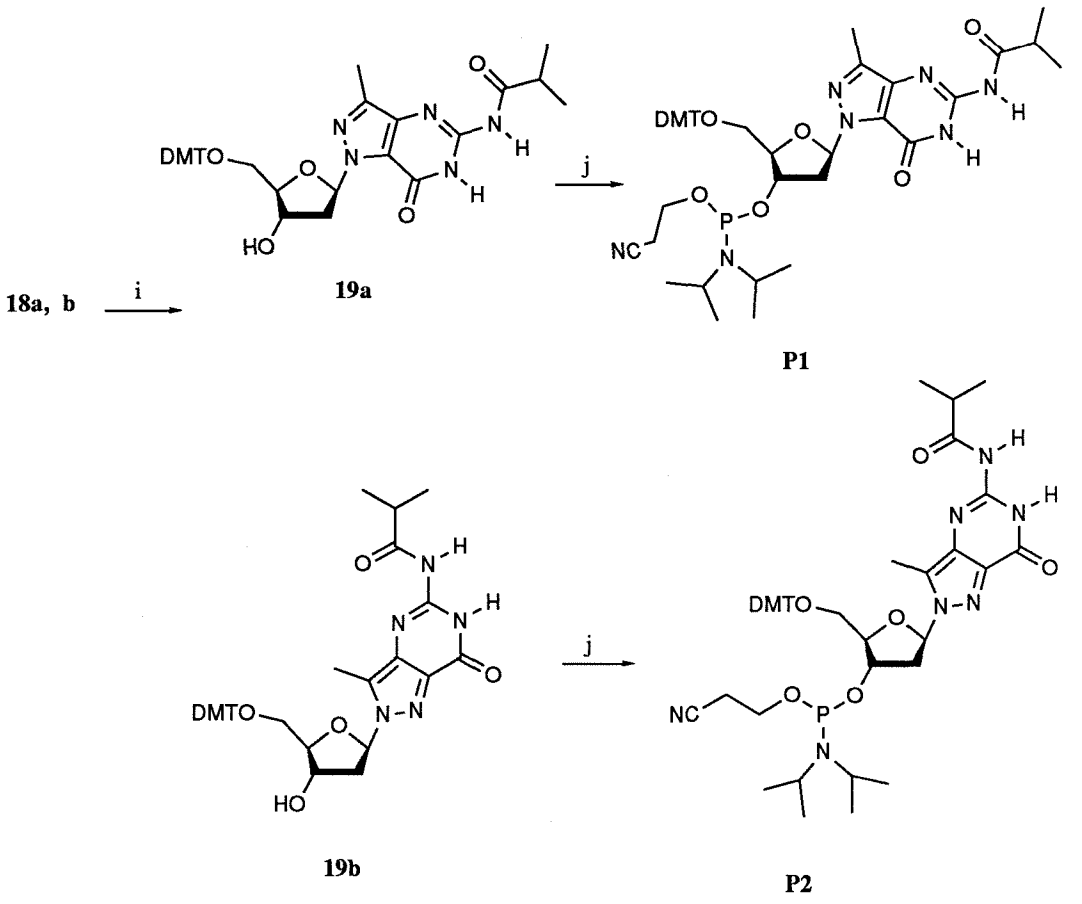

Figure 3. Scheme for the synthesis of **P1** and **P2** a) NaH, acetonitrile b) ammonia, MeOH c) 10% Pd/C, H_2, EtOH/water d) phenylisocyanate, pyridine 150°C e) NH_4OH f) H_2O_2 g) sat. ammonia 160°C h) TMSCl, isobutyric anhydride, pyridine i) DMTCl, pyridine j) diisopropylethylamine, 2-cyanoethyl-N, N-diisopropyl-chlorophosphoramidite, methylene chloride.

in 46% yield and N2 β anomer **13b** in 44% yield. The toluyl protecting groups and the ethyl ester group were removed in saturated ammonia in methanol and hydrogenation of **14a** (50psi, H_2, 10% Pd/C) reduced the nitro group to an amine. Ring closure of **15a** with phenylisocyanate gave **16a** (36). The SH group was oxidized to a sulfonic acid group, and the sulfonic acid displaced with saturated aqueous ammonium hydroxide in a sealed

pressure bottle at 160°C to give **17a**. The amine was selectively acylated by the transient protection method (37). The 5' hydroxy groups were protected with dimethoxytrityl chloride (DMTCl) to give **19a**. Reaction of **19a** with 2-cyanoethyl-N,N-diisopropylchlorophosphoramidite and di-isopropylethylamine (DIPEA) afforded the 5'-DMT-protected phosphoramidite (37) **P1** (Phosphoamidous acid, bis(1-methylethyl)-, 2-cyanoethyl ester, 3'-ester with N-[1-[5-O-[bis(4-methoxyphenyl)-phenylmethyl]-2-deoxy-β-D-erthro-pentofuranosyl]]-4,7-dihydro-3-methyl-7-oxo-1H-pyrazolo[4,3-d]pyrimidin-5-yl]-2-methyl-propanamide). **P2** (Phospho-amidous acid, bis(1-methylethyl)-, 2-cyanoethylester, 3'-ester with N-[2-[5-O-[bis(4-methoxyphenyl)phenylmethyl]-2-deoxy-β-D-erthro-pentofuranosyl]4, 7-dihydro-3-methyl-7-oxo-2H-pyrazolo[4, 3-d]pyrimidin-5-yl]-2-methyl-propanamide) was prepared by the same method. Abasic phosphoramidite(5-O-(4,4'-dimethoxytrityl)-1,2-dideoxy-D-ribose-3-(β-cyano-ethylN,N-diisopropyl)phosphoramidite) was a generous gift from Dr. Dave Horne.

Structural analysis of compounds 13a and 13b. The structures of **13a** and **13b** were analyzed by NMR and X-ray crystallography. In a NOE study, irradiation of the C-H1' proton enhanced the methylene proton peaks of the 5-ethylcarboxlate of **13a** and 5-methyl protons of **13b**. **13b** was recrystallized from a solution of ether and hexane (1:1 v/v). X-ray crystallographic analysis revealed the structure assigned from the NOE study (Figure 3). It crystallized in the orthorhombic system, in the space group $P2_12_12_1$.

Synthesis of oligonucleotides containing novel base heterocycles. Oligonucleotides **20-31** were synthesized using standard solid phase β-cyanoethyl-phosphoramidite chemistry (38). The novel base phosphor-

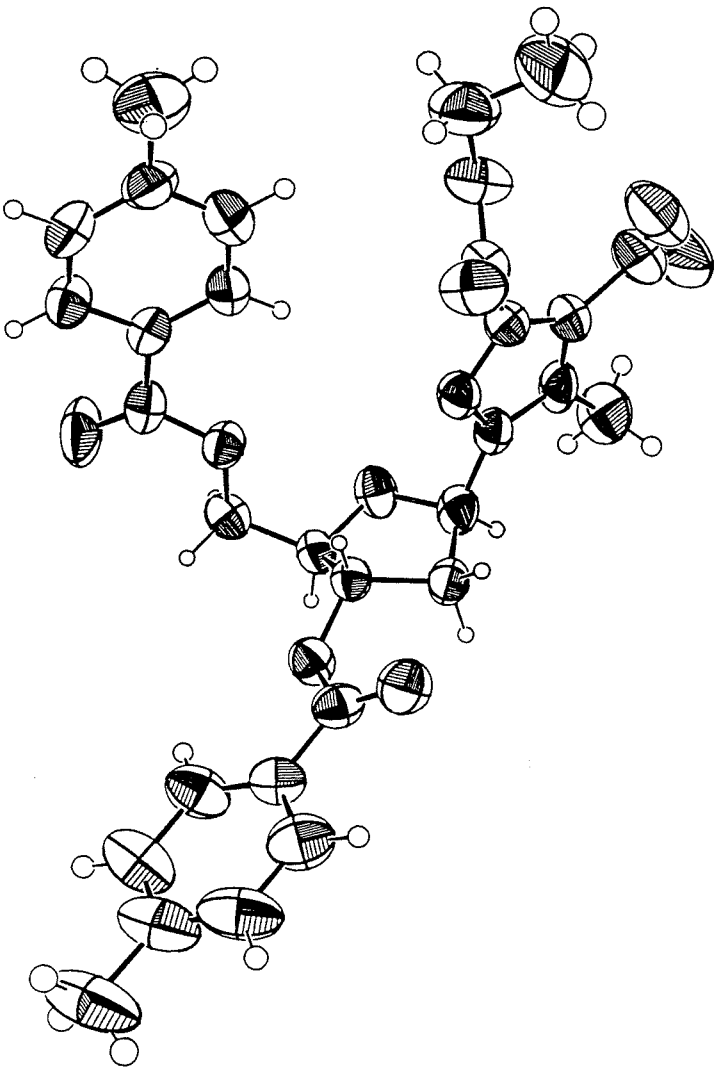

Figure 4. Structure of **13b** as determined by X-ray crystallography.

amidites P1, P2 and abasic phosphoramidite were coupled with an efficiency comparable to A, G, C, and T phosphoramidites; however deoxyriboisoguanosine phosphoramidite coupled with a a lower yield of ~60%.

It has been reported that isoguanosine derivatives are more easily depurinated in an acidic solution than either guanosine or adenosine (39). Because oligonucleotides **20-31** contain dT* (thymidine-EDTA) (40), 0.1N

NaOH was substituted in the deprotection steps for NH_4OH to circumvent possible ammonolysis of the T* ethylesters. To examine the stability of the novel bases through several machine synthesis coupling and base deprotection cycles, the 4-mers 5'-T-T-P1-T-3' and 5'-T-T-P2-T-3' were synthesized on a 10 μmol scale for NMR and FABMS studies. The glycosidic bonds of P1 and P2 were found to be stable under these conditions. From the NMR and FABMS data it was shown that the isobutyrylamido group of P1 or P2 was completely removed to give a free amine, and that the novel bases were stable in the machine synthesis.

Product Analysis of Oligonucleotides by Enzyme Digestion. The individual oligonucleotide and its nucleoside composition can be analyzed by HPLC to ensure that the nucleoside is not chemically changed during automated synthesis. Purified oligonucleotides were digested with snake venom phosphodiesterase and calf intestine alkaline phosphatase to give their nucleosides (Figure 5a) (41-42). Snake venom phosphodiesterase treatment of oligonucleotides gives 5'-monophosphate nucleotides, and subsequent treatment with calf intestine alkaline phosphatase gives the corresponding nucleosides. HPLC analysis of the digestion products was carried out on a C18 reverse phase column using 10 mM ammonium phosphate pH 5.1/ 8% MeOH as the eluent (Figures 5b, c, d, and e). Analysis of the oligonucleotide 5'-T*$(T)_4$$(P1T)_5$-3' gave T*, P1 and T nucleosides after enzyme digestion (Figures 5c and 5d). The oligonucleotide 5'-T*$(T)_3$C$(T)_4$P1$_6$T-3' gave T*, T, C, and P1 nucleosides (Figures 5e and 5f). The oligonucleotide 5'-TP2TT-3' gave T and P2 nucleosides. These analyses suggest that the P1 and P2 nucleosides can be used in automated DNA synthesis without complications.

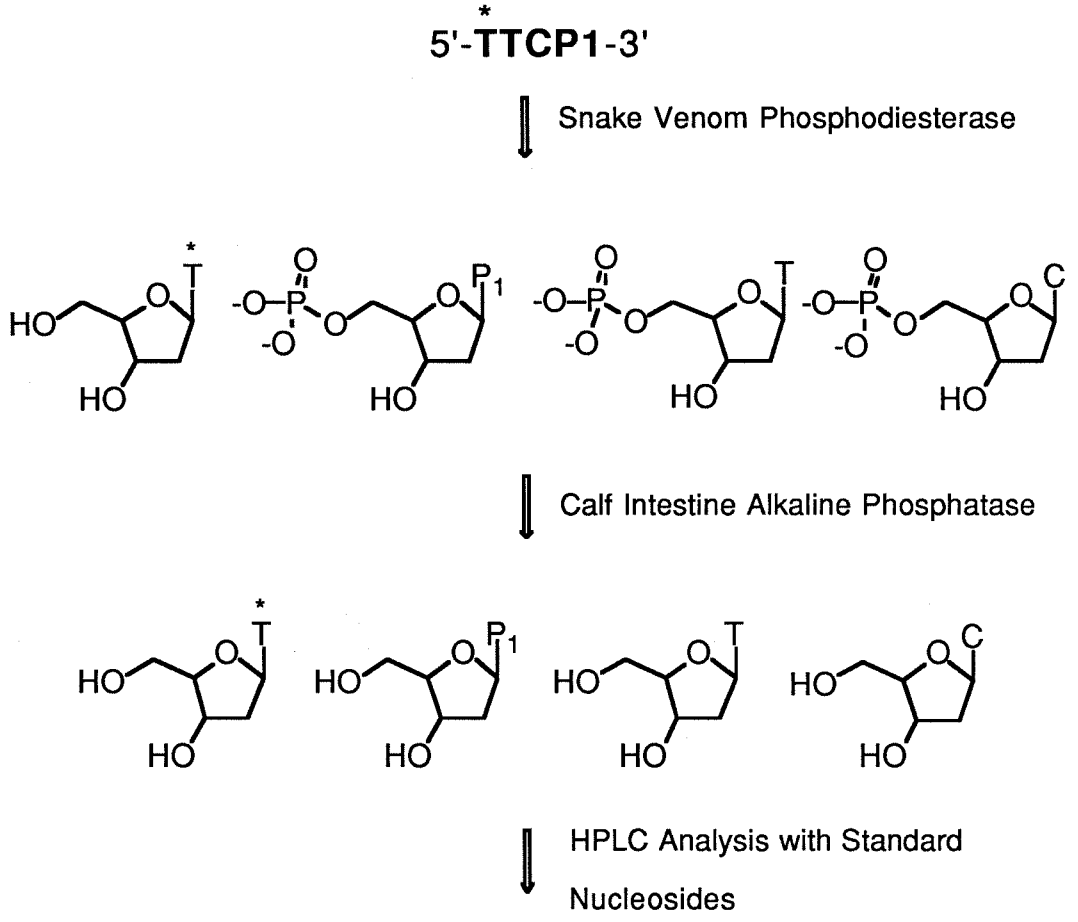

Figure 5a. Scheme for the enzyme digestion of oligonucleotides for HPLC analysis.

Cleavage of oligonucleotide 30 mer complex. The use of oligonucleotides equipped with the DNA-cleaving moiety thymidine-EDTA•Fe(II)(T*) allowed a qualitative ordering of relative stabilities of triple helices formed between 30 base pair (bp) DNA duplexes containing

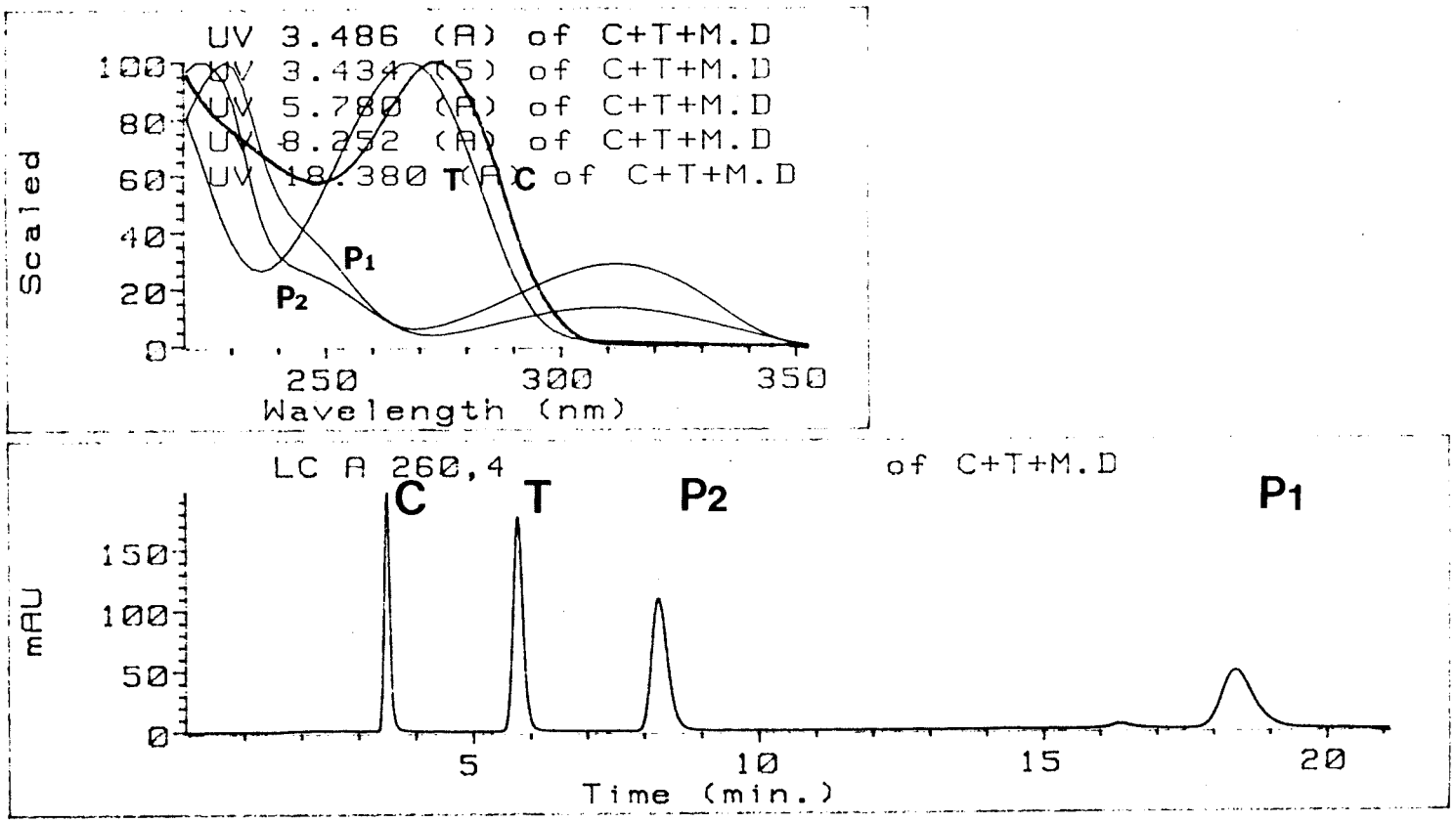

Figure 5b. HPLC chromatogram (monitored at 260 nm) of the nucleosides C, T, P1, and P2. The samples were eluted on a C18 reverse phase column with 8% MeOH in 10 mM ammonium phosphate pH 5.1 at a flow rate of 1 mL/min. The UV-Vis spectra of the different peaks are recorded in the upper left panel.

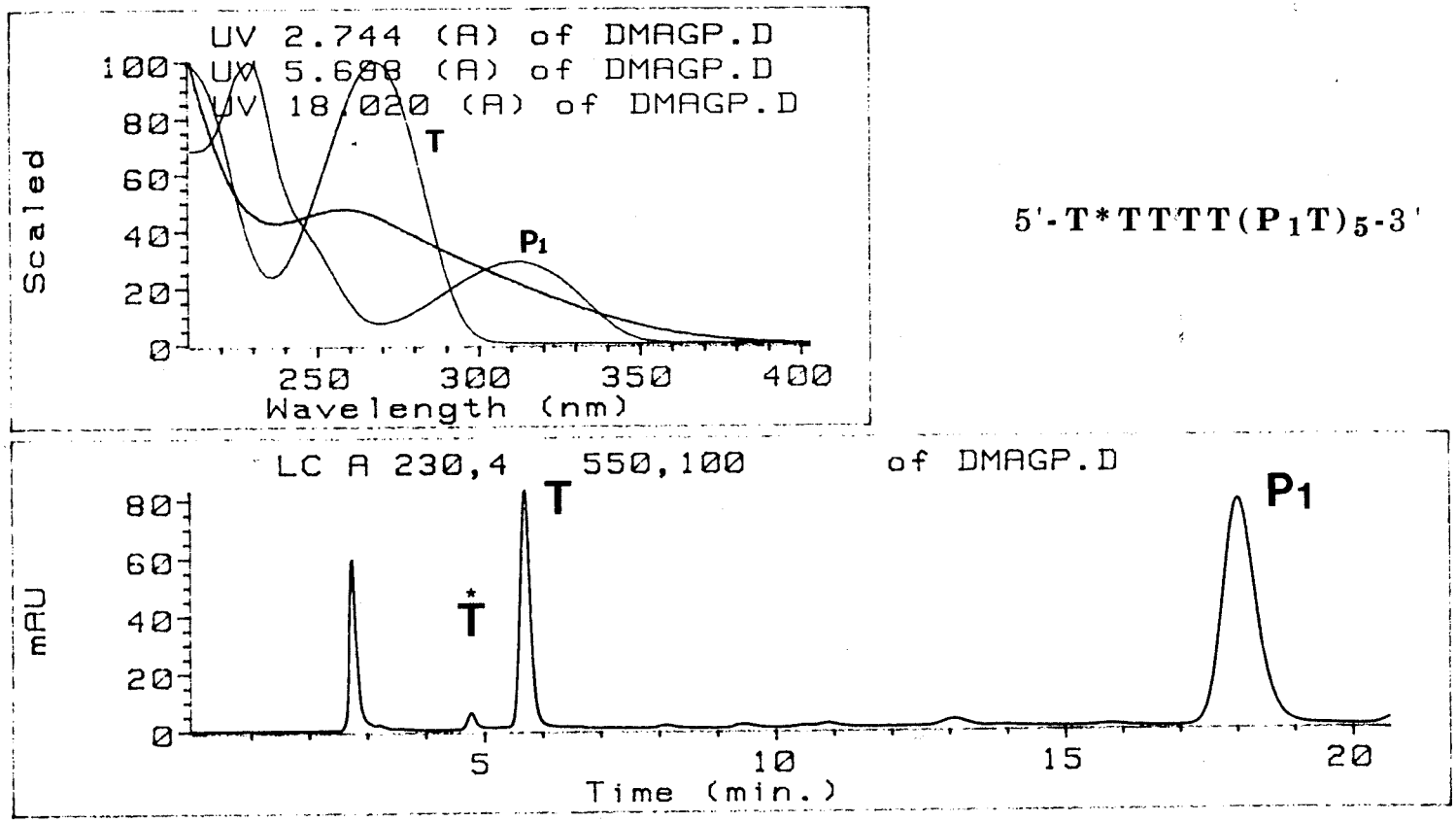

Figure 5c. HPLC chromatogram (monitored at 230 nm) of the mixture of the enzyme digested products of oligonucleotide **27** (**5'-T*TTTT(P1T)$_5$-3'**). The samples were eluted on a C18 reverse phase column with 8% MeOH in 10 mM ammonium phosphate pH 5.1 at a flow rate of 1 mL/min. The UV-Vis spectra of the different peaks are recorded in the upper left panel.

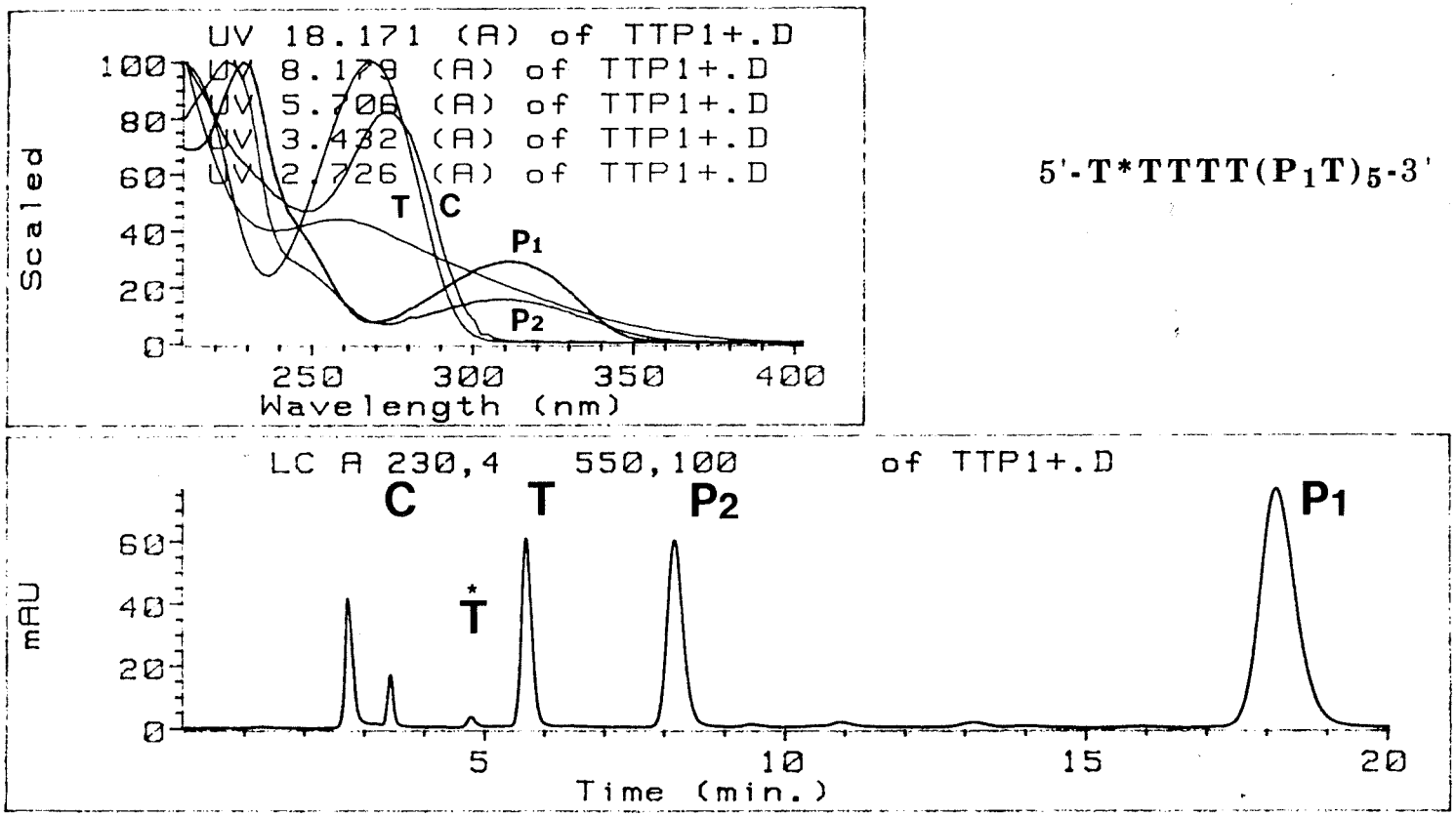

Figure 5d. HPLC chromatogram (monitored at 230 nm) of the mixture of the enzyme digested products of oligonucleotide **27** (**5'-T*TTTT(P$_1$T)$_5$-3'**) and nucleosides C, T, P1, and P2. The samples were eluted on a C18 reverse phase column with 8% MeOH in 10 mM ammonium phosphate pH 5.1 at a flow rate of 1 mL/min. The UV-Vis spectra of the different peaks are recorded in the upper left panel.

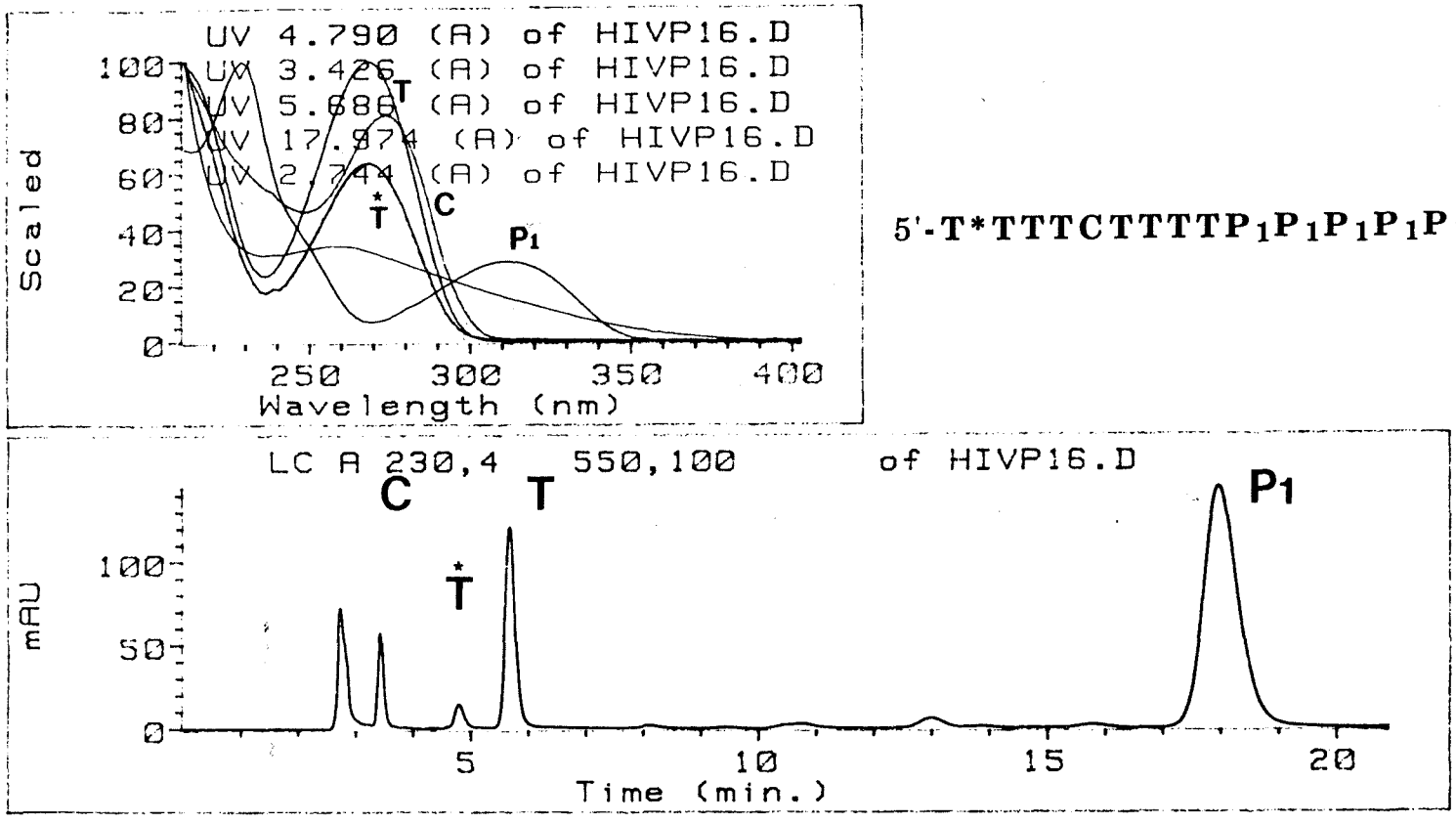

Figure 5e. HPLC chromatogram (monitored at 230 nm) of the mixture of the enzyme digested products of oligonucleotide **31** (**5'-T*TTTCTTTTP$_1$P$_1$P$_1$P$_1$P$_1$P$_1$T-3'**). The samples were eluted on a C18 reverse phase column with 8% MeOH in 10 mM ammonium phosphate pH 5.1 at a flow rate of 1 mL/min. The UV-Vis spectra of the different peaks are recorded in the upper left panel.

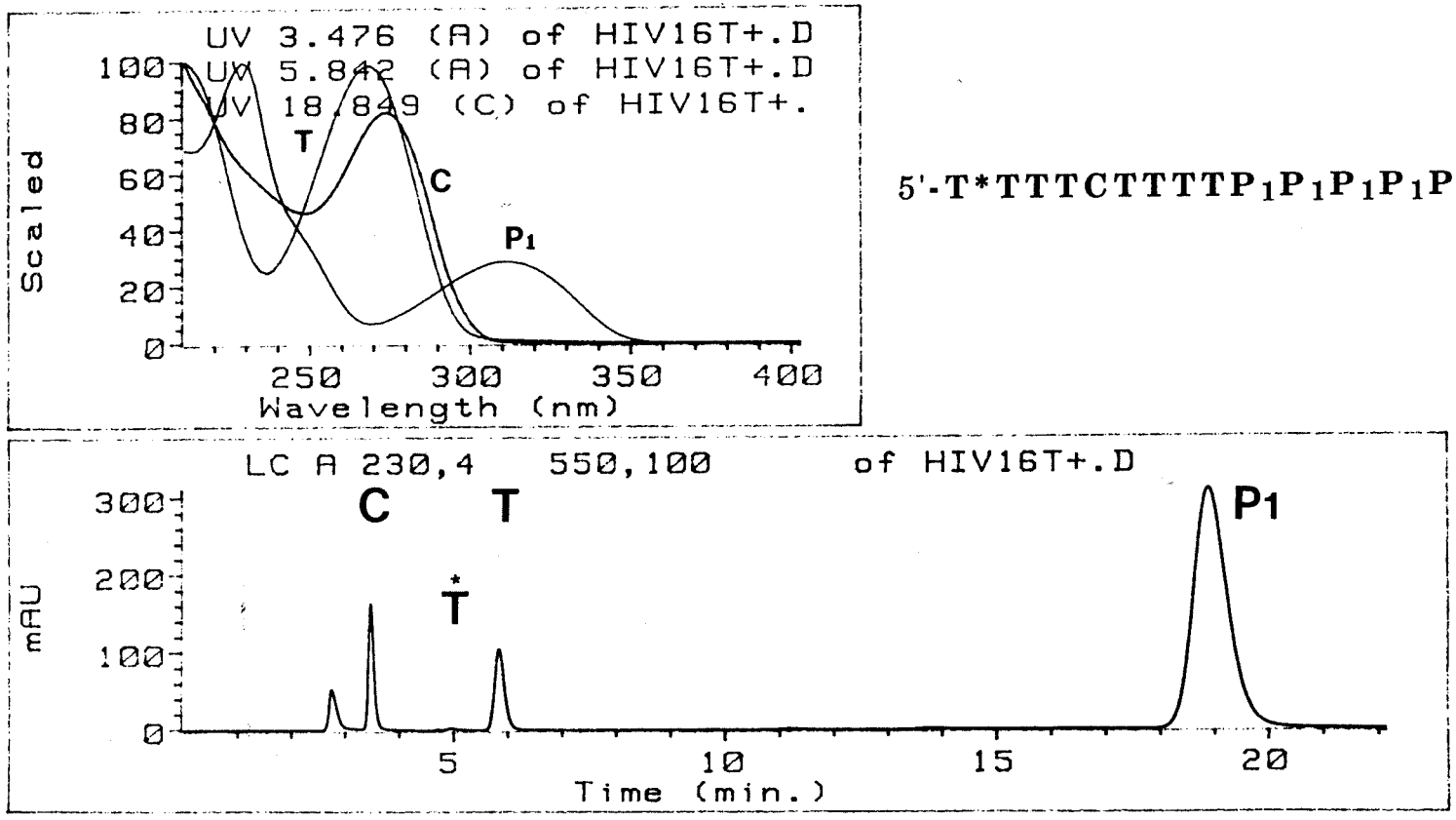

Figure 5f. HPLC chromatogram(monitored at 230 nm) of the mixture of the enzyme digested products of oligonucleotide **31** (**5'-T*TTTCTTTTP$_1$P$_1$P$_1$P$_1$P$_1$P$_1$T-3'**) and nucleosides C, T, P1, and P2. The samples were eluted on a C18 reverse phase column with 8% MeOH in 10 mM ammonium phosphate pH 5.1 at a flow rate 1 mL/min. The UV-Vis spectra of the different peaks are recorded in the upper left panel.

the site d(A7XA7)/d(T7YA7) (XY=AT, GC, TA or CG) and a series of 15 nt oligonucleotides differing at one base position d(T7NT7)(N=C, G', P1, P2, Ab) (Figure 6). The 30-bp duplexes were labeled with ^{32}P at the 5' end of the target site strand d(T7YT7). The DNA cleavage reactions of oligonucleotides **20-21** were performed to compare the base specificity and binding affinity. The most intense cleavage patterns were observed when N=C, XY=GC and N=G', XY=GC (Figure 7a). A bar graph representing the relative cleavage is shown in Figure 7b. The DNA binding reactions of oligonucleotide **21** were performed at various temperatures in the presence of 40% ethanol (Figure 8a). As the temperature increased, the cleavage efficiency of base triplets decreased sharply for all the base triplets except for G'•GC. The most intense cleavage pattern was observed for N=G', XY=GC under stringent conditions (pH 7.4, 35°C, 40% ethanol) (Figure 8a). The relative cleavage is shown in Figure 8b. The strong cleavage pattern in G'•GC suggests that isoguanosine (G') can recognize GC base pair selectively as C+ does (Figure 8c). The DNA cleaving reactions of **20**, **22**, **23**, and **24** were also performed under conditions that were sensitive to the stability of the variable base triplet in the middle of the thymine 15 nt fragment within the triple helix (pH 7.4, 35°C, 40% ethanol). The most intense cleavage patterns were observed when N=C, XY=GC and N=P1, XY=GC (Figure 9a). The cleavage for the C+GC triplet (lane 4 in Figure 9a) represents the known ability of C to bind GC base pairs. Strong cleavage patterns were observed for the base P1 in P1•GC base triplets (lane 8 in Figure 9a), while moderate cleavage patterns were observed for the base P2 in the P2•GC triplet (lane 12 in Figure 9a). The abasic compound shows a preference for pyrimidine/purine base pairs (CG and TA) over purine/pyrimidine base

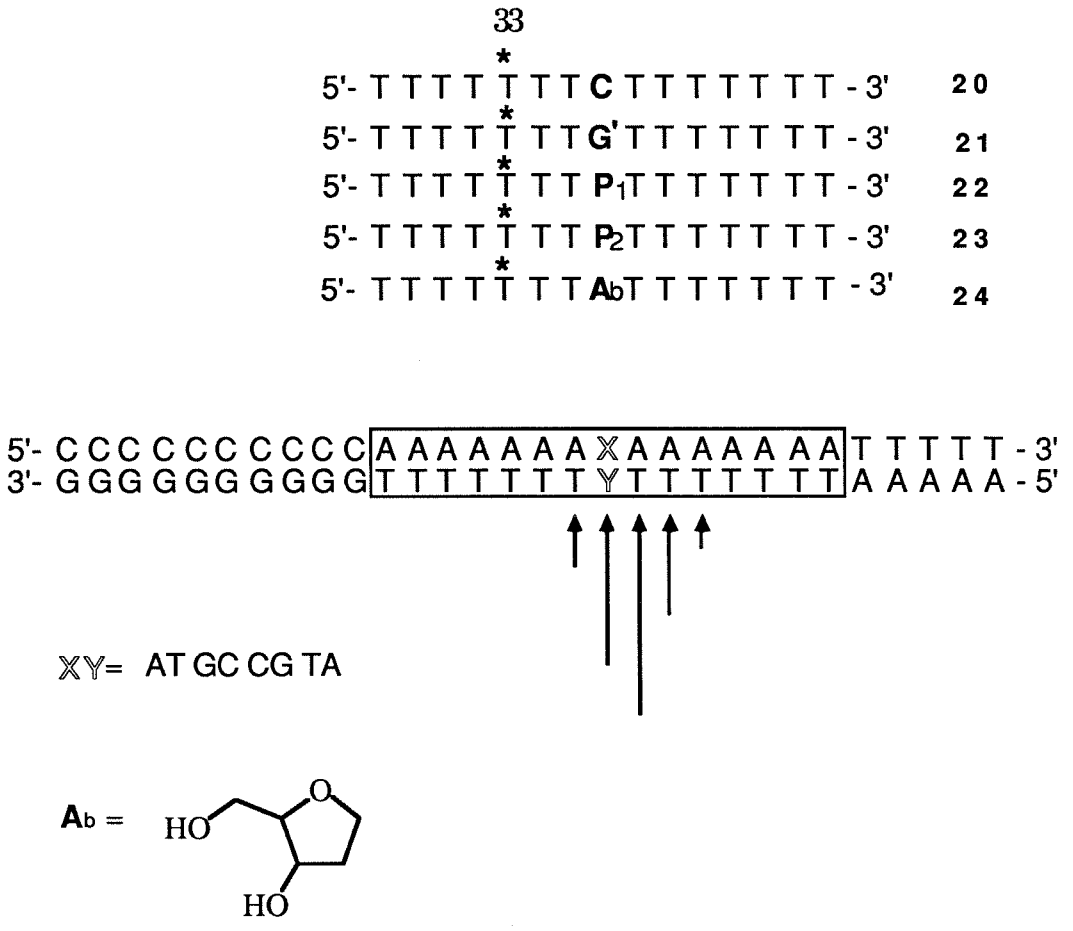

Figure 6. (**Above**) Sequence of oligonucleotides-EDTA **20-24** where T* is thymidine-EDTA. The oligonucleotides differ at one base position indicated in bold type. (**Below**) The box indicates the double stranded sequence bound by oligonucleotides-EDTA•Fe(II) **20-24.** The Watson-Crick base pair (AT, GC, TA or CG) opposite the varient base in the oligonucleotide is also in bold type.

pairs (AT and GC). The bases P1 and P2 were designed to form two hydrogen bonds to the GC base pair.

The strong cleavage pattern in P1•GC suggests that two hydrogen bonds are formed in the P1•GC triplets like C+GC. The weak cleavage pattern in P2•GC suggests that the position of the backbone in P2•GC is not appropriate or that the methyl group disfavors the anti conformation of base P2 (Figures 9c, d, and e).

Figure 7a. Autoradiogram of the 20 percent denaturing polyacrylamide gel. The cleavage reactions were carried out by combining a mixture of oligonucleotide-EDTA (2 μM), spermine(1mM), and Fe(II) (25 μM) with the ^{32}P labeled 30-mer duplex (40,000 cpm) in a solution of tris-acetate, pH 7.0 (50 mM, pH 7.4), NaCl (100 mM), calf thymus DNA (100μM bp), and 40% ethanol and incubated at 25°C for 1 hour. Cleavage reactions were initiated by the addition of DTT (3 mM) and allowed to proceed for 6 h at 25°C. The reactions were stopped by freezing and lyopholization and the cleavage products were analyzed by gel electrophoresis (1,500-2,000V, BPB 25 cm). Lanes 1-8: duplex containing 5' end-labeled ($A_5T_7YT_7G_{10}$). Lanes 1-8: DNA cleavage products produced by oligonucleotide-EDTA•Fe(II) (**20-21**); **20** (lanes 1 to 4); **21** (lanes 5 to 8). XY=AT (lanes 1 and 5); XY=GC (lanes 2 and 6); XY=CG (lanes 3 and 7); XY=TA (lanes 4 and 8).

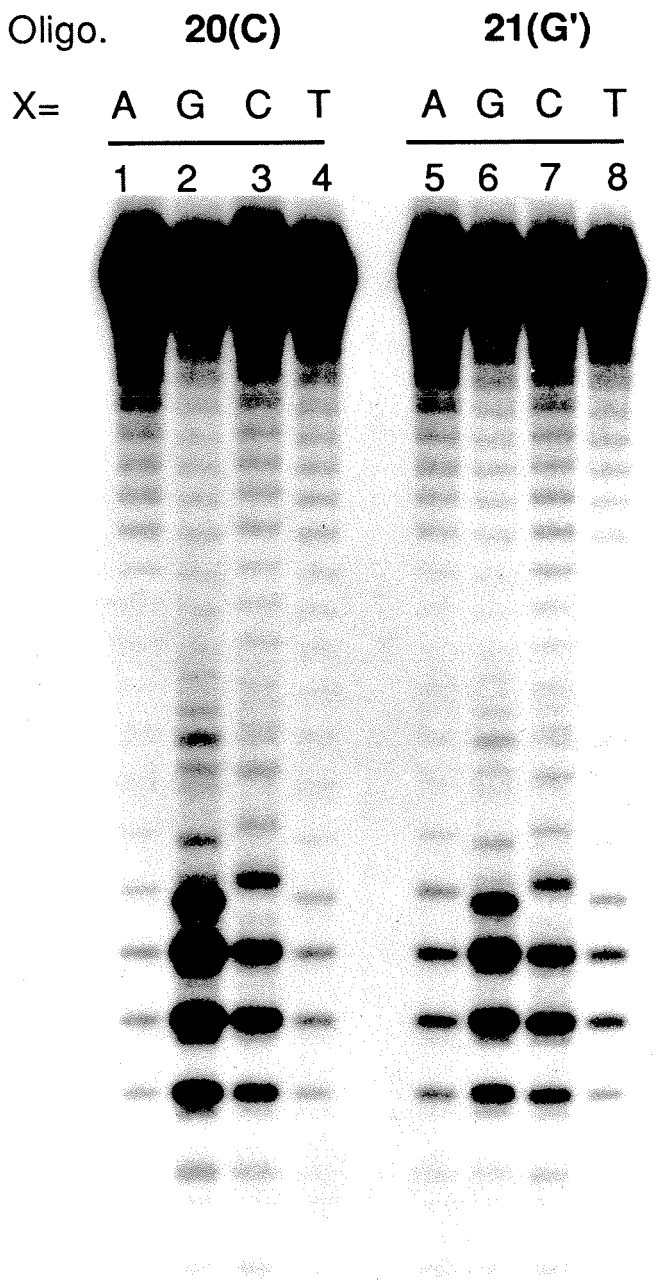
Oligo.
20(C)
21(G')
X=
A G C T
A G C T
1 2 3 4
5 6 7 8

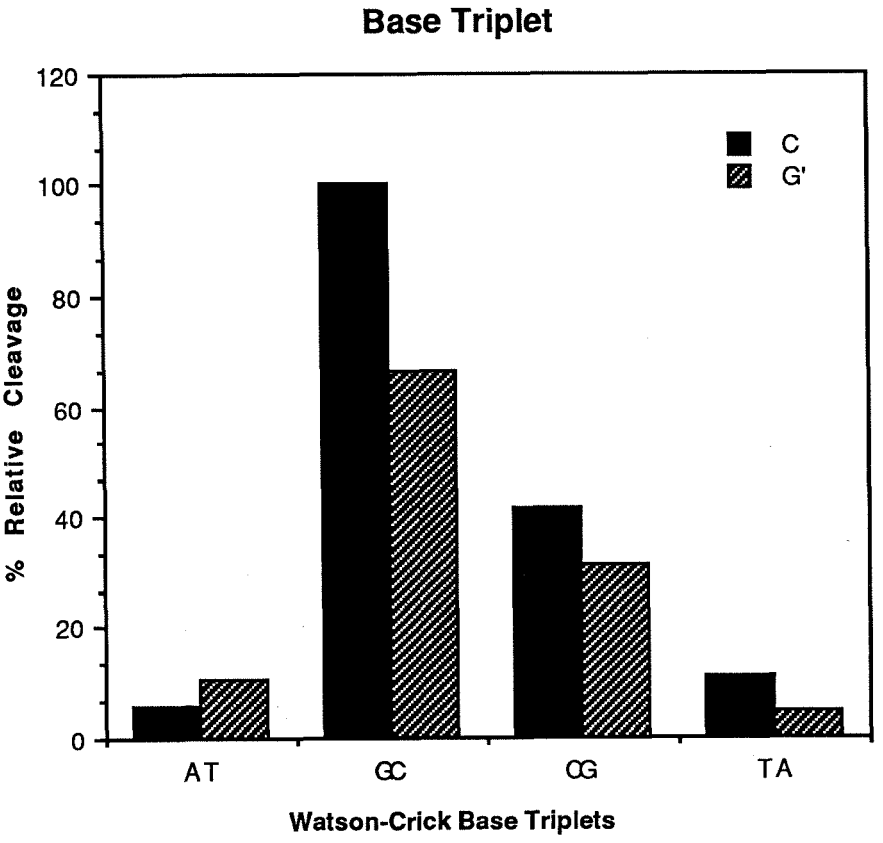

Figure 7b. Bar graph representing the relative cleavage data from densitometric analysis of Fig. 7a. Eight base triplets were examined for binding specificity compatible with the pyrimidine triple helix motif shown by the experiment described in Fig. 7a.

Figure 8a. Autoradiogram of the 20 percent denaturing polyacrylamide gel. The cleavage reactions were carried out by combining a mixture of oligonucleotide-EDTA (2 μM), spermine (1 mM), and Fe(II) (25 μM) with the ^{32}P labeled 30-mer duplex (40,000 cpm) in a solution of tris-acetate (50 mM pH 7.4), NaCl (100 mM), calf thymus DNA (100μM bp), and 40% ethanol and incubated at 20°C, 25°C, 30°C, and 35°C for 1 hour. Cleaving reactions were initiated by the addition of DTT (3 mM) and allowed to proceed for 6 h at each temperature. The reactions were stopped by freezing and lyopholization and the cleavage products were analyzed by gel electrophoresis (1,500-2,000V, BPB 25cm). Lanes 1-18: duplex containing 5' end-labeled ($A_5T_7YT_7G_{10}$). Lane 1: control showing intact 5' labeled 30 bp DNA standard obtained after treatment according to the cleavage reaction in the absence of oligonucleotide-EDTA. Lane 2: products of Maxam-Gilbert G+A sequncing reaction (43). Lane 3-18: DNA cleavage products produced by oligonucleotide-EDTA•Fe(II) (**21**); 20°C (lanes 3 to 6); 25°C (lanes 7 to 10); 30°C (lanes 11 to 14); 35°C (lanes 15 to 18). XY=AT (lanes 3,7,11, and 15); XY=GC (lanes 4, 8, 12, and 16); XY=CG (lanes 5, 9, 13, and 17); XY=TA (lanes 6, 10, 14, and 18).

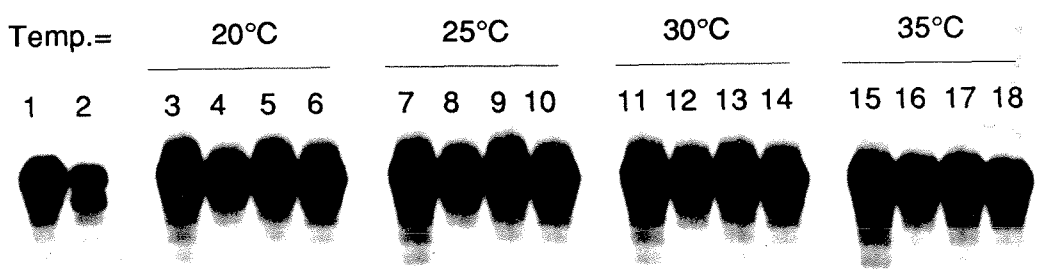
Temp.=
20°C
25°C
30°C
35°C
1 2
3 4 5 6
7 8 9 10
11 12 13 14
15 16 17 18

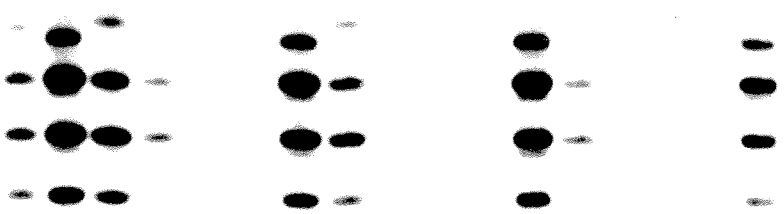

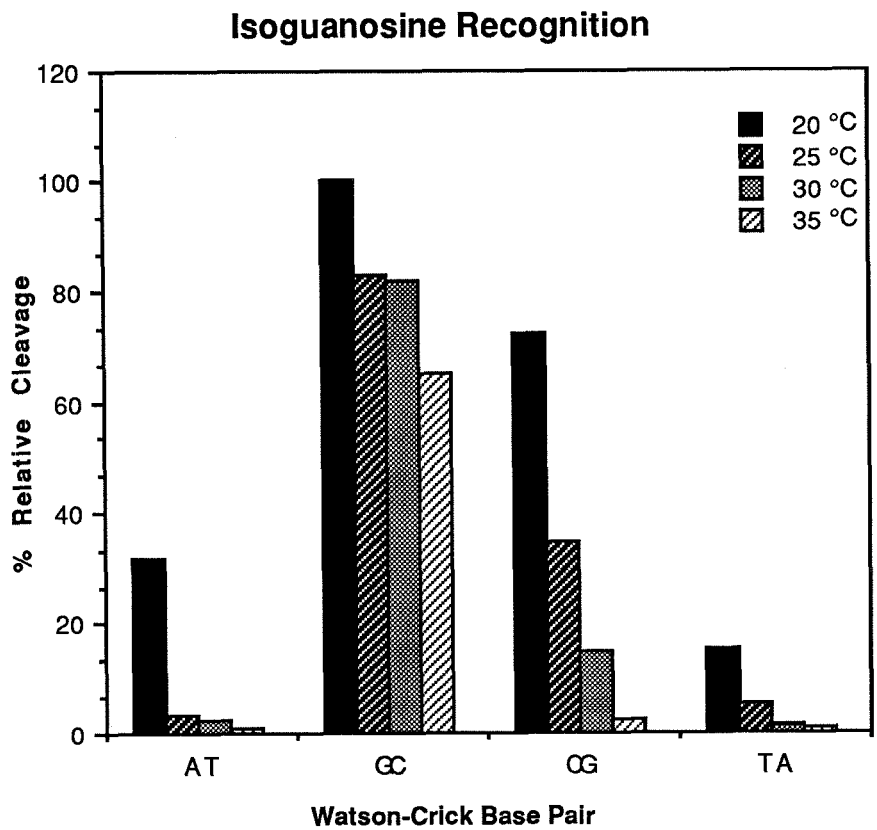

Figure 8b. Bar graph representing the relative cleavage data from densitometric analysis of Fig. 8a. Sixteen base triplets were examined for binding specificity compatible with the pyrimidine triple helix motif shown by the experiment described in Fig. 8a.

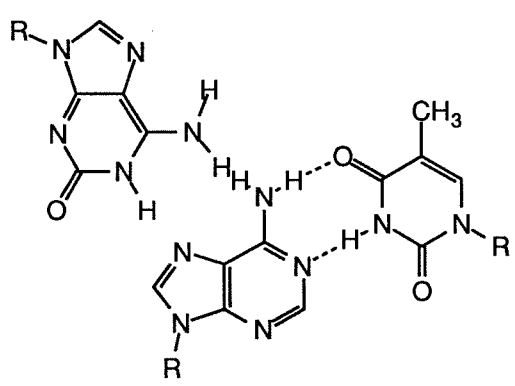

G'•AT

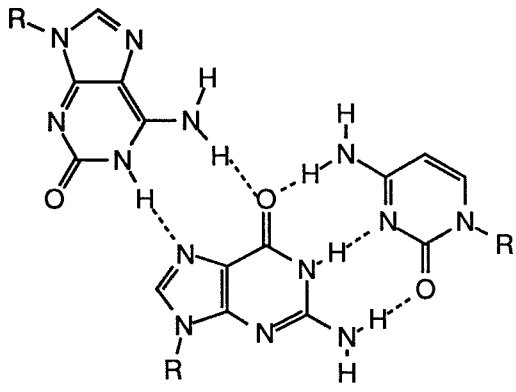

G'•GC

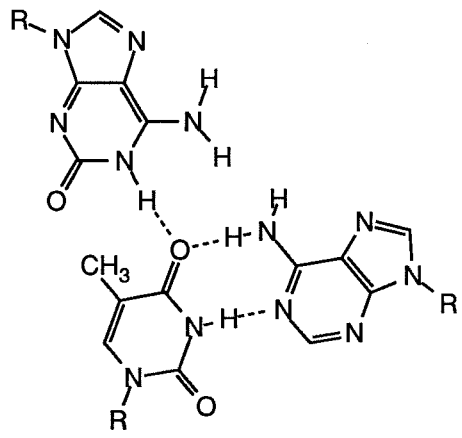

G'•TA

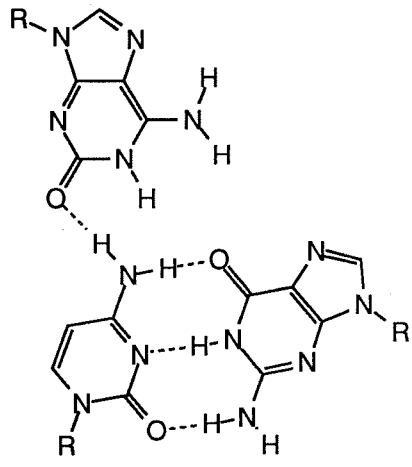

G'•CG

Figure 8c. Possible base triplets G'•AT, G'•GC, G'•CG, G'•TA. For each base triplet the positioning of the third base with respect to the Watson-Crick base pair is based upon forming possible hydrogen bonds, and an anti- confomation at the glycosidic link.

Figure 9a. Autoradiogram of the 20 percent denaturing polyacrylamide gel. The cleavage reactions were carried out by combining a mixture of oligonucleotide-EDTA (2 μM), spermine (1 mM), and Fe(II) (25 μM) with the ^{32}P labeled 30-mer duplex (40,000 cpm) in a solution of tris-acetate (50 mM pH 7.4), NaCl (100 mM), calf thymus DNA (100 μM bp), and 40% ethanol and incubated at 20°C, 25°C, 30°C, and 35°C for 1 hour. Cleaving reactions were initiated by the addition of DTT (3.3 mM) and allowed to proceed for 6 h at each temperature. The reactions were stopped by freezing and lyopholization and the cleavage products were analyzed by gel electrophoresis (1,500-2,000V, BPB 25 cm). Lanes 1 to 18: duplex containing 5' end-labeled ($A_5T_7YT_7G_{10}$). Lane 1: control showing intact 5' labeled 30 bp DNA standard obtained after treatment according to the cleavage reaction in the absence of oligonucleotide-EDTA. Lane 2: products of Maxam-Gilbert G+A sequnce reaction. Lanes 3 to 18: DNA cleavage products produced by oligonucleotide-EDTA•Fe(II) (**20**, **22**-**24**); **20** (lanes 3 to 6); **22** (lanes 7 to 10); **23** (lanes 11 to 14); **24** (lanes 15 to 18). XY=AT (lanes 3,7,11,and 15); XY=GC (lanes 4, 8, 12, and 16); XY=CG (lanes 5, 9, 13, and 17); XY=TA (lanes 6, 10, 14, and 18).

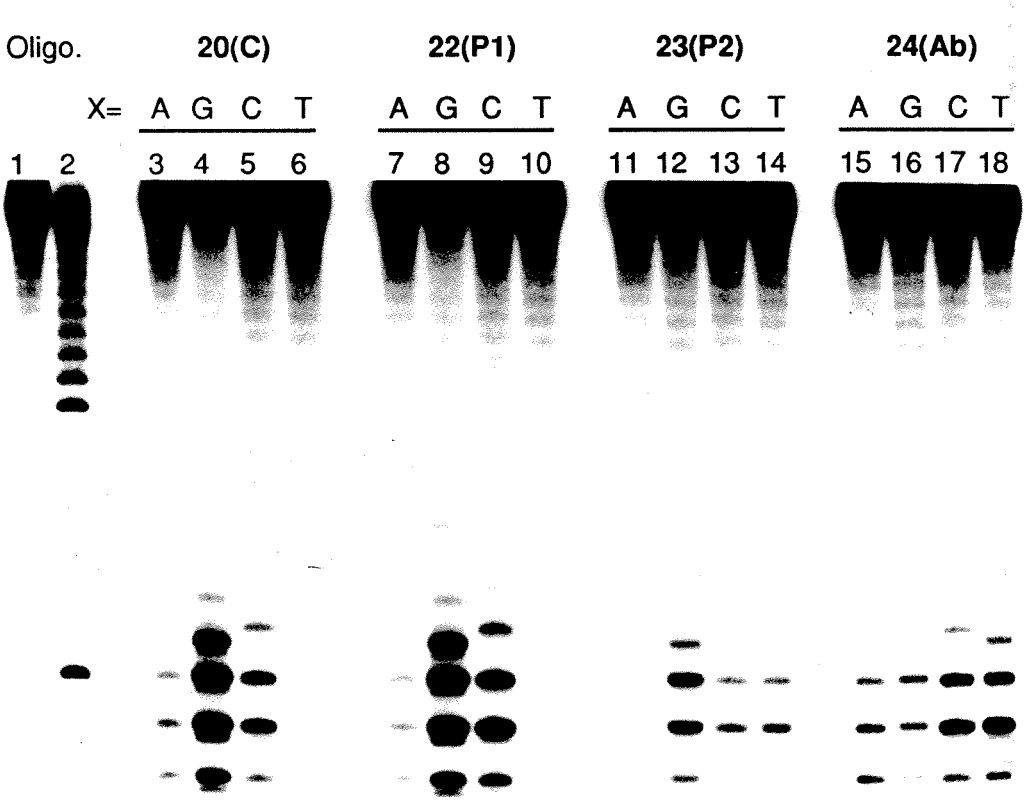
Oligo.
20(C)
22(P1)
23(P2)
24(Ab)
X= A G C T A G C T A G C T A G C T
1 2 3 4 5 6 7 8 9 10 11 12 13 14 15 16 17 18

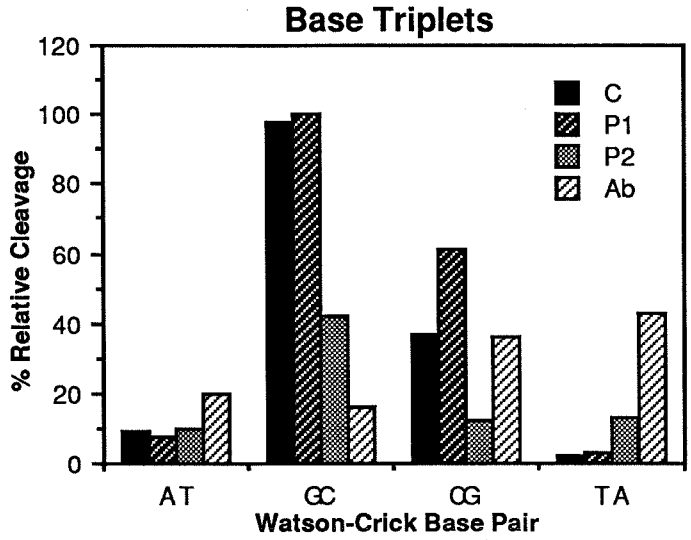

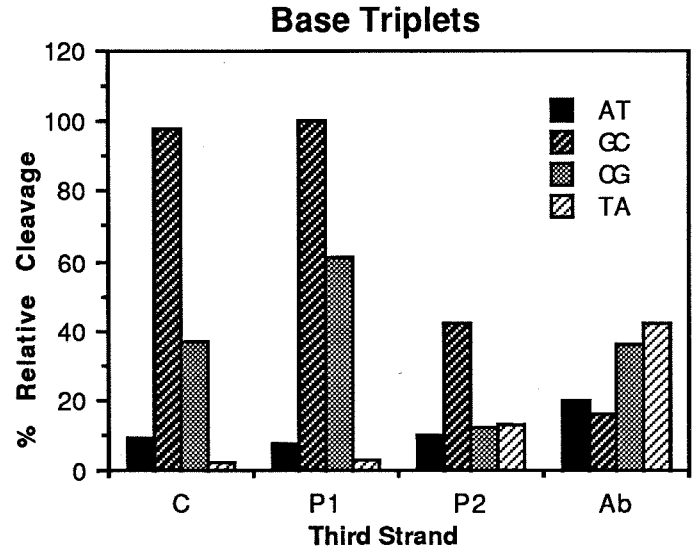

Figure 9b. Bar graph representing the relative cleavage data from densitometric analysis of Fig. 9a. Sixteen base triplets were examined for binding specificity compatible with the pyrimidine triple helix motif shown by the experiment described in Fig. 9a.

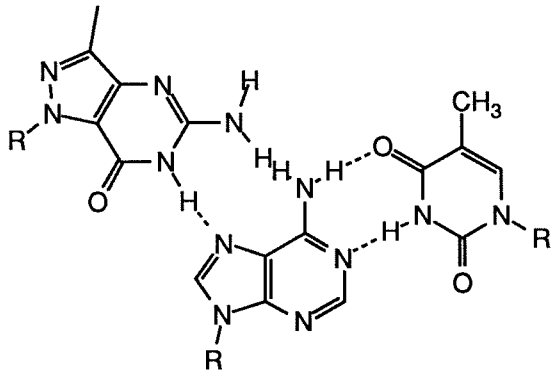

P1•AT

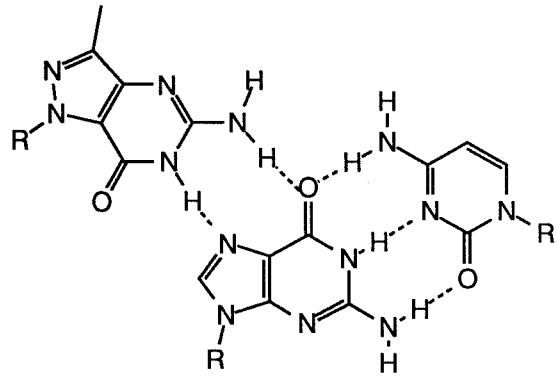

P1•GC

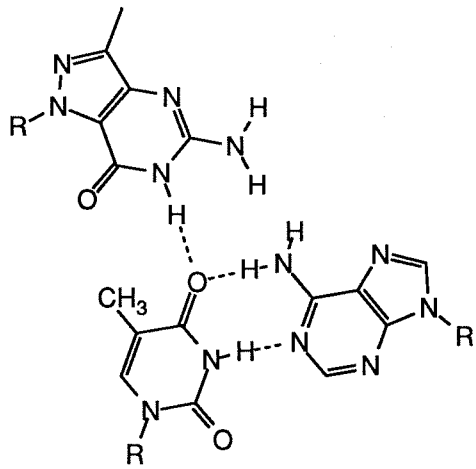

P1•TA

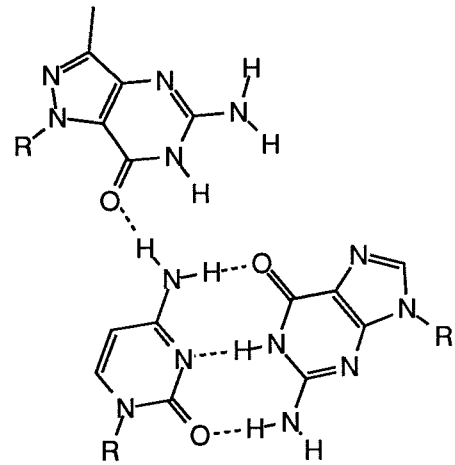

P1•CG

Figure 9c. Possible base triplets P1•AT, P1•GC, P1•CG, P1•TA. For each base triplet the positioning of the third base with respect to the Watson-Crick base pair is based upon forming possible hydrogen bonds, and an anti- confomation at the glycosidic link.

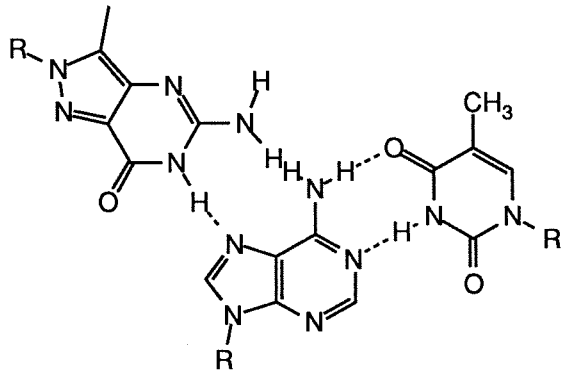

P2•AT

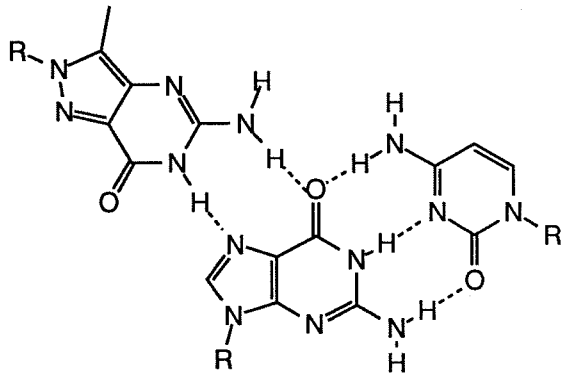

P2•GC

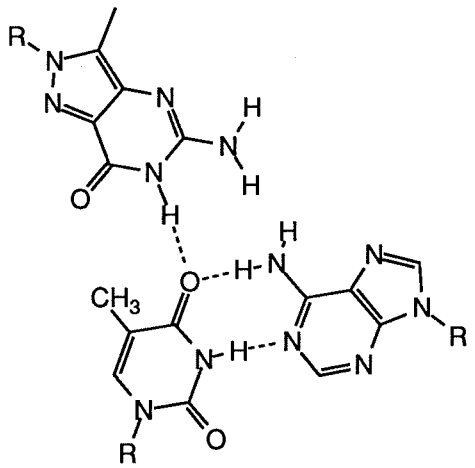

P2•TA

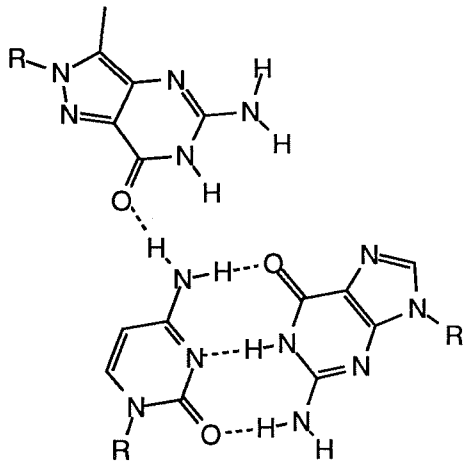

P2•CG

Figure 9d. Possible base triplets P2•AT, P2•GC, P2•CG, P2•TA. For each base triplet the positioning of the third base with respect to the Watson-Crick base pair is based upon forming possible hydrogen bonds, and an anti- confomation at the glycosidic link.

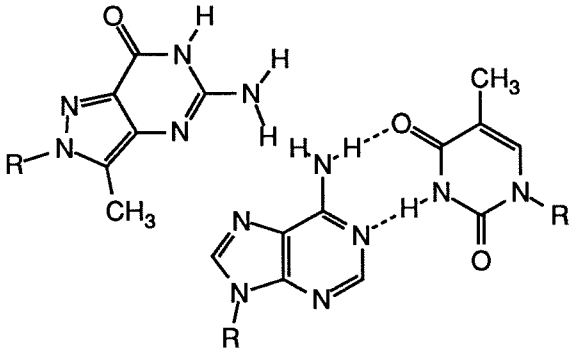

P2•AT

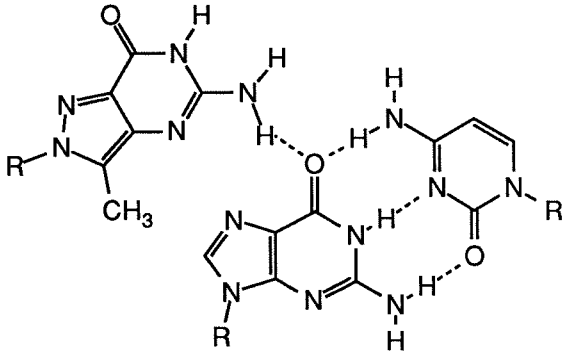

P2•GC

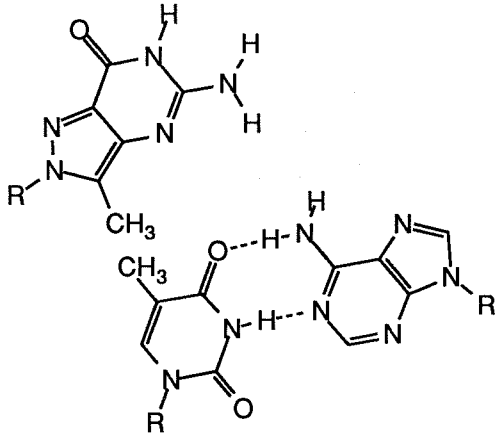

P2•TA

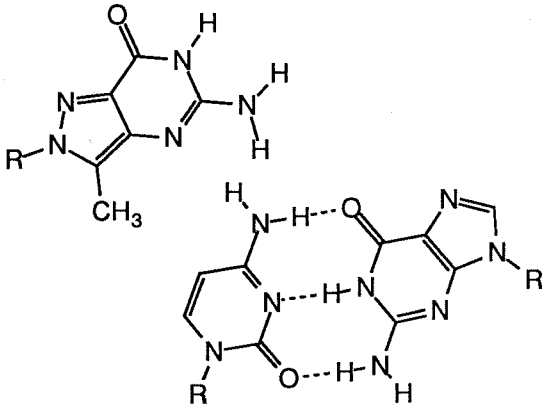

P2•CG

Figure 9e. Possible base triplets P2•AT, P2•GC, P2•CG, P2•TA. For each base triplet the positioning of the third base with respect to the Watson-Crick base pair is based upon forming possible hydrogen bonds, and a syn-confomation at the glycosidic link.

P2•GC suggests that the position of the backbone in P2•GC is not appropriate or that the methyl group disfavors the anti conformation of base P2 (Figures 9c, d, and e).

Site-specific double strand cleavage of pDMAG10 DNA. The ability of oligonuceotides **25-28** to execute site-specific double strand breaks in pDMAG10 is documented in Figure 10a. The plasmid was linearized with StyI and labeled with α-^{32}P-dTTP, producing a 4.06 kb restriction fragment specifically labeled 1.02kb from the target sequence d(AAAAAGAGAGAGAGA). The ^{32}P-end-labeled DNA was allowed to react with oligonucleotide-EDTA•Fe(II) in the presence of DTT at various pH's at 25°C. The separation of the cleavage products by agarose gel electrophoresis revealed one major cleavage site. The cleavage efficiency of oligonucleotide **25** containing C and T decreases sharply above pH 7.0. Replacement of C with mC (oligonucleotide **26**) extended the stability of triple helix formation to pH 7.4, but not to pH 7.8. Incorporation of P1 in place of C (oligonucleotide **27**) afforded the same cleavage efficiency as C and mC below pH 7.0, and extended the pH range to pH 7.8 for binding of the target (Figure 10b). Despite apparent GC recognition by P2 in the previous experiment, oligonucleotide **28** showed no cleavage even at lower pH (Figure 10 b).

Site-specific double strand cleavage of pHIV-CAT Plasmid DNA. The ability of oligonucleotides **29-31** to cause site-specific double strand breaks in HIV-CAT plasmid DNA is documented in Figure 11a. pHIV-CAT was digested with BamHI to produce a 4.95-kbp fragment, which contained the 3' LTR of HIV with the site d(AAAAGAAAAGGGGGGA) located 1.72 kbp and 3.23 kbp from the ends. The ^{32}P end-labeled DNA was allowed to react with oligonucleotide-EDTA•Fe(II) in the presence of ascorbate at 30°C (pH 6.2 to 7.0).

5'-T* T T T T T C T C T C T C T C T - 3' **25**

5'-T* T T T T T C^m T C^m T C^m T C^m T C^m T - 3' **26**

5'-T* T T T T T P1 T P1 T P1 T P1 T P1 T - 3' **27**

5'-T* T T T T T P2 T P2 T P2 T P2 T P2 T - 3' **28**

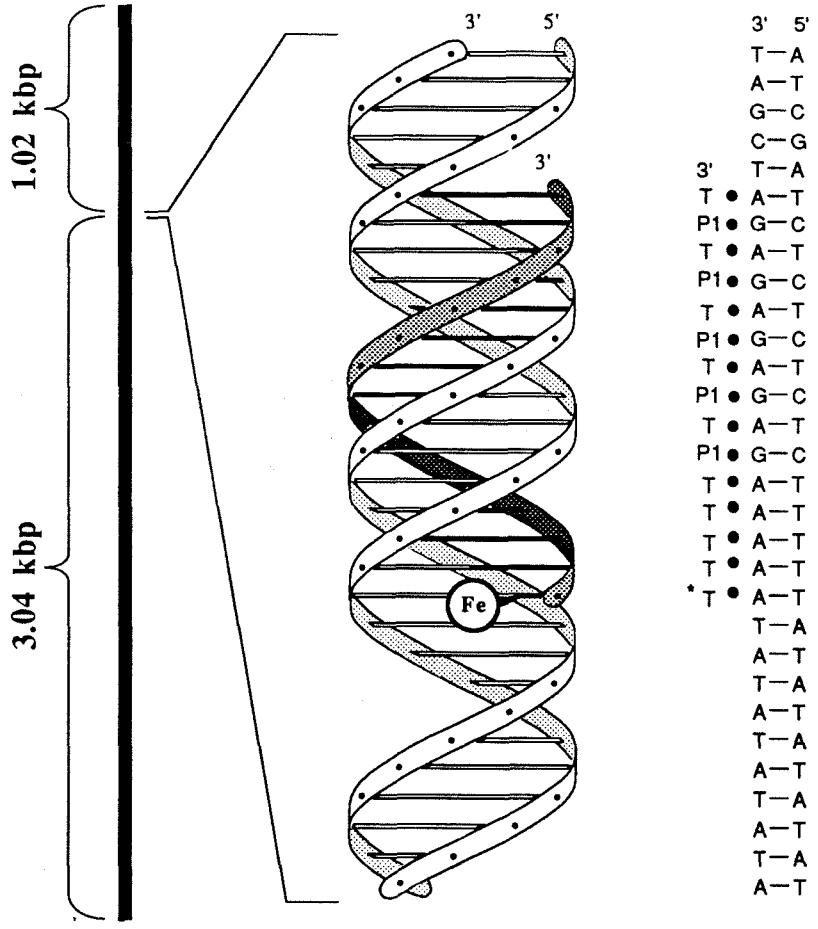

Figure 10a. (**Top**) Oligonucleotides **25-28** constructed from deoxyribonucleotide phosphoramidites containing cytosine (C), 5-methylcytosine mC), thymidine, P1, P2 and thymidine-EDTA (T*). (**Bottom**) Coarse resolution pattern for cleavage of plasmid DNA (4.06 kbp) by oligonucleotides-EDTA **25-28** with a simplified model of the triple helical complex between oligonucleotide **27** (T/P1) and a 15 base pair single site.

Figure 10b. Double strand cleavage of plasmid DNA analyzed on a 0.9% agarose gel. Plasmid pDMAG10 was linearized with StyI and labeled with (α-^{32}P)TTP, producing a 4.06 kbp restriction fragment. The 3' ^{32}P-end-labeled DNA was dissolved in a buffer containing NaCl, Tris, and spermine and was mixed with oligonucleotide **25-28** previously equilibrated for 30 minutes with 1.5 equiv. of Fe(II). After incubation at 25°C for 30 minutes, the reaction was initiated by the addition of DTT (final concentration: 25 mM tris-acetate, 1 mM spermine,100 mM NaCl, 100 μM calf thymus, 2 μM oligonucleotide-EDTA•Fe(II), and 2.5 mM DTT). The cleavage reactions were allowed to proceed for 6 h at 25°C. The reactions were stopped by precipitation with ethanol and the cleavage products were analyzed by gel electrophoresis. (**Top**) Lane 1: DNA size markers obtained by digestion of StyI linear pDMAG10 with EcoRI (1060 bp), BamHI (998), Asp700 (1460),and PstI (1814); (lane 2) control containing no oligonucleotide-EDTA•Fe(II); (lanes 3 to 5) **25**•Fe(II); (lanes 6 to 8) **28**•Fe(II); (lanes 9 to 11) **27**•Fe(II). (Lanes 3, 6 and 9) at pH 6.2; (lanes 4, 7, and 10) at pH 7.0; (lanes 5, 8 and 11) at pH 7.8. (**Bottom**) (Lane 1) DNA size markers as above. Lane 2: control containing no oligonucleotide-EDTA•Fe(II); (lanes 3 to 5) **26**• Fe(II); (lanes 6 to 8) **27**•Fe(II).Lanes 3 and 6: at pH 7.0; (lanes 4 and 7) pH 7.4; (lanes 5 and 8) at pH7.8.

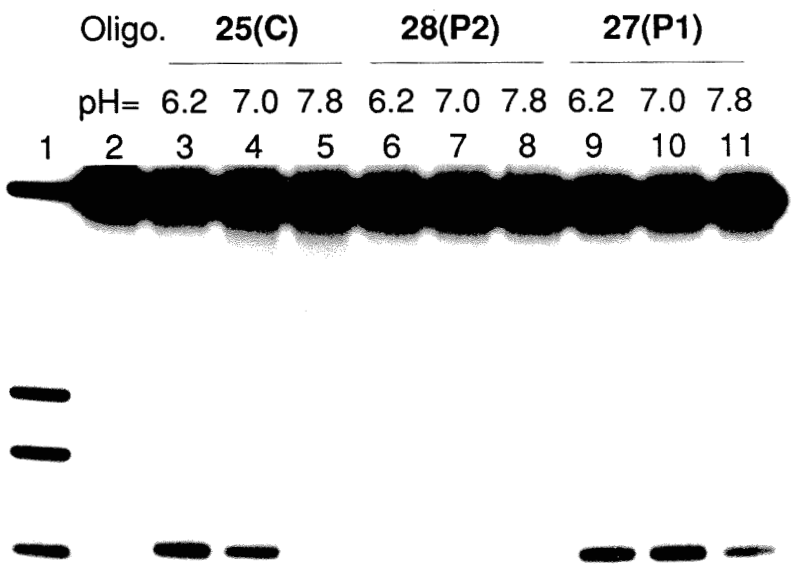
Oligo. 25(C) 28(P2) 27(P1)
pH= 6.2 7.0 7.8 6.2 7.0 7.8 6.2 7.0 7.8
1 2 3 4 5 6 7 8 9 10 11

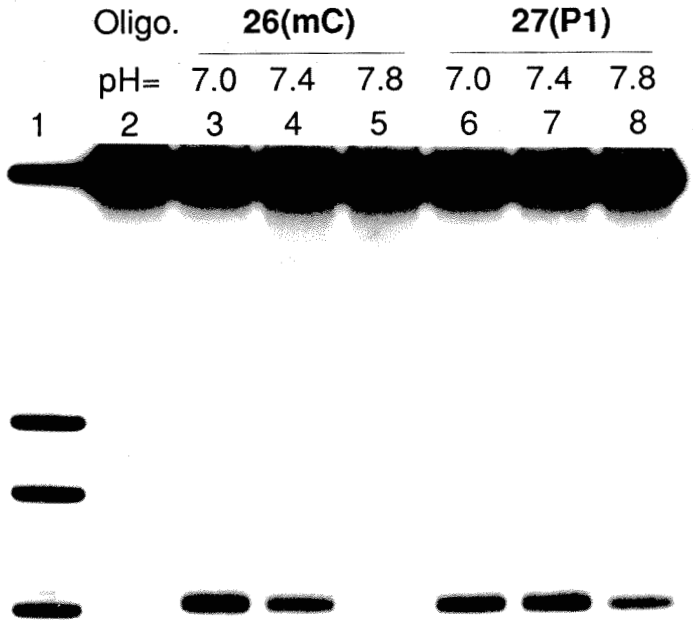
Oligo. 26(mC) 27(P1)
pH= 7.0 7.4 7.8 7.0 7.4 7.8
1 2 3 4 5 6 7 8

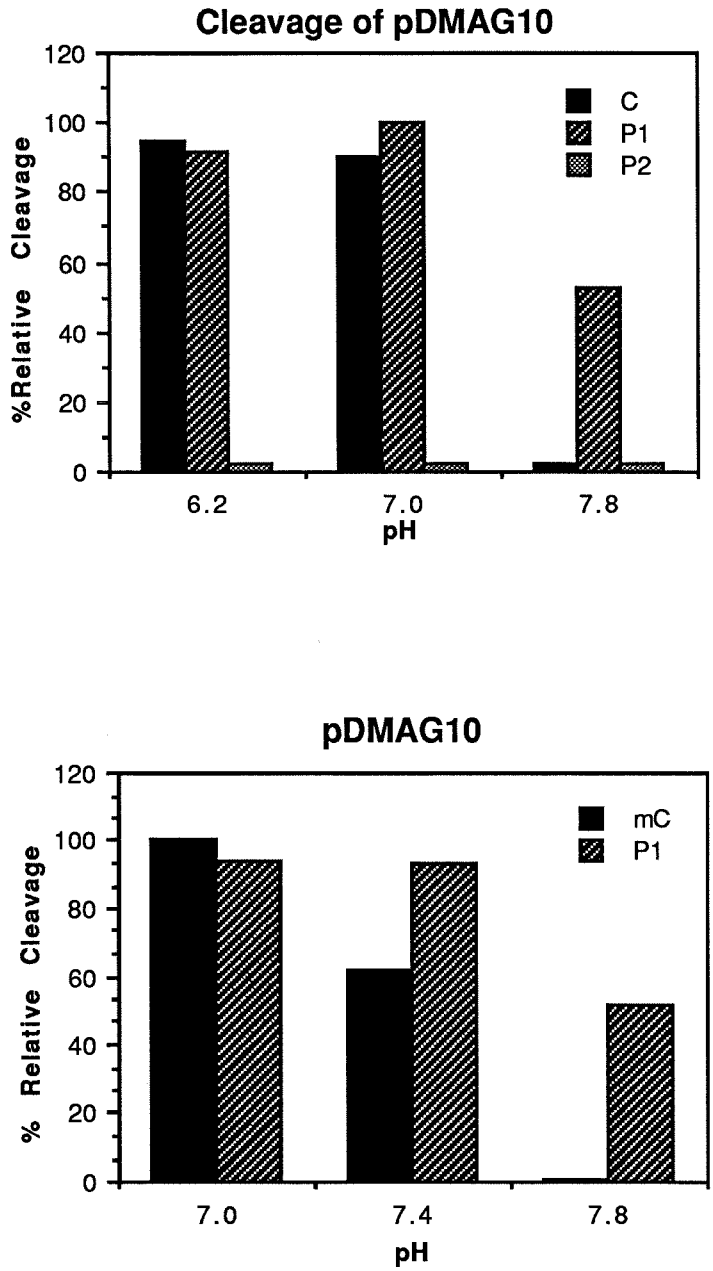

Figure 10c. Bar graph presenting the reaction cleavage data from the densitometric analysis of Fig. 10b (Top and Bottom).

Separation of cleavage products by agarose gel electrophoresis revealed a major cleavage site producing two DNA fragments, 1.72 and 3.23 kb in size (Figure 11b). Cleavage efficiency by oligonucleotides **29** and **30** was very sensitive to the pH and no cleavage was observed above pH 6.6 (Figure 11c). Interestingly, 5-methylcytosine did not extend the pH range for this target sequence. However, oligonucleotide **31** cleaved double-stranded DNA up to pH 7.4 at 30°C. The temperature dependence of cleavage by oligonucleotide-EDTA-Fe(II) **31** at pH 7.0 is shown in Figures 11d. These data suggest that the 16 nt oligonucleotide **31** can bind the HIV-LTR at physiological temperature and pH (37°C, pH 7.0).

5' T* T T T T C T T T T T C C C C C C T 29

5' T* T T T T C T T T T T C^m C^m C^m C^m C^m C^m T 30

5' T* T T T T C T T T T T P_1 P_1 P_1 P_1 P_1 P_1 T 31

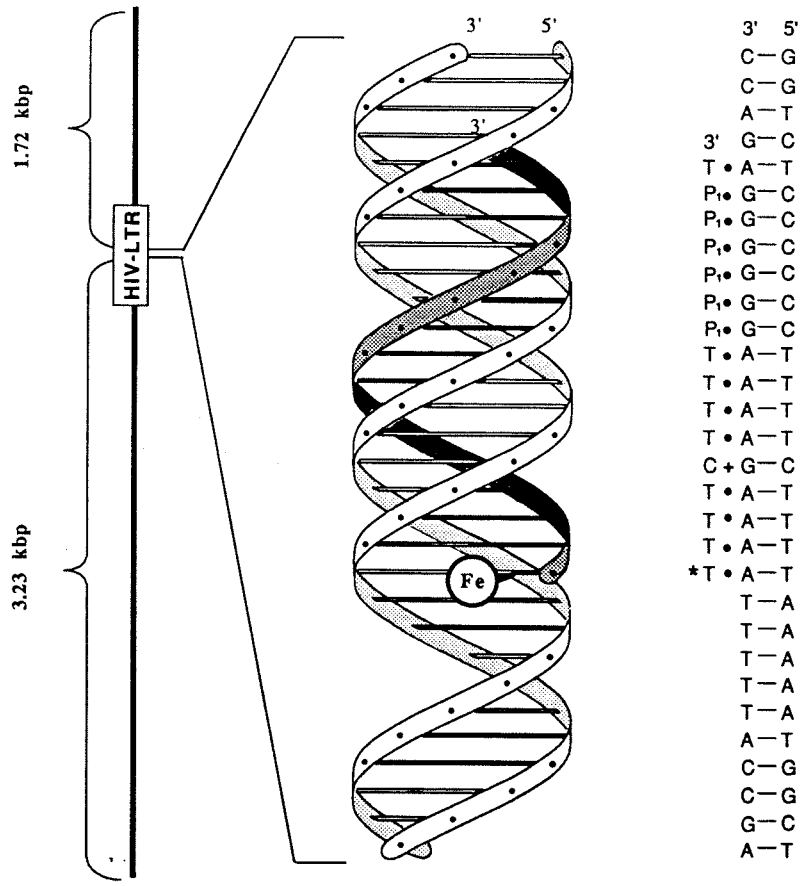

Figure 11a. (**Top**) Oligonucleotides **29-31** constructed from deoxyribonucleotide phosphoramidites containing cytosine (C), 5-methylcytosine (mC), thymidine, P1 and thymidine-EDTA (T*). (**Bottom**) Coarse resolution pattern for cleavage of plasmid DNA (4.95 kbp) by oligonucleotides-EDTA **29-31** with a simplified model of the triple helical complex between olgonucleotide **31** (T/P1) and a 16 base pair single site.

Figure 11b Autoradiogram of double strand cleavage of pHIV-CAT DNA (4.95 kbp) analyzed on a 0.9% agarose gel. The reactions were carried out by combining a mixture of oligonucleotide-EDTA **29-31** (2 μM), spermine (1 mM), and Fe(II) (2 μM) with the ^{32}P-labeled linearized plasmid [~100 μM(bp) (~40,000 cpm)] in a solution of Tris-acetate (25 mM), NaCl(100 mM), Calf thymus DNA [100 μM (bp)] and incubated for 1 hour at the reaction temperature. Cleavage reactions were initiated by the addition of ascobate (1 mM) and allowed to proceed for 10 h at 30°C. The reactions were stopped by precipitation with ethanol and the cleavage products were analyzed by agarose gel electophoresis. Lanes 1 to 8: pHIV-CAT linearized with Bam HI and 3'-end labeled at both ends. Lane 1: control containing no oligonucleotide-EDTA•Fe(II); (lane 2) DNA size markers obtained by digestion of BamHI linearized pHIV-CAT with HindIII and XhoI: 4950 (undigested), 3725, 3003, 1947, 1225 bp; (lanes 3 to 6) DNA cleavage products produced by **29**•Fe(II); (lanes 7 to 10) DNA cleavage products produced by **30**•Fe(II); (lanes 11 to 14) DNA cleavage products produced by **31**•Fe(II). (Lanes 3, 7 and 11) at pH 6.2; (lanes 4, 8 and 12) at pH 6.6; (lanes 5, 9 and 13) at pH 7.0; (lanes 6, 10 and 14) at pH 7.4.

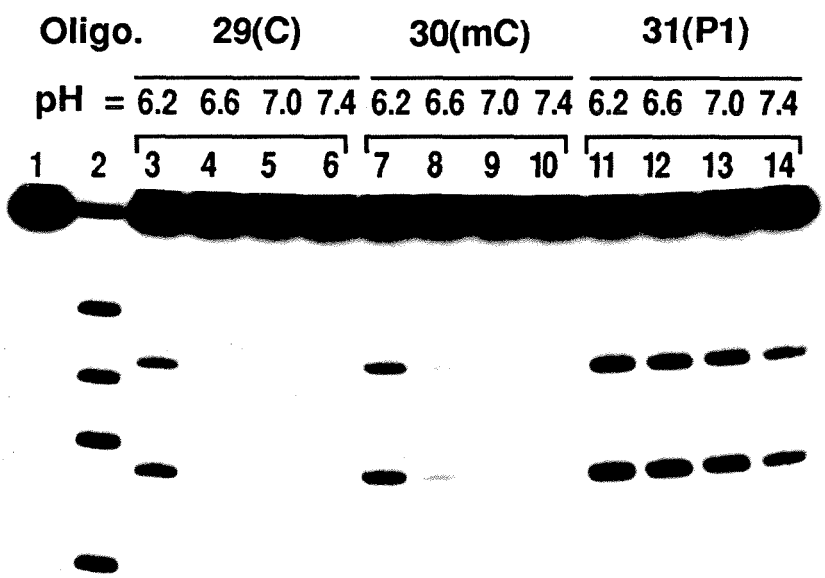
Oligo.
29(C)
30(mC)
31(P1)
pH = 6.2 6.6 7.0 7.4 6.2 6.6 7.0 7.4 6.2 6.6 7.0 7.4
1 2 3 4 5 6 7 8 9 10 11 12 13 14

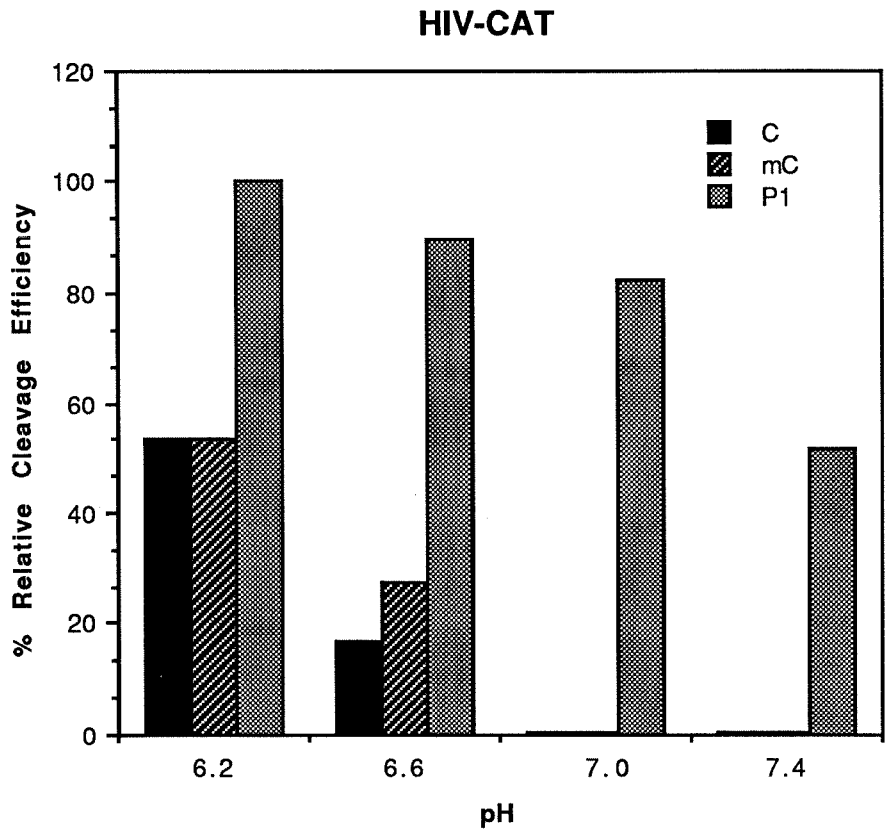

Figure 11c. Bar graph presenting the relative cleavage data from the densitometric analysis of Figure 11b.

Figure 11d. Autoradiogram of double strand cleavage of pHIV-CAT DNA (4.95 kbp) analyzed on a 0.9% agarose gel. The reactions were carried out by combining a mixture of oligonucleotide-EDTA **31** (2 μM), spermine (1 mM), and Fe(II) (2μM) with the ^{32}P-labeled linearized plasmid [~100 nM (bp) (~40,000 cpm)] in a solution of Tris-acetate (25 mM, pH 7.0), NaCl (100 mM), calf thymus DNA [100 μM (bp)] and incubated for 1 hour at the reaction temperature. Cleavage reactions were initiated by addition of ascorbate(1 mM) and allowed to proceed for 10 h at the reaction temprature. The reactions were stopped by precipitation with ethanol and the cleavage products were analyzed by agarose gel electophoresis. Lanes 1 to 5: pHIV-CAT linearized with Bam HI and 3'-end labeled at both ends. Lane 1: control containing no oligonucleotide-EDTA•Fe(II); (lane 2) DNA size markers obtained by digestion of BamHI linearized pHIV-CAT with HindIII and XhoI: 4950 (undigested), 3725, 3003, 1947, 1225 bp; (lane 3) DNA cleavage products produced by **31**•Fe(II) at 25°C; (lane 4) DNA cleavage products produced by **31**•Fe(II) at 30°C; (lane 5) DNA cleavage products produced by **31**•Fe(II) at 37°C.

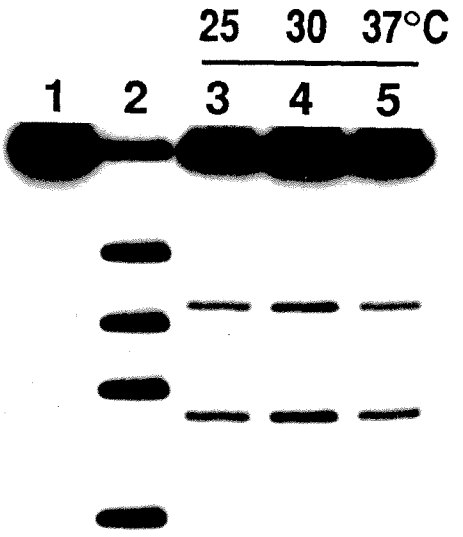
25 30 37°C
1 2 3 4 5

Conclusions

The novel bases isoguanosine (**G'**) and the two 3-methyl-5-amino-pyrazolo(4, 3-d)pyrimidine-7-ones, **P1** and **P2**, enable the selective binding and cleavage of a target site containing GC base pairs by triple helix formation. The utility of isoguanosine (**G'**) in oligonucleotide synthesis has limitations due to its instability in the conditions of automated synthesis. It is possible that the benzoyl protected isoguanosine base may be depurinated during the deprotection of DMT by trichloroacetic acid. P1 and P2 are stable under the conditions of automated synthesis, and P1 can be used to substitute for any cytosine base in oligonucleotides used for triple helix formation. Replacement of C with P1 in a $dT^*T_4(CT)_5$ (T*=thymidine-EDTA) probe extended the pH range for binding to pH 7.8 for the plasmid containing the $dA_5(GA)_5$ site. Although P2 has the same hydrogen bond donor groups as P1, its ability to recognize GC is weak. One possible explanation for this weak binding is that the backbone position is positioned inappropriately. Another explanation is that the 5-methyl group of P2 disfavors the *anti* conformation of P2 nucleotides as an 8-bromo substituent on guanosine does. Oligonucleotide $dT^*T_4(P2T)_5$-EDTA-Fe(II) (**28**) does not appreciably cleave its target site at pH values between 6.2 and 7.8, suggesting that unfavorable interactions within the 15 nt site disfavor triple helix formation. The HIV-DNA data suggested that triple helix formation with oligonucleotides containing consecutive cytosines or 5-methylcytosines is very sensitive to pH. Although 5-methylcytosine extended the pH range of triple helix formation for the plasmid containing $dA_5(GA)_5$ site, no pH extention was observed in HIV-DNA containing the $dA_4GA_4G_6A$ site. It has been suggested that the presence of hydrogen bonding can raise the pK_a

at N3 of cytosine. For a (CT)n sequence in a third strand, thymidine next to cytosine can facilitate the binding, and raise the pK_as of N3 of cytosine and 5-methylcytosine, respectively. However, for a (C)n sequence in a third strand, protonation of consecutive cytosines may result in charge repulsion that disfavors protonation. Oligonucleotide **31,** containing P1, shows less pH sensitivity in triple helix formation than its cytosine or 5-methylcytosine analogs. It is able to bind the sequence $dA_4GA_4G_6A$ in HIV DNA at pH 7.4, 30°C. Presumably, the base P1 does not require protonation to form 2 hydrogen bonds in triple helix formation. The pDMAG10 and HIV DNA data suggest that the P1 base can be put at any cytosine position in the third strand to achieve pH- independent triple helix formation.

Experimental and Materials

Synthesis. ^{1}NMR spectra were recorded at 400 MHz on a JEOL-GX 400 NMR spectrometer. The NOE spectra were measured in $CDCl_3$ after degassing in a freeze-thaw cycle vacuum line. Chemical shifts are reported in parts-per-million downfield from tetramethylsilane. IR spectra were recorded on a Shimadzu IR-435 Infrared Spectrometer. High resolution Fast Atom Bombardment Mass Spectra (FABMS) and EI mass spectra were obtained at the University of Nebraska, Lincoln, and the Mass Spectra Lab at the University of California, Riverside. Flash chromatography was carried out under positive air pressure using EM science Kieselgel 60 (230-400 mesh). Elemental analyses were performed by the analytical lab at Caltech. Reagent grade chemicals were used as received, except for diisopropylethylamine, which was distilled from CaH_2. A Beckman System1 Plus DNA synthesizer was utilized for the synthesis of oligonucleotides. Concentrations of oligonucleotides were determined by UV using a Perkin-Elmer Lambda 4C UV-VIS spectrometer. Analytical HPLC was performed with a Hewlett-Packard 1090 Liquid Chromatograph. Analytical reverse phase HPLC was performed on a BrownLee Labs Aquapore OD-300 4.6 mm x 22 cm 7 micron C18 column using no precolumn. Densitometry was performed by an LKB Ultrascan XL laser densitometer and scintilation counting was performed by a Beckman LS 3801 scintillation counter. All enzymes for DNA manipulation were purchased from Boehringer Mannheim or New England Bio Lab.

5-amino-1-[3,5-O-(1,1,3,3-tetraisopropyldisiloxanyl)-β-D-ribofuranosyl]-imidazole-4-carboxamide (**2**). To a solution of 5-amino-1-β-D-ribofuranosylimidazol-4-carboxamide (**1**, 5.16 g, 20mmol) in pyridine (50

mL) was added 1,3-dichloro-1,1,3,3-tetraisopropyldisiloxane (6.9 g, 22 mmol) and the mixture was stirred under argon at room temperature for 3 h. Water (50 mL) was added to the solution and the mixture was extracted with three 100 mL portions of ethyl acetate. Concentration of the dried (Na_2SO_4) solution gave a syrup, which was purified over a silica gel column using ethyl acetate to give desired product **2** (Rf= 0.45 in chloroform:ethyl acetate (1:1 v/v) (7.9 g, 79%). IR (KBr), 3450,3400, 3380, 3300, 2900, 2880, 1650, 1570, 1470, 1270, 1230 cm^{-1}. ^{1}NMR (DMSO-d_6) δ 7.21 (s, 1H), δ 6.74 (s, 1H), δ 6.64 (s, 1H), δ 5.80 (s, 2H), δ 5.61 (d, 1H, J=4.12, 2'hydroxy), δ 5.52 (s, 1H), δ 4.30 (m, 1H), δ 3.80-4.20 (m, 4H), δ 0.90-1.04 (m, 28H), EIMS calcd. for $C_{21}H_{40}N_4O_6Si_2$ (M+) 500.2486. Found 500.2473.

5-amino-1-[3,5-O-(1,1,3,3-tetraisopropyldisiloxanyl-2-O-phenoxythiocarbonyl)-β-D-ribofuranosyl]imidazol-carboxamide (3) Compound **2** (6.8 g, 13.6 mmol), phenoxythiocarbonyl chloride (3.74g, 21.6 mmol), N, N-dimethylaminopyridine (10.4 g, 86.4 mmol) were dissolved in acetonitrile (300 mL). The mixture was stirred for 3 h at room temperature under nitrogen atmosphere and then poured onto ice water (ca 200 g). The mixture was extracted with 500 mL portions of chloroform. The organic layer was washed with water (500 mL), dried over Na_2SO_4, and concentrated *in vacuo* to give a crude sample of **3**, which was chromatographed over a silica gel column with chloroform/ethyl acetate (50:50 v/v Rf= 0.74) as the eluent to give **3** (4.23 g, 49 %). IR (KBr), 3300, 2900, 2880, 1650, 1574, 1470, 1270, 1180 cm^{-1}. ^{1}NMR (DMSO-d_6) δ 7.36 (t, 2H, J=8.23, phenoxy), δ 7.27 (m, 2H), δ 7.16 (d, 2H, J=8.23, phenoxy), δ 6.74 (s, 1H), δ 6.64 (s, 1H), δ 6.07 (d, 1H, J=6.98, H1'),δ 5.94 (m, 2H), δ 4.72 (m, 1H), δ 4.12 (m, 1H), δ 3.98 (m, 2H), δ 0.90-1.04 (m, 28H), EIMS calcd. for $C_{28}H_{44}N_4O_7SSi_2$ (M+) 636.2469. Found 636.2468.

5-amino-1-[3,5-O-(1,1,3,3-tetraisopropylsiloxanyl)-β-D-deoxyribofuranosyl]imidazole-4-carboxamide (**4**). To a refluxing solution of **3** (4.0 g, 6.28 mmol) and a catalytic amount of 2',2'-azobis(2-methylpropionitrile) in toluene (100 mL) was added n-Bu_3SnH (10 mL) and the mixture was refluxed for 30 minutes under nitrogen. The solvent was evaporated *in vacuo* to give yellow syrup, which was purified with a silica gel column using chloroform/ethylacetate (50:50, v/v Rf=0.44) to give a white product (2.07 g, 4.29 mmol Y=68%). IR (KBr), 3310, 2940, 2850, 1614, 1550, 1470, 1135, 1120 cm^{-1}. ^{1}NMR(DMSO-d_6) δ 7.23 (s, 1H), δ 6.74 (s, 1H), δ 6.65 (s, 1H), δ 6.07 (d, 1H, J=5.76, H1'),δ 5.83 (m, 3H), δ 4.60 (m, 1H), δ 3.90 (m, 2H), δ 3.76 m, 1H), δ 2.27 (m, 1H), δ2.21 (m, 1H), δ 0.90-1.04 (m, 28H), EIMS calcd. for $C_{21}H_{40}N_4O_5Si_2$ (M+) 484.2537. Found 484.2528.

5-(N1-benzoylcarbamoyl)amino-1-[3,5-O-[1,1,3,3-tetraisopropylsiloxanyl)-β-D-deoxyribofuranosyl]imidazole-4-carbonitrile (**5**). A solution of compound **5** (1.5 g, 3.09 mmol) and benzoylisothiocyanate (628 mg, 3.3 mmol) in DMF (10 mL) was stirred at room temperature for 7 h. To the resulting solution was added N, N'-dicyclohexyl-carbodiimide (DCC) (1.4g, 7.0 mmol) and the mixture was continuously stirred at room temperature for 15 h. The solvent was then removed *in vacuo* (50°C) to an oil residue. The residue was chromatographed on a silica gel column using 14% ethyl acetate in chloroform to afford product **5** (1.2 g, 65%). IR (KBr), 3200, 2950, 2930, 2250, 1700,1670, 1570, 1250, 1030, 850 cm^{-1} . ^{1}NMR (DMSO-d_6) δ 11.46 (s, 1H), δ 10.58 (s, 1H), δ 8.03 (d, 2H, J=6.96, benzoyl), δ 8.00 (s, 1H), δ 7.69 (t, 1H, J=6.96, benzoyl), δ 7.55 (m, 2H), δ 6.01 (t, 1H, J=3.30, H1'),δ 4.54 (m, 1H), δ 3.93 (m, 2H), δ 3.76 (m, 1H), δ 2.64 (m, H), δ 2.43 (m, 1H), δ 0.90-1.04 (m, 28H), EIMS calcd. for $C_{29}H_{43}N_5O_6Si_2$ (M+) 613.2779. Found 613.2749.

3,5-O-(1,1,3,3-tetraisopropylsiloxanyl)deoxyriboisoguanosine(6). Compound **5** (1.2 g, 1.95 mmol) was suspended in a mixture of ethanol (20 mL) and 33% aqueous ammonia (20 mL) in a round bottom flask. The flask was well tightened with a rubber stopper, and the mixture was stirred for 72 h at 10°C. After 72 h, the ammonia was removed *in vacuo* at room temperature and a white solid was collected by filteration to give **6** (530 mg, 1.027 mmol, Y=52.6%). IR (KBr) 3100, 2950, 1670, 1620, 1530, 1470, 1410 cm^{-1}. ^{1}NMR (DMSO-d_6) δ 7.80 (s, 2H), δ 6.04 (t, 1H, J=4.23, H1'),δ 4.79 (m, 1H), δ 3.82 (m, 2H), δ 3.75 (m, 1H), δ 2.63 (m, H), δ2 .42 (m, 1H), δ 0.90-1.04 (m, 28H), FABMS calcd. for $C_{22}H_{39}N_5O_5Si_2Li$ (M+Li) 516.2649. Found 516.2625.

6-N,N-dibenzoyl-2-O-benzoyl-7-[3,5-O-(1,1,3,3-tetraisopropylsiloxanyl)-deoxyribofuranosyl]-isoguanosine (7). To a solution of compound **6** (700 mg, 1.35 mmol) in pyridine (10 mL) was added benzoylchloride (2.37g, 16.27 mmol) and the mixture was stirred for 72 h at 4°C. After 72 h, 5 mL cold water was added to the solution and the mixture was extracted with ethyl acetate. The organic layer was dried over Na_2SO_4 and concentrated *in vacuo* to give residue. The residue was chromatographed on silica gel using 7% ethyl acetate (Rf=0.32) in chloform to give compound **7** (1 g, 1.12 mmol, Y=83%). IR (KBr) 2980, 2930, 1750, 1710, 1600, 1583, 1500, 1230, 1125 cm^{-1}. ^{1}NMR (DMSO-d_6) δ 8.71 (s, 1H), δ8.01 (d, 1H, J=7.32, benzoyl), δ 7.79 (m, 5H), δ7.60 (m, 3H), δ7.43 (m, 5H), δ6.31 (m, 1H),δ5.12 (m, 1H), δ3.70-3.90 (m, 3H), δ2.97 (m, 1H), δ2.61 (m, 1H), δ0.90-1.04 (m, 28H), FABMS calcd. for $C_{43}H_{51}N_5O_8Si_2$ (M+H)+ 885.2832. Found 885.1860.

6-N,N-dibenzoyl-2-O-benzoyl-deoxyriboisoguanosine (8). To a solution of compound **7** (960 mg, 1.08 mmol) in tetrahydrofuran (THF) (50 mL) was added dropwise 1 M tetrabutylammonium fluoride solution in THF (2.3 mL)

at 4°C. The cooling bath was removed and the mixture was stirred for 2 h. After 2 h, water (50 mL) was added and the mixture was extracted with ethylacetate (150 mL). The organic layer was dried over Na_2SO_4 and concentrated under reduced pressure to give a residue. The residue was chromatographed on silica gel using ethyl acetate (Rf=0.33) to give compound **8** (420 mg, 0.74 mmol Y=60.4%) IR (KBr), 3400, 3295, 2980, 1750, 1710, 1600,1582, 1500 cm^{-1}. ^{1}NMR (DMSO-d_6) δ 8.81 (s, 1H), δ8 .03 (d, 2H, J=7.34, benzoyl), δ 7.78 (m, 5H), δ 7.60 (m, 3H), δ 7.45 (m, 5H), δ 6.39 (t, 1H, J=6.23, H1'), δ 5.38 (d, 1H, J=4.35, 3' hydroxy), δ 4,91 (t, 1H, J=5.23, 5' hydroxy), δ 4.40 (m, 1H), δ 3.83 (m, 1H), δ 3.56 (m, 2H), δ 2.72(m, 1H), δ 2.18 (m, 1H), FABMS calcd. for $C_{31}H_{26}N_5O_7$ (M+H)+ 580.1832. Found 580.1860.

6-N,N-dibenzoyl-2-O-benzoyl-7-[5-O-(4,4'-dimethoxytrityl)deoxyribo-fura-nosyl]-isoguanosine (**9**). To a solution of compound **8** (193 mg, 0.33 mmol) in pyridine (3 mL) was added 4,4'-dimethoxytritylchloride (113 mg, 0.33 mmol) and the mixture was stirred under argon for 24 h. After 24 h, ethyl acetate (50 mL) was added and washed with water (50 mL). The organic layer was dried over Na_2SO_4 and concentrated in reduced pressure to afford a yellowish residue. The residue was chromatographed on silica gel using 25% ethyl acetate (Rf=0.6) in chloroform to give compound **9** (230 mg, 0.26 mmol Y=79%). IR (KBr), 3295, 2980, 1750, 1710, 1600, 1580, 1500, 1230, 1120 cm^{-1}. ^{1}NMR (DMSO-d_6) δ 8.20 (s, 1H), δ 7.98 (d, 2H, J=7.34, benzoyl), δ 7.77 (m, 1H), δ 7.70 (d, 4H, J=8.12), δ 7.63 (t, 2H, J=8.12), δ 7.58 (t, 2H, J=8.12),δ 7.48 (m, 4H), δ 7.24 (m, 2H), δ 7.12 (m, 7H), δ 6.75 (d, 2H, J=8.97, methoxyphenyl), δ 6.70 (d, 2H, J=8.96, methoxyphenyl), δ 6.43 (t, 1H, J=5.45, H1'), δ 5.39 (d, 1H, J=4.56, 3' hydroxy), δ 4,41 (m, 1H), δ 3.95 (m, 1H),

δ 3.75 (m, 6H),δ 3.11 (m, 1H), δ 3.05 (m, 1H), δ 2.83 (m, 1H), δ 2.20 (m, 1H), FABMS calcd. for $C_{52}H_{44}N_5O_9$ (M+H)+ 882.3139. Found 882.3137.

Phosphoramidite (10). To a solution of compound **10** (160 mg, 0.19 mmol), N, N-diisopropyl ethylamine (93.7 mg, 0.8 mmol) in dry methylene chloride (3 mL) was added 2-cyanoethyl-N, N-diisopropylamino-chlorophosphoramidite (71 mg, 0.3 mmol). The reaction mixture was stirred for 3 h and ethyl acetate (50 mL) was added. The ethyl acetate solution was washed with sat. sodium bicarbonate solution (50 mL) 2 times and sat. sodium chloride solution (50 mL) 2 times. The organic layer was washed over Na_2SO_4 and concentrated under reduced pressure to give a yellowish residue. The residue was chromatographed on silica gel using methylene chloride: triethylamine: isopropyl alcohol (97:1:2 v/v) solution (Rf=0.65) to afford compound **10** (140 mg, 0.13 mmol). ^{1}NMR (DMSO-d_6) δ 8.21 (d, 1H, J=18.12), δ 8.02 (d, 2H, J=7.46, benzoyl), δ 7.81 (m, 4H), δ 7.60 (m, 1H), δ 7.43 (m, 4H), δ 7.12-7.28 (m, 13H), δ 6.76 (m, 4H), δ 6.43 (t, 1H, J=5.67, H1'), δ 4.64 (m, 1H), δ 4,22 (m, 1H), δ 3.21-3.80 (m, 10H), δ 2.60-2.80 (m, 2H), δ 2.60 (t, 1H, J=5.98, methylene), δ 2.41 (t, 1H, J=5.98, methylene), δ 1.00-1.30 (m, 14H), FABMS calcd. for $C_{61}H_{61}N_7O_{10}P$ (M+H)+ 1082.4217. Found 1082.4268.

1H-Pyrazole-5-carboxylic acid, 1-[2-deoxy-3, 5-bis-O-(4-methylbenzoyl)-β-D-erythro-pentofuranosyl]-3-methyl-4-nitro-, ethyl ester (**13a**) and **1H-Pyrazole-3-carboxylic acid, 1-[2-deoxy-3, 5-bis-O-(4-methylbenzoyl)-β–D-erythro-pentofuranosyl]-5-methyl-4-nitro-, ethyl ester** (**13b**). Ethyl(3-methyl-4-nitropyrazole-carboxlate) (**11**) was prepared by the method of Townsend (32). 1-Chloro-2-deoxy-3,5-di-o-p-toluoyl-α-D-erythro-pentofuranose (**12**) was prepared by Hoffer's method (34). Sodium hydride (60% dispersion in oil, 4.4

g, 1.11 mol) was added to a suspension of **11** (19.9 g, 0.1 mol) in dry CH_3CN (1 L). The mixture was stirred under argon at room temperature for thirty minutes. **12** (42.8 g, 0.11 mol) was added portionwise with stirring over a period of 30 minutes. After stirring under argon at room temperature for an additional hour, the reaction was filtered to remove a small amount of insoluble material and evaporated. Flash chromatography (hexane: ether, 2:1, v/v, TLC, Rf=0.3, 0.45) yielded 25.3 g of **13a** (Rf=0.45) and 24.3 g of **13b** (Rf=0.3). Crystallization from hexane/ether gave pure white needles. **13a** ^{1}NMR ($CDCl_3$) δ 7.96 (d, 2H, J=8.03, toluoyl), δ 7.95 (d, 2H, J=8.03, toluoyl), δ 7.24 (d, 2H, J=8.03, toluoyl), δ 7.19 (d, 2H, J=8.03, toluoyl), δ 6.38 (t, 1H, J=6.72, H1'), δ 5.81 (m, 1H),δ 4.62 (m, 2H),δ 4.20 (m, 3H) δ 3.32 (m, 1H), δ 2.63 (m, 1H), δ 2.40 (s, 6H), δ 2.38 (s, 3H), δ 1.37 (t, 3H, J=6.72, methyl). IR 3000, 1730, 1720, 1610, 1503, 1380, 1250, cm^{-1} EIMS calcd. for $C_{28}H_{29}N_3O_9$ (M+) 551.1903. Found 551.1898. Elemental Analysis calcd. for $C_{28}H_{29}N_3O_9$ C, 60.97; H, 5.30; N, 7.61. Found C, 60.98; H, 5,35; N, 7.63. **13b** ^{1}NMR ($CDCl_3$) δ 7.93 (d, 2H, J=8.06), δ 7.90 (d, 2H, J=8.06), δ 7.22 (d, 2H, J=8.06), δ 7.18 (d, 2H, J=8.06), δ 6.21 (t,1H, J=6.74, H1'), δ 5.26 (m, 1H), δ 4.23-4.62 (m, 5H), δ 3.61 (m, 1H), δ 2.71 (s, 3H), δ 2.65 (m, 1H), δ 2.37 (s, 3H), δ 2.42 (s, 3H) δ 1.32 (t, 3H, J=6.76, methyl). IR 3000, 1735, 1730, 1710, 1618, 1380, 1270, 1130 cm^{-1} EIMS calcd. for $C_{28}H_{29}N_3O_9$ (M+) 551.1903. Found 551.1897. EA calcd. for $C_{28}H_{29}N_3O_9$ C, 60.97; 5.30; N, 7.61. Found C, 60.98; H, 5.32; N, 7.63.

1H-Pyrazole-5-carboxamide,1-(2-deoxy β-D-erythro-pento-furanosyl) -3-methyl-4-nitro-(14a). **13a** (22.04 g, 40 mmol) was stirred in saturated NH_3/ MeOH (500 mL) in a 1 L round bottom flask equipped with a tight stopper at room temperature for 4 h. The mixture was evaporated, and dried under vacuum to give a light yellow residue. Flash chromatography

(MeOH/EtOAc, 1:19, v/v, TLC; Rf=0.42) yielded 10.8 g of a clear colorless product. ^{1}NMR (DMSO-d_6) δ 8.49 (s, 1H), δ 8.28 (s, 1H), δ 6.00 (t, 1H, J=6.13, H1'), δ 5.28 (d, 1H, J=4.25, 3' hydroxy), δ .71 (t, 1H, J=5.12, 5' hydroxy), δ 4.32 (m, 1H), δ 3.83 (m, 1H), δ 3.45 (m, 1H), δ 3.35 (m, 1H), δ 2.68 (m, 1H), δ 2.43 (s, 3H), δ 2.23 (m, 1H). IR (KBr) 3330, 3170, 2950, 1690, 1650, 1435, 1320, 1080, 1020 cm^{-1}. FABMS calcd. for $C_{10}H_{15}N_4O_6$ $(M+H)^+$287.0991. Found 287.0974.

1H-Pyrazole-3-carboxamide, 1-(2-deoxy-β-D-erythro-pentofuranosyl)-5-methyl-4-nitro- (14b). **13b** (22.04 g, 40 mmol) was stirred in saturated NH_3 in MeOH (500 mL) as described for the synthesis of **14a**.The mixture was evaporated, and dried under vacuum to a give light yellow residue. Flash chromatography (MeOH/EtOAc, 1;18, v/v, TLC, Rf=0.20) yielded 10.08 g (95%) of a clear colorless product. ^{1}NMR (DMSO-d_6) δ 7.95 (s, 1H), δ 7.70 (s, 1H), δ 6.24 (t, 1H, J=6.87), δ 5.30 (d, 1H, J=4.26, 3'hydroxy), δ 4.7 1(t, 1H, J=5.14, 5' hydroxy), δ 4.34 (m, 1H), δ 3.80 (m, 1H), δ 3.20-3.50 (m, 3H), δ 2.82 (m, 1H), δ 2.64 (s, 3H), δ 2.22 (m, 1H). IR (KBr) 3350, 2950, 1670,1500,1370, 1380,1080,1060cm^{-1}. FABMS calcd. for $C_{10}H_{15}N_4O_6$ $(M+H)^+$ 287.0991. Found 287. 0974.

1H-Pyrazole-5-carboxamide, 1-(2-deoxy-β-D-erythro-pentofuranosyl)-3-methyl-4-amino- (15a). A solution of the nitro compound **14a** (8.6 g, 30 mmol) in 300 mL (EtOH/H_2O 8:2, v/ v) was shaken with 10% Pd/C (800 mg) under H_2 (50 psi) for 5 h, using a parr apparatus. Filtration and evaporation afforded 7.9 g of a clear colorless oil, which crystallized upon standing. ^{1}NMR (DMSO-d_6) δ 7.49 (s, 2H), δ 6.56 (t, 1H, J=6.13, H1'), δ 5.12 (d, 1H, J=4.25, 3' hydroxy), δ 4.72 (t, 1H, J=5.12, 5' hydroxy), δ 4.32 (m, 3H), δ 3.71 (m, 1H), δ 3.42 (m, 1H), δ 3.23 (m, 1H), δ 2.76 m, 1H), δ 2.04 (m, 4H).IR

(KBr) 3400, 2950, 1700, 1590, 1215cm^{-1}. EIMS calcd. for $C_{10}H_{16}N_4O_4$ (M+) 256.1172 Found 256.1167.

1H-Pyrazole-3-carboxamide, 1-(2-deoxy-β-D-erythro-pentofuranosyl)-5-methyl-4-amino- (15b). A nitro group of **14b** (8.6 g, 30 mmol) was reduced by the procedure described for **15a**. Filtration and evaporation gave 7.7 g of a colorless oil, which crystallized upon standing. ^{1}NMR (DMSO-d_6) δ 7.08 (s, 1H), δ 7.04 (s, 1H), δ 6.04 (t, 1H, J=6.14, H1'), δ 5.13 (d, 1H, J=4.24, 3' hydroxy), δ 4.66 (t, 1H, J=5.12, 5' hydroxy), δ 4.31-4.50 (m, 3H), δ .75 (m, 1H), δ 3.20-3.50 (m, 2H), δ 2.93 (m, 1H), δ 2.15 (m, 4H). IR (KBr) 3400,2950, 1672, 1600, 1320, 1300 cm^{-1}. EIMS calcd. for $C_{10}H_{16}N_4O_4$ 256.1171. Found 256.1167.

7H-Pyrazolo[4, 3-d]pyrimidin-7-one, 1-(2-deoxy-β-D-erythro-pento–furanosyl)-1, 4, 5, 6-tetrahydro-3-methyl-5-thioxo- (16a). Nucleoside **15a** (5.12 g, 20 mmol) and phenylisocyanate (7.8 g, 60 mmol) was dissolved in pyridine (50 mL) in a round bottom flask and the solution heated at reflux temperature for 16 h. The solution was taken to dryness and ethanol (50 mL) was added and removed *in vacuo*. Flash chromatography (5% MeOH in EtOAc) yielded 4.1 g (70%) of **16a** as a white solid. ^{1}NMR (DMSO-d_6) δ 13.02 (s, 1H), δ 12.02 (s, 1H), δ 6.68 (t, 1H, J=6.15, H1'), δ 5.27 (d, 1H, J=4.16, 3'hydroxy), δ 4.68 (t, 1H, J=5.25, 5'hydroxy), δ 4.35 (m, 1H), δ 3.78 (m, 1H), δ 3.45 (m, 1H), δ 3.31 (m, 1H), δ 2.71 (m, 1H), δ 2.31 (s, 3H), δ 2.20 (m, 1H).IR (KBr) 3400, 3100, 1700, 1600, 1290, 1200, 1160 cm^{-1}. EIMS calcd. for $C_{11}H_{14}N_4O_4S$ (M+) 298.0735. Found 298.0737.

7H-Pyrazolo(4,3-d)pyrimidine-7-one,2-(2-deoxy-β-D-erythropento-furanosyl)-2, 4, 5, 6-tetrahydro-3-methyl-5-thioxo- (16b). Nucleoside **15b** (5.12 g, 20 mmol) and phenylisocyanate (7.8 g, 60 mmol) was dissolved in

pyridine (60 mL) and the solution heated at reflux temperature for 16 h. The solution was evaporated to give an oil and triturated in ethyl acetate to give a white precipitate. The precipitate was filtered and dried to give 4.3 g of a white solid. ^{1}NMR(DMSO-d_6) δ12.61 (s, 1H), δ12.08 (s, 1H), δ6.25 (t, 1H, J=6.15, H1'),δ5.29 (d, 1H, J=4.24, 3'hydroxy), δ 4.73 (t, 1H, J=5.15, 5'hydroxy), δ 4.37 (m, 1H), δ3.81 (m, 1H), δ 3.21-3.50 (m, 2H), δ 2.90 (m, 1H), δ 2.47 (s, 3H), δ 2.25 (m, 1H). IR (KBr) 3300, 3100, 1700, 1620, 1600, 1280.cm^{-1} EIMS calcd. for $C_{11}H_{14}N_4O_4S$ 298.1735. Found 298.0727.

7H-Pyrazolo(4,3-d)pyrimidin-7-one,1-(2-deoxy-β-D-erythro-pentofuranosyl)1, 4, 5, 6-tetrahydro-3methyl-5-amino- (17a). Nucleoside **16a** (2.98 g, 10 mol) was dissolved in 10 mL concentrated NH_4OH and evaporated until the solid appeared. The mixture was cooled to 0°C, and 2.98 mL of 30% hydrogen peroxide solution was added dropwise and stirred for 20 minutes at 0°C. The reaction mixture was saturated with ammonia gas at 0°C. The solution was transferred to a pressure reaction bottle and the reaction was carried out at 150°C for 10 h, then cooled to 0°C. The light brown solution was evaporated to give a brown solid. The solid was recrystallized in water to give 2.01 g of white crystal (71%). ^{1}NMR(DMSO-d_6) δ 10.96 (s, 1H), δ 6.73 (t,1H, J=6.92), δ 6.13 (s, 2H), δ 5.18 (d, 1H, J=4.32, 3' hydroxy), δ 4.69(t, 1H, J=5.23, 5' hydroxy), δ 4.44 (m, 1H), δ 3.76 (m, 1H), δ 3.30-3.65 (m, 2H), δ 2.72 (m, 1H), δ 2.22 (s, 3H), δ 2.13 (m, 1H). IR (KBr) 3400, 3330, 2950, 1690, 1650, 1570, 1435, 1320cm^{-1}. UV (H_2O) λmax 228, 310 nm (ε_{228}=20,950, ε_{260}=3,387, and ε_{310}=6,020). FABMS calcd. for $C_{11}H_{16}N_5O_4(M+H)^+$ 282.1202. Found 282.1212.

7H-Pyrazolo[4, 3-d]pyrimidin-7-one, 2-(2-deoxy-β-D-erythro-pentofuranosyl)-2, 4, 5, 6-tetrahydro-3-methyl-5-amino- (17b). Nucleoside **16b** (2.98 g,

10 mmol) was transformed to amine by the same procedure described for **17a**. The light brown solution was evaporated to give a brown solid. The solid was dissolved in pyridine and filtered to remove ammonium sulfite. The solvent was evaporated to a brown solid. Flash chromatography (MeOH) yielded 1.9 g of a white solid. ^{1}HNMR (DMSO-d_6) δ 10.55 (s, 1H), δ6.33 (t, 1H, J=6.67, H1'), δ 6.00 (s, 2H), δ 5.32 (d, 1H,J=4.34, 3'hydroxy), δ 4.75 (t, 1H, J=5.23, 5'hydroxy), δ .40 (m, 1H), δ .79 (m, 1H), δ 3.39 (m, 1H), δ 3.26 (m, 1H), δ 2.92 (m, 1H), δ 2.31 (s, 3H), δ 2.24 (m, 1H). IR (KBr) 3400, 3320, 2960, 1695, 1630, 1600, 1320 cm^{-1}. UV (H_2O) λmax 224, 310 nm (ε_{224}=23,000, ε_{260}=4,142, and ε_{310}=3,857). FABMS calcd. $C_{11}H_{16}N_5O_4$ $(M+H)^+$ 282.1202. Found 282.1210.

Propanamide, N-[1-(2-deoxy-β-D-erythro-pento–furanosyl)-4, 7-dihydro-3-methyl-7-oxo-2H-pyrazolo[4, 3-d]pyridine-5-yl]-2-methyl- (18a). Amine compound **17a** (1.41 g, 5 mmol) was suspended in dry pyridine (25 mL) in a 100 mL round bottom flask equipped with a drying tube and cooled in an ice bath; trimethylchlorosilane (5 eq., 2.16 mL, 25 mmol) was added dropwise with stirring. After 30 minutes isobutyric anhydride (5 eq., 3.95 mL, 25 mmol) was added dropwise to the stirring solution. The reaction was allowed to warm to room temperature and stirred for 3 h. The reaction mixture was neutralized by addition of saturated aqueous $NaHCO_3$, then rotoevaporated several times with toluene and EtOH. The residue was dissolved in ethyl acetate and washed with water and dried over Na_2SO_4. Chromatography (ethyl acetate Rf=0.5) yielded 1.31 g (75%) of isobutyryl protected nucleoside. ^{1}HNMR(DMSO-d_6) δ 12.15 (s, 1H), δ 11.55 (s, 1H), δ 6.77 (dxd, 1H, J=6.41, 6.74, H1'), δ 5.23 (d, 1H, J=4.27, 3' hydroxy), δ 4.68 (t, 1H, J=5.65, 5' hydroxy), δ 4.49 (m, 1H), δ 3.79 (m, 1H), δ 3.48 (m, 1H), δ 3.31

(m, 1H), δ 2.75 (m, 2H), δ 2.31 (s, 3H), δ 2.21 (m, 1H), δ 1.05 (d, 6H, J=6.84, methyl). IR (KBr) 3250, 2980, 1680, 1610, 1490, 1300 cm^{-1}. FABMS calcd. for $C_{15}H_{22}N_5O_5$ $(M+H)^+$ 352.1620. Found 352.1608.

Propanamide, N-[2-(2-deoxy-β-D-erythro-pento–furanosyl)-4, 7-dihydro-3-methyl-7-oxo-2H-pyrazolo[4, 3-d]pyrimidine-5-yl]-2-methyl- (**18b**). The synthesis of **18b** was carried out as described for the synthesis of **18a**. Chromatography (EtOAc, Rf=0.35) yielded 1.30 g of a light yellow solid (75%). ^{1}HNMR(DMSO-d_6) δ11.89 (s, 1H), δ11.37 (s, 1H), δ6.32 (dxd, 1H, J=5.86, 6.35, H1'), δ5.28 (d, 1H, J=4.18, 3'hydroxy), δ4.69 (t, 1H, J=5.24, 5'hydroxy), δ4.39 (m, 1H), δ3.81 (m, 1H), δ3.37 (m, 1H), δ3.22 (m, 1H), δ2.94 (m, 1H), δ2.69 (m, 1H), δ2.43 (s, 3H), δ2.22 (m, 1H), δ1.07 (d, 6H, J=6.83, methyl). IR (KBr) 3250, 2980, 1680, 1610, 1490, 1300.cm^{-1} FABMS calcd. for $C_{15}H_{22}N_5O_5$ $(M+H)^+$ 362.1620. Found 352.1610.

Propanamide, N-[1-[5-O-[bis(4-methoxyphenyl)methyl]2-deoxy-β–D-erythro-pentofuranosyl]-4, 7-dihydro-3-methyl-7-oxo-1H-pyrazolo(4,3-d)pyrimidin-5-yl]-2-methyl- (**19a**). Protected nucleoside **18a** (1.06 g, 3 mmol) was dissolved in dry pyridine(6 mL). 4, 4-dimethoxytritylchloride (TMTCl) (1.14 g, 3.3 mmol) was added to the solution, and this mixture was stirred at 4°C overnight. An additional portion of DMTCl (35 mg, 0.1 mmol) was added until most of the starting material was converted to product as determined by TLC. The reaction was stopped by the addition of MeOH (2 mL) and diluted in methylene chloride (50 mL). The organic layer was washed three times with water, dried over anhydrous Na_2SO_4, filtered, and evaporated to a yellow foam. Chromatography (CH_2Cl_2/EtOAc, 2:1, v/v, Rf=0.31) yielded 1.46 g (75%) of the product as a white solid. ^{1}HNMR (DMSO-d_6) δ 12.28 (s, 1H), δ 11.59 (s, 1H), δ 7.31 (d, 2H, J=7.84, phenyl), δ 7.16 (m, 7H), δ 6.76 (m,

5H), δ 5.27 (d, 1H, J=4.70, 3' hydroxy), δ 4.45 (m, 1H), δ 3.92 (m, 1H), δ 3.70 (s, 3H), δ 3.69 (s, 3H), δ 3.00 (m, 2H), δ 2.73 (m, 2H), δ 2.26 (m, 1H), δ 2.18 (s, 3H), δ 1.10 (d, 6H, J=6.84, methyl). IR (KBr) 3400, 3200, 2980, 1670, 1610, 1500, 1250 cm^{-1}. FABMS calcd. for $C_{36}H_{40}N_5O_7$ $(M+H)^+$ 654.2927. Found 654.2938.

Propanamide, N-[2-[5-O-[bis (4-methoxyphenyl)phenylmethyl]-2-deoxy-β-D-erthro-pentofuranosyl]-4, 7-dihydro-3-methyl-7-oxo-2H-pyrazolo[4, 3-d]pyrimidin-5-yl]-2-methyl- (19b). The procedure for the synthesis of **18a** was followed for the 5'-OH protection of **18b** (1.06 g, 3 mmol). Chromatography (CH_2Cl_2/EtOAc, 2:1, v/v, Rf=0.23) yielded 1.52 (76 %) of **19b**. ^{1}HNMR (DMSO-d_6) δ 11.94 (s, 1H), δ11.39 (s, 1H), δ .00-δ7.30 (m, 9H), δ .75 (d, 2H, J=8.98,4-methoxyphenyl), δ 6.73 (d, 2H, J=8.55, 4-methoxyphenyl), δ 6.41 (q, 1H), δ 5.35 (d, 1H, J=5.13, 3'hydroxy), δ 4.57 (m, 1H), δ 3.96 (m, 1H), δ 3.68 (m, 3H), δ 3.66 (s, 3H), δ 3.00 (m, 2H), δ 2.81 (m, 1H), δ 2.72 (m, 1H), δ 2.55 (s, 3H), δ 2.27 (m, 1H), δ 1.09 (d, 6H, J=6.86, methyl). IR (KBr) 3400, 3200, 2980, 1670, 1620, 1500, 1470,1290, 1250 cm^{-1}. FABMS calcd. $C_{36}H_{40}N_5O_7$ $(M+H)^+$ 654.2927. Found 654.2950.

Phosphoramidous acid, bis(1-methylethyl)-, 2-cyanoethyl ester, 3'-ester with N-[1-[5-O-[bis(4-methoxyphenyl)phenylmethyl]-2-deoxy-β-D-erythro-pentofuranosyl]-4, 7-dihydro-3-methyl-7-oxo-1H-pyrazolo(4,3-d)pyrimidin-5-yl]-2-methyl-propanamide (P1). 2-cyanoethyl-N, N-diisopropyl-chlorophosphoramidite (200 mL, 0.90 mmol) was added dropwise to a solution of **19a** (392 mg, 0.60 mmol) and diisopropylethylamine (312 mL, 1.80 mmol) in dry CH_2Cl_2 (4 mL, purified by passing through basic aluminum oxide) under argon. After 1 hour, the reaction was quenched with ethanol (1.0 mL), diluted with EtOAc (60 mL), and washed with saturated aqueous $NaHCO_3$ (2x60 mL) and brine (2x60 mL). The organic layer was dried over

anhydrous Na_2SO_4 and then concentrated. The phosphoramidite diastereomers were purified by flash chromatography (EtOAc/CH_2Cl_2/TEA/isopropyl alcohol, 5:90:2:2, v/v/v/v, Rf=0.70) to give a white solid. ^{1}HNMR (DMSO-d_6) δ 12.29 (s, 1H), δ 11.61 (s, 1H), δ 7.37 (m, 2H), δ 7.16 (m, 7H), δ 6.76 (m, 5H), δ 6.76 (m, 5H), δ 4.75 (m, 1H), δ 4.06 (m, 1H), δ 3.40-3.85 (m, 10H), δ3 .09 (m, 1H), δ 2.80 (m, 2H), δ 2.72 (m, 2H), δ 2.65 (m, 1H), δ 2.45 (m, 1H), δ 2.18 (s, 3H), δ 0.90-1.40 (m, 18H). IR (KBr) 3200, 2980, 2250, 1680, 1610, 1500, 1305, 1250 cm^{-1}. FABMS calcd. for $C_{45}H_{57}N_7O_8P$ $(M+H)^+$ 854.4006. Found 854. 4036.

Phosphoramidous acid, bis(1-methyethyl)-, 2-cyanoethylester, 3'-ester with N-[2-[5-O-[bis(4-methoxyphenyl)phenylmethyl]-2-deoxy-β-D-erythro-pentofuranosyl]-4, 7-dihydro-3-methyl-7-oxo-2H-pyrazolo(4,3-d)pyrimidin-5-yl]-2-methyl-propanamide (P2). **P2** was prepared by the same procedure described for the synthesis of **P1** (400 mg, 0.6 mmol). Chromatography of the phosphoramidite diastereomers (EtOAc/CH_2Cl_2/TEA/isopropyl alcohol, 5:90:2:2, v/v/v/v, Rf=0.48) gave **P2** in an 82% yield. ^{1}HNMR (DMSO-d_6) δ 11.94 (s, 1H), δ 11.40 (s, 1H), δ 6.9-7.4 (m, 9H), δ6.75 (m, 4H), δ 6.50 (t, 1H, J=4.27, H1'), δ 4.89 (m, 1H), δ 4.10 (m, 1H), δ 3.40-3.80 (m, 10H),δ 3.21 (m, 1H), δ 3.05 (m, 1H), δ 2.30-2.80 (m, 8H), δ 0.8-δ 1.50 (m, 18H). IR (KBr) 3250, 2990, 1680, 1610, 1245 cm^{-1}. FABMS calcd. for $C_{45}H_{57}N_7O_8P$ $(M+H)^+$ 854.4006. Found 854.4026.

Oligonucleotides. Oligonucleotides **20-31** were machine synthesized using β-cyanoethyl phosphoramidite chemistry. Modified nucleosides coupled with >97% efficiency except phosphoramidite **10**. The oligonucleotides were removed from the support and deprotected by treatment with 0.1 N NaOH (1.5 mL/1 μmol, 55°C, 24 h), neutralized with

glacial acetic acid (6-7 μL/1.5 mL 0.1 N NaOH), applied to a column of Sephadex G-10-120 (Sigma), and eluted with water. The crude oligonucleotides were lyophilized and purified by electrophoresis (550V, 20 h) on a 2 mm-thick 20% polyacrylamide gel (Maxam-Gilbert). The major UV-absorbing bands were excised and eluted (0.2N NaCl, 1 mM EDTA, 37°C, 24 h), then passed through Sephadex G-10-120, and dialyzed against water for 3 days. Oligonucleotide 4 mers 5'- T-T-P1-T-3', 5'-T-T-P2-T-3' were synthesized on a 10 mmol scale in a similar manner as in the NMR and FABMS studies. The crude deprotected 4-mers were filtered, lyophilized, and chromatographed on a Sephadex G-10-120 column to give 6.12 mg of a white solid. ^{1}HNMR (DMSO-d_6) T-T-P1-T δ 11.30 (m, 4H), δ 7.90 (s, 1H), δ 7.87 (s, 1H), δ 7.81 (s, 1H), δ 6.71 (t, 1H, J=5.01, H1'), δ 6.31 (s, 2H), δ 6.18 (m, 3H), δ 5.89 (m, 1H), δ 4.82 (m, 2H), δ 4.75 (m, 1H), δ 4.45 (m, 1H), δ 3.50-4.20 (m, 13H), δ 2.98 (m, 1H), δ 2.25 (s, 3H), δ 2.00-2.50 (m, 7H), δ 1.85 (s, 6H), δ 1.29 (s, 3H). FABMS calcd. for $C_{41}H_{52}N_{11}O_{25}P_3Na_3$ $(M+H)^+$ 1260.2041. Found 1260.2009. 1HNMR (DMSO-d_6) T-T-P2-T δ 11.20 (m, 4H), δ 7.81 (s, 1H), δ 7.79 (s, 1H), δ 7.74 (s, 1H), δ 6.22 (m, 4H), δ 6.01 (m, 1H), δ 5.78 (m, 1H), δ 4.81 (m, 1H), δ 4.72 (m, 1H), δ 4.65 (m, 1H), δ 4.38 (m, 1H), δ 4.31 (m. 1H), δ 3.22-4.00 (m, 16H), δ3.00 (m, 1H), δ 2.31 (s, 3H), δ 1.90-2.60 (m, 7H), δ 1.78 (s, 6H), δ 1.73 (s, 3H). FABMS calcd. for $C_{41}H_{52}N_{11}O_{25}P_3Na_3(M+H)^+$ 1260.2041. Found 1260.2075.

HPLC Analysis. 3 nmoles of purified oligonucleotide was digested simultaneously with snake venom phosphodiesterase (3 μL, 2 μg/ μL), calf intestine alkaline phophotase (3 μL, 1 u/ μL), 50 mM Tris-pH 8.1, 100 mM $MgCl_2$. The reaction mixture was incubated at 37°C for 2 h and lyophilized to dryness. The dry sample was dissolved with 10 μL of Milli-Q water. 5 μL

of the solution was injected onto a C18 reverse phase column utilizing 10 nM ammonium phosphate pH 5.1/8.0% MeOH as eluent. 5 μL of the standard solution containing C (4 nmols), T (4 nmols), P1 (12 nmols) and P2 (12 nmols) was also injected under same conditions as a standard. Each peak was compared with the peaks of the standard solution. 5 μL of digested solution was mixed with 5 μL of the solution containing standard nucleosides, and 5 μL of resulting solution was injected to show that each nucleoside peak was identical.

DNA manipulation. Distilled, deionized water was used for all aqeuous reactions and dilutions. Enzymes were purchased from either Boehringer-Mannheim or New England Biolabs. Deoxynucleoside triphosphates were purchased from Pharmacia as 100 mM solutions. 5'[α-^{32}P]dNTPs (3000 Ci/mmol) and 5'[γ-^{32}P]ATP (7000 Ci/mmol) were obtained from Amersham. The plasmid pDMAG10 was a gift from D. Mendel, who constructed it by inserting a duplex containing d(AAAAAGAGAGAGAGA) into the large BamHI/HindIII restriction fragment of pBR322. The plasmid pHIV-CAT was a gift from Dr. Alan Frankel and Tom Povsic. DNA reactions were typically carried out in 1.5 mL polypropylene tubes obtained from Tekma company. Calf thymus DNA was purchased from Sigma, sonicated, and extracted with 3x0.2 volume water saturated phenol, 0.2 volume 24:1 $CHCl_3$/isoamyl alcohol, and 0.2 volume $CHCl_3$. After extensive dialysis against water, the DNA was passed through a 4.5 μm Centrex filter (Schleicher Schuell) and assayed for concentration by UV assuming ε_{260}=11,800 L/mol.bp.cm. DNA was precipitated from either 0.3M NaOAc pH5.2/EtOH (1:3) or NH_4OAc/EtOH (1:2.5). DNA pellets were dried in a Savant speed vac. Agarose gel

electrophoresis was carried out using 40 mM tris-acetate, 5 mM NaOAc, 1 mM EDTA, pH 7.9 buffer. The ten-fold concentration (10x) loading buffer for agarose gels was 25% (w/v) ficoll solution, which contained 0.2% (w/v) bromophenol blue (BPB) and xylene cyanol (XC) tracking dyes. Polyacrylamide gel electrophoresis was carried out using 100 mM tris-borate, 1mM EDTA, pH 8.3 buffer. The loading buffer for denaturing polyacrylamide gels was 80% formamide in 100 mM tris-borate, 1mM EDTA, pH 8.3 buffer. 3' labeling of DNA was prepared by standard procedures (47). Specific radioactivity was measured with a Beckman LS 2801 scintillation counter. Gels were dried (after transferring them to Whatman 0.3 mm paper) on a Bio-Rad Model 483 slab dryer at 80°C. Autoradiography was carried out using Kodak X-Omat film. Optical densitometry was performed using LKB Broma Ultrascan XL Laser Densitometer operating at 633 nm. The relative peak area for each cleavage band or locus was equated to the relative cleavage efficiency at that site.

Cleavage of 5' ^{32}P end-labeled 30 mer duplex. 50 picomoles of each single-stranded oligonucleotide $A_5T_7YT_7G_{10}$ (Y=T, C, G, A) were dissolved in 28 μL water, 5 μL 10x kinase buffer (10x=700 mM Tris.HCl, 100 mM $MgCl_2$, 1 mM spermidine, 1 mM EDTA, pH 7.6), and 5 μL 10 mg/ml DTT. This solution was treated with 10 μL 5' [α-^{32}P]ATP and 2 μL T4 polynucleotide kinase (10 u/μL). The 5' end labeling was allowed to proceed for 45 minutes at 37°C. The end-labeled DNA was precipitated from NaOAc/EtOH, washed with 70% EtOH, and dried. The pellets were dissolved in 100 mM NaCl, 50 mM tris-acetate, pH 7.4, and 50 picomoles of the complementary 30 mer in a total volume of 30 μL. To effect hybridization of the 30 mers, the oligonucleotide mixture was heated to 90°C for 5 minutes

and allowed to cool to room temperature. The oligonucleotide mixtures were treated with 5 μL 25% ficoll loading buffer, loaded onto a nondenaturing polyacrylamide gel and electrophoresed at 240 V until the BPB tracking dye was near the bottom of the gel. The four bands (Y=T, C, G, A) of end-labeled DNA were visualized by autoradiography, excised from the gel, crushed, transferred to 1.5 mL polypropylene tubes, and eluted into 0.2 N NaCl at 37 °C for 24 h. The end- labeled DNA 30 mer duplexes were recovered by passing the eluents through a 4.5 mL Centrex filter and extensive dialysis against water. The labeled DNA solution was used for the cleavage reaction. For the cleavage reactions the DNA (20,000 cpm/reaction) was mixed with salts, buffer, spermine and the oligonucleotide-EDTA with Fe(II). This solution was incubated for 30 minutes at 37°C before the cleavage reaction was initiated by the addition of DTT to make a final volumn of 40 μL. The reaction was stopped by lyophilization. To each eppendorf tube a certain volume of formamide loading buffer was added (80% formamide, 20% 5X TBE buffer, 0.02% bromophenol blue and 0.02 % xylene cyanol) to give approximately 3,000 cpm/μL for each reaction. To dissolve the solid the tubes were vortexed (10 sec). 5 μL of the resulting solutions were transferred to new tubes and counted afterwards. The volume of buffer was loaded on each lane to give the same amount of radioactivity (~6000 cpm/lane) for each reaction. Electrophoretic separation of the cleavage products was achieved on a 20% denaturing polyacrylamide gel until the bromophenol blue was 25 cm from the starting position. Cleavage products were visualized by autoradiography without drying the gel. The relative cleavage was analyzed by LKB densitometry.

Double strand cleavage of pDMAG10. The plasmid pDMAG10 was precipitated twice from NaOAc with ethanol, rinsed with 70% ethanol, briefly dried *in vacuo* and digested with StyI, which produces an asymetric cleavage site that enables a selective labeling at only one of two ends. The linearized plasmid (10 ng) was labeled with [α-^{32}P]dTTP and DNApolymerase (large Klenow fragment, reaction volumn =100 µL) according to standard procedures (44). 100 µL Milli-Q water was added to reaction mixture. The resulting DNA solution was extracted with 2x1 volume water saturated phenol and 3x1 volume ether. Half of the resulting DNA-solution (100 µL) was passed through the column containing 1 mL Sephadex G-50-80 resin to remove mononucleotides. The labeled DNA solution was used for the cleavage reaction. For the cleavage reactions the DNA (20,000 cpm/reaction) was mixed with salts, buffer, spermine and the oligonucleotide-EDTA with Fe. This solution was incubated for 30 minutes at 25°C before the cleavage reaction was initiated by the addition of DTT to make a final volumn of 40 µL. The reaction was stopped by precipitation: 60 µL water was added followed by 20% NaOAc-solution (10 µL) and 300 µL cold ethanol, and the DNA was precipitated as usual. The pellets were rinsed once with 70% cold ethanol (50 µL) and briefly dried *in vacuo.* To each pellet a certain volume of ficoll loading buffer was added (2.5% ficoll 400, 1xTAE-buffer, 0.02% bromophenol blue and 0.02 xylene yanol) to give approximately 600 cpm/µL for each reaction. To dissolve the pellet the tubes were vortexed 10 sec). 20 µL of the resulting solutions were transferred to new tubes and counted afterwards. The volume of buffer was loaded on each lane to give the same amount of radioactivity (~6000 cpm/lane) for each reaction. Electrophoretic separation of the cleavage products was achieved

on a 0.9% agarose gel (20x14x0.4 cm, TAE-buffer, 120 V, 4.0 h) until the bromophenol blue was 15 cm from the starting position. The gel was dried on a Bio-Rad Slab Gel Dryer Model 483 (1.5 h at 80°C) and cleavage products were visualized by autoradiography.

Double strand cleavage of HIV-CAT DNA. HIV-CAT was precipitated twice from NaOAc with ethanol, rinsed with 70% ethanol, briefly dried *in vacuo* and digested with BamHI according to conditions provided by the manufacturers. The linearized DNA was labeled with α-[^{32}P]GTP using DNA polymerase according to standard procedures. Purification of the labeled DNA and performance of the cleavage experiments were carried out exactly as described for the double-stranded cleavage of pDMAG10 except where sodium ascorbate was used instead of DTT as the reducing agent.

References and notes

(1) Lyamichev, V. I.; Mirkin, S. M.; Frank-Kamenetski, M. D.; Cantor, C. R. *Nucl. Acids Res.* **1988**, *16*, 2165.

(2) Doan, T. L; Perrouault, L.; Praseuth, D.; Habhoub, N.; Decaut, J.-L.; Thoung, N. T.; Lhomme, J.; Helene, C. *Nucl. Acids Res.* **1987**, *15*, 7749.

(3) Praseuth, D.; Perrouault, L.; Doan, T. L.; Chassignol, M.; Thuong, N.; Helene, C. *Proc. Natl. Acad. Sci. U. S. A.* **1988**, *85*, 1349.

(4) Moser, H. E.; Dervan, P. B. *Science* **1987**, *238*, 645.

(5). Povsic, T. J.; Dervan, P. B. *J. Amer. Chem. Soc.* **1989**, *111*, 3059.

(6) Strobel, S. A.; Moser, H. E.; Dervan, P. B. *J. Amer. Chem. Soc.* **1988**, *110*, 7927.

(7) Felsenfeld, G.; Davies, D. R.; Rich, A. *J. Amer. Chem. Soc.* **1957**, *79*, 2023.

(8). Michelson, A. M.; Massoulie, J.; Guschlbauer, W. *Prog. Nucl. Acid. Res. Mol. Biol.* **1967**, *6*, 83.

(9) Felsenfeld, G.; Miles, H. T. *Annu. Rev. Biochem.* **1967**, *36*, 407.

(10) Lipsett, M. N. *Biochem. Biophys. Res. Commun.* **1963**, *11*, 224.

(11) Howard, F. B.; Frazier, J.; Lipsett, M. N.; Miles, H. T. *Biochem. Biophys. Res. Commun.* **1964**, *17*, 93.

(12) Lipsett, M. N. *J. Biol. Chem.* **1964**, *239*, 1256.

(13) Miller, J. H.; Sobell, J. M. *Proc. Natl. Acad. Sci. U. S. A.* **1966**, *55*, 1201.

(14) Morgan, A. R.; Wells, R. D. *J. Mol. Biol.* **1968**, *37*, 63.

(15) Lee, J. S.; Johnson, D. A.; Morgan, A. R. *Nucleic Acids. Res.* **1979**, *6*, 3073.

(16) Arnott, S.; Bond, P. J. *Nature New Biology* **1973**, *244*, 99.

(17) Arnott, S.; Selsing, E. *J. Mol. Biol.* **1974**, *88*, 509.

(18) Arnott, S.; Bond, P. J.; Selsing, E.; Smith, P. J. C. *Nucleic Acids Res.* **1976**, *3*, 2459.

(19) Saenger, W. *Priciples of Nucleic Acid Structure*, edited by Cantor, C. R.; Springer-Verlag, New York Inc. (**1984**), p. 242.

(20) Hoogsteen, K. *Acta Crysta.* **1959**, *12*, 822.

(21) Moser, H. E.; Dervan, P. B., unpublished results.

(22) Mace, H. A. F.; Pelhan, H. R. B.; Travers, A. *Nature* **1983**, *304*, 555.

(23) Nickol, J. M.; Felsenfeld, G. *Cell* **1982**, *35*, 467.

(24) Larsen, A.; Weintraub, H. *Cell* **1982**, *29*, 609.

(25) Schon, E.; Evans, T.; Welsh, J.; Efstratiadis, A. *Cell* **1983**, *35*, 837.

(26). Hanvey, J. C.; Shimizu, M.; Wells, R. D. *Proc. Natl. Acad. Sci.* **1988**, *85*, 6292.

(27) Mirkin, S. M.; Lyamichev, V. I.; Drushlyak, K. N.; Dobrynin, V. N.; Filippov, S. A.; Frank-Kamenetskii, M. D. *Nature* **1987**, *330*, 495.

(28) Kohwi-Shigematsu, T; Kohwi, Y. *Cell* **1985**, *43*, 199.

(29) Htun, H.; Dahlberg, J. E. *Science* **1989**, *243*, 1571.

(30) Sugawara, T.; Ishikura, T.; Itoh, T.; Mizuno, Y. *Nucleosides and Nucleotides* **1982**, *1*, 239.

(31) Chern, J.; Lee, H.; Huang, M.; Shish, F. *Tetrahedron Letters* **1987**, *28*, 2151.

(32) Long, R. C.; Gerster, J. F.; Townsend, L. B. *J. Heterocycl. Chem.* **1970**, *17*, 863.

(33) Robins, R. K.; Holum, L. B.; Furcht, F. W. *J. Org. Chem.* **1956**, *21*, 833.

(34) Hoffer, M. *Chem. Ber.* **1960**, *93*, 2777.

(35) Kazimierczuk, Z.; Lottam, H. B.; Revanker, G. R.; Robins, R. K. *J. Amer. Chem. Soc.* **1984**, *106*, 6379.

(36) Imai, K.; Marumoto, R.; Kobayashi, K. *Chem. Pharm. Bull.* **1971**, *19*, 576.

(37) a) Atkinson, T; Smith, M. *Oligonucleotide Synthesis: A practical Approach*; edited by Gait, M. J. IRL Press, Oxford(**1985**). b) Ti, G. C; Gaffney, B. L.; Jones, R. A. *J. Amer. Chem. Soc.* **1982**, *104*, 1316.

(38) Sinha, N. D.; Biernat, J.; MaManus, J.; Koster, H. *Nucleic Acids Res.* **1984**, *12*, 4539.

(39) Itaya,T.; Harada, T. *Tetrahedron Letters* **1982**, *23*, 2203.

(40) Dreyer, G. B.; Dervan, P. B. *Proc. Natl. Acad. Sci. U. S. A.* **1985**, *82*, 968.

(41) Usman, N.; Ogilvie, K. K.; Jiang, M.-Y.; Cedergren, R. J. *J. Amer. Chem. Soc.* **1987**, *109*, 7845.

(42) Mclaughlin, L. W.; Cramer, F.; Sprinzl, M. *Anal. Biochem.* **1981**, *112*, 60.

(43) Maxam, A. M.; Gilbert, W. *Methods Enzymol.* **1980**, *65*, 499.

(44) Maniatis, T.; Fritsch, E. F.; Sambrook, J. *Molecular Cloning C. S. H.* **1982**.

Appendix

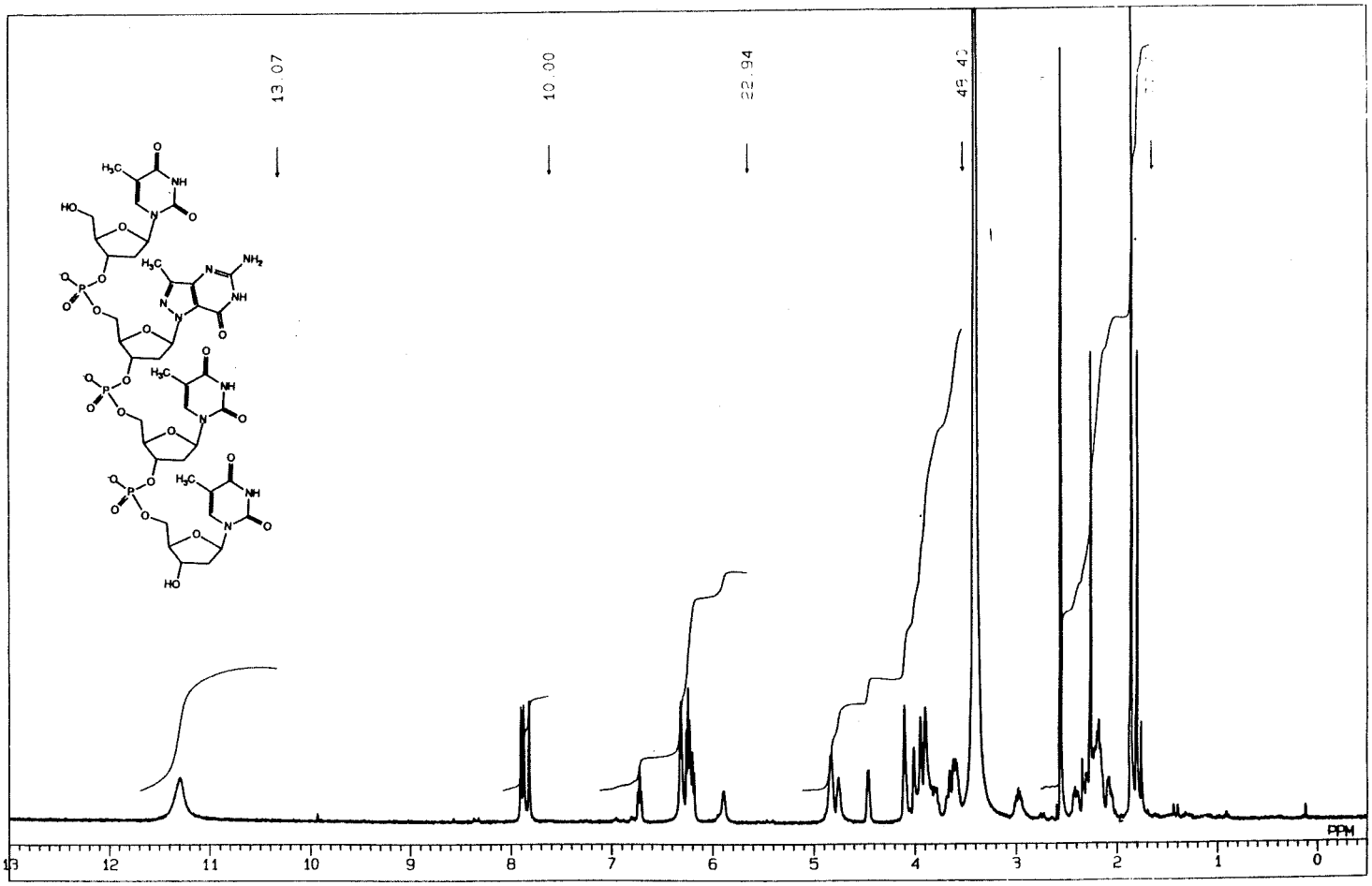

Figure 1. ^{1}HNMR (Me_2SO-d_6) of oligonucleotide tetramer 5'-T-T-P1-T-3'.

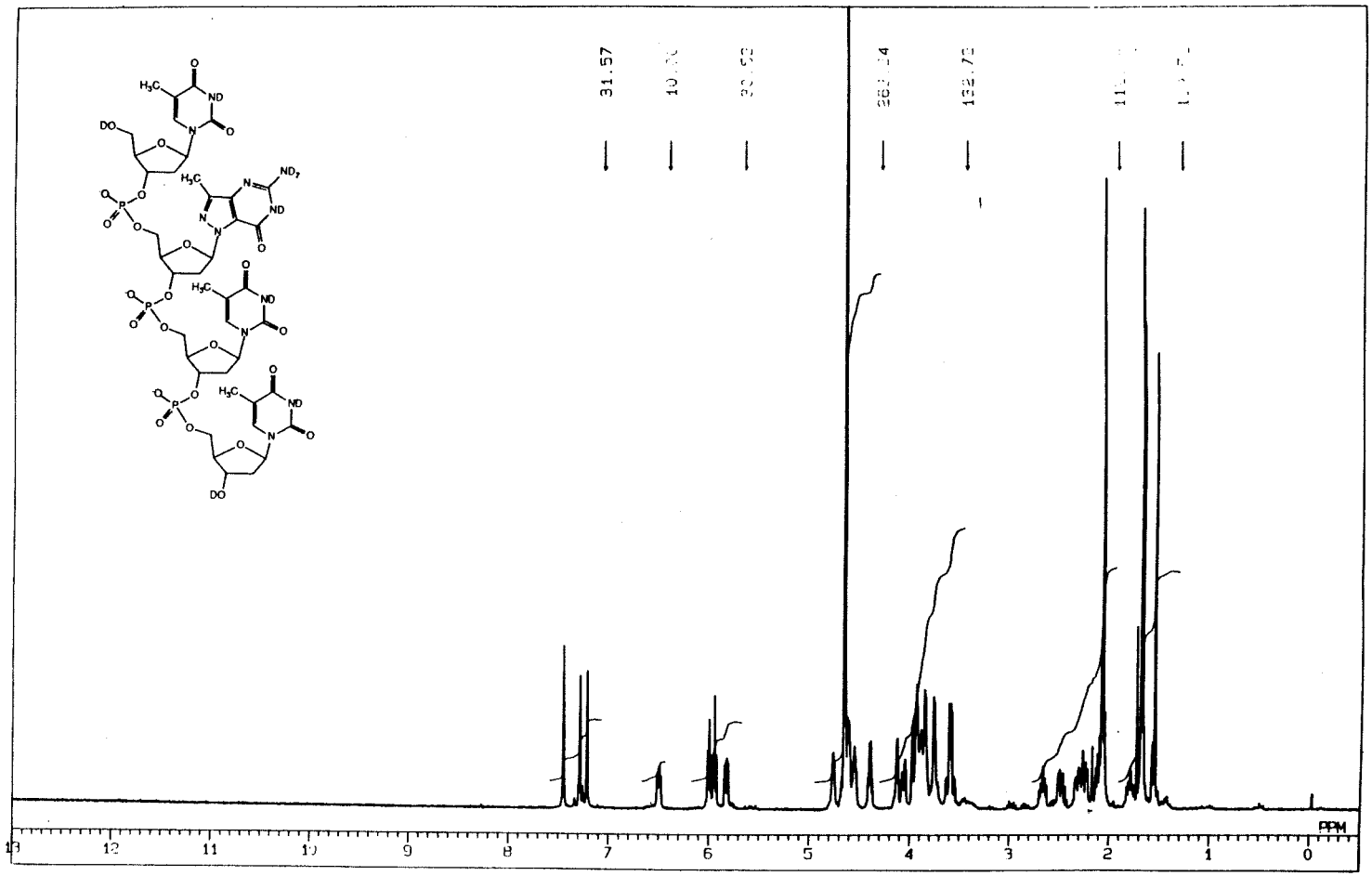

Figure 2 . ^{1}HNMR (D_2O) of oligonucleotide tetramer 5'-T-T-P1-T-3'.

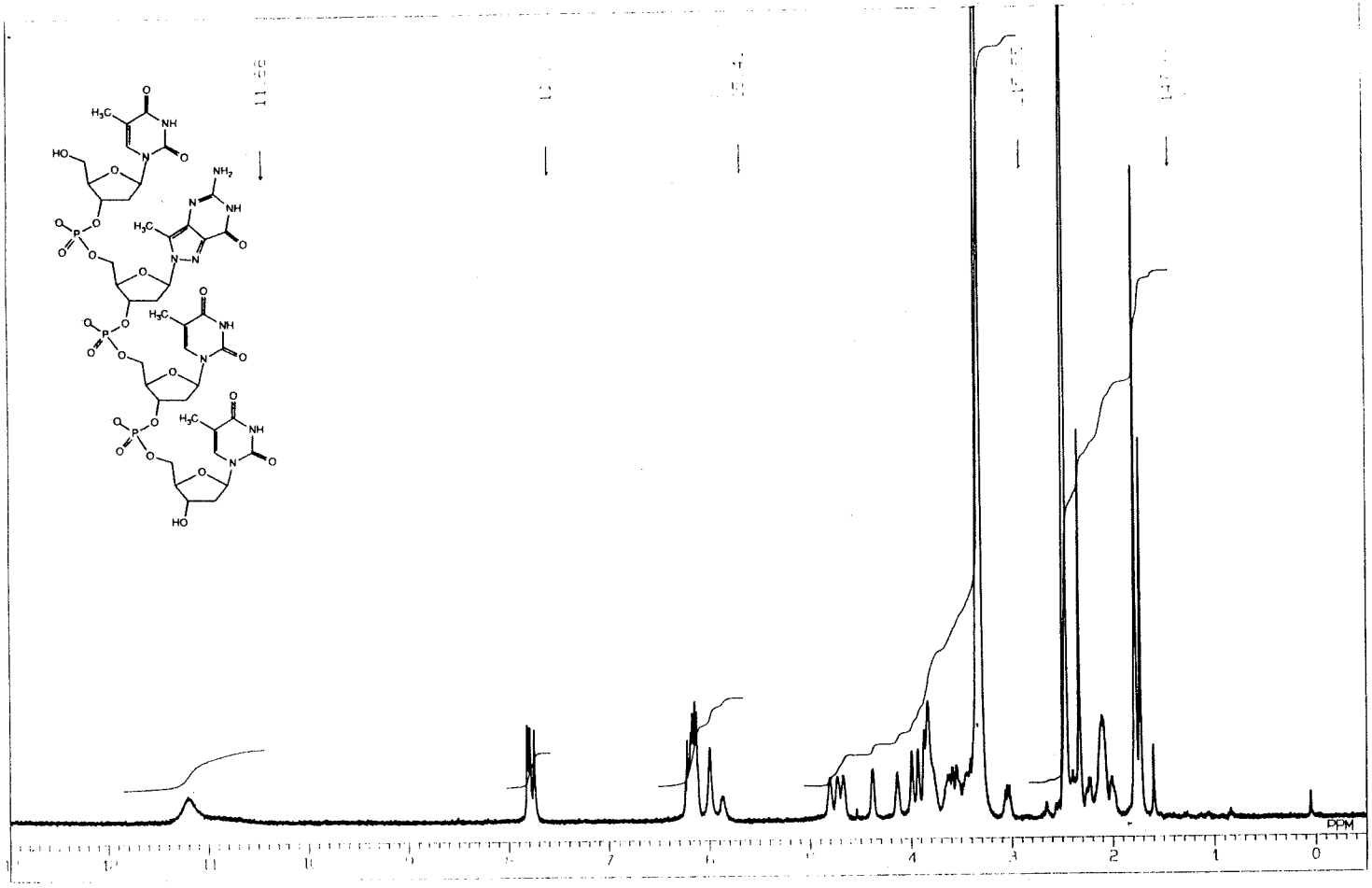

Figure 3. ^{1}HNMR (Me_2SO-d_6) of oligonucleotide tetramer 5'-T-T-P2-T-3'.

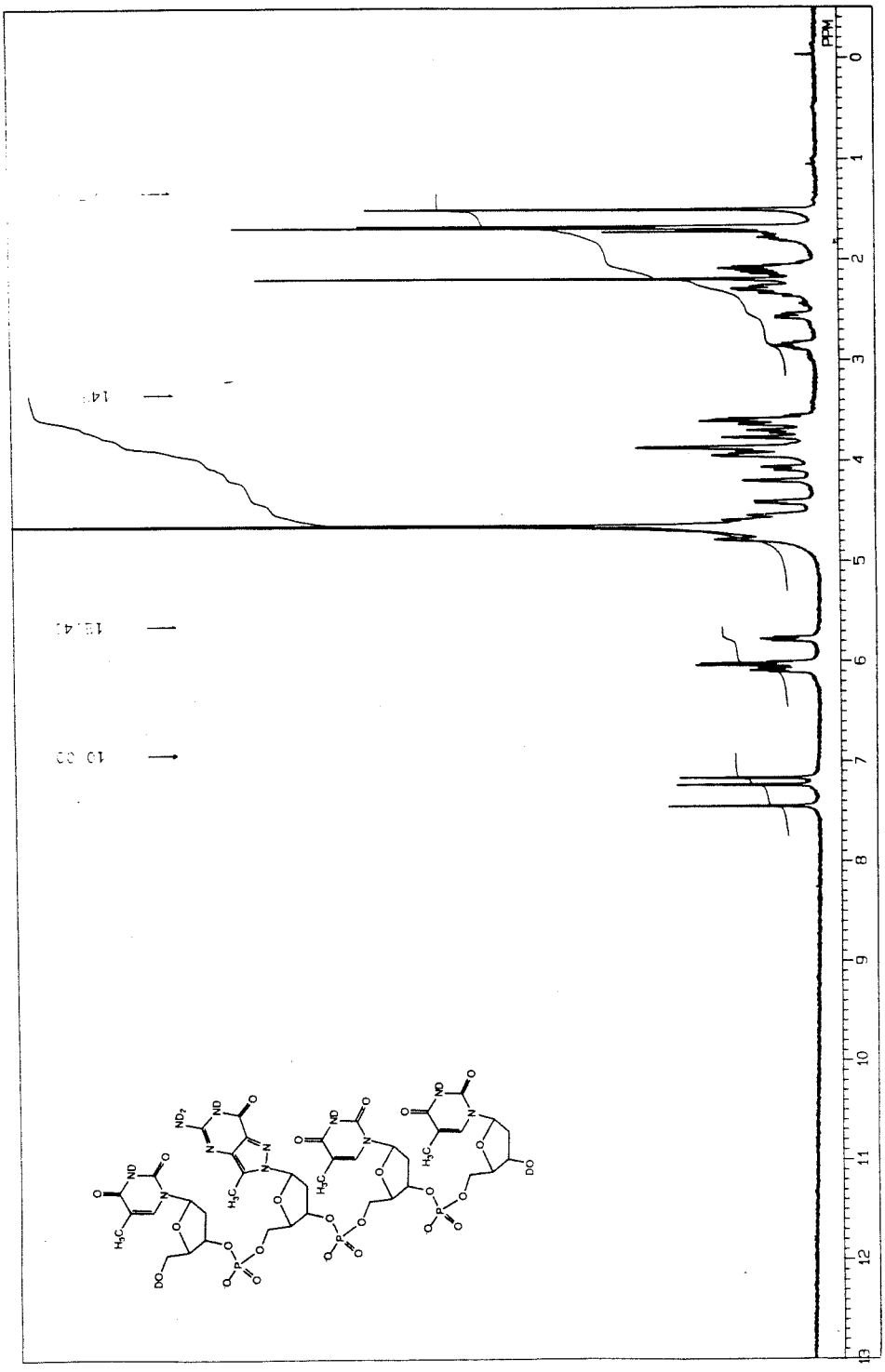

Figure 4. ^{1}HNMR (D_2O) of oligonucleotide tetramer 5'-T-T-P2-T-3'.

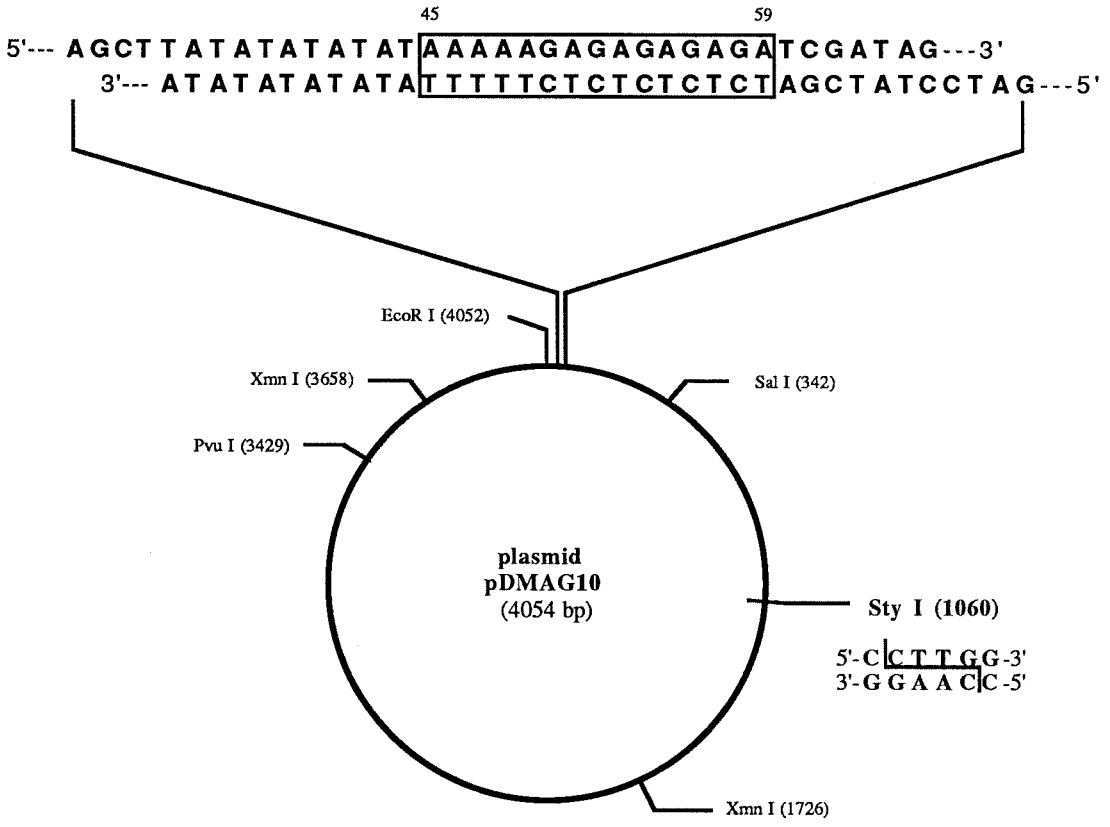

Figure 5. Schematic of plasmid pDMAG10 and the sequence of the target site.

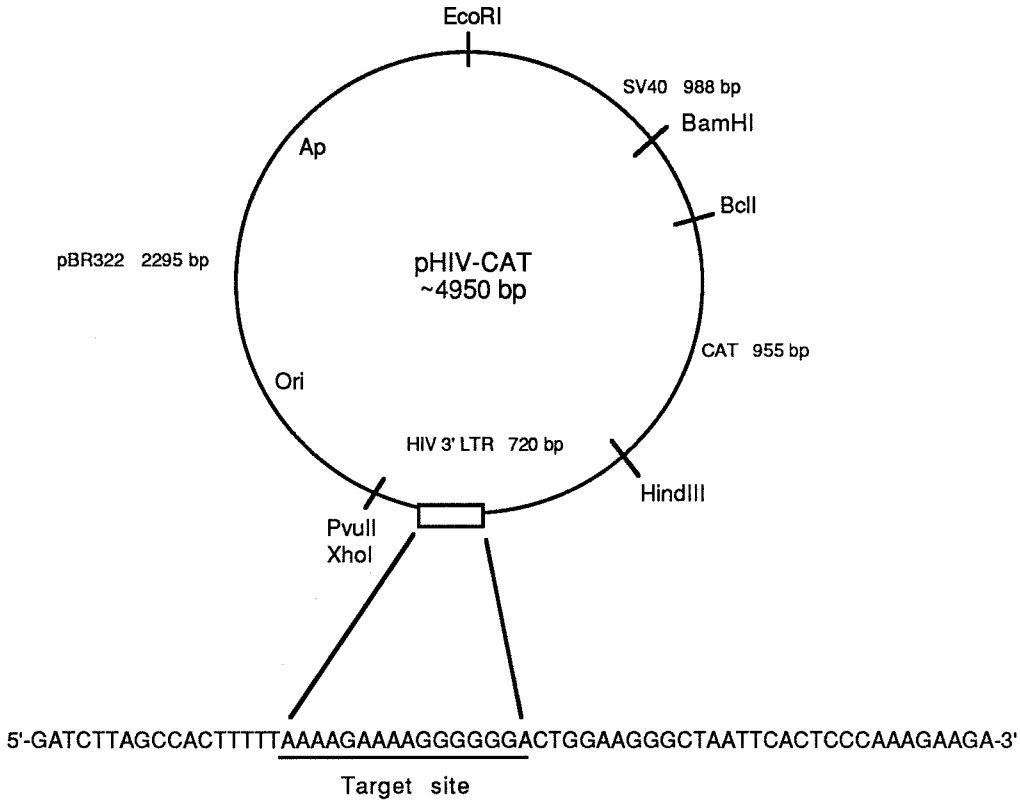

Figure 6. Schematic of plasmid HIV-CAT, which contains the entire HIV promoter region on a Xho-HindIII fragment derived from the Long Terminal Repeat (LTR) of HIV DNA, and the sequence of the target site.

Chapter 2

Extension of Triple Helix Formation. Design of Novel Bases for Recognition of CG Base Pairs

Introduction

The sequence specific recognition of double helical DNA is essential for the recognition of cellular functions including transcription, replication and cell division. The ability to design synthetic molecules that bind specifically to unique sequences on human DNA could have major implications for the treatment of genetic, neoplastic, and viral diseases (1-3).

Triple Helix Formation. Double helical DNA recognition using pyrimidine oligonucleotides by triple helix formation offers a powerful chemical approach for the sequence-specific binding of double helical DNA. Specificity arises from base triplets (T•AT and C+GC) formed by Hoogsteen base pairing of the second pyrimidine strand with the purine strand of the double helix (4-20). It is believed that each base pair (bp) in a homopurine double helical DNA sequence involves two specific hydrogen bonds for triple helix formation in which the pyrimidine oligonucleotide is oriented in the major groove of DNA parallel to the Watson-Crick purine strand (4-7, 18). In the pyrimidine-Hoogsteen triple strand model, a binding site size of >15 homopurine base pairs affords >30 discrete sequence-specific hydrogen bonds to duplex DNA. An oligonucleotide 15 nucleotides (nt) in length could conceivably bind uniquely to one site on a human chromosome.

Moser and Dervan have reported that homopyrimidine oligodeoxyribonucleotides with EDTA•Fe(II) attached at a single position bind the corresponding homopyrimidine/homopurine tracts within large double-stranded DNA by triple helix formation and cleave at those sites (4). Cleavage efficiency by homopyrimidine probes is sensitive to single base mismatches. Cleavage by triple strand formation is not observed in the

absence of cations such as spermine or cobalt hexamine, which are necessary to overcome the repulsion between the anionic chains of the Watson-Crick duplex and the third negatively charged phosphodiester backbone. The binding affinities of oligonucleotides containing cytosine are sensitive to pH. The sensitivity of binding also depends on the number and position of cytosines in the oligonucleotides (21). This is probably influenced by the requirement for protonation of cytosine N-3 in the third strand to enable the formation of two Hoogsteen hydrogen bonds.

Povsic and Dervan have shown that oligonucleotide-EDTA•Fe(II) probes containing 5-bromouracil and 5-methylcytosine bind and cleave at the target site $dA_5(GA)_5$ with specificity comparable to those of their thymine-cytosine analogs, but with greater affinities and over an extended pH range (5). However, because the protonation of N3 is still required for 5-methylcytosine, triple helix formation at consecutive G-rich sequences is still limited over a wide range of pH. Recently, an oligonucleotide-EDTA•Fe(II) probe containing 3-methyl-5-amino-pyrazolo(4, 3-d)pyrimidine-7-one (**P1**) was shown to bind and cleave duplex DNA containing the sequence $dA_4GA_4G_6A$ with specificity comparable to 5-methylcytosine, but with greater affinities and over an extended pH range (22). This finding allows the recognition of the consecutive G-rich double helical DNA via triple helix formation over an extended pH range.

Less well understood is purine oligonucleotide recognition of double helical DNA (purine•purine•pyrimidine triplets) (23-26). Purine oligonucleotides have been postulated to bind parallel to the purine strand in duplex DNA by triple helix formation (A•AT and G•GC base triplets) (26). α-Oligonucleotides have also been observed to form triple-stranded structures (27, 28).

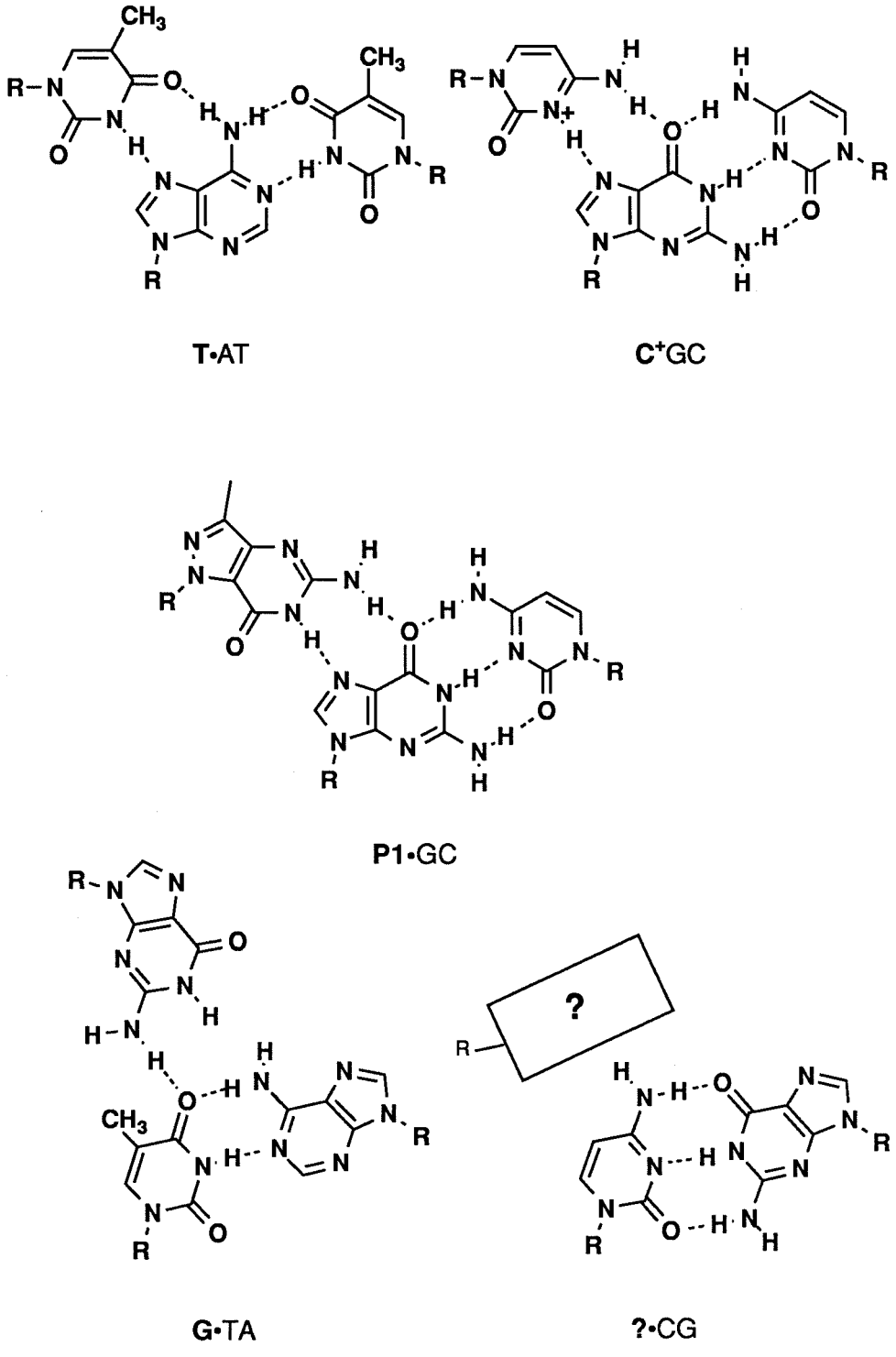

Figure 1. (**Top**) Isomorphous base triplets **T**•AT and **C+**•GC. (**Middle** and **Bottom**) New base triplets **P1**•GC, **G**•TA and unknown base triplet **?**•CG.

Extension of triple helix formation. Because homopyrimidine, homopurine and synthetic base oligonucleotides limit triple helix formation to homopurine tracts containing AT and GC base pairs, it is desirable to study whether oligonucleotides can be designed to bind to all four base pairs of DNA (Figure 1). A general solution would allow targeting of oligonucleotides (or their analogs) to any given sequence. Recently, Horne and Dervan have shown that the incorporation of a 3'-3' phosphodiester and 1,2-dideoxy-D-ribose linker permits construction of a pyrimidine oligonucleotide that binds to a stretch of purines on one strand of the DNA double helix and then crosses over the major groove to bind to a stretch of purines on the opposite side of the major groove (29). This work extended the triple helix formation to mixed DNA sequences of the type $(purine)_nNN(pyrimidine)_n$. Griffin and Dervan found that guanine contained within a pyrimidine oligonucleotide specifically recognized thymine•adenine base pairs (G•TA base triplets, Figure 1) (30). Although there are sequence-composition effects, this finding extended specific recognition within the pyrimidine triple helix motif to three of the four possible base pairs in double helical DNA.

It is our goal to design and synthesize a novel base that can bind CG base pairs strongly and selectively for the extension of triple helix formation to the four possible base triplets in double helical DNA. From model building studies we have chosen isoguanosine analogs (**G'** and **G"**), 3-methyl-5-amino-pyrazolo(4,3-d)pyrimidine-7-one analogs (P1 and P2), and cytosine analogs (**C**, **C'** and **C"**) as initial targets (Figure 2) and an abasic compound as a reference for the relative recognition. Enzymatic digestion of oligonucleotides containing synthetic bases gives their corresponding

nucleosides as detected by HPLC except oligonucleotides containing 2-pyrimidinone (**C'**). Oligonucleotides containing 2-pyrimidinone gave the α-anomer, β-anomer and pyrimidinone, which indicates that the β-anomer undergoes anomerization and acid catalyzed hydrolysis during oligonucleotide synthesis. Isoguanosine analogs **G'** and **G"**, and isocytosine (**C"**) have been found to recognize CG base pairs very weakly. However, cytosine, 2-pyrimidinone (a mixture of α-anomer, β-anomer and acid and

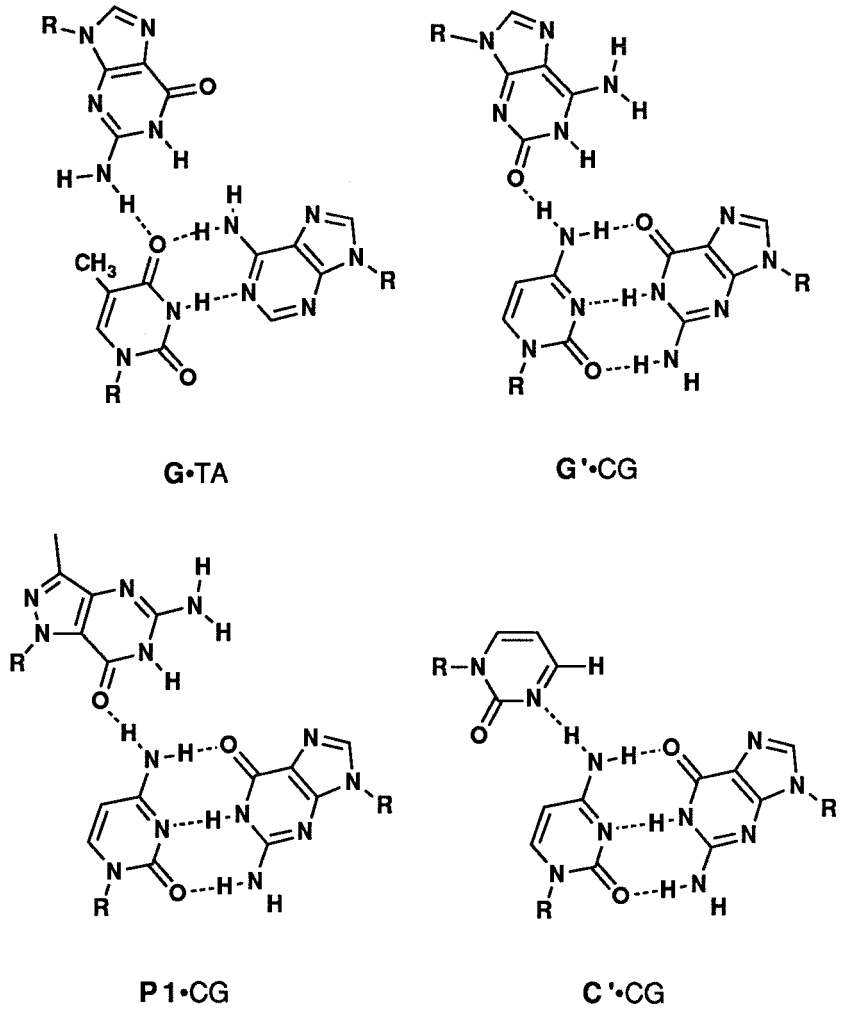

Figure 2. Possible base triplets **G•TA**, **G'•CG**, **P1•CG** and **C'•CG**.

acid hydrolyzed products) and P1 have been found to recognize moderately CG base pairs relative to T•AT, C•GC, P1•GC, and G•AT. The utility of cytosine, 2-pyrimidone, and P1 is demonstrated in the site-specific binding of an 18 base pair sequence in SV40 DNA and 16 base pair sequence in HIV DNA containing all four base pairs.

Result and Disscussion

Synthesis of nucleosides. The synthetic scheme of phosphoramidite **9** (**G''**) is shown in Figure 3. 5-Methylamino-1-(2',3',5'-triacetyl-β-D-ribofuranosyl)imidazole-4-carboxamide **1** was prepared by the published method (31). Dehydration of compound **1** in the presence of phosphorous oxychloride gave nitrile **2** in 75% yield (32). Compound **2** was reacted with benzoyl isocyanate and subsequent annulation gave 3-methylisoguanosine (**3**). Benzoyl protected 3-methylisoguanosine **4** was prepared by the known method from **3** (33). Compound 4 was protected with 1,3-dichloro-1,1,3,3-tetraisopropylsiloxane ($TIPDCl_2$) to give compound **5** (34) and subsequent methylation of **5** gave compound **6** (35). Deprotection of **6** by tetrabutylammoniun fluoride (TBAF) gave compound **7**. The 5' hydroxyl group of compound **7** was protected with 4,4-dimethoxytritylchloride (DMTCl) to give compound **8**, and the reaction of **8** with 2-cyanoethyl-N,N-diisopropylchlorophosphoramidite afforded the phosphoramidite **9** (**G''**).
1-(2'-deoxy-5'-dimethoxytrityl-β-D-ribofuranosyl)-2(1H)-pyrimidinone-3'-N, N'-diisopropylamino-2-cyanoethylphosphoramidite (**C'**, **10**) was synthesized according to the method of Rolf Altermatt and Christoph Tamm (Figure 4) (36-38). N^2-Benzoyl-(2'-deoxy-5-dimethoxytrityl-β-D-ribofuranosyl)-isocytidine-3'-N,N'-diisopropylamino-2-cyanoethylphosphoramidite (**C''**, **11**) was prepared by the published method (39,40). Synthesis of protected isoguanosine (**G'**) and 3-methyl-5-amino-pyrazolo(4, 3-d)pyrimidine-7-one phosphoramidites (**P1** and **P2**) was prepared according to the method of J.S. Koh and P.B. Dervan (22). Abasic phosphoramidite (5-O-(4,4'-dimethoxytrityl)-1,2-dideoxy-D-ribose-3-(β-cyanoethyl-N, N-diisopropyl)-phosphoramidite) (**Ab**) was a generous gift from Dr. David Horne.

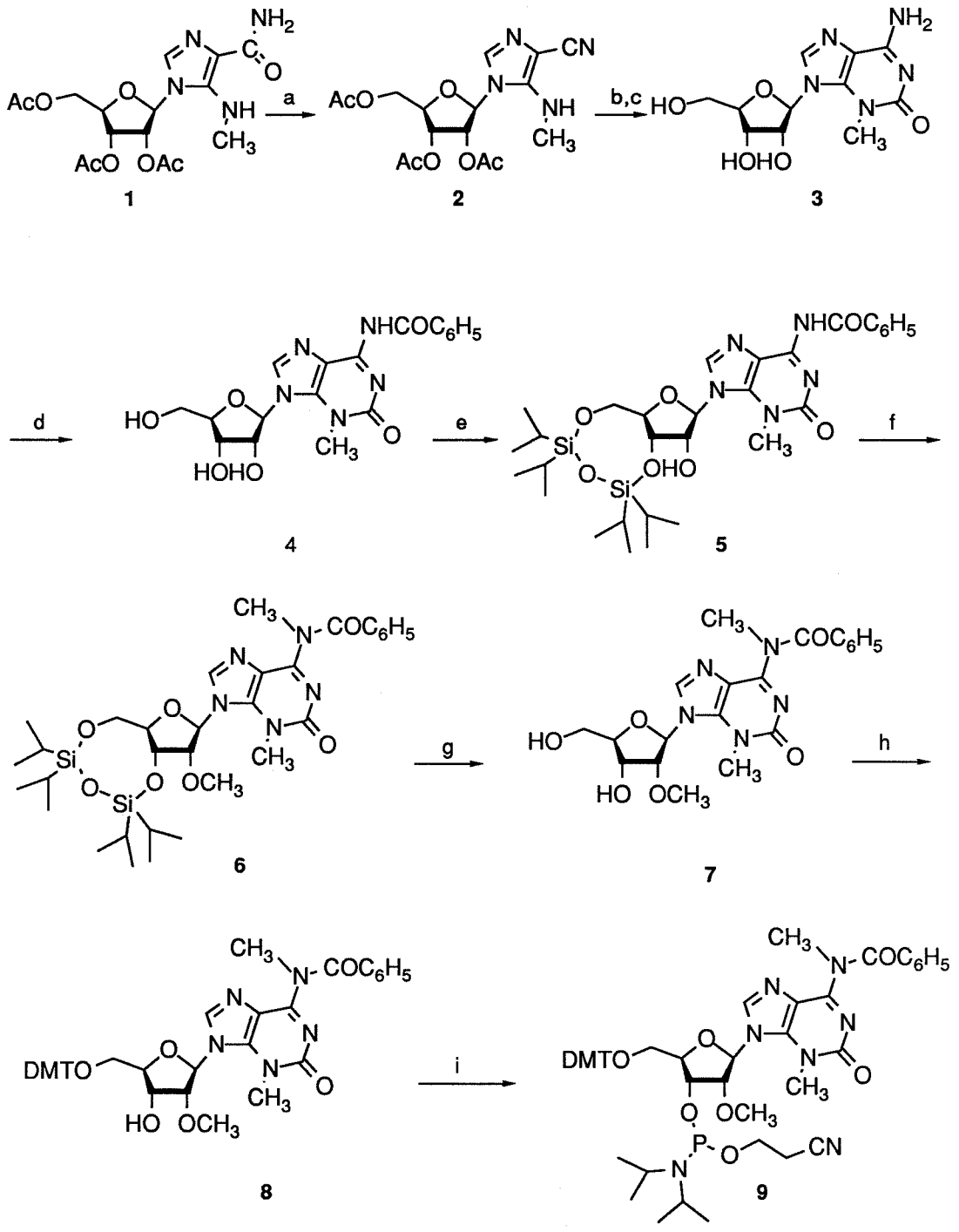

Figure 3. Synthetic scheme of phosphoramidite **9** (**C'**). a) $POCl_3$/TEA b) $OCNCOC_6H_5$/DMF c) NH_4OH/EtOH d) BzCl/py/NaOH e) $TIPDCl_2$/py f) CH_3I/Ag_2O g) TBAF/THF h) DMTCl/py i) 2-cyanoethyl N, N-diisopropylchlorophosphoamidite/diisopropylamine/methylene chloride.

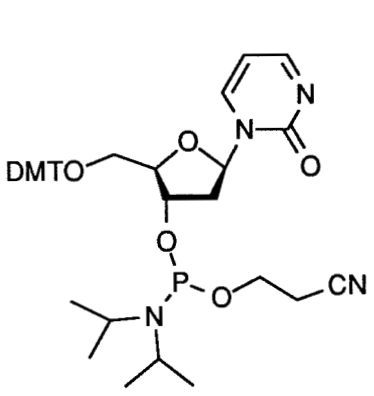

10

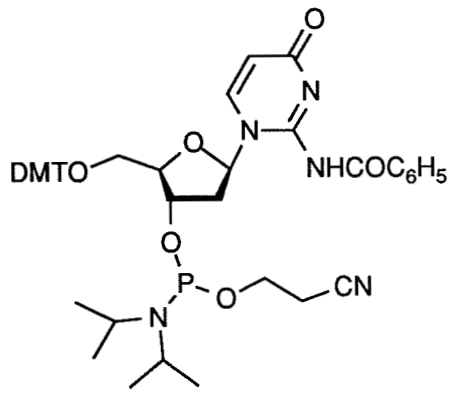

11

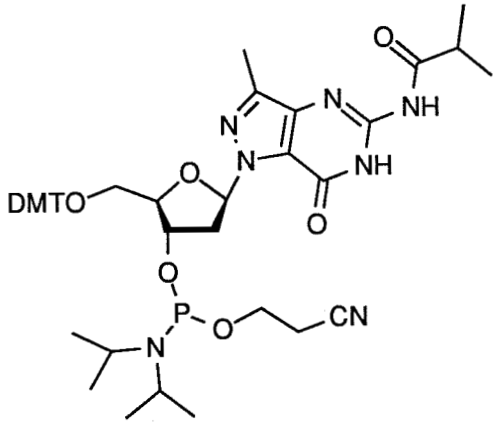

P1

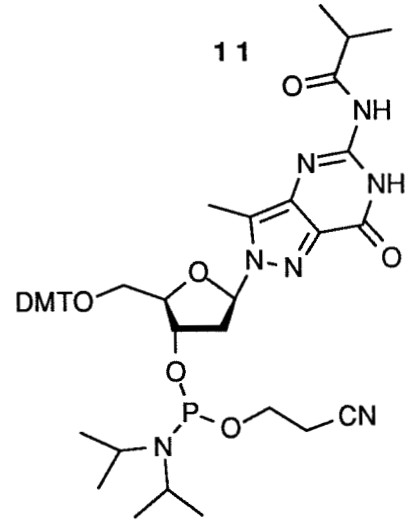

P2

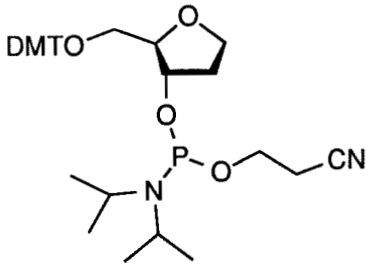

Ab

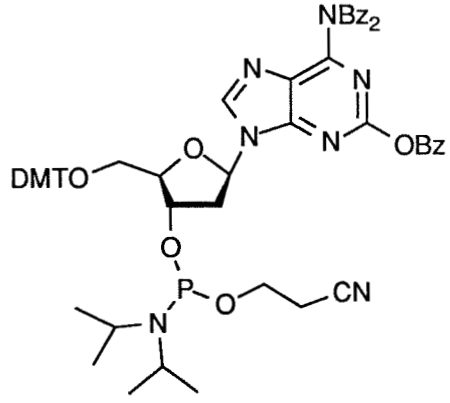

G'

Figure 4.The structures of phosphoramidites **10** (**C'**) , **11** (**C"**), **P1**, **P2**, **Ab** and **G'**.

The chemical structures of **C'**, **C"**, **P1**, **P2**, **Ab**, **G'** are shown in Figure 4.

Synthesis of oligonucleotides containing novel base heterocycles. Oligonucleotides **12-31** were synthesized using β-cyano-phosphoramidite chemistry (41). The novel base phosphoramidites P1, P2, G" C" and the abasic phosphoramidite were coupled with an efficiency equal to A, G, C and T phosphoramidites, but deoxyriboisguanosine (**G'**) and 2-pyrimidinone (**C'**) showed lower yields due to depurination, anomerization or depyrimidination during oligonucleotide synthesis (42). It has been reported that deoxyriboisoguanosine derivatives and 2-pyrimidinone are acid labile (42). Because oligonucleotides **12-31** contain thymidine-EDTA (dT*), 0.1N NaOH was substituted in the deprotection steps for NH_4OH to circumvent possible aminolysis of the T* ethylester (43).

Enzyme digestion product analysis of oligonucleotides. The stability of the synthetic bases during automated synthesis and base deprotection is very important. The oligonucleotide and its composition of bases obtained from the oligonucleotide synthesizer can be analyzed by HPLC to ensure that the individual base is not chemically changed during the synthesis. Purified oligonucleotides were digested with snake venom phosphodiesterase and calf intestine alkaline phosphatase to give corresponding nucleosides. Snake venom phosphodiesterase treatment of oligonucleotides gives 5'-monophosphate nucleotides, and subsequent calf intestine alkaline phosphatase treatment of the mononucleotide gives the corresponding nucleosides. HPLC analysis of the enzyme digested products was carried out on a C18 reverse phase HPLC column using 10 mM ammonium phosphate pH 5.1/8% MeOH as the eluent. All of the oligonucleotides gave only their corresponding nucleosides except for oligonucleotides containing **C'**.

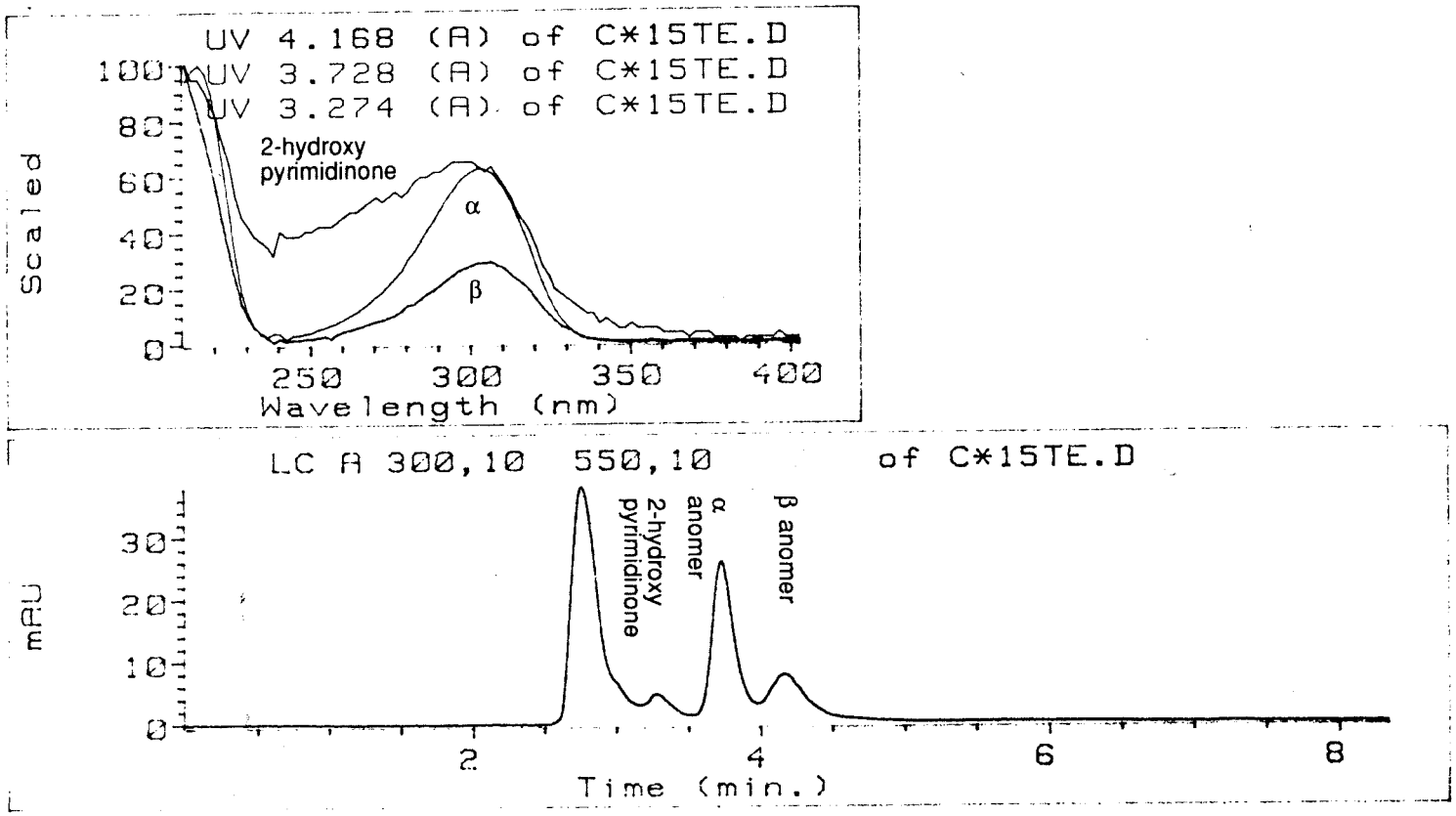

Figure 5. HPLC chromatogram (monitored at 300 nm) of the mixture of the enzyme digested products of oligonucleotide **16** (5'-**TTTTT*TTC'TTTTTTT**-3'). The samples were eluted on a C18 reverse phase column with 8% MeOH in 10 mM ammonium phosphate pH 5.1 at a flow rate of 1 mL/min. The UV-Vis spectra of the different peaks are recorded in the upper left panel.

Oligonucleotides containing **C'** gave the 2-hydroxypyrimidinone base, the β-anomer and α-anomer (Figure 5). It is believed that 1-(β-D-2'-deoxyribosyl)-2-pyrimidinone undergoes anomerization during the deprotection of DMT by trichloroacetic acid and then loses the base slowly in water (42). The proposed mechanism of anomerization is described in Figure 6. The β-anomer can form the oxonium ion in the presence of acid. Subsequent nucleophilic reaction can give a mixture of anomers.

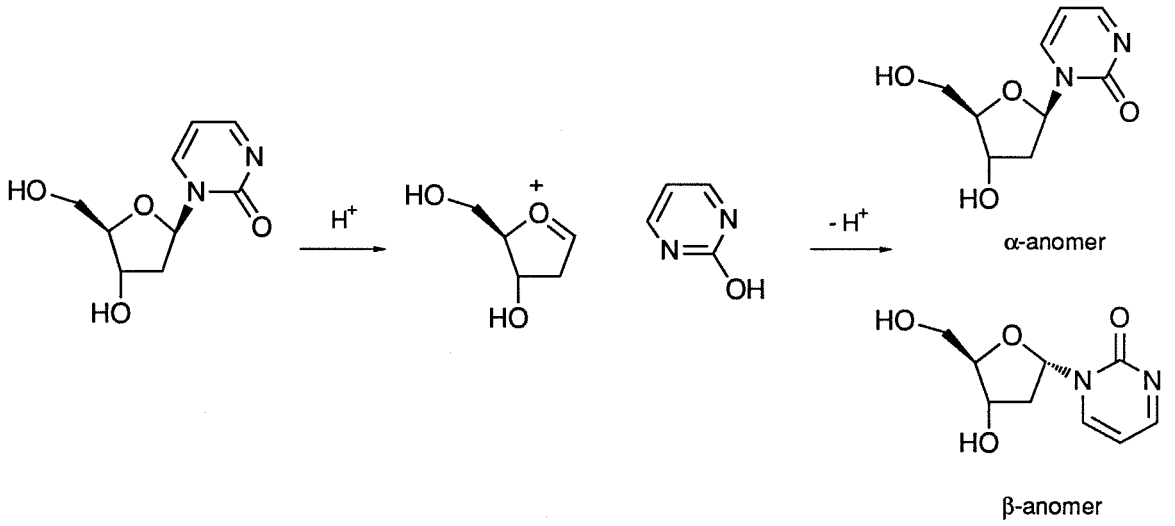

Figure 6. The possible mechanism of anomerisation of 1-(β-D-2'-deoxyribosyl)-2-pyrimidinone.

Binding-cleavage of oligonucleotide to 30 mer complex. The relative affinities of the bases thymidine (T) , cytosine (C), guanosine (G), isocytosine (**C"**), 2-pyrimidinone (**C'**, a mixture of α , β- anomer and hydrolyzed products), P1, P2, Ab, isoguanosine (**G'**), and 3-methyl-N^6-methyl-isoguanosine (**G"**) for all possible base pair combinations within a pyrimidine triple helix motif were examined (Figure 7a). The use of oligonucleotides equipped with the DNA cleaving moiety thymidine-

EDTA•Fe(II) (T*) allowed the relative stabilities of triple helix formation between 30 base pair (bp) DNA duplexes containing the sites $d(A_7XA_7)/d(T_7YA_7)$ (XY=AT, GC, TA or CG) and a series of 15 nt oligonucleotides differing at one base position $d(T_7NT_7)$(N=T, C, G, C', C'', P1, P2, Ab, G' and G'') to be determined by the affinity cleaving method. The 30-bp duplexes were labeled with ^{32}P at the 5' end of the target site strand $d(T_7YT_7)$. The DNA binding-cleaving reactions of oligonucleotides **12-21** were performed under conditions that were sensitive to the stability of the base triplet formed upon hybridization of a T_7NT_7 oligonucleotide and triple helix formation (pH 7.4, 35°C, 40% ethanol). The most intense cleavage patterns were observed for the conditions N=T, XY=AT, N=C, XY=GC, N=P1, XY=GC, N=C', XY=CG, N=G, XY=TA (Figure 7b, c and d). The cleavage observed for three of these combinations represents the previously known ability of T to bind AT, C to bind GC, P1 to bind GC and G to bind TA base pairs. P1 strongly recognizes the GC base pair as reported (22). Strong and selective cleavage patterns are observed for the base C' in C'•CG base triplets, while moderate cleavage patterns are observed for the base P1 in P1•CG, Ab in Ab•CG and C in C•CG triplet. Isoguanosine analogs G' and G'' show selectivity for GC recognition but not for CG recognition. The selectivty of C' in the C'•CG triplet is due to the removal of the amino group of C. It is not clear why cleavage is stonger in the C'•CG triplet than in the C•CG triplet, since the oligonucleotide contains a mixture of the α-anomer, β-anomer and hydrolyzed base. Although isocytosine can accept one hydrogen bond at N3 in C''•CG, C'' shows only very weak cleavage and is selective for AT and CG base pairs over GC and TA base pairs. From model building studies, it is possible that the C5

hydrogen in the C of the Watson-Crick strand can interact with the N2 hydrogen in third strand in the C"•CG triplet (Figure 8). The bases P1 and C" were designed to form one hydrogen bond each to the CG base pair, as is postulated for the G•TA and C•CG triplets, but the cleavage efficiency is low. The difference in cleavage efficiency might be due to the different hydrogen bond acceptor, base stacking or the backbone position.

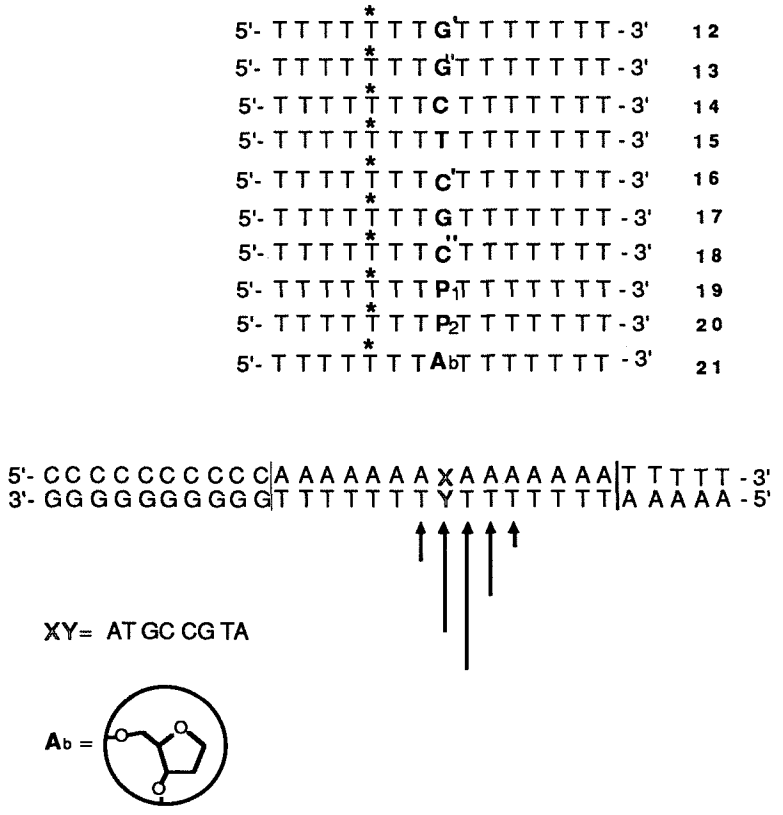

Figure 7a. (**Above**) Sequence of oligonucleotides-EDTA (**12-21**) where T* is the position of thymidine-EDTA. The oligonucleotides differ at one base position indicated in bold type. (**Below**) The box indicates the double-stranded sequence bound by oligonucleotide-EDTA•Fe(II) (**12-21**). The Watson-Crick base pair (AT, GC, TA or CG) opposite the variant base in the oligonucleotide is also in bold type. The arrow indicates a cleavage site and intensity.

Figure 7b. Autoradiogram of the 20 percent denaturing polyacrylamide gel. The cleavage reactions were carried out by combining a mixture of oligonucleotide-EDTA (2μM), spermine (1 mM), and Fe(II) (25μM) with the ^{32}P labeled 30-mer duplex (40,000 cpm) in a solution of tris-acetate (25 mM pH 7.4), NaCl (100 mM), calf thymus DNA (100μM bp), and 40% ethanol and incubating at 35°C for 1 hour. Cleaving reactions were initiated by the addition of DTT (3 mM) and allowed to proceed for 6 h at 35°C. The reactions were frozen and lyophilized and the cleavage products were analyzed by gel electrophoresis. Lanes 1 to 14: duplex containing 5' end-labeled($A_5T_7YT_7G_{10}$). Lane 1: control showing intact 5'labeled 30 bp DNA standard obtained after treatment according to the cleavage reaction in the absence of oligonucleotide-EDTA. Lane 2: products of Maxam-Gilbert G+A sequnce reaction. Lanes 3 to 18: DNA cleavage products produced by oligonucleotide-EDTA•Fe(II) (**12**, **13** and **14**); **12** (lanes 3 to 6); **13** (lanes 7 to 10); **14** (lanes 11 to 14); XY=AT (lanes 3, 7,and 11); XY=GC (lanes 4, 8, and 12); XY=CG (lanes 5, 9, and 13); XY=TA (lanes 6, 10, and 14).

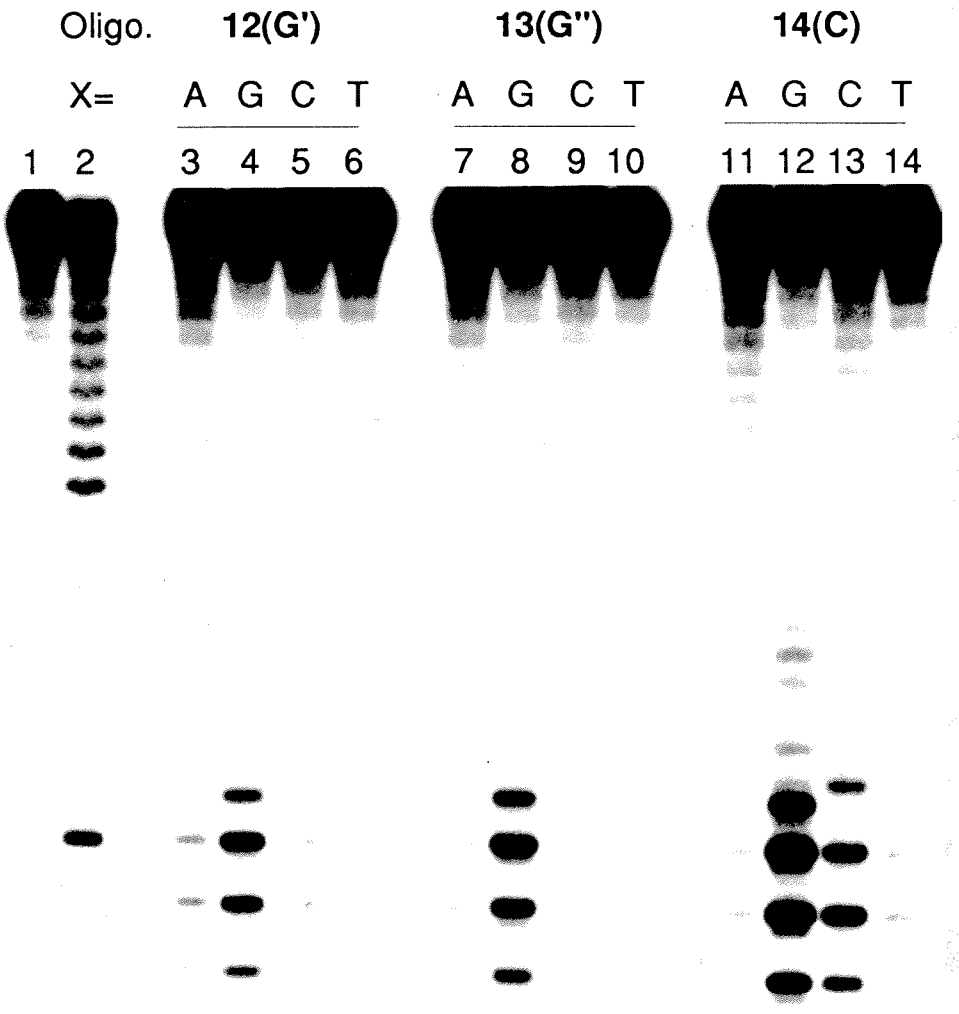
Oligo.
12(G')
13(G")
14(C)
X=
A G C T
A G C T
A G C T
1 2
3 4 5 6
7 8 9 10
11 12 13 14

Figure 7c. Autoradiogram of the 20 percent denaturing polyacrylamide gel. The cleavage reactions were carried out by combining a mixture of oligonucleotide-EDTA (2 μM), spermine (1 mM), and Fe(II) (25 μM) with the ^{32}P labeled 30-mer duplex (40,000 cpm) in a solution of tris-acetate (25 mM pH 7.4), NaCl (100 mM), calf thymus DNA (100 μM bp), and 40% ethanol and incubating at 35°C for 1 hour. Cleaving reactions were initiated by the addition of DTT (3.3 mM) and allowed to proceed for 6 h at 35°C. The reactions were frozen and lyophilized and the cleavage products were analyzed by gel electrophoresis. Lanes 1 to 22: duplex containing 5' end-labeled($A_5T_7YT_7G_{10}$). Lane 1: control showing intact 5' labeled 30 bp DNA standard obtained after treatment according to the cleavage reaction in the absence of oligonucleotide-EDTA. Lane 2: products of maxam-Gilbert G+A sequnce reaction. Lanes 3 to 22: DNA cleavage products produced by oligonucleotide-EDTA•Fe(II) (**14-18**); **14** (lanes 7 to 10); **15** (lanes 3 to 6); **16** (lanes 11 to 14); **17** (lanes 15 to 18); **18** (lanes 19 to 22). XY=AT (lanes 3, 7, 11, 15, and 19); XY=GC (lanes 4, 8, 12, 16, and 20); XY=CG (lanes 5, 9, 13, 17, and 21); XY=TA (lanes 6, 10, 14, 18, and 22).

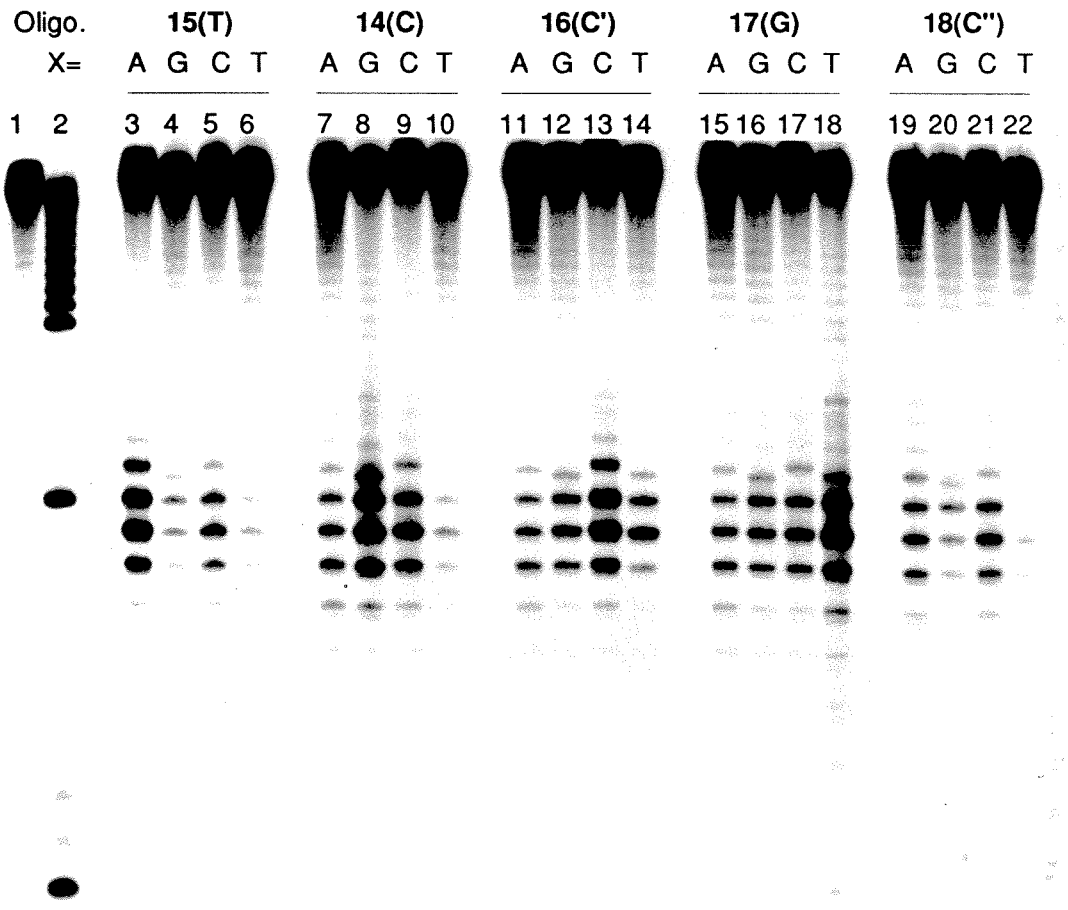
Oligo.
X=
15(T)
A G C T
14(C)
A G C T
16(C')
A G C T
17(G)
A G C T
18(C")
A G C T
1 2
3 4 5 6
7 8 9 10
11 12 13 14
15 16 17 18
19 20 21 22

Figure 7d. Autoradiogram of the 20 percent denaturing polyacrylamide gel. The cleavage reactions were carried out by combining a mixture of oligonucleotide-EDTA 2 μM), spermine (1 mM), and Fe(II) 25 μM) with the ^{32}P labeled 30-mer duplex (40,000 cpm) in a solution of tris-acetate (25 mM pH 7.4), NaCl (100 mM), calf thymus DNA (100 μM bp), and 40% ethanol and incubating at 35°C for 1 hour. Cleaving reactions were initiated by the addition of DTT (3.3 mM) and allowed to proceed for 6 h at 35°C. The reactions were stopped, frozen and lyophilized, and the cleavage products were analyzed by gel electrophoresis. Lanes 1 to 18: duplex containing 5' end-labeled($A_5T_7YT_7G_{10}$). Lane 1: control showing intact 5' labeled 30 bp DNA standard obtained after treatment according to the cleavage reaction in the absence of oligonucleotide-EDTA. Lane 2: products of Maxam-Gilbert G+A sequnce reaction. Lanes 3 to 18: DNA cleavage products produced by oligonucleotide-EDTA•Fe(II) (**14**, **19-21**); **14** (lanes 3 to 6); **19** (lanes 7 to 10); **20** (lanes 11 to 14); **21** (lanes 15 to 18). XY=AT (lanes 3, 7, 11, and 15); XY=GC (lanes 4, 8, 12, and 16); XY=CG (lanes 5, 9, 13, and 17); XY=TA (lanes 6, 10, 14, and 18).

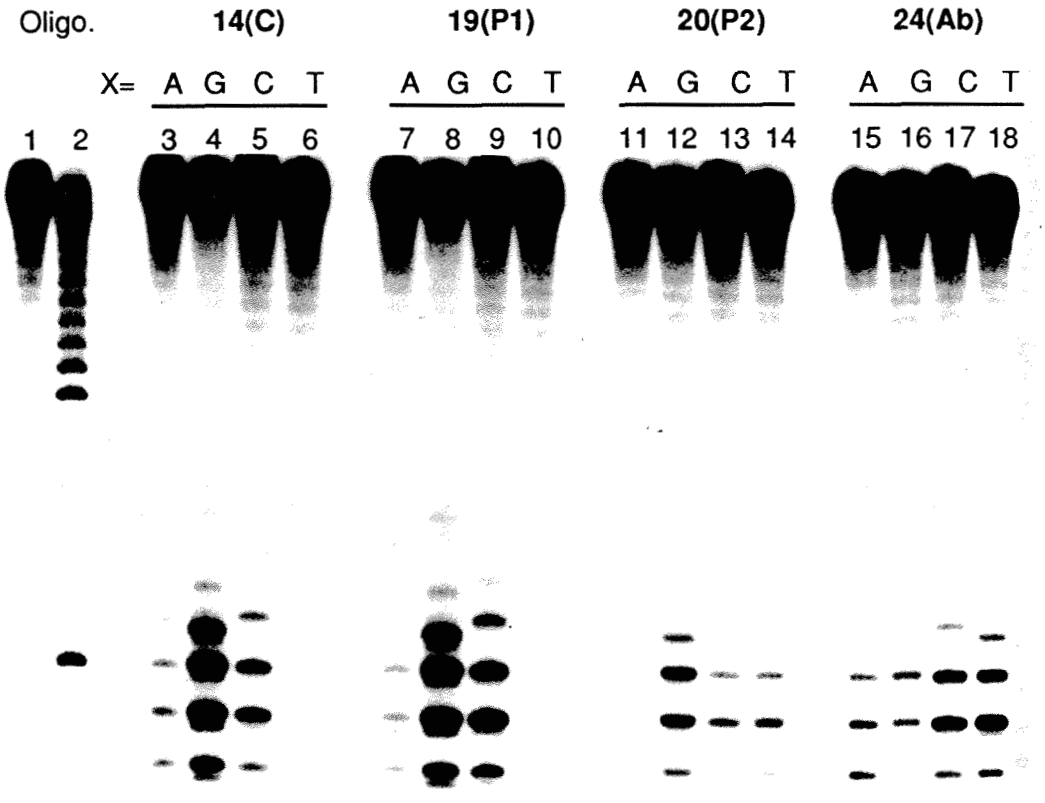
Oligo.
14(C)
19(P1)
20(P2)
24(Ab)
X= A G C T A G C T A G C T A G C T
1 2 3 4 5 6 7 8 9 10 11 12 13 14 15 16 17 18

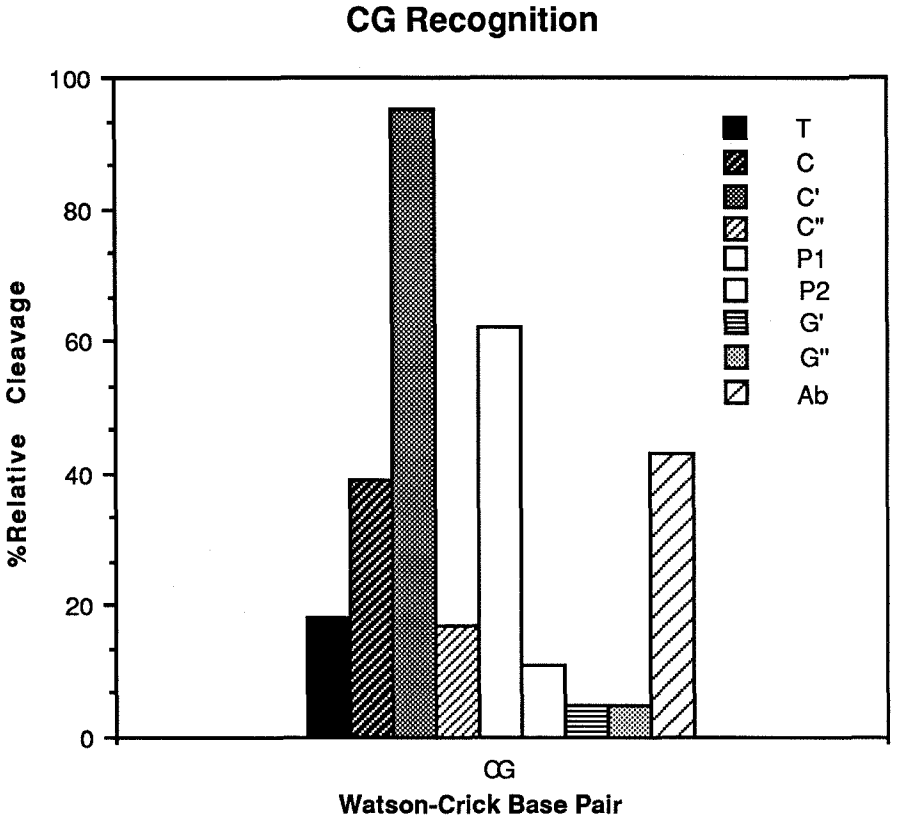

Figure 7e. Bar graph representing the relative cleavage data from densitometric analysis of Figures 7b, 7c and 7d. 36 base triplets were examined for binding specificity compatible with the pyrimidine triple helix motif shown by the experiment described in Figures 7b, c and d.

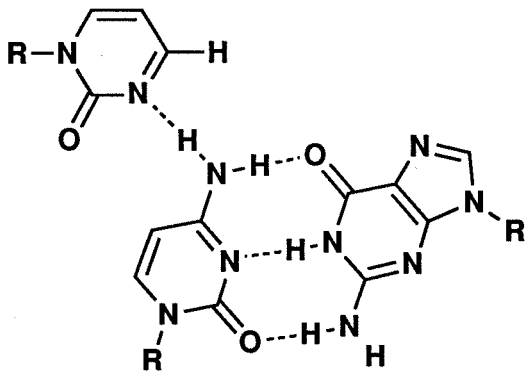

C '•CG

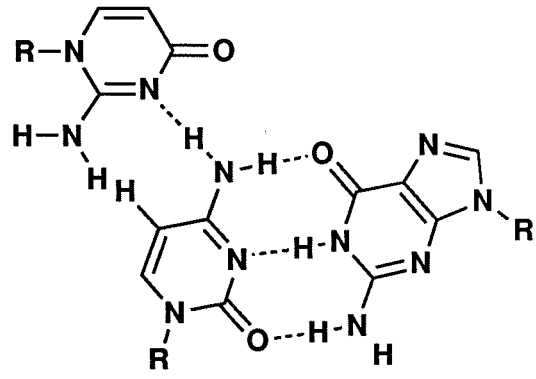

C"•CG

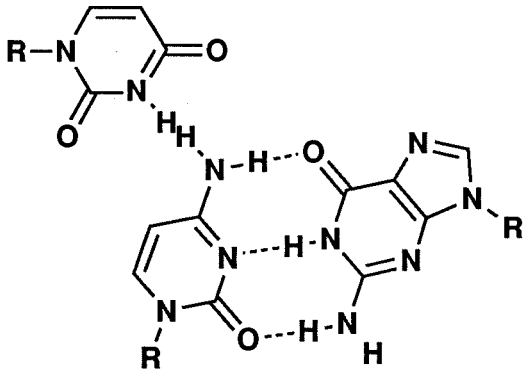

T•CG

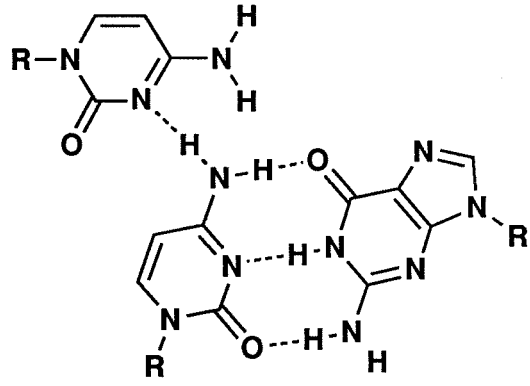

C•CG

Figure 8. Possible base triplets C"•CG, C'•CG, T•CG and C•CG triplets. For each base triplet the positioning of the third base with respect to Watson-Crick base pair is based on forming possible hydrogen bonds with the anti conformation at the glycosidic link.

5'-T* T G T T T C C T C T C T T C T-3' **22**
5'-T* T G T T T C C T C T C T T C' T-3' **23**
5'-T* T G T T T C C T C T C T T P1 T-3' **24**

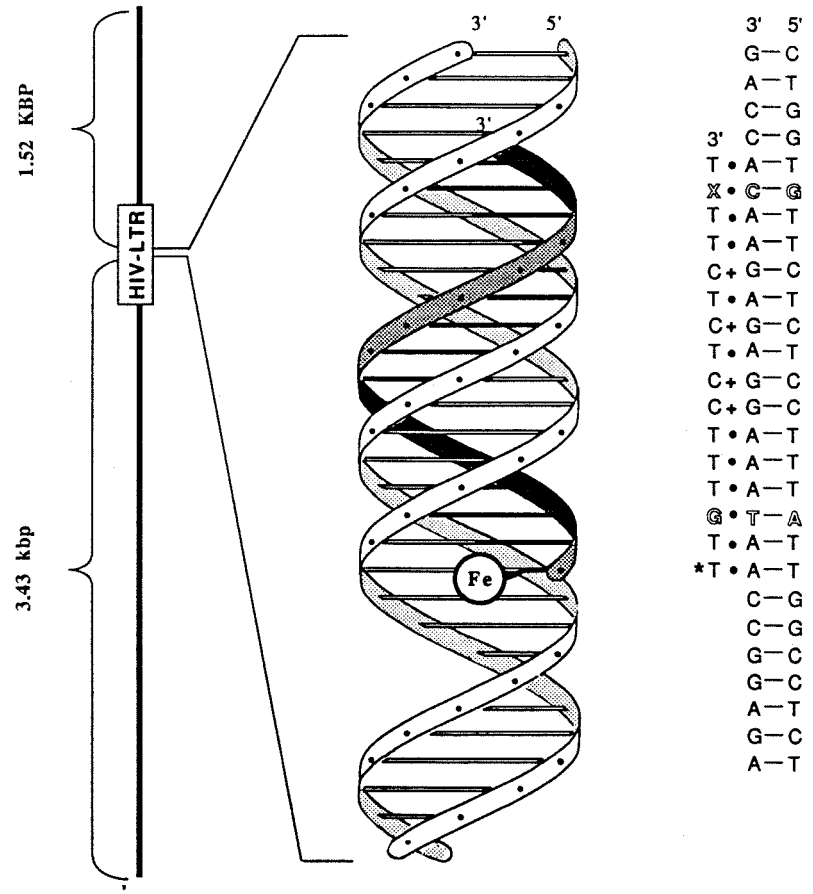

Figure 9a. (**Top**) Oligonucleotides **22-24** constructed from deoxyribonucleotide phosphoramidites containing cytosine (C), 2-pyrimidinone (C'), thymidine, P1 and thymidine-EDTA (T*). (**Bottom**) Coarse resolution pattern for cleavage of plasmid DNA (4.95 kbp) by oligonucleotides-EDTA **22-24** with a simplified model of the triple helical complex between oligonucleotids **22-24** and a 16 base pair single site.

Figure 9b. Autoradiogram of double strand cleavage of pHIV-CAT DNA (4.95 kbp) analyzed on a 0.9% agarose gel. The reactions were carried out by combining a mixture of oligonucleotides-EDTA **22-24** (2 μM), spermine 1 mM), and Fe(II) (2 μM) with the ^{32}P labeled linearized plasmid [~100 nM (bp) (~40,000 cpm)] in a solution of tris-acetate (25 mM pH 6.2, 6.6, 7.0, 7.4), NaCl (100 mM), calf thymus DNA [100 μM (bp)]. Reactions were incubated for 1 h at 25°C, initiated by the addition of ascorbate (1 mM) and allowed to proceed for 10 h at 25°C. The reactions were stopped by precipitation with ethanol and the cleavage products were analyzed by agarose gel electophoresis (120 V, BPB run near the bottom of the gel). Lanes 1 to 14: pHIV-CAT linearized with BamHI and 3'-end labeled at both ends. Lane 1: control containing no oligonucleotide-EDTA•Fe(II). Lane 2: DNA size markers obtained by digestion of BamHI linearized pHIV-CAT with HindIII and XhoI: 4950 (undigested), 3725, 3003, 1947, and 1225 bp. (Lanes 3 to 6) DNA cleavage products produced by **22**•Fe(II). (Lanes 7 to 10) DNA cleavage products produced by **23**•Fe(II). (Lanes 11 to 14) DNA cleavage products produced by **24**•Fe(II). (Lanes 3, 7 and 11) at pH 6.2, (lanes 4, 8 and 12) at pH 6.6, (lanes 5, 9 and 13) at pH 7.0, (lanes 6, 10 and 14) at pH 7.4.

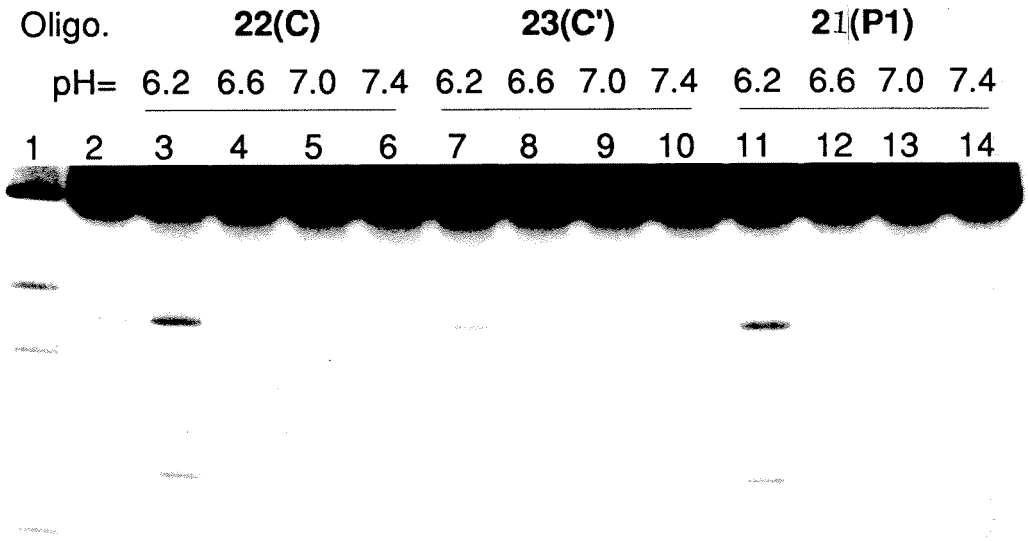
Oligo.
22(C)
23(C')
21(P1)
pH=
6.2 6.6 7.0 7.4 6.2 6.6 7.0 7.4 6.2 6.6 7.0 7.4
1 2 3 4 5 6 7 8 9 10 11 12 13 14

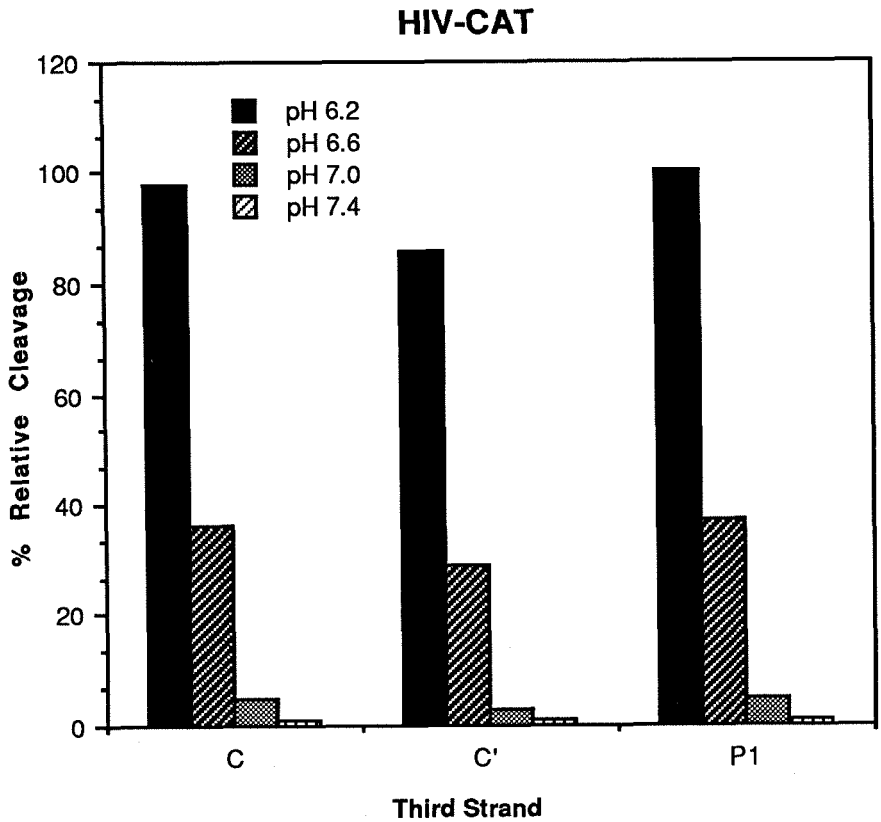

Figure 9c. Bar graph presenting the relative cleavage data from the densitometric analysis of Figure 9b.

Site-specific double strand cleavage of pHIV-CAT plasmid DNA. The ability of oligonucleotides **22-24** to cause site-specific double strand breaks in HIV-CAT plasmid DNA is documented in Figure 9a. pHIV-CAT was digested with Bam HI to produce a 4.95 kbp fragment, which contained the 3' long terminat repeat (LTR) of HIV with the site d(AA$\mathbb{T}$AAAGGAGAGAA$\mathbb{C}$A) located 1.52 kbp and 3.43kbp from the ends. Cleavage at this site demonstrates binding to a sequence containing all four base pairs. The ^{32}P end labeled DNA was allowed to react with

oligonucleotide-EDTA•Fe(II) in the presence of ascorbate at 30°C (pH 6.2 to 7.0). Separation of the cleavage products by agarose gel electrophoresis revealed one major cleavage site producing two DNA fragments, 1.52 and 3.43 kb in size (Figure 9b). The cleavage efficiency by oligonucleotides **22-24** was very sensitive to pH, and very little cleavage was observed above pH 6.6 (Figure 9b). Interestingly, oligonucleotide-EDTA•Fe(II) containing 2-pyrimidinone (**23**) does not show significantly strong cleavage efficiency. This finding is not consistent with the oligonucleotide data where the cleavage intensity observed for the C'•CG base triplet is greater than for the C•CG and P1•CG base triplets.

Cleavage of SV40 PpuMI-BglI restriction fragment at a site containing a TA and CG base pair. The cleavage of a 596 bp SV40 restriction fragment by the oligonucleotides-EDTA•Fe(II) series **25-28** (5'-T*$T_2GT_4CTNT_5CT$-3') was examined (Figures 10a, b, and c). This restriction fragment contains the 18-bp sequence d(AAA**T**AAAGA**C**AAAAAGA), which represents a purine-rich site containing two pyrimidines (T and C). Cleavage at this site demonstrates binding of a sequence containing all four base pairs. The cleavage efficiencies of oligonucleotides **25-28,** which differ at one base position opposite the CG Watson-Crick base pair, were examined under conditions sensitive to the stability of the base triplets at the CG sites (pH 7.4, 37°C). Oligonucleotides-EDTA **26** (C•CG) and **27** (P1•CG) produced the most significant site specific cleavage on the 596-bp fragment. Oligonucleotides-EDTA•Fe(II) **25** (T•CG) and **28**(P2•CG) show only moderate cleavage. This finding is consistent with oligonucleotide data where the cleavage intensities observed for the T•CG and P2•CG base triplets are very weak.

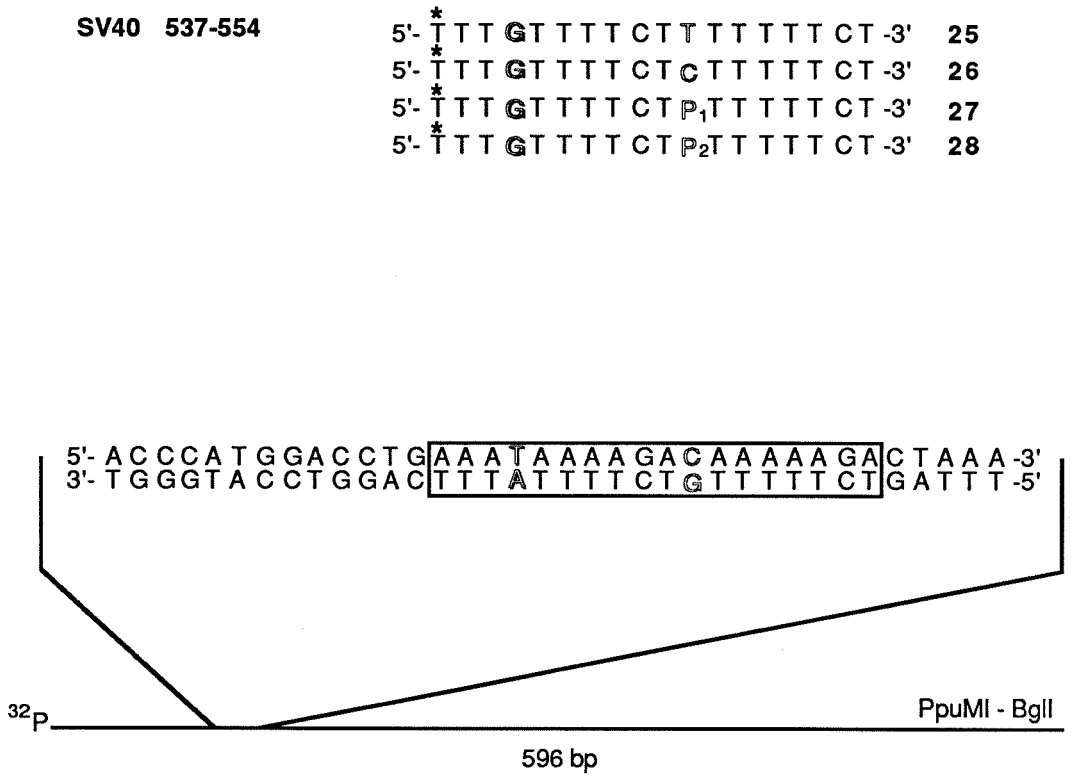

Figure 10a. (**Above**) Sequence of oligonucleotides-EDTA **25-28** where T* is the position of thymine-EDTA. The oligonucleotides differ at one base position indicated by bold type. (**Below**) The box indicates the double strand sequence bound by oligonuceotides-EDTA•Fe(II) **25-28** in SV40 restriction fragment.

Figure 10b. (Left) Autoradiogram of an 8 percent denaturing polyacrylamide gel of the cleavage reactions on a PpuMI-BglI restriction fragment of SV40 DNA. The cleavage reactions were carried out by combining a mixture of oligonucleotide-EDTA (2 μM), spermine (1 mM), and Fe(II) (25 μM) with the ^{32}P labeled restriction fragment [~100 nM(bp) (20,000 cpm)] in a solution of Tris-acetate, pH 7.4 (50 mM), NaCl (100 mM), and calf thymus DNA [100 μM (bp)]. This was incubated at 37°C for 1 hour. Cleavage reactions were initiated by the addition of DTT (3 mM) and allowed to proceed for 4 h at 37°C. The reactions were stopped by precipitation with ethanol and the cleavage products were analyzed by gel electrophoresis (BPB 30 cm). Lanes 1 to 6: 3' end-labeled PpuMI-BglI restriction fragment of SV40. Lane 1: control containing no oligonucleotide-EDTA•Fe(II). Lane 2: Maxam-Gilbert G sequencing reactions. Lanes 3 to 6: DNA cleavage products by oligonucleotide-EDTA•Fe(II) (**25-28**): **25** (lane 3); **26** (lane 4); **27** (lane 5); **28** (lane 6).

Figure 10c. (Right) Autoradiogram of an 8 percent denaturing polyacrylamide gel of the cleavage reactions on a PpuMI-BglI restriction fragment of SV40 DNA. The cleavage reactions were carried out by combining a mixture of oligonucleotide-EDTA (2 μM), spermine (1 mM), and Fe(II) (25 μM) with the ^{32}P labeled restriction fragment [~100 nM(bp) (20,000 cpm)] in a solution of Tris-acetate, pH 7.4 (50 mM), NaCl (100 mM), and calf thymus DNA [100 μM (bp)]. This was incubated at 37°C for 1 h. Cleavage reactions were initiated by addition of DTT (3 mM) and allowed to proceed for 4 h at 37°C. The reactions were stopped by precipitation with ethanol and the cleavage products were analyzed by gel electrophoresis (BPB 30 cm). Lanes 1 to 6: 5' end-labeled PpuMI-BglI restriction fragment of SV40. Lane 1: control containig nooligonucleotide-EDTA•Fe(II). Lane 2: Maxam-Gilbert G sequencing reactions. Lanes 3-6: DNA cleavage products by oligonucleotide-EDTA•Fe(II) (**25-28**); 25 (lane 3); **26** (lane 4); **27** (lane 5); **28** (lane 6).

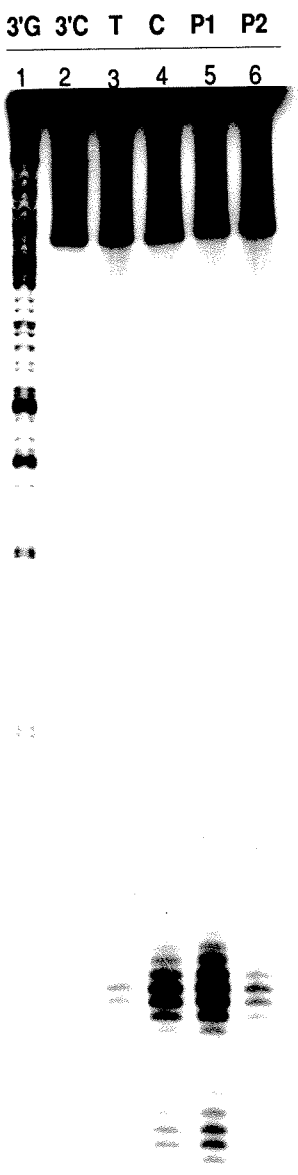
3'G 3'C T C P1 P2
1 2 3 4 5 6

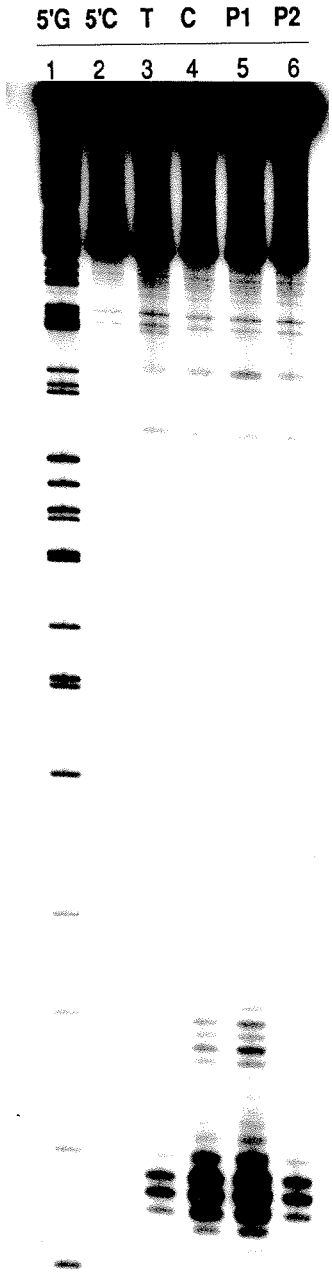
5'G 5'C T C P1 P2
1 2 3 4 5 6

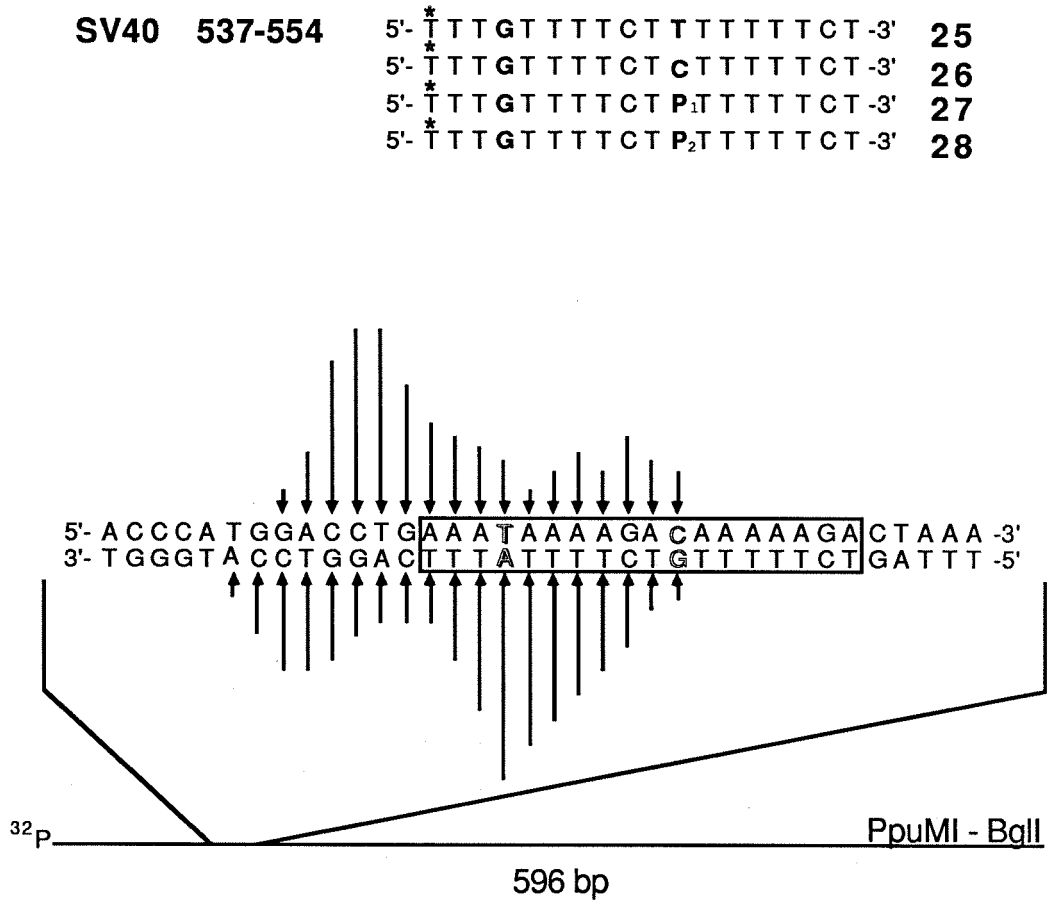

Figure 10d. (Top) Sequence of oligonucleotides-EDTA **25, 26, 27,** and **28** where T* is thymidine-EDTA.(**Below**) Histogram of the DNA cleavage patterns for oligonucleotides **27** derived from densitometry of autoradiogram in Figures 9b and c. The box indicates the original target sequence.

Double Strand Cleavage of SV40 DNA. The double strand cleavage of SV40 DNA by the oligonucleotide-EDTA•Fe(II) series **25-27, 29-31** (5'-$T^*T_2GT_4CTNT_5CT$-3') was examined. SV40 contains the 18-bp sequence d(AAA$\mathbb{T}$AAAGA$\mathbb{C}$AAAAAGA), which represents a purine-rich site containing two pyrimidines (T and C). Cleavage at this site demonstrates

binding to a sequence containing all four base pairs. The cleavage efficiencies of oligonucleotides **25, 26, 27, 29, 30,** and **31** which differ at a single position opposite a CG Watson-Crick base pair, were examined under conditions sensitive to the stability of the base triplets at the CG sites (pH 7.4, 37°C). SV40 DNA was digested with BclI to produce a 5.24 kbp fragment, which contained the sequence d(AAATAAAAGACAAAAAGA) located 2.21 kbp and 3.03 kbp from the ends. The ^{32}P end-labeled DNA was allowed to react with oligonucleotide-EDTA•Fe(II) in the presence of ascorbate (pH 7.0, 30°C or 37°C). Separation of the cleavage products by agarose gel electophoresis reveals one major cleavage site producing two DNA fragments, 2.21 and 3.03 kb in size (Figures 11a and b). Interestingly, oligonucleotide-EDTA•Fe(II) **29** which contains the abasic compound (Ab•CG) produced significant site specific cleavage, which is consistent with earlier oligonucleotide studies. Oligonucleotides-EDTA•Fe(II) **26** (C•CG) and **27** (P1•CG) also produced significant site specific cleavage. However, oligonucleotides **25, 30** and **31** did not produce significant site-specific cleavage. The effects of temperature on binding to this sequence for oligonucleotides **26, 27, 29, 30, 31** are presented in bar graph form in Figure 11d. Raising the temperature increases the stringency of triple helix formation.

5'- T T T G T T T T C T T T T T T C T - 3' **25**
5'- T T T G T T T T C T C T T T T T C T - 3' **26**
5'- T T T G T T T T C T P1 T T T T T C T - 3' **27**
5'- T T T G T T T T C T Ab T T T T T C T - 3' **29**
5'- T T T G T T T T C T C' T T T T T C T - 3' **30**
5'- T T T G T T T T C T C'' T T T T T C T - 3' **31**

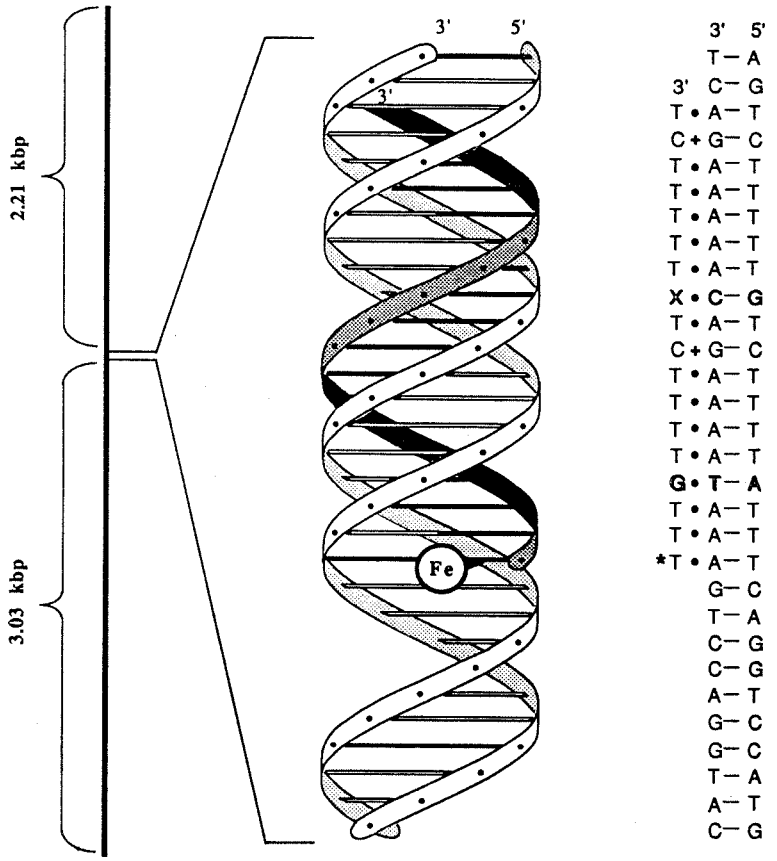

Figure 11a. (**Top**) Oligonucleotides **25, 26, 27, 29, 30** and **31** constructed from deoxyribonucleotide phosphoramidites containing cytosine(C), 2-pyrimidinone(C'), isocytidine(C''), thymidine, P1, Ab and thymidine-EDTA (T*). (**Bottom**) Coarse resolution pattern for cleavage of plasmid DNA (4.95 kbp) by oligonucleotides-EDTA **25, 26, 27, 29, 30** and **31** with a simplified model of the triple helical complex between oligonucleotides **25, 26, 27, 29, 30** and **31** (T, C , G, T*/X, X=T, C, P1, Ab, C' and C'') and an 18 base pair single site.

Figure 11b Autoradiogram of double strand cleavage of SV40 DNA (5.24 kbp) analyzed on a 0.9% agarose gel. The reactions were carried out by combining a mixture of oligonucleotide-EDTA (2 μM), spermine (1 mM), and Fe(II) (2 μM) with the ^{32}P labeled linearized plasmid [~100 nM (bp) (~40,000 cpm)] in a solution of tris-acetate (25 mM, pH 7.4), NaCl (100 mM), Calf thymus DNA [100 μM (bp)] and incubated for 1 h at the reaction temperature. Cleavage reactions were initiated by addition of ascorbate (1 mM) and allowed to proceed for 10 h at 37°C. The reactions were stopped by precipitation with ethanol and the cleavage products were analyzed by agarose gel electophoresis (BPB run near the bottom of the gel). Lanes 1-6: SV40 linearized with BclI and 3'end-labeled at both ends. Lane 1: control containing no oligonucleotide-EDTA•Fe(II). Lane 2: DNA size markers obtained by digestion of BclI linearized SV40 with HaeII and BglI: 5243 (undigested), 3305, 2778, 2465, 1938 bp. Lane 3: DNA cleavage products produced by **29**•Fe(II). Lane 4: DNA cleavage products produced by **26**•Fe(II). Lane 5: DNA cleavage products produced by **27**•Fe(II). (Lane 6) DNA cleavage products produced by **25**•Fe(II).

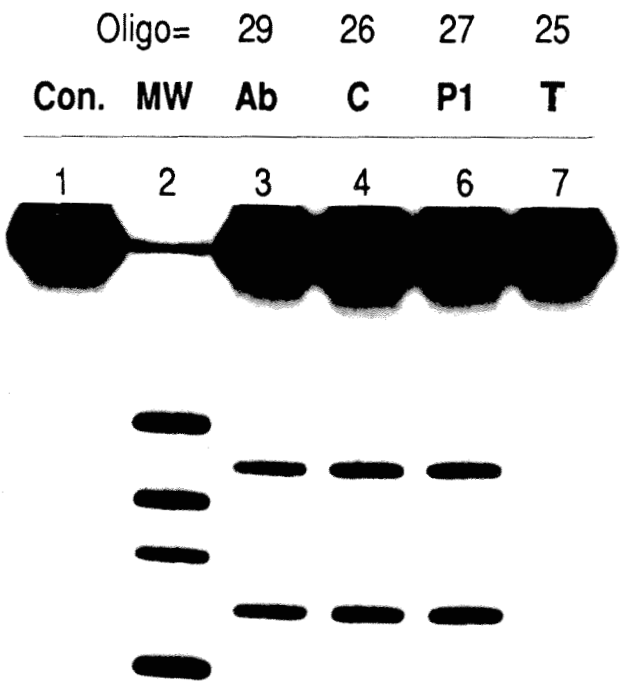
Oligo=
29
26
27
25
Con.
MW
Ab
C
P1
T
1
2
3
4
6
7

Figure 11c Autoradiogram of double strand cleavage of SV40 DNA (5.24 kbp) analyzed on a 0.9% agarose gel. The reactions were carried out by combining a mixture of oligonucleotide-EDTA (2 μM), spermine (1 mM), and Fe(II) (2 μM) with the ^{32}P labeled linearized plasmid [~100 nM (bp) (~40,000 cpm)] in a solution of tris-acetate (25 mM, pH 7.4), NaCl (100 mM), calf thymus DNA [100 μM (bp)] and incubated for 1 h at the reaction temperature. Cleavage reactions were initiated by addition of ascorbate(1 mM) and allowed to proceed for 10 h at the reaction temperature. The reactions were stopped by precipitation with ethanol and the cleavage products were analyzed by agarose gel electophoresis (BPB run near the bottom of the gel). Lanes 1-12: SV40 linearized with BclI and 3'end-labeled at both ends. Lane1: Control containing no oligonucleotide-EDTA•Fe(II). Lane 2: DNA size markers obtained by digestion of BclI linearized SV40 with HaeII and BglI: 5243 (undigested), 3305, 2778, 2465, 1938 bp. Lanes 3 to 7: reaction at 30°C. Lanes 8-12: reaction at 37°C. Lanes 3 and 8: DNA cleavage products produced by **29**•Fe(II). Lanes 4 and 9: DNA cleavage products produced by **26**•Fe(II). Lanes 5 and 10: DNA cleavage products produced by **27**•Fe(II). Lanes 6 and 11: DNA cleavage products produced by **30**•Fe(II). Lanes 7 and 12: DNA cleavage products produced by **31**•Fe(II).

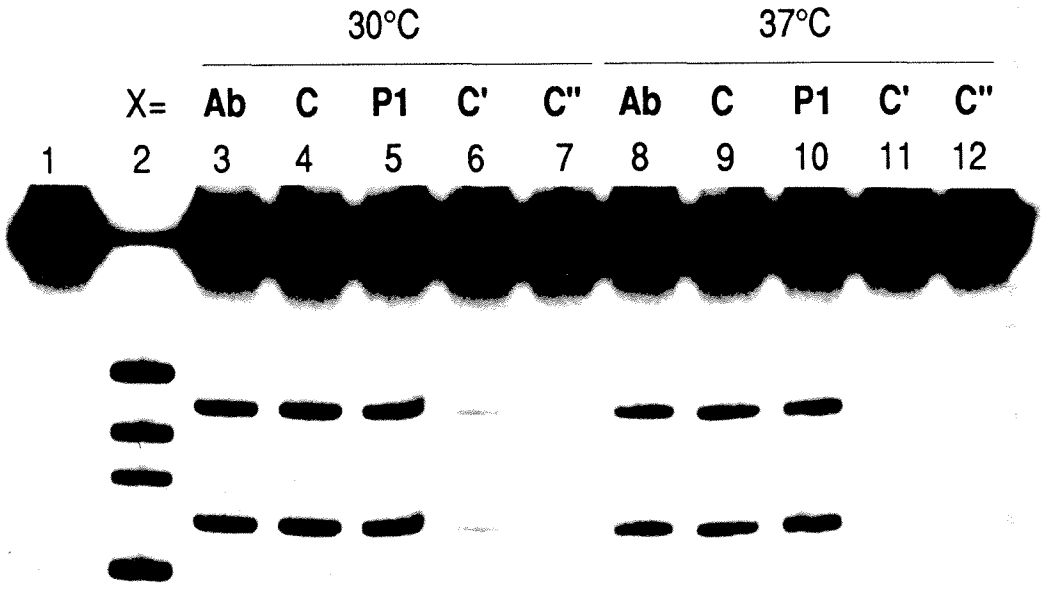
30°C
37°C
X=
Ab
C
P1
C'
C"
Ab
C
P1
C'
C"
1
2
3
4
5
6
7
8
9
10
11
12

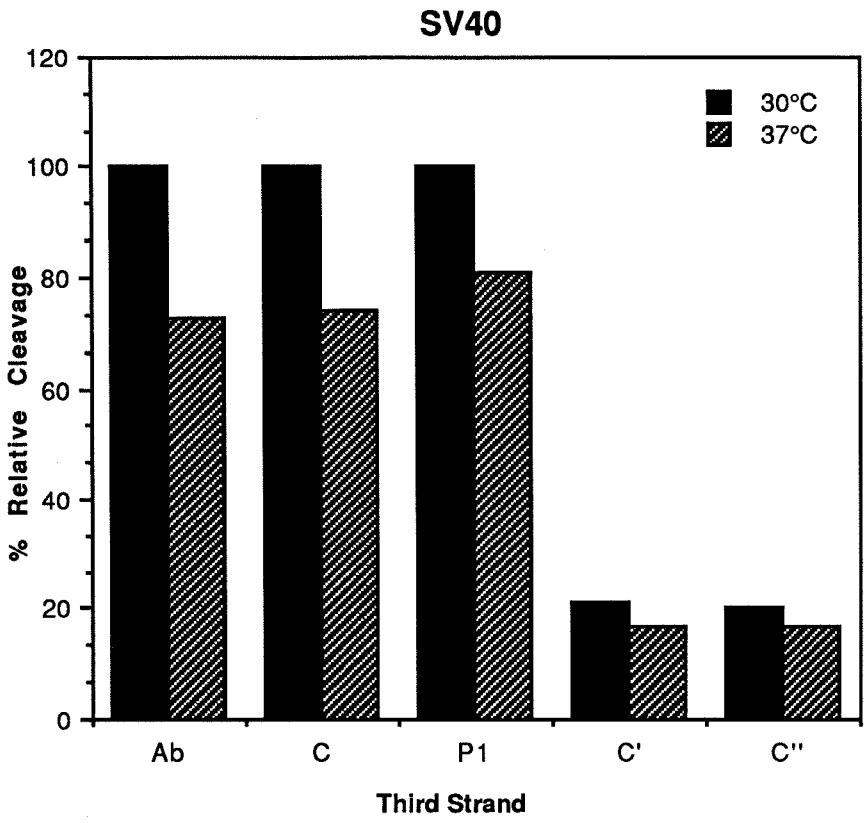

Figure 11d. Bar graph representing the relative cleavage data from the densitometric analysis in Figure 11c.

Conclusions

The novel base 3-methyl-5-amino-pyrazolo(4, 3-d)pyrimidine-7-one (P1), cytosine and an abasic compound (Ab) enable the selective cleavage of a site containing all four base pairs by triple helix formation. However isoguanosine analogs (G and G") and isocytidine (C") do not recognize a CG base pair in triple helix formation. Because oligonucleotides containing the 2-α–pyrimidinone (C') nucleoside give a mixture of α-anomer, β-anomer and hydrolyzed products due to its acid sensitivity, it is not clear whether this base recognizes a CG base pair in triple helix formation. Although the P1•CG, C•CG and Ab•CG triplets within a pyrimidine oligonucleotide extend triple helix specificity to all four possible base pairs of double helical DNA, some limitations on sequence composition exist. This result provides important structural ideas for the design of nucleosides (or their analogs) with nonnatural heterocycles directed toward a more general solution to sequence-specific recognition of double helical DNA at any sequence.

Experimental method and Materials

Synthesis. ^{1}NMR spectra were recorded at 400 MHz on a JEOL-GX 400 NMR spectrometer. Chemical shifts are reported in parts-per-million downfield from tetramethylsilane. IR spectra were recorded on a Shimadzu IR-435 Infrared Spectrometer. High resolution Fast Atom Bombardment Mass Spectra (FABMS) and EI mass spectra were obtained at the University of Nebraska, Lincoln and the Mass Spectra Lab at the University of California, Riverside. Flash chromatography was carried out under positive air pressure using EM Science Kieselgel 60 (230-400 mesh). Elemental analyses were performed by the analytical lab at Caltech. Reagent grade chemicals were used as received, except for diisopropylethylamine, which was distilled from CaH_2. A Beckman System1 Plus DNA synthesizer was utilized for the synthesis of oligonucleotides. Concentrations of oligonucleotides were determined by UV using a Perkin-Elmer Lambda 4C UV-Vis spectrometer. Analytical HPLC was performed on a BrownLee Labs Aquapore OD-300 4.6 mm x 22 cm 7 micron C18 column using no precolumn. All enzymes for DNA manipulation were purchased from Boehringer Mannheim.

5-methylamino-1-(2', 3', 5'-triacetyl-β-D-ribofuranosyl)imidazole-4-car–bonitrile (**2**). To a solution of compound **1** (2.8 g, 7.03 mmol) and triethylamine in chloroform (100 mL) was added phosphorous oxychloride (3.22g , 21 mmol), and the mixture was stirred for 30 minutes under argon. Cold water (100 ml) was added to the reaction solution and the mixture was extracted with chloroform (200 mL). The organic layer was washed with water (100 mL), dried over Na_2SO_4, and concentrated *in vacuo* to give a crude product of **3**, which was then chromatographed on a silica gel

column with chloroform and 10% ethanol in chloroform (v/v, Rf=0.48) to give **2** (2.0 g, Y=75%). ^{1}NMR (DMSO-d_6) δ 7.58 (s, 1H), δ 6.54 (m, 1H) , δ 5.79 (d, 1H, J=6.12, H1'), δ 5.56 (t, 1H, J=6.12, H2'), δ 5.32 (m, 1H), δ 4.25 (m, 3H), δ 2.95 (d, 3H, J=3.12, methyl), δ 2.10 (s, 3H), δ 2.07 (s, 3H), δ 2.05 (s, 3H). IR (KBr) 2200 cm^{-1}. FABMS calcd. for $C_{16}H_{21}N_4O_7$ (M+H)+ 381.1410. Found 381.1418.

3-Methylisoguanosine (**3**). A solution of compound **2** (2.0 g, 5.26 mmol) and benzoylcyanate (1.16 g, 7.80 mmol) in DMF was stirred at room temperature overnight. The solvent was then evaporated *in vacuo* (50°C) to afford an oily residue. The residue was suspended in a mixture of ethanol (40 mL) and 33% aqueous ammonia (40 mL) in a round bottom flask. The flask was well tightened with a rubber stopper, and the mixture was stirred at room temperature for 72 h. After 72 h, the solvent was removed under reduced pressure to give a yellowish residue. The residue was triturated with ethyl acetate, and the precipitated solid was collected by filtration to give **3** (920 mg, Y=58%). ^{1}HNMR (DMSO-d_6) δ 8.03 (s, 1H), δ 7.31 (s, 2H), δ 6.00 (d, 1H, J=6.22, H1'), δ 5.63 (d, 1H, J=4.23, 2' hydroxy), δ 5.27 (d, 1H, J=4.12, 3' hydroxy,), δ 5.07 (t, 1H, J=5.11, 5' hydroxy), δ 4.35 (t, 1H, J=6.22, H2'), δ 4.06 (m, 1H), δ 3.91 (1H, m), δ 3.57 (m, 5H). FABMS calcd. for $C_{11}H_{15}N_5O_4$ (M+) 281.1124. Found 281.1130.

N^6-benzoyl-3-methylisoguanosine (**4**). Compound **3** (500 mg, 1.69 mmol) was suspended in dry pyridine (25 mL) in a 100 mL round bottom flask equipped with a drying tube and cooled in an ice bath, and benzoyl chloride (2.44 g, 16.8 mmol) was added dropwise to the stirring solution. The reaction was allowed to warm to room temperature and stirred for 6 h. The reaction mixture was neutralized by addition of saturated $NaHCO_3$,

evaporated several times with toluene and ethanol. Ethyl acetate (100 mL) was added to this residue and washed with water (50 mL) and concentrated to give a residue. To this residue was added 20 ml of pyridine-methanol-water solution (65:35:5, v/v/v) and cooled in an ice bath. 2N NaOH solution (20 mL) in pyridine-methanol-water (65:35:5) was added dropwise to the reaction mixture with stirring at 0°C. The reaction mixture was stirred over 40 minutes at 0°C, and 2.4 g of ammonium chloride in water (5 mL) was added to neutralize the solution. The resulting solution was concentrated *in vacuo* to give a solid mixture. 20 ml of 20% methanol in ethyl acetate was added and insoluble solid was filtered and washed with 8 ml of water. The remaining solid was dried to give 470 mg of compound **4** (Y=68%). ^{1}HNMR (DMSO-d_6) δ 12.50 (s,1H), δ 8.21(s, 1H), δ 8.09 (m, 2H), δ 7.53 (m, 1H), δ 7.47 (m, 2H), δ 6.06 (d, 1H, J=5.23, H1'), δ 5.70 (d, 1H, J=5.24, 2' hydroxy), δ 5.32 (d, 1H, J=5.01, 3' hydroxy), δ 5.13 (t, 1H, J=4.34, 5' hydroxy), δ 4.38 (m, 1H), δ 4.12 (m, 1H), δ 3.96 (m, 1H), δ 3.50-3.70 (m, 5H). FABMS calcd. for $C_{18}H_{20}N_5O_6$ $(M+H)^+$ 402.1413. Found 402.1420.

3-Methyl-N^6-benzoyl-9-(3', 5'-O-(1,1,3,3-tetraisopropyldisiloxanyl-β-D-ribofuranosyl)isoguanosine (**5**). To a solution of compound **4** (412 mg, 1 mmol) in pyridine (10 mL) was added 1,3-dichloro-1,1,3,3-tetra isopropyldisiloxane ($TIPDCl_2$) (346 mg, 1.1 eq.) and the mixture was stirred under argon at room temperature for 3 h. Water (20 mL) was added to the reaction solution and the mixture was extracted with three 50 mL portions of ethyl acetate. The extract was dried over Na_2SO_4; upon concentration it afforded a yellowish residue, which was purified on a silica gel using ethyl acetate-chloroform solvent (50:50 v/v, Rf=0.51) to give 500 mg of compound **5**. ^{1}HNMR (DMSO-d_6) δ12.73 (s, 1H), δ 8.23 (m, 2H), δ 7.93 (s, 1H), δ 7.53 (m,

1H), δ 7.46 (m, 2H), δ 6.21 (s, 1H), δ 5.98 (d, 1H, J=4.46, 2' hydroxy), δ 4.51 (t, 1H, J=3.12, H3'), δ 4.23 (m, 2H), δ 4.10 (d, 1H, J=8.97), δ 3.94 (d, 1H, J=13.43), δ 3.68 (s, 3H). δ 1.10(s, 28H) FABMS calcd. for $C_{30}H_{46}N_5O_7Si_2$ $(M+H)^+$ 644.3285. Found 644.3270.

3-methyl-N^6-benzoyl-N^6-methyl-9-(2'-O-methyl-3', 5'-O-(1,1,3,3,--tetra-isopropyldisiloxanyl-β-D-ribofuranosyl)isoguanosine(6). To a solution of compound **5** was added 12 mL of methyl iodide along with silver oxide (400 mg, 0.63 mmol), and the mixture was stirred under argon at room temperature for 3 h and filtered. (The reaction was carried out in the dark due to the light sensitivity of silver oxide.). The filtrate was evaporated to give a yellowish solid, which was chromatographed on silica gel using 40% ethyl actate in chloroform (v/v, Rf=0.55) to give 180 mg of **6** (Y=44%). ^{1}HNMR (Aceton-d_6) δ 7.93 (d, 2H, J=9.01, benzoyl), δ 7.61 (s, 1H), δ 7.46 (m, 1H), δ 7.38 (m, 2H), δ 6.21 (s, 1H), δ 4.54 (dxd, 1H, J=4.43, 3.35), δ 4.41 (d, 1H, J=4.12), δ 4.12 (m, 3H), δ 3.75 (s, 3H), δ 3.73 (s, 3H), δ 3.47 (s, 3H), δ 1.10 (m, 28H). FABMS calcd. for $C_{32}H_{50}N_5O_7Si_2(M+H)^+$ 672.3248. Found 672.3240.

3-Methyl-N^6-benzoyl-N^6-methyl-9-(2'-O-methyl-β-D-ribofuranosyl)-isoguanosine(7). To a solution of compound **6** (180 mg, 0.28 mmol) in tetrahydrofuran (THF) (5 mL) was added dropwise 0.56 mL of 1N tetrabutylammonium fluoride solution (TBAF) in THF at room temperature, and the reaction mixture was stirred at room temperature for 10 minutes, where upon 10 mL of cold water was added. The mixture was extracted with 80 ml ethyl acetate and washed with 10 mL of water. The organic layer was concentrated under reduced pressure to give a residue. The residue was chromatograped on silica gel using 10% methanol in ethyl acetate (v/v, Rf= 0.46) to give 100 mg of **7** (Y=85%). ^{1}HNMR(DMSO-d_6) δ 7.89

(s, 1H), δ 7.82 (d, 2H, J=8.56, benzoyl), δ 7.46 (m, 1H), δ 7.38 (m, 2H), δ 5.95 (d, 1H, J=6.11, H1'), δ 5.35 (d, 1H, J=5.16, 3' hydroxy), δ 5.02 (t, 1H, J=4.45, 5' hydroxy), δ 4.24 (m, 2H), δ 3.93 (m, 1H), δ 3.63 (s, 3H), δ 3.49 (m, 3H), δ 3.43 (s, 3H), δ 3.33 (s, 3H), δ1.10 (m, 14H). FABMS calcd. for $C_{20}H_{24}N_5O_6$ $(M+H)^+$ 430.1726. Found 430.1730.

3-methyl-N^6-benzoyl-N^6-methyl-9-(2'-O_methyl-5'-O-(4, 4'-dimethoxytrityl)-β-D-ribofuranosyl)isoguanosine (**8**). Compound **7** (90 mg, 0.21 mmol) and 4, 4'-dimethoxytritylchloride (DMTCl) was dissolved in dry pyridine (3 ml). The mixture was stirred at 4°C overnight. The reaction was stopped by the addition of methanol (2 mL) and diluted in ethyl acetate (50 mL). The organic layer was washed three times with water (20 mL), dried over anhydrous Na_2SO_4, filtered, and evaporated to a yellowish solid. This solid was chromatographed on silica gel using ethyl acetate to afford 125 mg of **8** (Y=83%). ^{1}HNMR (acetone-d_6) δ7.95 (d, 2H, J=8.46, benzoyl), δ 7.56 (s, 1H), δ 7.47 (m, 1H), δ 7.35 (m, 4H), δ 7.21 (m, 7H), δ 6.80 (d, 4H, J=13), δ 6.11 (d, 1H,J=6.34, H1'), δ 4.47 (t, 1H, J=5.03, H2'), δ 4.40 (m, 2H), δ 4.21 (m, 1H), δ 3.83 (s, 3H), δ 3.75 (s, 6H), δ 3.52 (s, 3H), δ 3.48 (s, 3H), δ 3.32 (m, 1H), δ 3.26 (m, 1H). FABMS calcd. for $C_{41}H_{42}N_5O_8$ $(M+H)^+$ 732.3011. Found 732.3031.

Phosphoramidite 9. 2-Cyanoethyl-N, N-diisopropyl-chlorophosphoramidite (69 mg, 0.29 mmol) was added dropwise to a solution of **8** (120 mg, 0.16 mmol) and diisopropylethylamine (90.4 mg, 70 mmol) in dry methylene chloride (3 mL) under argon. The reaction mixture was stirred at room temperature for 1 h and then diluted with ethyl acetate (50 mL) and washed with saturated $NaHCO_3$ (2x50 mL) and brine (3x50 mL). The organic layer was dried over Na_2SO_4 and concentrated under reduced pressure. The phosphoramidite diastereomers were purified by flash chromatography

(ethyl acetate/methylene chloride/isopropyl alchole/triethylamine, 30:64:1.5:1, v/v/v/v, Rf=0.52) to give 125 mg of **9** (Y=84%). ^{1}HNMR (acetone-d_6) δ 7.95 (d, 2H, J=8.45, benzoyl), δ 7.56 (s, 1H), δ 7.47 (m, 1H), δ 7.37 (m, 2H), δ 7.32 (m, 2H), δ 7.21 (m, 7H), δ 7.6.80 (d, 4H, J=13.10), δ 6.11 (d, 1H, J=6.11, H1'), δ 4.47 (t, 1H, J=4.98, H2'), δ 4.40 (m, 1H), δ 4.21 (m, 1H), δ 3.83 (s, 3H), δ 3.75 (s, 6H), δ 3.52 (s, 3H), δ 3.30-3.50 (m, 4H), δ .47 (s, 3H), δ 2.57 (t, 1H, J=5.11, methylene), δ 2.42 (t, 1H, J=5.11, methylene), δ 0.90-1.30 (m, 14H). FABMS calcd. for $C_{50}H_{58}N_7O_9P$ 932.4091. Found 932.4108.

Oligonucleotides Oligonucleotides **12-31** were machine synthesized using β-cyanoethyl phosphoramidite chemistry. Modified nucleosides coupled with >97% efficiency except phosphoramidites **12, 16, 23** and **30**. The oligonucleotides were removed from the support and deprotected by treatment with 0.1 N NaOH(1.5 mL/1 mmol, 55°C, 24 h), neutralized with glacial acetic acid (6-7 μL/1.5 mL 0.1 N NaOH), applied to a column of Sephadex G-10-120 (Sigma), and eluted with water. The crude oligonucleotides were lyophilized and purified by the electrophoresis (550V, 20 h) on a 2 mm-thick 20% polyacrylamide gel (Maxam-Gilbert). The major UV-absorbing bands were cut out and eluted (0.2 N NaCl, 1 mM EDTA, 37°C, 24 h), then passed through Sephadex G-10-120, and dialyzed against water for 3 days.

HPLC analysis. 3 nmols of purified oligonucleotide were digested simultaneously with snake venom phosphodiesterase (3 μL, 2 μg/μL) and calf intestine alkaline phophatase (3 μL, 1 u/μL), in 50 mM Tris, pH 8.1, and 100 mM $MgCl_2$. The reaction mixture was incubated at 37°C for 2 h and lyophilized to dryness. The dry sample was dissolved with 10 μL of Milli-Q water. 5 μL of the solution was injected onto a C18 reverse phase column

utilizing 8% MeOH in 10 mM ammonium phosphate, pH 5.1, as eluent. 5 μL of a standard solution containing dC (2 nmol), dT (2 nmol), 2-pyrimidinone (2 nmol) and C' (α and β anomer) (2 nmol) was also injected under identical conditions as a standard. 5 μL of the digested oligonucleotide was mixed in 5 μL of the solution containing the standard nucleosides, and 5 μL of the resulting solution was injected to show that each nucleoside peak is identical.

DNA manipulation. Doubly distilled water was used for all aqueous reactions and dilutions. Enzymes were purchased from either Boehringer-Mannheim or New England Biolabs. Deoxynucleoside triphosphates were purchased from Pharmacia as 100 mM solutions. 5'α-^{32}P-dNTPs (3,000 Ci/mmol) and 5'γ-^{32}P-ATP (7,000 Ci/mmol) were obtained from Amersham. The plasmid SV40 was purchased from Bethesda Research Laboratories. The plasmid pHIV-CAT was a gift from Dr. Alan Frankel and Tom Povsic. DNA reactions were typically carried out in 1.5 mL polypropylene tubes obtained from Tekma company. Calf thymus DNA was purchased from Sigma, sonicated, and extracted with 3x0.2 volume water-saturated phenol, 0.2 volume 24:1 $CHCl_3$/isoamylalcOhol, and 0.2 volume $CHCl_3$. After extensive dialysis against water, the DNA was passed through a 0.45 micron Centrex filter (Schleicher Schull) and assayed for concentration by UV assuming ε_{260}=11,800 L/mol.bp.cm. Agarose gel electrophoresis was carried out using 40 mM Tris-acetate, 5 mM NaOAc, 1 mM EDTA, pH 7.9 buffer. Ten-fold concentration (10x) loading buffer for agarose gels was 25% (w/v) ficoll solution, which contained 0.2% (w/v) bromophenol blue (BPB) and xylene cyanol (XC) tracking dyes. Polyacrylamide gel electrophoresis was carried out using 100 mM tris-borate, 1 mM EDTA, pH 8.3 buffer.

Loading buffer for denaturing polyacrylamide gels was 80% formamide in 100 mM Tris-borate, 1mM EDTA, pH 8.3 buffer. The DNA were labeled by standard procedures (47). Specific radioactivity was measured with a Beckman LS 2801 Scintillation counter. Gels were dried (after transferring them to Whatman 0.3 mm paper) on a Bio-Rad Model 483 slab dryer at 80°C. Autoradiography was carried out using Kodak X-Omat film. Optical densitometry was performed using LKB Broma Ultrascan XL Laser Densitometer operating at 633nm. The relative peak area for each cleavage band or locus was equated to the relative cleavage efficiency at that site.

Procedure for the preparation of 5' ^{32}P end-labeled 30 mer duplex. 50 picomoles of each single-stranded oligonucleotide $A_5T_7YT_7G_{10}$ (Y=T, C, G, A) were dissolved in 28 μL water, 5 μL 10x kinase buffer (10x700 mM Tris:HCl, 100 mM $MgCl_2$, 1 mM spermidine, 1 mM EDTA, pH 7.6), and 5 μL 10 mg/ml DTT. This solution was treated with 10 μL 5' γ-^{32}P ATP and 2 μL T4 polynucleotide kinase (20 u). The 5' end-labeling was allowed to proceed for 45 minutes at 37°C. The end-labeled DNA was precipitated with NaOAc/EtOH, washed with 70% EtOH, and dried. The pellets were dissolved in 100 mM NaCl, 50mM tris-acetate, pH 7.4, and 50 picomoles of the complementary 30 mer in a total volume of 30 μL. To effect hybridization of the 30 mers, the oligonucleotide mixture was heated to 90°C for 5 minutes and allowed to cool to room temperature. 15 μL 25% ficoll loading buffer was added and the mixture was loaded onto a nondenaturing polyacrylamide gel (15%) and electrophoresed at 240 V until the BPB tracking dye was near the bottom of the gel. The four bands (Y=T, C, G, A) of end-labeled DNA were visualized by autoradiography, excised from the gel, crushed, transferred to 1.5 ml polypropylene tubes, and eluted into 0.2 N NaCl at 37°C

for 24 h. The end-labeled DNA 30mer duplexes were recovered by passing the eluents through a 0.45 micron Centrex filter and extensive dialysis with water. The labeled DNA solution was used for the cleavage reaction. For the cleavage reactions the DNA (20,000 cpm/reaction) was mixed with salts, buffer, spermine and the oligonucleotide-EDTA with Fe(II). This solution was incubated for 30 minutes at 37°C before the cleavage reaction was initiated by the addition of DTT to make a final volumn of 40 μL. The reaction was stopped by lyophilization. To each eppendorf tube a certain volume of formamide loading buffer was added (80% formamide, 20% 5X TBE buffer, 0.02% bromophenol blue and 0.02 % xylene cyanol) to give approximately 3,000 cpm/μL for each reaction. To dissolve the solid the tubes were vortexed (10 sec). 5 μL of the resulting solutions were transfered to new tubes and counted afterwards. The volume of buffer was loaded on each lane to give the same amount of radioactivity (~6000 cpm/lane) for each reaction. Electrophoretic separation of the cleavage products was achieved on a 20% denaturing polyacrylamide gel until the bromophenol blue was 25 cm from the starting position. Cleavage products were visualized by autoradiography without drying the gel. The relative cleavage was analyzed by LKB densitometry.

Cleavage of SV40 PpuMI-BglI restriction fragment. 3' and 5' end-labeling were carried out by standard methods (47). For the cleavage reactions the DNA (20,000 cpm/reaction) was mixed with calf thymus DNA (100 μM bp), NaCl (100 mM), Tris-acetate (50 mM pH 7.4), spermine (1 mM) and the oligonucleotide-EDTA (2μM) with Fe(II) (25 μM). This solution was incubated for 30 minutes at 25°C before the cleavage reaction was initiated by the addition of sodium ascorbate (1 mM) to make a final volumn of 40 μL.

The cleavage reactions were carried out at 37°C. The reaction was stopped by precipitation: 60 μL water was added followed by 20% NaOAc solution (10 μL) and 300 μL cold ethanol, and the DNA was precipitated as usual. The pellets were rinsed with 70% cold ethanol (50 μL), and briefly dried *in vacuo*. To each pellet a certain volume of formamide loading buffer was added (80% formamide, 20% 5X TBE buffer, 0.02% bromophenol blue and 0.02% xylene cyanol) to give approximately 1,800 cpm/μL for each reaction. To dissolve the pellet the tubes were vortexed (10 sec). 10 μL of the resulting solutions was transferred to new tubes and counted afterwards. The tubes were heated at 90°C for 2 minutes and cooled to 0 °C. The volume of buffer loaded on each lane was controlled to give each reaction the same amount of radioactivity (~6000 cpm/lane). Electrophoretic separation of the cleavage products was achieved on an 8% denaturing polyacrylamide gel until the bromophenol blue was 30 cm from the starting position. The gel was dried on a Bio-Rad Slab Gel Dryer Model 483 (1.5 h at 80°C) and cleavage products visualized by autoradiography. The relative cleavage was analyzed using the LKB densitometer

Double strand cleavage of pHIV-CAT. The plasmid pHIV-CAT was precipitated twice from NaOAc with ethanol, rinsed with 70% ethanol, briefly dried *in vacuo* and digested with BamHI according to the conditions provided by the manufacturer. The linearized plasmid (10 ng) was labeled with α-^{32}P-dGTP and DNA polymerase (large Klenow fragment, reaction volumn =100 μL) according to standard procedures. 100 μL Milli-Q water was added to the reaction mixture. The resulting DNA solution was extracted with 2x1 volume water saturated phenol and 3x1 volume ether. Half of the resulting DNA-solution (100 μL) was passed through a column

containing 1 mL Sephadex G-50-80 resin to remove unincorporated mononucleotides. The labeled DNA solution was used for the cleavage reaction. For the cleavage reactions the DNA (20,000 cpm/reaction) was mixed with NaCl (50 mM), tris-acetate (25 mM), spermine (1 mM) and the DNA EDTA (2 μM) with Fe(II) (2 μM). This solution was incubated for 30 minutes at 25°C before the cleavage reaction was initiated by the addition of sodium ascorbate (1 mM) to make a final volume of 40 mL. The reactions were carried out at 25°C. The reactions were stopped by precipitation: 60 μL water was added followed by 20% NaOAc solution (10 μL) and 300 μL cold ethanol, and the DNA was precipitated as usual. The pellets were rinsed with 70% cold ethanol (50 μL), and briefly dried in vacuo. To each pellet a certain volume of ficoll loading buffer was added (2.5% ficoll 400, 1xTAE-buffer, 0.02% bromophenol blue and 0.02% xylene cyanol) to give approximately 600 cpm/μL for each reaction. To dissolve the pellet the tubes were vortexed (10 sec). 20 μL of the resulting solutions were transferred to new tubes and counted afterwards. The volume of buffer was loaded on each lane to give the same amount of radioactivity (~6000 cpm/lane) for each reaction. Electrophoretic separation of the cleavage products was achieved on a 0.9% agarose gel (20x14x0.4 cm, TAE-buffer, 120 V, 4.0 h) until the bromophenol blue was 15 cm from the starting position. The gel was dried on a Bio-Rad Slab Gel Dryer Model 483 (1.5 h at 80 °C) and cleavage products visualized by autoradiography.

Double -strand cleavage of SV40 DNA. HIV-CAT was precipitated twice from NaOAc with ethanol, rinsed with 70% ethanol, briefly dried *in vacuo* and digested with BaclI according to conditions provided by the manufacturer. The linearized DNA was labeled with α-^{32}P-GTP using

DNA polymerase according to standard procedures. Purification of the labeled DNA and performance of the cleavage experiments were carried out exactly as described for the double-stranded cleavage of pDMAG10 except sodium ascorbate was substituted for DTT.

References and notes

(1) Dervan, P. B. *Science* **1986**, *232*, 464.

(2) Dervan, P. B. in *Nucleic Acids and Molecular Biology,* edited by Eckstein, F; Lilley, D. M. J. Ed.; (Springler-Verlag, Heidelberg (**1988**) vol. 2, pp. 49-64.

(3) Barton, J. K. *Science* **1986**, *233*, 727.

(4) Moser, H. E.; Dervan, P. B. *Science* **1987**, *238*, 645.

(5). Povsic, T. J.; Dervan, P. B. *J. Amer. Chem. Soc.* **1989**, *111*, 3059.

(6) Strobel, S. A.; Moser, H. E.; Dervan, P. B. *J. Amer. Chem. Soc.* **1988**, *110*, 7927.

(7) Felsenfeld, G.; Davies, D. R.; Rich, A. *J. Amer. Chem. Soc.* **1957**, *79*, 2023.

(8). Michelson, A. M.; Massoulie, J.; Guschlbauer, W. *Prog. Nucl. Acid. Res. Mol. Biol.* **1967**, *6*, 83.

(9) Felsenfeld, G.; Miles, H. T. *Annu. Rev. Biochem.* **1967**, *36*, 407.

(10) Lipsett, M. N. *Biochem. Biophys. Res. Commun.* **1963**, *11*, 224.

(11) Howard, F. B.; Frazier, J.; Lipsett, M. N.; Miles, H. T. *Biochem. Biophys. Res. Commun.* **1964**, *17*, 93.

(12) Lipsett, M. N. *J. Biol. Chem.* **1964**, *239*, 1256.

(13) Miller, J. H.; Sobell, J. M. *Proc. Natl. Acad. Sci. U. S. A.* **1966**, *55*, 1201.

(14) Morgan, A. R.; Wells, R. D. *J. Mol. Biol.* **1968**, *37*, 63.

(15) Lee, J. S.; Johnson, D. A.; Morgan, A. R. *Nucleic Acids. Res.* **1979**, *6*, 3073.

(16) Arnott, S.; Bond, P. J. *Nature New Biology* **1973**, *244*, 99.

(17) Arnott, S.; Selsing, *J. Mol. Biol.* **1974**, *88*, 509.

(18) Arnott, S.; Bond, P. J.; Selsing, E.; Smith, P. J. C. *Nucleic Acids Res.* **1976**, *3*, 2459.

(19) Saenger, W. *Principles of Nucleic Acid Structure*, edited by Cantor, C. R.; Springer-Verlag, New York Inc. (**1984**).

(20) Hoogsteen, K. *Acta Crysta.* **1959**, *12*, 822.

(21) Moser, H. E.; Dervan, P. B., unpublished results.

(22) Koh, J. S.; Dervan, P. B. *J. Amer. Chem. Soc.* in preparation.

(23) Marck, C.; Thiele, *Nucleic Acids Res.* **1978**, *5*, 1017.

(24) Briotman, S. L.; Im, D. D.; Fresco, J. R. *Proc. Natl. Acad. Sci. U. S. A.* **1987**, *84*, 5120.

(25) Letai, A. J. *et al. Biochemistry* **1988**, *27*, 9108.

(26) Cooney, M. *et. al. Science* **1988**, *241*, 456.

(27) Doan, T. L. *et al. Nucleic Acids Res.* **1987**, *15*, 7749.

(28) Praseuth, C. *et al. Proc. Natl. Acad. Sci. U. S. A.* **1988**, *85*, 1349.

(29) Horne, D. A.; Dervan, P. B. *J Amer. Chem. Soc.* **1990**, *112*, 2435.

(30) Griffin, L. C.; Dervan P. B. *Science* **1989**, *245*, 967.

(31) Itaya, T.; Matsumoto, H.; Watanabe, T. *Chem. Pharm. Bull.* **1982**, *30*, 86.

(32) Ienaga,K.; Pfleiderer, W. *Tetrahedron Letters* **1978**, *16*, 1447.

(33) Atkinson, T.; Smith, M. *Oligonucleotide Synthesis: A practical approach;* edited by Gait, M. J.; IRL Press (**1985**), Oxford.

(34) Sugawara, T.; Ishikura, T.; Itoh, T.; Mizuno, Y. *Nucleosides and Nucleotides* **1982**, *1*, 239.

(35) Kamimura, T.;Masegi, T.; Hata, T. *Chemistry Letters* **1982**, 965.

(36) Schneider, H.; Tamm, C. *Helvetica Chimica Acta* **1983**, *66*, 350.

(37) Altermatt, R.; Tamm, C. *Helvetica Chimica Acta* **1985**, *68*, 475.

(38) McLaughlin, L. M.; Gildea, B. *Nucleic Acids Res.* **1989**, *17*, 2261.

(39) Kimura, J.; Yagi, K.; Suzuki, H. Mitsunobo, O. *Bull. Soc. Chem. Jpn.* **1980**, *53*, 3670.

(40) Switzer, C. Moroney, S.; Benner, S. *J. Amer. Chem. Soc.* **1989**, *111*,8322.

(41) Sinha, N. D.; Biernat, J.; MaManus, J.; Koster, H. *Nucleic Acids Res.* **1984**, *12*, 4539.

(42) Iocono, J. A.; Gildea, B. Mclaughlin, L. W. *Tetrahedron Letters* **1990**, *31*, 175.

(43) Dreyer, G. B.; Dervan, P. B. *Proc. Natl. Acad. Sci. U. S. A.* **1985**, *82*, 968.

(44) Usman, N.; Ogilvie, K. K.; Jiang, M.-Y.; Cedergren, R. J. *J. Amer. Chem. Soc.* **1987**, *109*, 7845.

(45) Mclaughlin, L. W.; Cramer, F.; Sprinzl, M. *Anal. Biochem.* **1981**, *112*, 60.

(46) Maxam, A. M.; Gilbert, W. *Methods Enzymol.* **1980**, *65*, 499.

(47) Maniatis, T.; Fritsch, E. F.; Sambrook, J. *Molecular Cloning C. S. H.* **1982**.

PART II

Design of DNA-Cleaving Functional Groups

Chapter 3

Design of New DNA-Cleaving Functional Groups and Studies of Their DNA-Cleaving Mechanisms

Introduction

Nucleases, molecules which cleave DNA either at specific sites along the strand or in an indiscriminant, nonspecific fashion, have become the molecular scalpels of the biochemist. The reactions performed by both site-specific and nonspecific cleaving molecules are quite remarkable and intriguingly complex. These reactions can be broken down in terms of two distinct chemical events: (1) the binding step, involving recognition of a particular aspect of DNA base sequence or structure; and (2) the cleaving step, involving a series of transformations which lead either directly or indirectly to hydrolysis of the phosphodiester linkage and scission of the DNA backbone. There has been an explosion in the research effort directed toward the isolation and evaluation of naturally occurring DNA cleaving agents and toward the design and synthesis of model compounds that can sequence-specifically recognize and cut DNA. The potential scope of the utility of these compounds is enormous and ranges from the creation of synthetic restriction enzymes for use by molecular biologists to the development of chemotherapeutic agents that may be effective against a variety of neoplastic diseases. The work I describe here encompasses the design and synthesis of sequence-specific DNA cleaving molecules and studies of their DNA cleaving mechanisms.

DNA structure. DNA is a polymer in which each monomer is a nucleotide consisting of a phosphate group, a 5-carbon sugar moiety, and a purine or pyrimidine base. DNA contains the sugar deoxyribose and the bases adenine(A), thymine(T), guanine(G), and cytosine(C). The nucleotides are linked by phosphodiester bonds, creating a sugar phosphate backbone via the 3'- and 5'-positions of the sugar. The bases are

linked to the 1-position of the sugar. The phosphodiester is a strong acid, and the polymer has 1 negative charge/repeat unit. Most DNAs are double helical molecules in which the two strands run in opposite directions. The strands are held together through hydrogen bond interactions between the bases; A hydrogen bonds with T and G hydrogen bonds with C.

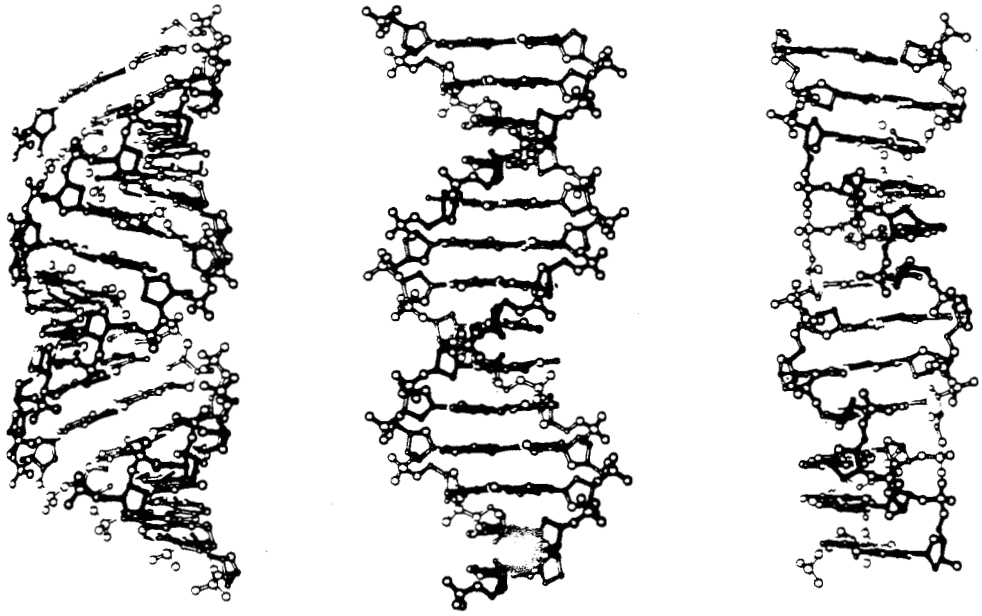

Figure 1. Structural conformers of double helical DNA.

The helical conformation of DNA can be classified into three general families: the A, B, and Z forms (Figure 1) (1). Although each conformation involves bases paired through Watson-Crick hydrogen bonding, the overall shapes of the helices are quite different. A-DNA is a right-handed helix seen in DNA fibers at low hydration. It is the predominant conformation of DNA-RNA hybrids and double-stranded RNA segments. B-DNA is a right-handed helix with base pairs oriented essentially perpendicular to the helix

axis and is the predominant conformation of DNA in solution. Z-DNA is a left-handed helix formed by a CpG dinucleotide. In this symmetrical unit the deoxyguanosine has an unusual glycosidic bond angle (syn) and deoxyribose pucker (C3'-endo) when compared with B-DNA.

Since B-DNA constitutes the dominant conformation of DNA under physiological conditions, the sequence-specific recognition of B-DNA is of great interest. The clearest view of the B conformation is derived from the crystal structure of a dodecamer determined by Richard B. Dickerson and coworkers (2). This structure shows the pronounced major and minor

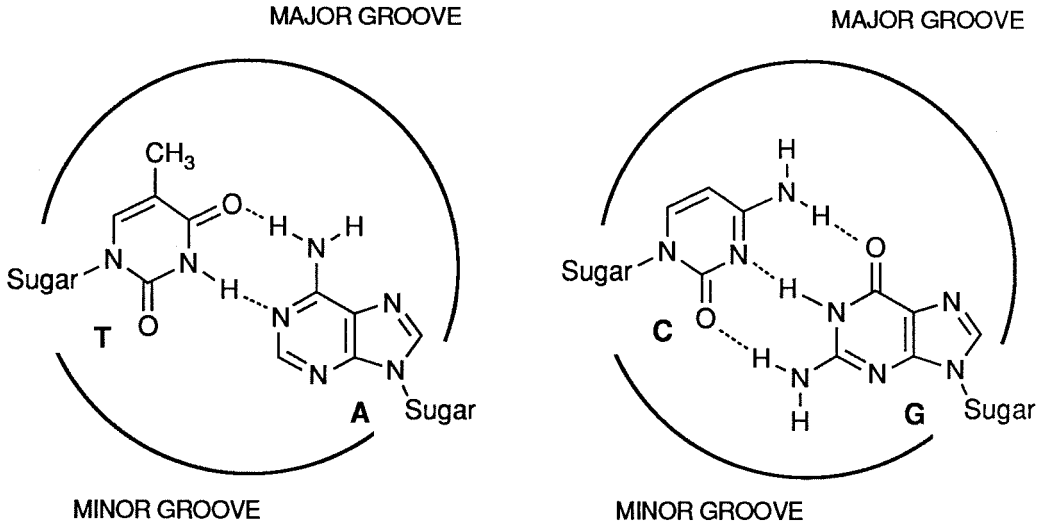

Figure 2 Effects of Watson-Crick base pairing on the availability of base functional groups.

grooves of B-DNA, which spiral along the helix axis. This structure also shows that local DNA conformational properties such as base propeller twist, roll, slide, tilt, and groove width vary with the local DNA sequence.

In addition, the pattern of hydrogen bond donor and acceptor groups found on the floors of the DNA major and minor grooves were observed.

In the minor groove when an A:T base pair is present, the lone pairs of electrons from adenine N3 and thymine O2 atoms are available for hydrogen bonding; while when a G:C base pair is present, the hydrogen from the exocyclic N2 amino group of guanine is available for hydrogen bonding (Figure 2). In the major groove when a A:T base pair is present, the lone pairs from adenine N7 and the hydrogen from the exocyclic N6 amino group of adenine are available for hydrogen bonding; when a G:C base pair is present, the lone pairs from N7 and O6 of guanine are available.

DNA binding molecule-DNA complexes. A variety of molecules have been observed to bind specifically to DNA. These compounds appear to exert antitumor and antibiotic activities by forming tight complexes with their cognate DNA sites, resulting in the blockage of transcription (3). Three modes of interaction have been observed in the DNA complexes of such molecules (4). One mode involves the intercalation of a flat aromatic molecule between two base pairs. In general, this mode has a relatively low specificity, presumably because a major interaction is the relatively nonspecific π-π stacking interaction (5). Usually there is a slight preference for G, C bp because of the increased width and flatter conformations of G, C sequences.

The other recognition modes involve interactions within one of the grooves of the helix. Either the major or minor groove could serve as a complexation site, with the appropriate segregation of base recognition elements. Examples of nonintercalative DNA binding molecules which

bind to the minor groove of A:T-rich regions include the oligo(N-methylpyrrolecarboxamide) antibiotics netropsin and ditamycin A (isolated from Streptomyces cultures) (3). The crystal structure of netropsin reveals that it has a crescent shape (in which amide NH and pyrrole C2H atoms form the concave edge) and a right-handed twist of one N-methylpyrrolecarboxamide residue relative to the other (6). Dodecamer-netropsin and dodecamer-distamycin A complexes have been examined recently by X-ray crystallography (7-9). In both cases the antibiotic is set deeply into the minor groove so that the pyrrole amide hydrogens form

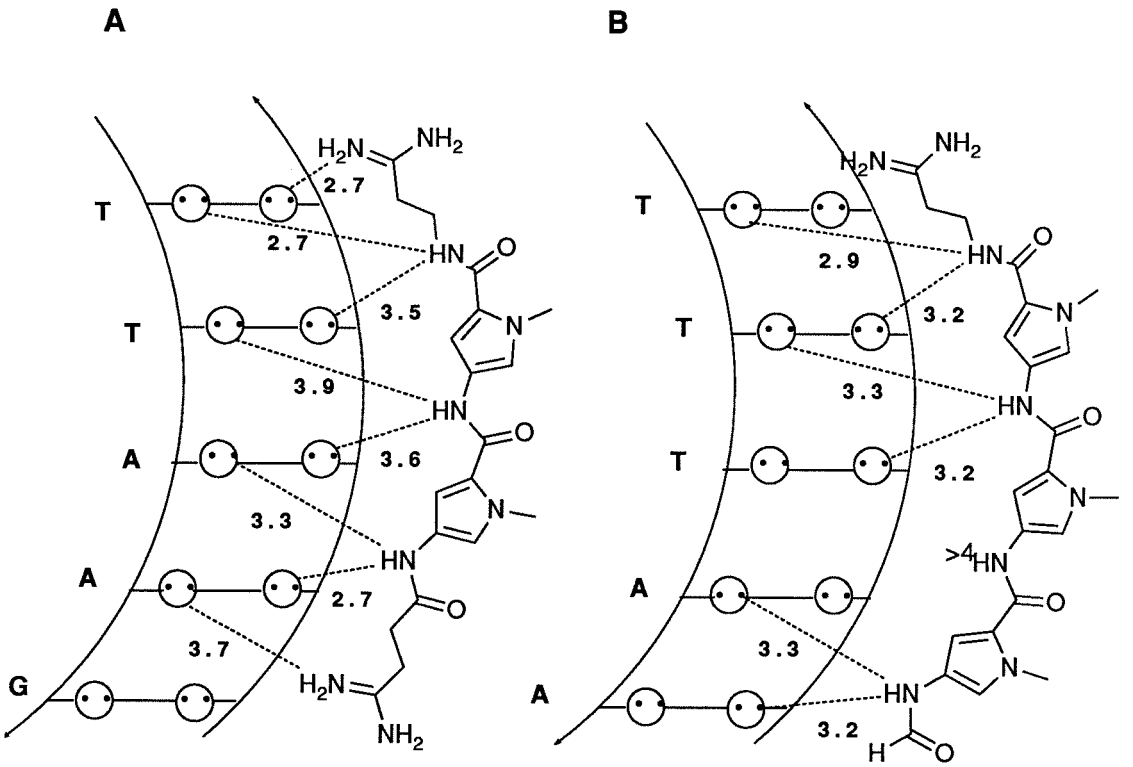

Figure 3 Structural features of the DNA complexes of netropsin and distamycin A (8-9). The small molecules are set deeply in the minor groove, in close van der Waals contact to the sugar phosphate backbones. Circles represent the lone pair electrons of the thymine O2 and adenine N3. Dashed lines represent hydrogen bonds existing in the complex. The distance in A between donor and acceptor atoms is shown beside each interaction.

bifuricated hydrogen bonds with the N3 of adenine and the O2 of thymine onthe floor of the groove. In the netropsin complex, the width of the minor groove has increased by an average of 1.7 Å. The adjustment allows the pyrrole rings to fill the minor groove completely and to form extensive van der Waals contacts with the sides of the grooves. These close contacts require the pyrrole rings to be parallel to the sides of the groove, increasing the overall screw sence of the antibiotic so that it matches the minor groove. The helix axis is bent away from the netropsin molecule by 8°, increasing the distance between the utmost T carbonyl by about 0.5Å. These carbonyls also form the strongest hydrogen bonds to the pyrrole amides, suggesting that the overall distance of the unbound DNA site is smaller than that required for optimum contacts with netropsin (10). A similar situation exists in the DNA-distamycin A cocrystal (9). ^{1}HNMR studies of netropsin-GGAATTCC (11), a netropsin-GGTATACC (12), and a distamycin-CGCGAATTCGCG complex (16) conclude that the structure in solution is very similar to that found in the solid state.

Site-specific DNA Cleavage. The prototypical system to examine site-specific recognition and reaction at a DNA is that of restriction enzymes and naturally occurring compounds such as bleomycine and neocarzinostatin. The restriction enzymes are able to recognize a particular sequence and, in the presence of divalent metal ions, cleave each of the two DNA strands producing 5'-phosphoryl and 3'-hydroxy termini through the phosphodiester hydrolysis (14). Metallobleomycin (BLM) (15) and neocarzinostatin (NCZ) (16) have the ability to recognize and noncovalently bind to specific sequences in DNA and then to perform chemistry on a specific deoxynucleoside residue that can ultimately lead to a strand

scission. The activity of BLM *in vitro* depends on Fe(II) and O_2 or Fe(II) and H_2O_2. The initial BLM•Fe(II)•O_2 complex undergoes a one-electron reduction to yield an activated BLM which can initiate DNA damage leadin to strand scission (Figure 4) (17). Pathway a in Figure 4 results in the formation of nucleic acid base propenal and a DNA strand scission that yields 3'-phosphoglycoate and 5'-phosphate termini. Pathway b in Figure 4 results in the liberation of nucleic acid base plus an alkali-labile site that cleaves at pH 12 with piperidine to afford a 3'-phosphate and a 5'-phosphate terminus.

Dervan and coworkers have shown that the coupling of the nonspecific nucleolytic chemistry of EDTA-Fe(II) to a sequence specific DNA-binding molecule creates a sequence-specific nuclease (18-20). One of the first examples of this is ferrous EDTA tethered to the antibiotic distamycin. Here the EDTA moiety is tethered to either the amino or carboxy terminus of tris-N-methylpyrrolcaboxamide yielding distamycin-EDTA(DE) or EDTA-distamycin (ED) (Figure 5). From sequencing gel analysis, both DE•Fe(II) and ED•Fe(II) are found to cleave the sites adjacent to five base pairs consisting of A-T-rich DNA sequences. A synthetic 52-residue peptide, forming the DNA-binding domain of Hin reconbinase which recognizes a 13 bp sequence, has also been equipped with the Fe(II)-EDTA-cleaving function, tethered, in this case, to the amino terminus of the peptide fragment (21). DNA cleaving is illustrated also in the attachment of EDTA-Fe(II) to a strand of homopyrimidineoligonucleotides containing 15-20 base residues. In this case, it is shown that this homopyridine nuclease specifically binds and cleaves at precisely the corresponding homopyrimi-

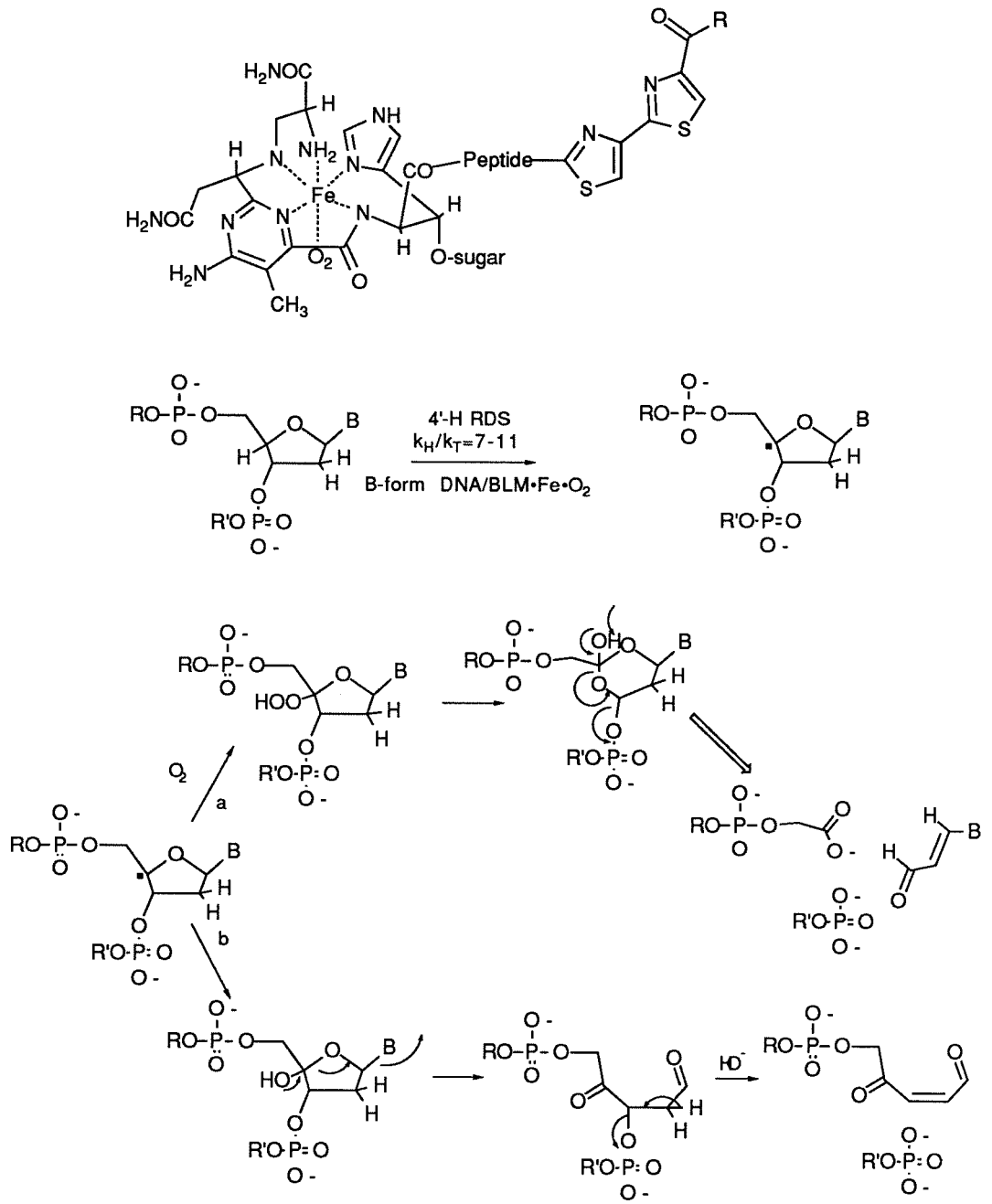

Figure 4. (**Top**) Proposed structure of the BLM•Fe•O2. (**Middle** and **Bottom**) Proposed unified mechanism for the cleavage of DNA by "activated BLM".

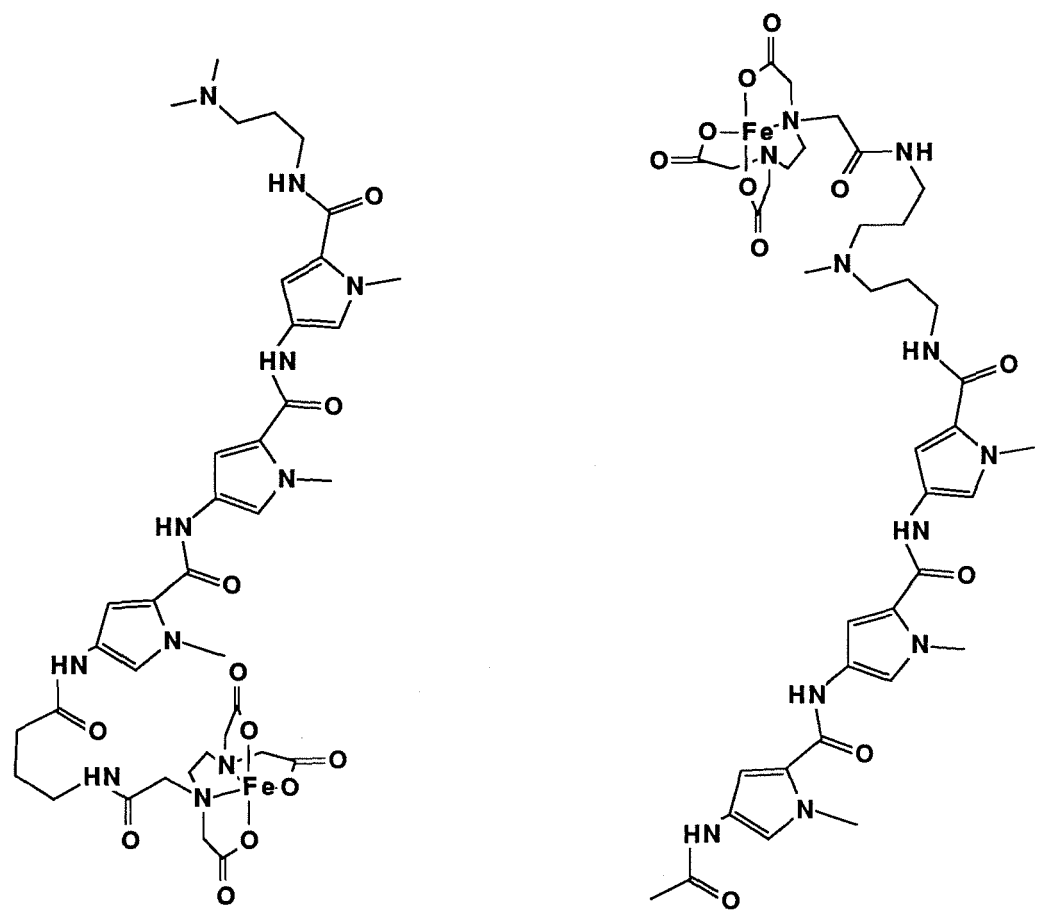

Figure 5. The structure of Distamycin-EDTA•Fe(DE•Fe) and EDTA-Distamycin•Fe(ED•Fe).

idine-homopurine tracts of DNA by triple helix formation (22). The studies of Sigman using a 1, 10-phenanthroline-copper complex [$(OP)_2Cu(I)$] tethered to the tryptophan gene repressor of *E. coli* (23) and Barton with chiral transition-metal complex[tris(4, 7-diphenylphenanthroline)cobalt-(III) ($Co(DIP)_3^{3+}$)] (24) have shown site-specific cleavage of DNA through

the scission of the DNA backbone. Since the DNA cleavage of EDTA•Fe(II) and 1, 10-phenanthroline-copper complex [$(OP)_2Cu(I)$] gives multiple cleavage patterns on double helical DNA (18, 24), we have turned our attention to the development of non-diffusible cleaving functions that would produce a single cleavage site. The design for the DNA-cleaving functions was based on the naturally occurring bleomycin (BLM), neocarzinostatin (NCZ), and dopamine-β-monohydroxylase. Bleomycin, as mentioned earlier, cleaves DNA at two base recognition sites in a reaction dependent on Fe(II)/dithiothreitol or Co(III)/UV (15, 17). Neocarzinostatin cleaves DNA through radical formation in the presence of thiol (16). Dopamine-β-monooxygenase, a copper-containing enzyme, catalyzes the hydroxylation of dopamine to norepinephrine (25).

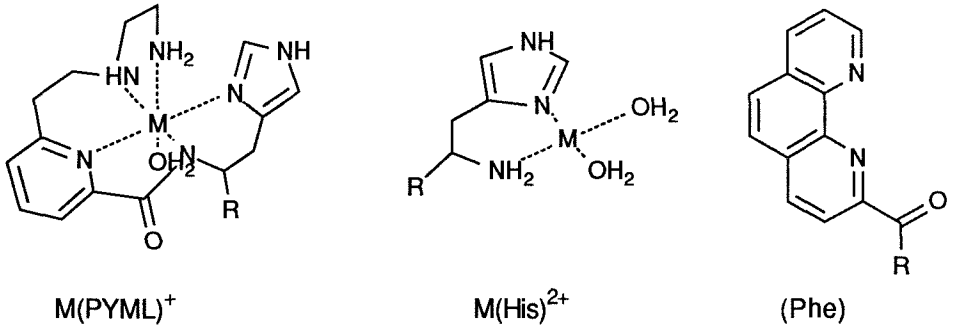

Figure 6a. Structure of ligand to be connected to sequence-specific DNA binding molecule R. M is Metal ions (Fe^{++}or Cu^{++}).

We designed and synthesized three different cleaving functional groups in an effort to create a nondiffusible cleaving moiety (Figure 6). Compound **19** (P3-M-PYML) shows the sequence-specific cleavage of DNA in the presence of Fe(II) and DTT, while compound **12** (P3-Ga-His) shows the sequence-specific cleavage of DNA in the presence of Cu(II) without

adding a reducing agent such as DTT. The cleavage of DNA by P3-M-PYML•Fe(II)/dithiothreitol (DTT) near the distamycin binding site is multiple as in an experiment of distamycin-EDTA•Fe(II), while the cleavage of DNA by P3-Ga-His•Cu(II) shows the less multiple cleavage. Interestingly, compound **23** (P3-Ga-Phe) shows the sequence-specific cleavage of DNA in the presence of UV light and β-carbonato(trien)cobalt(III)perchlorate complex. The end product analysis of the cleaved oligonucleotide shows 5'-phosphate and two different 3' products.

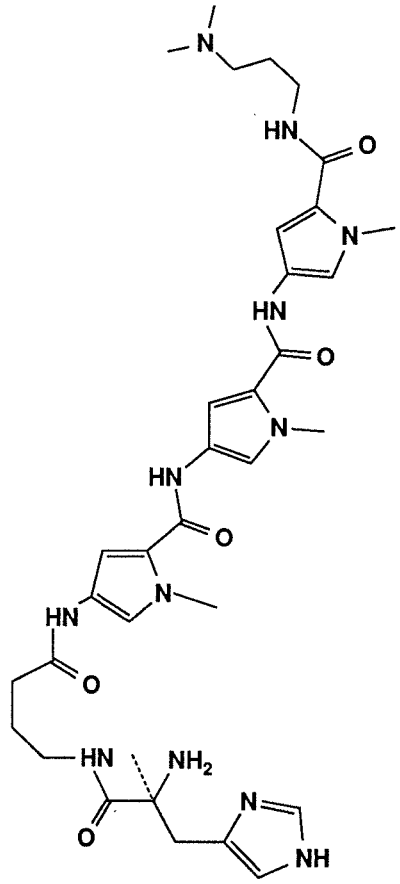

12 (P3-Ga-His)

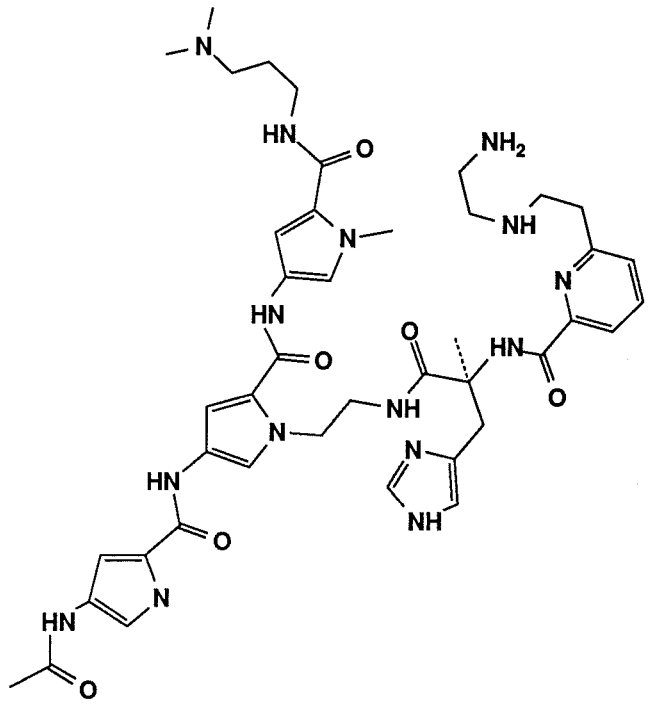

19 (P3-M-PYML)

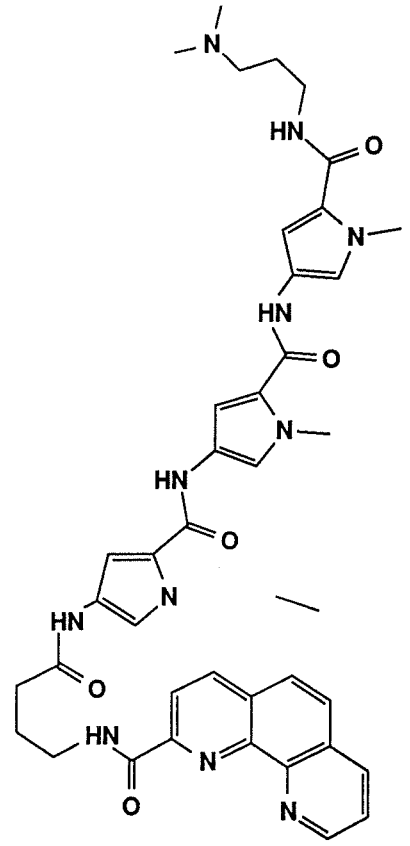

23 (p3-Ga-Phe)

Figure 6b. The chemical structures of P3-Ga-His (**12**), P3-M-PYML (**19**), and P3-Ga-Phe (**23**).

Results and Discussion

Synthesis (Figure 7, 8, 9 and 10). 4-Nitropyrrole-2-carboxlic acid ethylester **1** was prepared by the published method (26). The reaction of **1** with 2-bromoethyl amine t-butylcarbamate **2** and subsequent hydrolysis of **3** produced the pyrrole **4**. The coupling of **4** with N-methy-4-nitropyrrole-2-(N, N-dimethylpropylamino)-carboxamide **5** (27) produced compound **6**. Reduction of **6** and coupling with N-methy-4-nitropyrrole-2-carboxlic acid (27) produced compound **7**. Compound **9** was obtained in three steps from compound **7**. The coupling of **9** with l-Histidine-t-boc carbamate and subsequent deprotection of the t-boc group produced compound **10** (P3-M-His). Compound **11** was synthesized by the published method (27). Compound **12** (P3-Ga-His) was synthesized by coupling **11** with l-histidine-t-boc carbamate and subsequent deprotection as described above.

Compound **18** was synthesized by the known method (28). The coupling of **9** with **18** and subsequent deprotection of the resulting products produced compound **20** (P3-PYML). Compound **21** (P3-EDTA) was synthesized by coupling of **9** with the triester of EDTA and hydrolysis of the resulting ester product (27).The coupling of **9,** which was prepared by the published method (27), with 1,10-phenanthroline-2-carboxylic acid produced compound **21** (P3-M-Phe). The same method was applied for the synthesis of compound **23** (P3-Ga-Phe).

DNA cleavage by P3-M-PYML•Fe(II) 19 and P3-M-EDTA•Fe(II) 20.The cleavage of the 167 bp fragment from plasmid pBR322 by P3-M-PYML(19) in the presence of dithiothreitol and O_2 was studied.An autoradiograph of the cleavage patterns produced by P3-M-PYML•Fe(II) and P3-M-EDTA on the 167 base pair restriction fragment is shown in Figure 11a. The DNA cleavage patterns on this autoradiograph were anal-

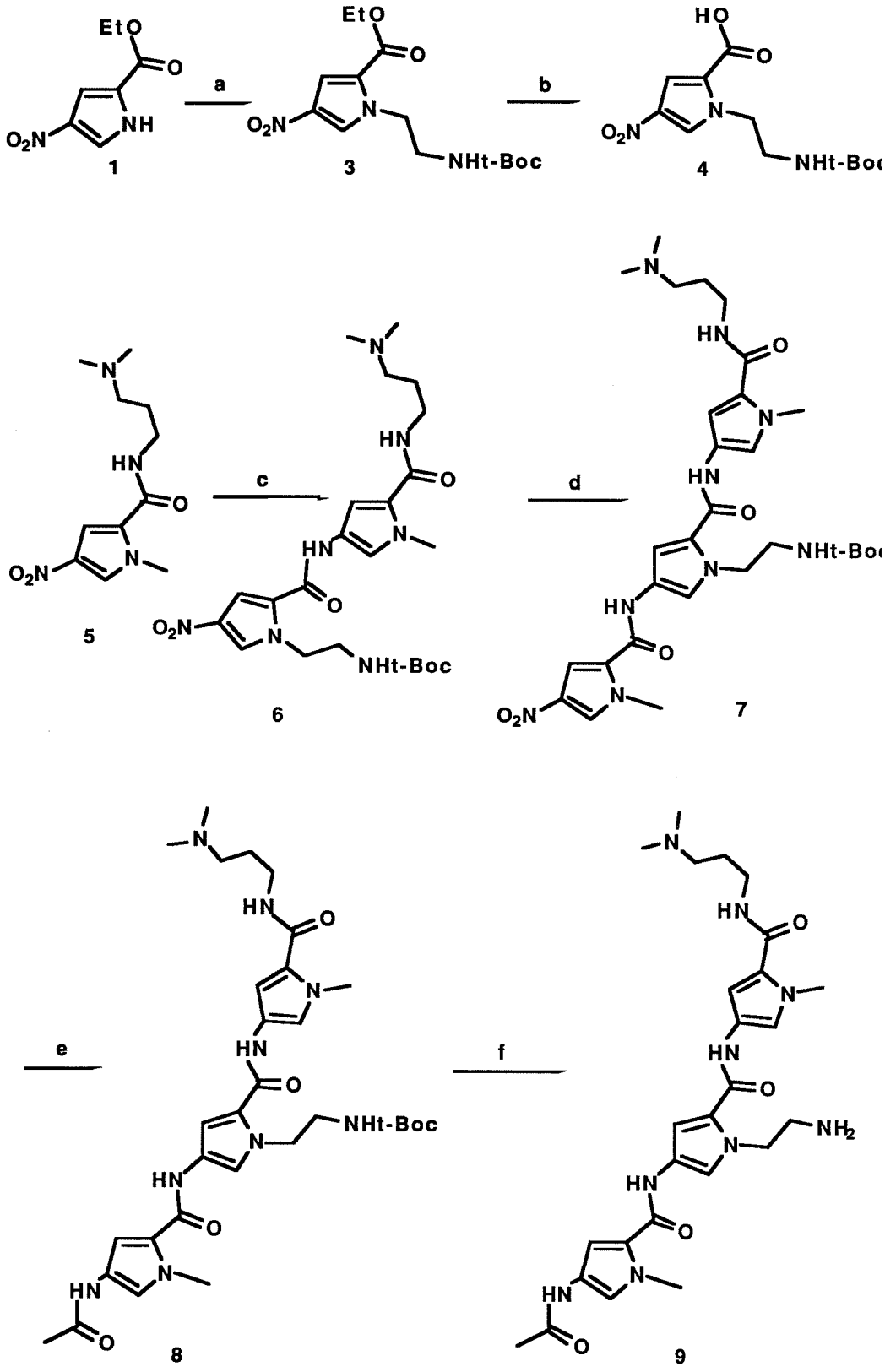
EtO
O
NH
O_2N
1
a
EtO
O
N
O_2N
NHt-Boc
3
b
HO
O
N
O_2N
NHt-Boc
4
N
HN
O
N
HN
O
N
O_2N
5
c
N
HN
O
N
HN
O
N
O_2N
NHt-Boc
6
d
N
HN
O
N
HN
O
N
HN
O
N
O_2N
NHt-Boc
7
e
N
HN
O
N
HN
O
N
HN
O
N
HN
O
NHt-Boc
8
f
N
HN
O
N
HN
O
N
HN
O
N
HN
O
NH_2
9

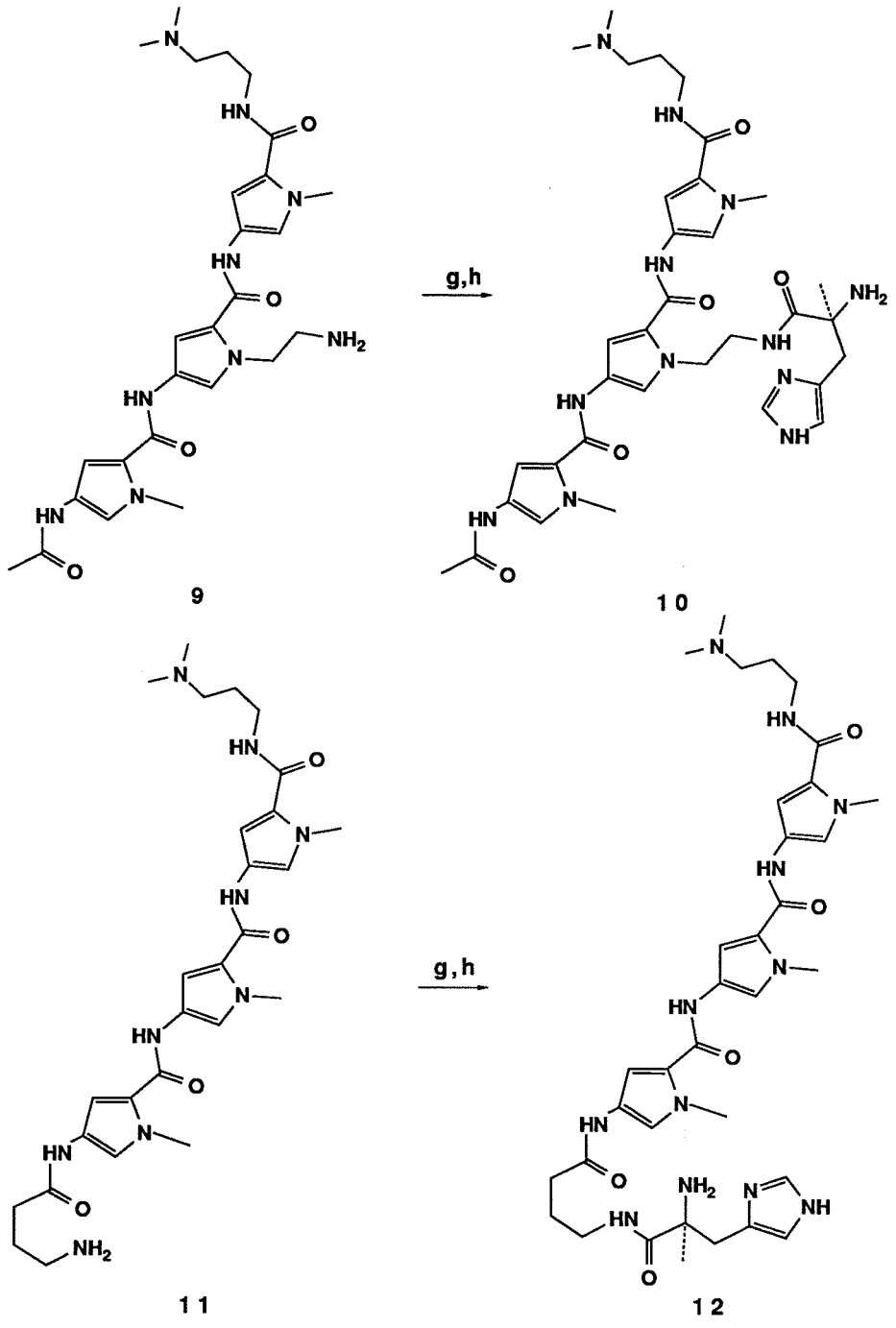

Figure 7. a) NaI/acetone, $BrCH_2CH_2NHCOOC(CH_3)_3$ b)OH^- c) H_2/Pd/C, n-hydroxybenzotriazole(1-HOBT)/dicyclohexylcarbodiimide (DCC)/DMF d) DCC/1-HOBT/ N-methyl-4-nitro-2-carboxylic acid/DMF e) H_2/Pd/C. carbonyl–diimidazole (CDI)/acetic acid/DMF f) trifluoroacetic acid g) l-histidine-t-boc/DCC/1-HOBT h) trifluoroactic acid.

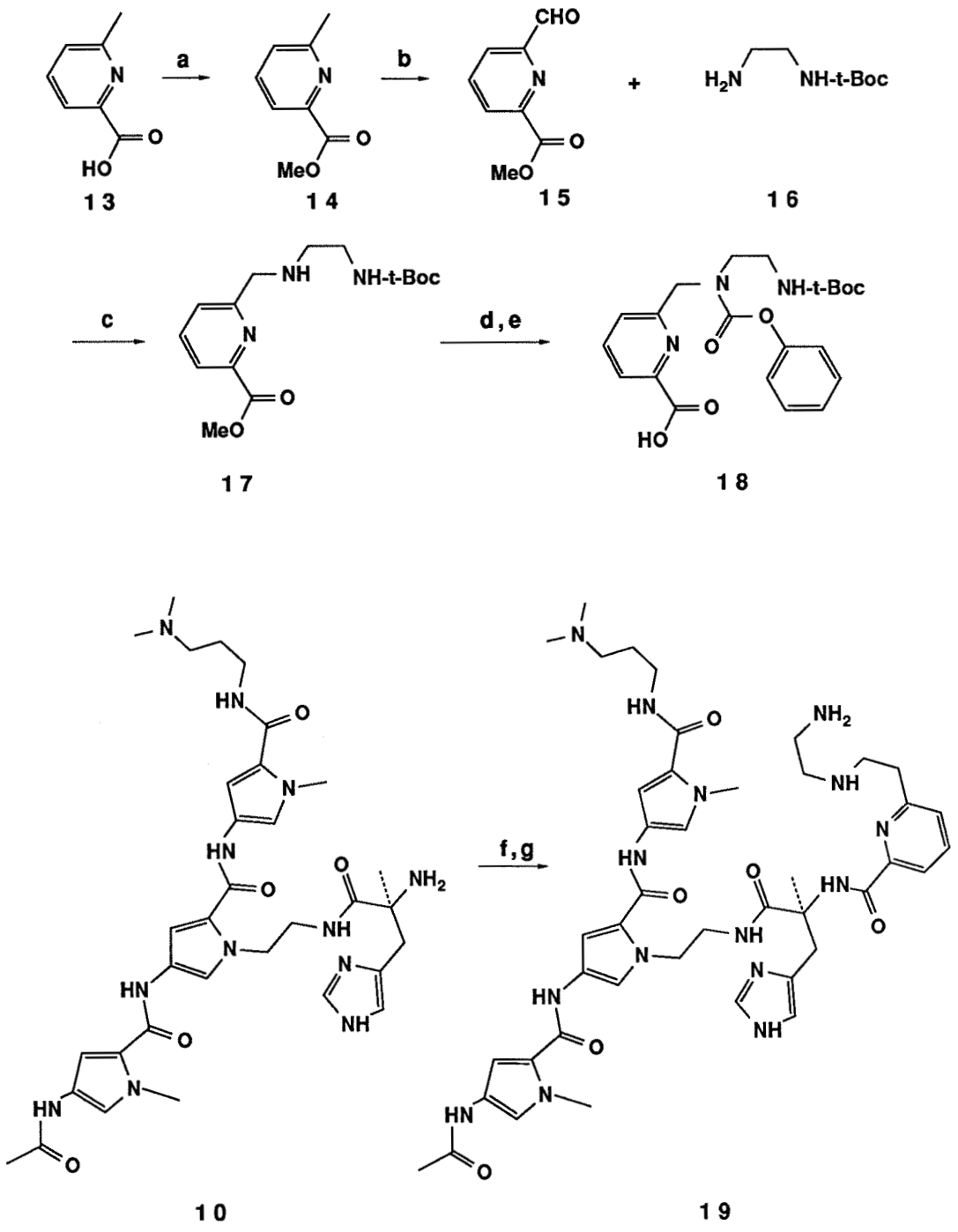

Figure 8. The synthetic scheme for the synthesis of P3-M-PYML(**19**). a) MeOH/H_2SO_4 b) I_2/DMSO c) Molecular Sieve 4Å/acetonitrile, H_2/Pd/C d) C_6H_5OCOCl/HO- e) OH^- f) **18**, DCC/1-HBT g) trifluoroacetic acid.

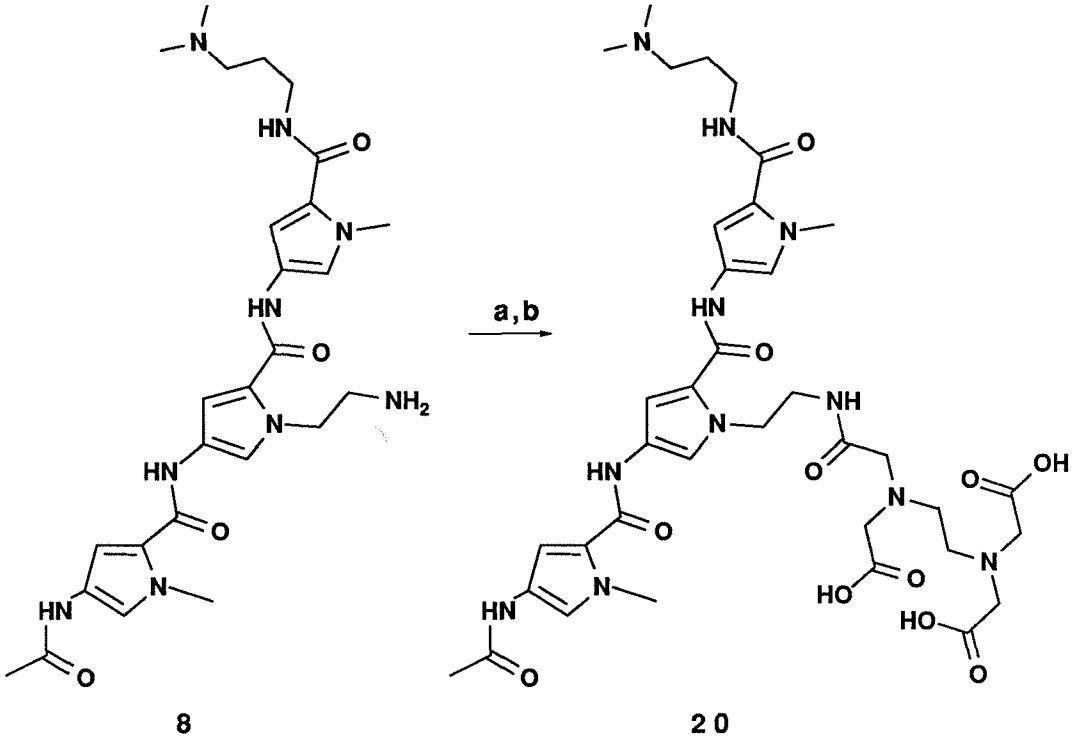

Figure 9. The synthetic scheme for the P3-M-EDTA (**20**). a) EDTA-ester/CDI b) HO^-.

lyzed by densitometry and converted to histogram (Figure 11b). It can be seen that P3-M-PYML•Fe(II) and P3-M-EDTA•Fe(II) produce specific DNA cleavage near the binding sites. The cleavage patterns produced by the two compounds near the distamycin binding site show mutiple sites of cleavage. Since the reactive group is in the middle of a molecule, the cleavage patterns do not show two orientations near the binding site as in distamycin-EDTA and EDTA-distamycin (which has a reactive group at the carboxy terminal or amino terminal of distamycin). The cleavage efficiency of DNA by P3-M-PYML•Fe(II) is better than that of P3-M-EDTA (20). The strongest cleavage site is 5'-GTTAAATTG-3'

DNA cleavage by P-Ga-His (12). The cleavage of a 167 bp fragment from bacterial plasmid pBR322 by compounds **10** and **12** was studied at various

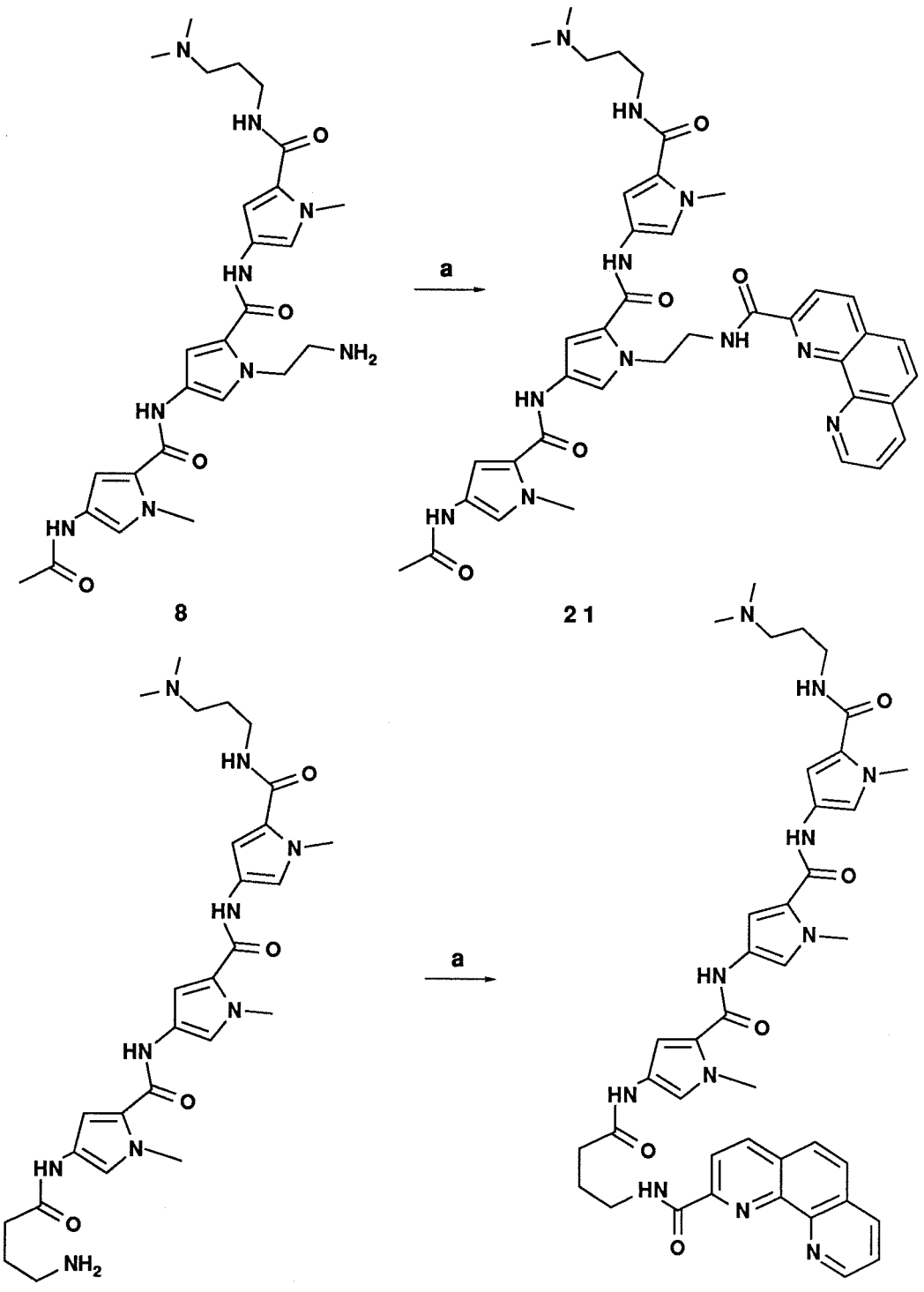

Figure 10. The synthetic scheme for the synthesis of P3-M-Phe (**21**) and P3-Ga-Phe (**23**). a) 1,10-phenanthroline-2-carboxylic acid/DCC/1-HOBT/DMF. minal of distamycin). The cleavage efficiency of DNA by P3-M-PYML•Fe(II) is better than that of P3-M-EDTA (**20**). The strongest cleavage site is 5'-GTTAAATTG-3'.

pH's in the presence of Cu(II) ion. Footprintings of DNA by MPE•Fe(II) for compounds **10** and **12** were also examined by using the 167 base pair restriction fragment. An autoradiograph of the cleavage patterns produced by P3-Ga-His (**12**) on the 167 base pair restriction fragment is shown in Figure 12a. The DNA cleavage patterns on this autoradiograph were analyzed by densitometry and converted to histogram form (Figure 12b). Here it can be seen that the P3-Ga-His compound (**12**) produces specific DNA cleavage near the binding site. The cleavage patterns near the binding site are different from those produced by distamycin-EDTA analogs. A single sites of cleavage is seen near the 5'-CGATAA site in 5' labeled 167 bp fragment. This cleavage pattern suggests that P3-Ga-His•Cu(II) cuts DNA cleavage via a nonfreely diffusing reactive species. Interestingly , P3-M-His (**10**) compound shows no cleavage of DNA (data not shown). It is believed that the histidine-Cu(II) complex of **10** is not accesible to minor groove because the molecule itself sits on the the minor groove.

The type of end products produced during DNA cleavage is dependent on the type of cleavage reaction. Maxam-Gilbert chemical sequencing reactions produce 3'- and 5'-phosphate terminal groups. DNAase reaction produce 3'-hydroxy and 5'-phosphate terminal groups (29). Distamycin-EDTA•Fe(II) and MPE•Fe(II) produce 5'-phosphate and a mixture of 3'-phosphate and 3'-phosphoglycolate termini (30). BLM•Fe(II) produces 5'-phosphate and 3'-phosphoglycolate termini under aerobic conditions (15,17). Neocarzinostatin produces 3'-phosphate termini and a mixture of 5'-phosphate and nucleoside 5'-aldehyde termini (11).

The DNA end products produced upon P3-Ga-His•Cu(II) cleavage were determined as part of an investigation into the mechanism by which

Figure 11a. Autoradiograph of DNA cleavage patterns produced by P3-M-EDTA•Fe(II)(**20**) and P3-M-PYML•Fe(II) (**19**) compounds on 5'-^{32}P end-labeled 167 base pair restriction fragments (EcoRI/RsaI) from plasmid pBR322 DNA in the presence of dioxygen and dithiothreitol. Cleavage patterns were resolved by electrophoresis on a 1:20 cross-linked 8% polyacrylamide, 50% urea denaturing gel. Lane 1: Maxam-Gilbert chemical sequencing G reaction (33); lane 2: Control with 25 μM Fe(II); lanes 3-5: P3-M-EDTA(**20**)•Fe(II) at 25 μM, 5μM, 1μM concentrations; lanes 6-9: P3-M-PYML(**19**)•Fe(II) at 25 μM, 5 μM, 1μM, and 0 μM concentrations.

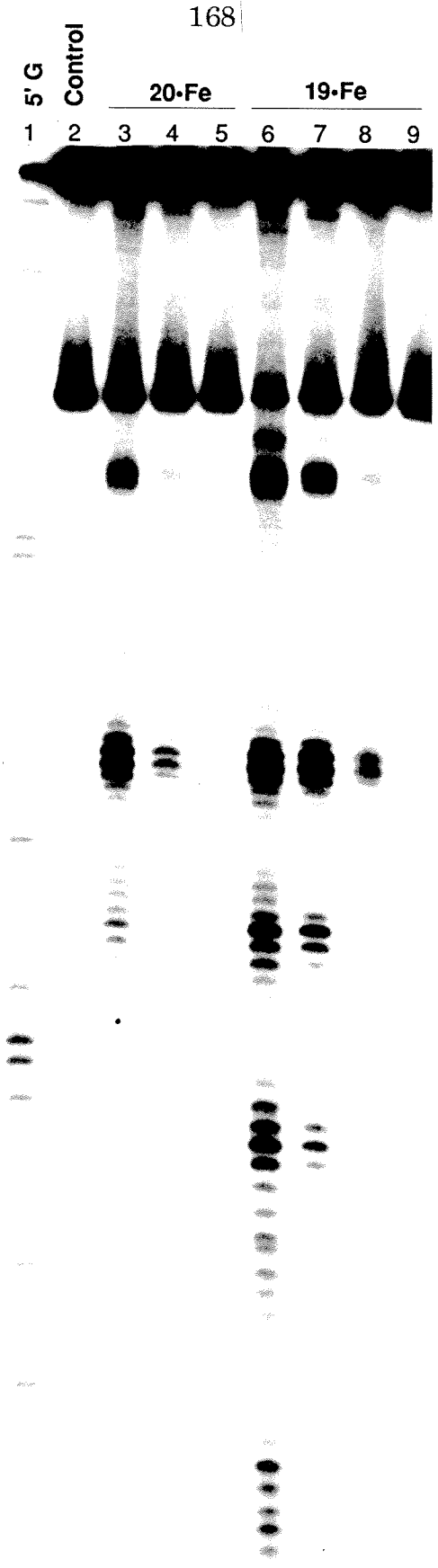
5' G
Control
20•Fe
19•Fe
1 2 3 4 5 6 7 8 9

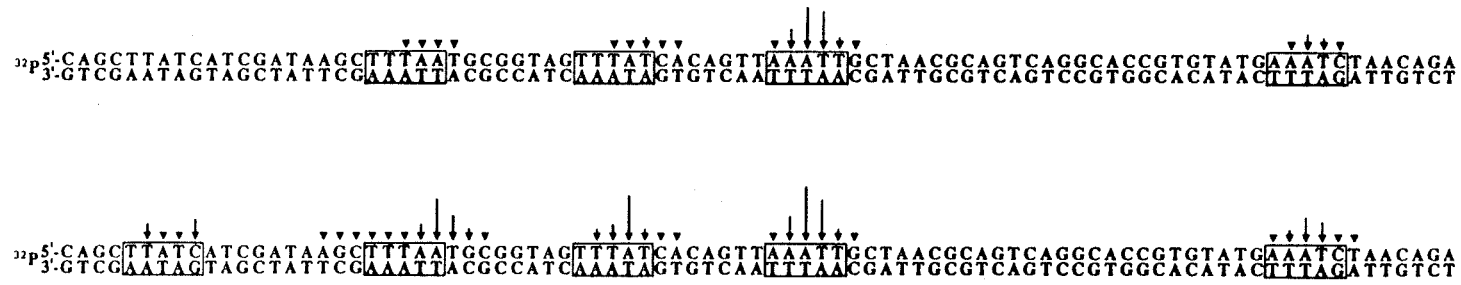

Figure 11b. Histogram of DNA cleavage produced by 5 μM P3-M-EDTA•Fe(II) (**20**) (**Top**) and 5 μM P3-M-PYML (**19**)•Fe(II) on 167 base pair fragment (EcoRI/RsaI) from plasmid pBR322 DNA in the presence of DTT and dioxygen (Figure 11a). Length of arrows corresponds to the relative amount of cleavage, determined by optical densitometry, which result in removal of indicated base. Boxes represent equilibrium binding site. Sequence positions of cleavage were determined by comparing the electromobilities of DNA cleavage fragments to bands in Maxam-Gilbert chemical sequencing lane.

P3-Ga-His•Cu(II) mediates DNA cleavage. The identities of DNA end products produced with P3-Ga-His•Cu(II) were determined by analyzing the electrophoretic mobilities of short DNA cleavage fragments on 15% denaturing polyacrylamide gels, and the way in which the mobilities of these fragments were affected by treatment with phosphatase enzymes. Figure 12c (left) shows an autoradiograph of cleavage patterns produced by Maxam-Gilbert reaction, DNAase reaction, MPE•Fe(II)/dithiothreitol reaction, P3-Ga-His•Cu(II) reaction, and digestion of these with T4 polynucleotide kinase (which converts 3'-phosphate groups to 3'-hydroxy groups) on the 3'-^{32}P end-labeled 167 base pair EcoRI/RsaI restriction fragment from pBR322. Electromobilities of the radio-labeled cleavage fragment produced on these substrates depend on their length and the nature of their 3'-termini. The doublets produced with MPE•Fe(II) are due to faster-running fragments that terminate in 3'-phosphoglycolate and slower-running fragments that terminate in 3'-phosphate groups (30). The short DNA fragments produced by P3-Ga-His•Cu(II) do not comigrate with 3'-phosphate, 3'-hydroxy, and 3'-phosphoglycolate except in the case of the shortest fragment. The electromobilities of these fragments are not reduced upon treatment with T4 polynucleotide kinase. Thus, P3-Ga-His•Cu(II) mediates the direct formation of DNA strand breaks having different 3'-ends from Maxam-Gilbert, DNAase, and MPE•Fe(II). Figure 12c (right) shows an autoradiograph of cleavage patterns produced by Maxam-Gilbert reaction, DNAase reaction, MPE•Fe(II)/dithio- thretol reaction, P3-Ga-His•Cu(II) reaction, and digestion with calf intestine alkaline phosphatase (CAP) (which converts 5'-phosphate groups to 5' hydroxy groups) on the 5'-^{32}P end-labeled 167 base pair EcoRI/RsaI restric-

Figure 12a. Autoradiograph of MPE•Fe(II) footprinting by P3-Ga-His and cleavage patterns produced by P3-Ga-His(**12**)•Cu(II) on 3'- and 5'- ^{32}P end-labeled 167 base pair fragments (EcoRI/RsaI) from plasmid pBR322 DNA in the presence of dioxygen. Cleavage patterns were resolved by electrophoresis on a 1:20 cross linked 8% polyacrylamide, 50% urea denaturing gel. Lanes 1, 3, 5, 7, and 9-11 were with 5' end-labeled DNA, whiles lanes 2, 4, 6, 8, and 12-14 were with 3' end-labeled DNA. Lanes 1 and 2, Maxam-Gilbert chemical sequencing G reactions; lanes 3-4, MPE•Fe(II) at 2 μM concentration; lane 5, MPE•Fe(II) at 2 μM concentration in the presence of P3-Ga-His (5 μM) and dioxygen; lane 6, MPE•Fe(II) at 2 μM in the presence of P3-Ga-His (5 μM) and dioxygen; lanes 7-8, Cu(II) at 200 μM concentration; lanes 9-11, P3-Ga-His at 5 μM concentration in the presence of Cu(II) (200 μM) and dioxygen at pH 7,5, 8,5, and 9.5; lanes 10-14, P3-Ga-His at 5 μM concentration in the presence of Cu(II) (200 μM) at pH 7.5, 8.5, and 9,5.

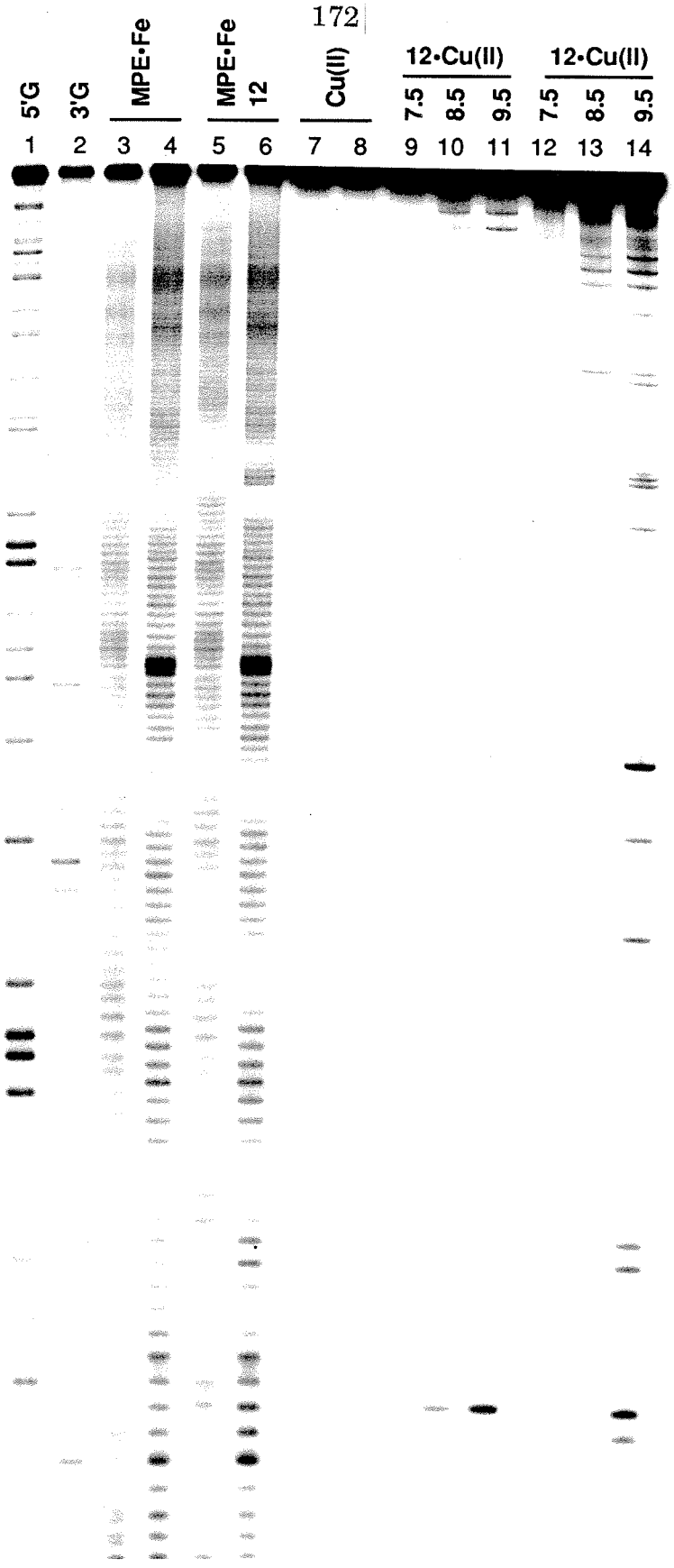
5'G
3'G
MPE•Fe
MPE•Fe
12
Cu(II)
12•Cu(II)
12•Cu(II)
7.5
8.5
9.5
7.5
8.5
9.5
1 2 3 4 5 6 7 8 9 10 11 12 13 14

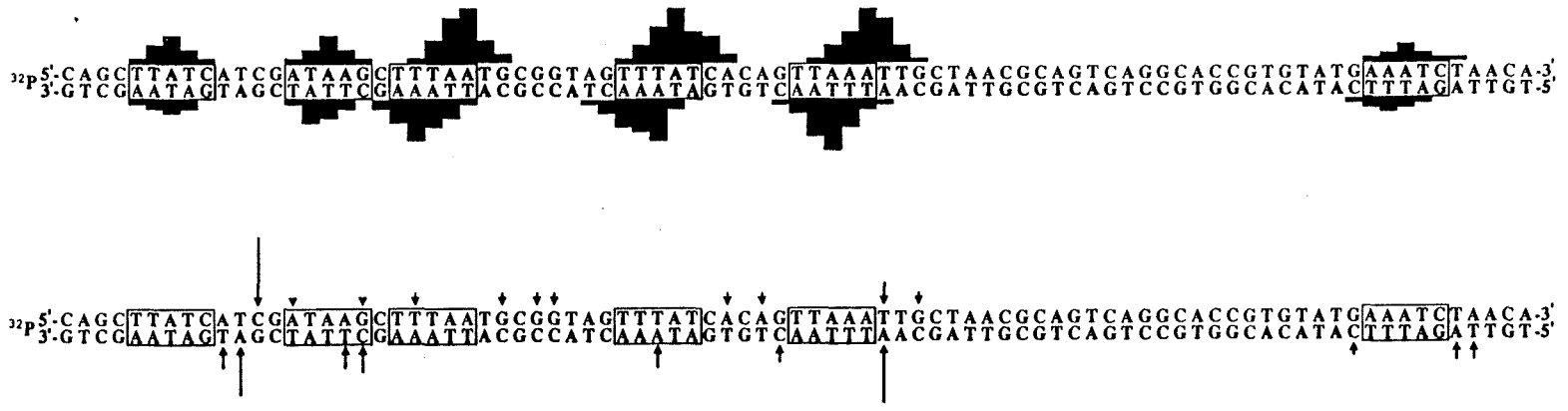

Figure 12b. (**Top**) MPE•Fe(II) protection patterns for 5 μM P3-Ga-His on the 167 bp fragment of PBR322. (**Bottom**)Histogram of DNA cleavage produced by P3-Ga-His•Cu(II) (**12**) on 167 base pair fragment (EcoRI/RsaI) from plasmid pBR322 DNA in the presence of dioxygen (Figure 12a). Length of arrows corresponds to the relative amount of cleavage, determined by optical densitometry, which result in removal of indicated base. Boxes represent equilibrium binding site. Sequence positions of cleavage were determined by comparing the electromobilities of DNA cleavage fragments to bands in Maxam-Gilbert chemical sequencing lane.

Figure 12c. (**left**) Analysis of DNA 3'-end products produced with P3-Ga-His(**12**)•Cu(II) on the 5'-^{32}P end-labeled 167 bp restriction fragment (EcoRI/RsaI) from pBR322 plasmid DNA. Cleavage patterns were resolved by electrophoresis on a 1:20 cross-linked 15% polyacrylamide, 40% urea denaturing gel. Lane 1, Maxam-Gilbert chemical sequencing G reaction; lane 2, DNase I reaction; lane 3, DNA cleavage by MPE•Fe(II) at 2 μM concentration in the presence of dithiothreitol (4.0 mM) and dioxygen; lane 4, DNA cleavage by P3-Ga-His at 5 μM concentration in the presence of $CuSO_4$ (200 μM) and dioxygen; lane 5, DNA cleavage by P3-Ga-His at 5 μM concentration in the presence of CuSO4 (200 μM) and dioxygen with subsequent 3'-dephosphorylation using T4 polynucleotide kinase. (**right**) Analysis of DNA 5'-end products produced with P3-Ga-His•Cu(II) (**12**) on the 3'-^{32}P end-labeled 167 bp restriction fragment(EcoRI/RsaI) from pBR322 plasmid DNA. Cleavage patterns were resolved by electrophoresis on a 1:20 cross-linked 15% polyacrylamide, 40% urea denaturing gel. Lane 1, Maxam-Gilbert chemical sequencing G reaction; lane 2, DNAase reaction; lane 3, DNA cleavage by MPE•Fe(II) at 2 μM concentration in the presence of dithiothreitol (4.0 mM) and dioxygen; lane 4, DNA cleavage by P3-Ga-His at 5 μM concentration in the presence of $CuSO_4$ (200 μM) and dioxygen; lane 5, DNA cleavage by P3-Ga-His at 5 μM concentration in the presence of $CuSO_4$ (200 μM) and dioxygen with subsequent 5'-dephosphorylation using calf intestine alkaline phosphatase (CAP).

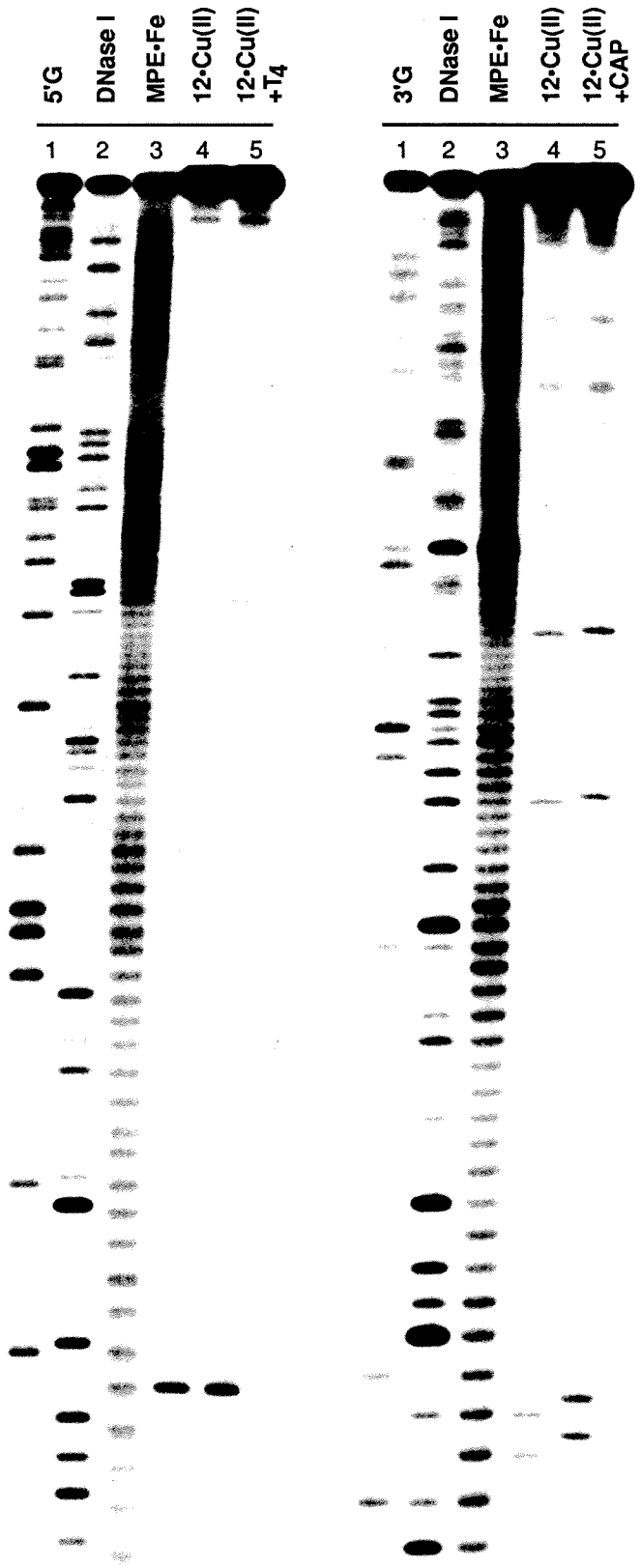
5'G
DNase I
MPE-Fe
12-Cu(II)
12-Cu(II) +T4
1 2 3 4 5
3'G
DNase I
MPE-Fe
12-Cu(II)
12-Cu(II) +CAP
1 2 3 4 5

tion fragment from pBR322. Electromobilities of radio-labeled cleavage fragments produced on these substrates depend on their length and the nature of their 5' termini. Fragments produced by the Maxam-Gilbert chemical reaction, DNAase, and MPE•Fe(II)/dithiothreitol terminate in 5'-phosphate group (30). The short DNA fragments produced by P3-Ga-His•Cu(II) comigrate with the MPE•Fe(II) DNA fragments having 5'-phosphate groups. The electromobilities of these fragments are reduced upon treatment with CAP. Thus, P3-Ga-His(II) mediates the direct formation of DNA strand breaks having 5'-phosphate termini.

DNA cleavage by P3-Ga-Phe (23). The sequence-specific cleavages of DNA by P3-M-Phe (**21**) and P3-Ga-Phe (**23**) in the presence of β-carbonato(trien)Co(III)perchlorate and UV light was examined using the 167 bp restriction fragment from pBR322. Footprinting of DNA by MPE•Fe(II) for P3-Ga-Phe and P3-M-Phe in the presence of dithiothreitol was also examined. An autoradiograph of the cleavage pattern produced by P3-Ga-Phe, P3-M-Phe and bleomycin•Co(III) on 167 base pair restriction fragments is shown in Figure 13a. The results of footprinting and cleavage sites were analyzed by densitometry and converted to histogram form (Figure 13b). Here it can be seen that P3-Ga-Phe produces the single DNA cleavage on 167 base restriction fragment which has 4 strong binding sites. Interestingly, P3-M-Phe (**21**) does not show any cleavage Bleomycine•Co(III) shows strong photochemical DNA cleavage as reported, with preference for G:C base pairs. The identities of DNA end products produced by P3-Ga-Phe (**23**) in the presence of UV light and β-carbonato(trien)Co(III)perchlorate were determined by analyzing the electrophoretic mobilities of short DNA cleavage fragments on 20% dena-

Figure 13a. Autoradiograph of MPE•Fe(II) footprinting by P3-M-Phe (**21**) and P3-Ga-Phe (**23**) in the presence of dithiothreitol and dioxygen, and cleavage patterns produced by P3-M-Phe (**21**) and P3-Ga-Phe (**23**) on 3'- and 5'-^{32}P end labeled 167 base pair fragments (EcoRI/RsaI) from plasmid pBR322 DNA in the presence of dioxygen, β-carbonato(trien)Co(III)perchlorate, and UV light (366 nm). Cleavage patterns were resolved by electrophoresis on a 1:20 cross linked 8% polyacrylamide, 50% urea denaturing gel. Lanes 1, 3, 5, 6, 9,11, 13, 15, 16, 19, 21 were with 5'end-labeled DNA, and lanes 2, 4, 7, 8, 12,14, 17, 18, 20, 22 were with 3'end-labeled DNA. Lanes 1 and 2, Maxam-Gilbert chemical sequencing G reaction; lanes 3-4, MPE•Fe(II) at 2μM concentrations; lanes 5 and 7, MPE•Fe(II) at 2 μM concentrations in the presence of P3-Ga-Phe (5 μM), dithiothreitol and dioxygen; lanes 6 and 8, MPE•Fe(II) at 2 μM in the presence of P3-M-Phe (5 μM) and dioxygen; lanes 9-10, P3-Ga-Phe at 5 μM concentrations in the presence of UV (366 nm) and dioxygen; lanes 11-12, P3-M-Phe at 5 μM concentration in the presence of UV(366 nm) and dioxygen; lanes 13-14, β-carbonato(trien)Co(III) at 25 μM concentration in the presence of UV(366 nm) and dioxygen; lanes 15 and 17, P3-Ga-Phe at 5 μM concentration in the presence of UV (366 nm), β-carbonato(trien)Co(III)perchlorate (25 μM), and dioxygen; lanes 16 and 18, P3-M-Phe at 5 μM concentration in the presence of UV(366 nm), β-carbonato(trien)Co(III)perchlorate (25 μM), and dioxygen; lanes 19 and 20, bleomycin (BLM)Co(III) at 5 μM concentration in the presence of UV (366 nm) and dioxygen; lanes 21 and 22, UV light (366 nm).

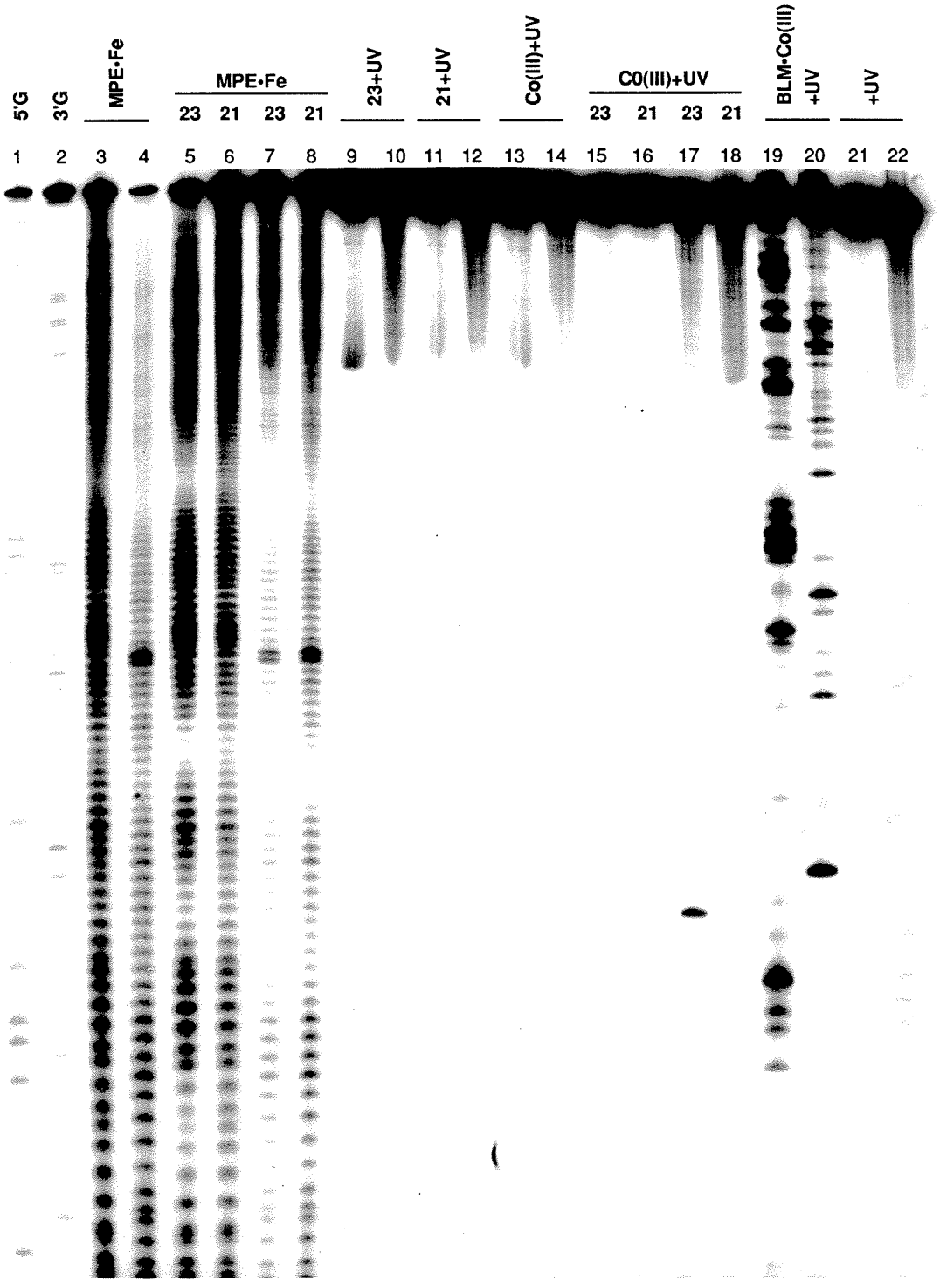
5'G
3'G
MPE-Fe
MPE•Fe
23
21
23
21
23+UV
21+UV
Co(III)+UV
C0(III)+UV
23
21
23
21
BLM•Co(III)
+UV
+UV
1 2 3 4 5 6 7 8 9 10 11 12 13 14 15 16 17 18 19 20 21 22

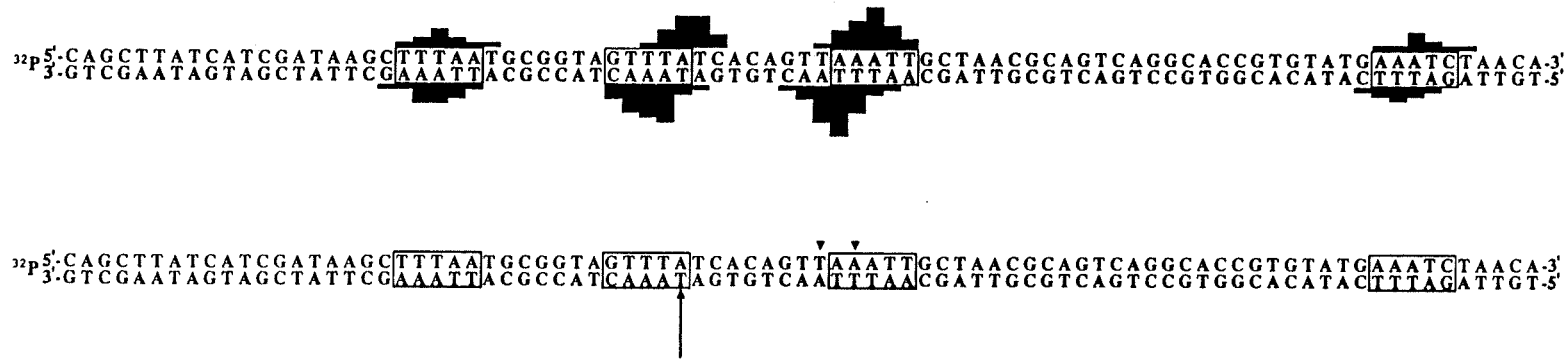

Figure 13b. (**Top**) MPE•Fe(II) protection patterns for 5 μM P3-Ga-Phe (**22**) on the 167 bp fragment of PBR322. (**Bottom**) Histogram of DNA cleavage produced by 5 μM P3-Ga-Phe (**22**) on 167 base pair fragment (EcoRI/RsaI) from plasmid pBR322 DNA in the presence of dioxygen, β-carbonato(trien)Co(III)perchlorate, and UV light (366 nm) (Figure 13a). Length of arrows corresponds to the relative amount of cleavage, determined by optical densitometry, which result in removal of indicated base. Boxes represent equilibrium binding site. Sequence positions of cleavage were determined by comparing the electromobilities of DNA cleavage fragments to bands in Maxam-Gilbert chemical sequencing lane.

turing polyacrylamide gels.

Oligonucleotide duplex **26** containing the same sequence near the strong cleavage site of the 167 base fragment was synthesized by β-cyanoethylchemistry and labeled on the 3'-end and the 5'-end of the cleaving strand (Figure 13c). 3' and 5' end labeled duplex oligonucleotide **26** were prepared by standard methods. Figure 13d shows an autoradiograph of cleavage patterns produced by Maxam-Gilbert G reaction, MPE•Fe(II)/dithiothreitol, P3-Ga-Phe (**23**)/β-carbonato(trien)Co(III)perchlorate/UV reaction, and digestions with T4 polynucleotide kinase (which converts 3'-phosphate groups to 3' hydroxy groups) on the 3'-^{32}P 27 mer oligonucleotide. Electromobilities of radio-labeled cleavage fragments produced on these substrates depend on their length and the nature of their 3'-termini. The doublets produced with MPE•Fe(II) are due to faster-running fragments that terminate in 3'-phosphoglycolate and slower-running fragments that terminate in 3'-phosphate groups. The DNA fragments produced by P3-Ga-Phe/β-carbonato(trien)Co(III)perchlorate/UV comigrate with 3'-phosphate and 3'-phosphoglycolate. The electromobilities of slower-running fragments are reduced upon treatment with T4 polynucleotide kinase. Thus, P3-Ga-Phe/β-carbonato(trien)Co(III)perchlorate/UV mediates the direct formation of DNA strand breaks having two different 3'-ends: 3'-phosphate and 3'-phosphoglycolate as in MPE•Fe(II).

Figure 13e shows an autoradiograph of cleavage patterns produced by Maxam-Gilbert G reaction, MPE•Fe(II)/dithiothreitol reaction, P3-Ga-Phe(**23**)/β-carbonato(trien)Co(III)perchlorate/UV reaction, and digestion with calf intestine alkali phosphatase (CAP) (which converts 5'-phosphate

Figure 13c . Oligonucleotides **24**, **25**, and **26** and the DNA cleavage with P3-Ga-Phe(**23**).

groups to 5'-hydroxy groups) on the 5'-^{32}P end-labeled 27 mer oligonucleotide DNA. Electromoblities of radio-labeled cleavage fragments produced on these substrate depends on their length and the nature of their

5'-termini. Fragments produced by Maxam-Gilbert chemical G reaction, and MPE•Fe(II)/dithiothreitol terminate in 5'-phosphate group. The DNA fragments produced by P3-Ga-Phe (**23**)/β-carbonato(trien)Co(III)perchlorate/UV comigrate with the DNA fragments having 5'-phosphate groups produced by MPE•Fe(II). The electromobilities of these fragments are reduced upon treatment with CAP. Thus, P3-Ga-Phe (**23**)/β-carbonato(trien)Co(III)perchlorate/UV mediates the direct formation of DNA strand breaks having 5'-phosphate termini.

Figure 13d. Analysis of DNA 3'-end products produced by P3-Ga-Phe (**23**) /β-carbonato(trien)Co(III)perchlorate/UV light/dioxygen on the 5'-^{32}P end-labeled 27 bp oligonucleotide (**26**). Cleavage patterns were resolved by electrophoresis on a 1:20 cross-linked 20% polyacrylamide, 40% urea denaturing gel. Lane 1, uncleaved DNA; lane 2, UV light (366 nm); lane 3, Maxam-Gilbert chemical sequencing G reaction; lanes 4-5, DNA cleavage by MPE•Fe(II) at 10 μM concentration in the presence of dithiothreitol (4.0 mM) and dioxygen; lane 6, DNA cleavage by P3-Ga-Phe at 5 μM concentration in the presence of dioxygen, β-carbonato(trien)Co(III)perchlorate (25 μM), and UV light (366 nm); lane 7, DNA cleavage by P3-Ga-Phe at 5 μM concentration in the presence of dioxygen, β-carbonato(trien)Co(III)perchlorate (25 μM), and UV light (366 nm) with subsequent 3'-dephosphorylation using T4 polynucleotide kinase.

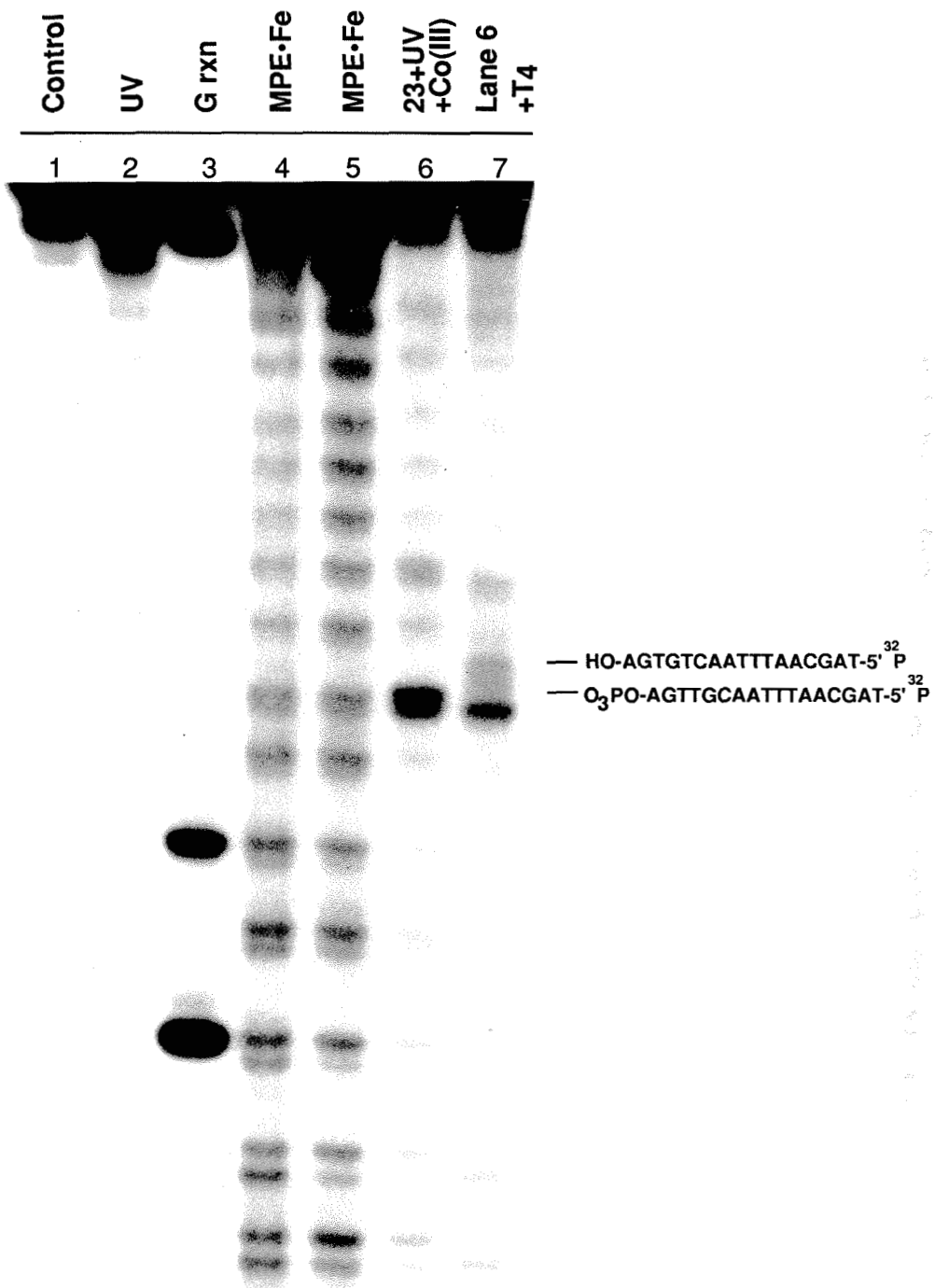
Control
UV
G rxn
MPE·Fe
MPE·Fe
23+UV +Co(III)
Lane 6 +T4
1
2
3
4
5
6
7
— HO-AGTGTCAATTTAACGAT-5' 32P
— O3PO-AGTTGCAATTTAACGAT-5' 32P

Figure 13e. Analysis of DNA 5'-end products produced with P3-Ga-Phe /β-carbonato(trien)Co(III)perchlorate/UV light/dioxygen on the 5' ^{32}P end-labeled 27 bp oligonucleotide (**26**). Cleavage patterns were resolved by electrophoresis on a 1:20 cross-linked 20% polyacrylamide, 40% urea denaturing gel. Lane 1, uncleaved DNA; lane 2, UV light (366 mm); lane 3, Maxam-Gilbert chemical sequencing G reaction; lane 4, DNA cleavage by MPE•Fe(II) at 10μM concentration in the presence of dithiothreitol (3.0 mM) and dioxygen; lanes 5 and 7, DNA cleavage by P3-Ga-Phe at 5 μM concentration in the presence of dioxygen, β-carbonato(trien)Co(III)perchlorate (25 μM), and UV light (366 nm); lanes 6 and 8, DNA cleavage by P3-Ga-Phe at 5 μM concentration in the presence of dioxygen, β-carbonato(trien)Co(III)perchlorate (25 μM), and UV light (366 nm) with subsequent 3'-dephosphorylation using T4 polynucleotide kinase.

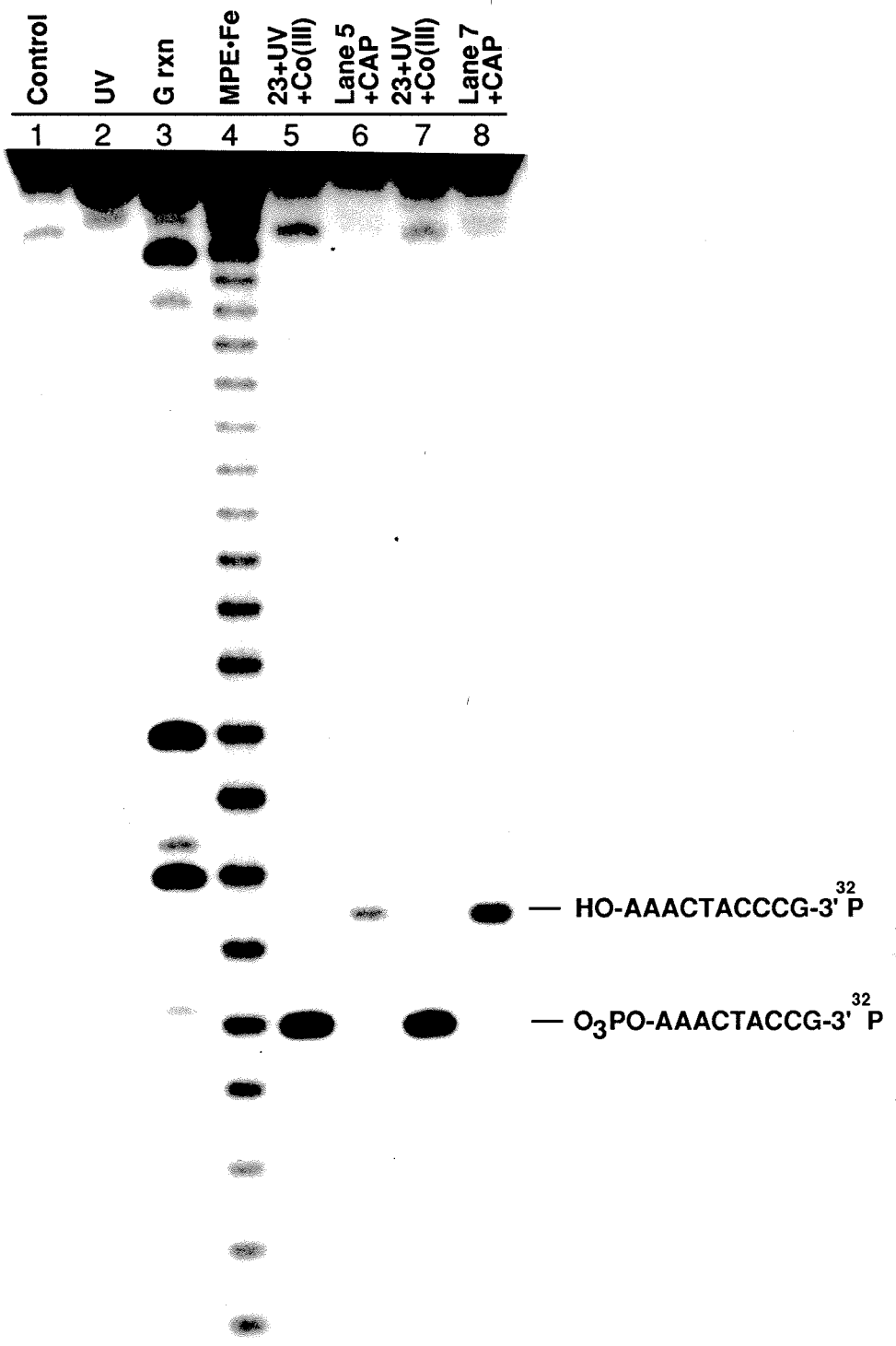
Control
UV
G rxn
MPE•Fe
23+UV +Co(III)
Lane 5 +CAP
23+UV +Co(III)
Lane 7 +CAP
1
2
3
4
5
6
7
8
— HO-AAACTACCCG-3' 32P
— O3PO-AAACTACCG-3' 32P

Discussion

Both P3-M-PYML•Fe(II) (**19**) and P3-M-EDTA (**20**) produced multiple cleavage patterns near the binding site. Since these patterns are indicative of diffusible reactive species, the DNA-cleaving mechanism of P3-M-PYML•Fe(II)/DTT appears to be similar to that of EDTA•Fe(II)/DTT (18,30), which produces a diffusible hydroxyl radical that abstracts a proton of the sugar ring of DNA and induces breakdown of the deoxyribose.

In the light of the results described in P3-Ga-His•Cu(II) (**12**) mediated DNA cleavage, several observations about the mechanism(s) by which P3-Ga-His•Cu(II) mediates DNA cleavage may be made. First, DNA cleavage stems from oxidative modification and breakdown of deoxyribose residues. Second, given that the DNA cleaving species is located in the DNA minor groove, C-H bonds within or on the edges of the minor groove (C-H1', C-H2', C-H4', C-H5') should be considered as the most likely candidates for activation. Third, since the cleavage patterns are not diffused, it must be considered that the reactive species is not diffusible and may be a metal oxo.

Figure 14 depicts four possible pathways, each of which involves the activation of a deoxyribose C-H bond located within or on the edge of the minor groove by P3-Ga-His•Cu(II) to afford hydroxylated products. Considering the work of Klinman *et al.* (25) on dopamine β-monooxygenase (enzymes catalyzing the hydroxylation of dopamine to norepinephrine), C-H activation is likely to involve hydroxylation by copper-mediated oxidant species. The disproportionation of Cu(II) complex into Cu(I) and Cu(III) complexes may also produce a reactive species as in copper-mediated oxidative C-terminal N-dealkylation of peptide (38-39).

C-H1' activation would produce a hemiortho ester which could decompose to an unstable 3' dehydrolactone derivative, liberating a free base and a DNA fragment with a 5'-phosphate group. The dehydrolactone

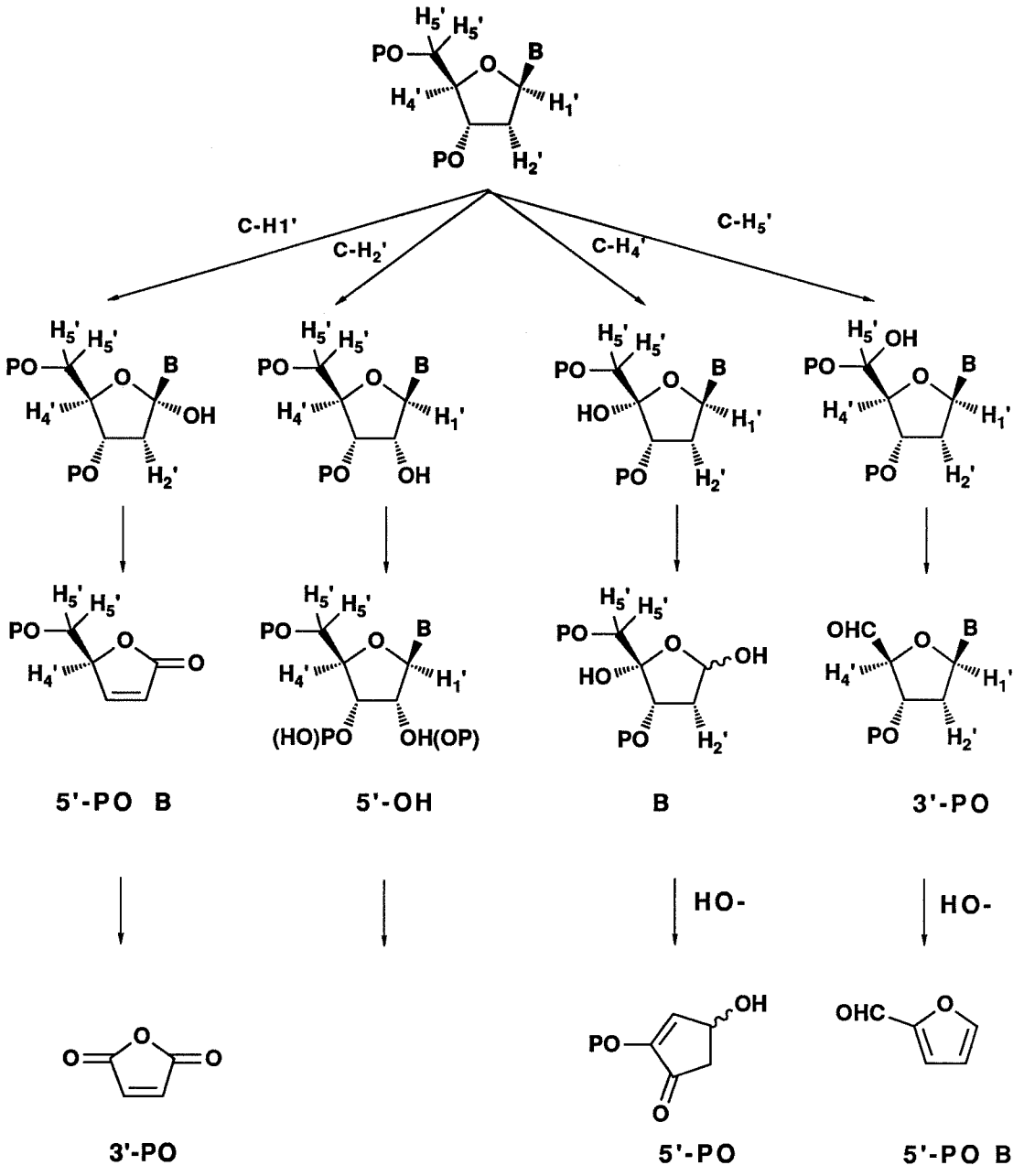

Figure 14. Four possible pathways of cleavage mediated by P3-Ga-His•Cu(II).

would undergo further decomposition under mild conditions (room temperature at neutral pH) to liberate an unstable methylene dehydrolactone and a DNA fragment with a 3'-phosphate group. Activation of C-H1' bonds has been shown to occur during DNA cleavage with bis(1,10-phenanthroline)copper(II) (31). It is likely that NCZS and the related antibiotics Esperamicin A1 and Calicheamicin $\gamma 1^I$ activate C-H1' bonds (32).

C-H2' activation could afford a ribonucleotide residue within a DNA molecule. Ribonucleotides may be hydrolyzed under basic conditions to liberate DNA fragments having 5' hydroxy groups and 3'- or 2'-phosphate.

C-H4' activation would afford an unstable hemiacetal derivative which could decompose, liberating free base and creating a bis hemiacetal. This species represents the base labile lesion produced by BLm•Fe(II) in the absence of sufficient dioxygen (33). In the presence of base this species decomposes to a DNA fragment having a 5'-phosphate group and a DNA fragment having a 3'-nonphosphate group (15, 17).

C-H5' activation could afford a hemiacetal phosphate ester which should decompose under ambient conditions to liberate a DNA fragment with a 3-phosphate group and a DNA fragment with a nucleoside 5'-aldehyde group. These products are produced upon DNA cleavage with NCZS or the related antibiotics Esperamicin A1 and Calicheamicin $\gamma 1\pm$. DNA fragments terminating in nucleoside 5'-aldehyde groups can be converted to the corresponding fragments that terminate in 5'-phosphate groups by base workup, which would also liberate the DNA base and furyfural (34).

The cleavage products of DNA by P3-Ga-His•Cu(II) are unknown 3'-end (which is not 3'-phosphate, 3'-phosphoglycolate, or 3'hydroxy group)

and one 5'-phosphate. Thus, the most possible mechanism is C-H4' activation which produces 3'-nonphophate group and 5'-phosphate group. Higher cleavage efficiency at high pH might be due to the pH-dependence of decomposition of hydroylated product though C-H4' activation or the pH dependence of complex formation.

Bleomycin Co(III) (35) and lamda-tris(diphenyl phenanthroline)-Co(III) (24) cleave DNA in the presence of UV light. It is well known that when the Co(III) amine complex is excited, Co(II) and cation amine radical are produced as intermedates (36, 37). The appearance of DNA cleavage by P3-Ga-Phe/UV/β-carbonato(trien)Co(III)perchlorate with the same 3'- and 5'- end products as in the MPE•Fe(II)/DTT DNA cleavage reaction suggests that the active radical species produced by P3-Ga-Phe/UV/β-carbonato(trien)cobalt(III)perchlorate photoreaction attacks the deoxyribose ring, and subsequent reactions lead to strand scission It is likely that the phenanthroline cation radical is generated by intermolecular electron transfer to the excited Co(III) complexes when the reaction mixture is irradiated at 366 nm (the ligand field excitation of β-carbonato(trien)cobalt(III)perchlorate). Intramolecular electron transfer from phenanthroline to cobalt(III) mediated by the transient cobalt(III) phenanthroline complex cannot be excluded. The single cleavage site (T) on the 167 base fragment which has 4 binding sites indicates that reactive species are not diffusible like free hydroxyl radical. Since the distance between binding site and reactive sugar is sequence-dependent, the observation of a single cleavage event suggests that only one of the 5 sites has the right distance and orientation.

Experimental

Methods and materials. ^1H NMR spectra were recorded at 90 MHz on Varian EM-390 or JEOL FX-90Q instruments, or at 400 MHz on a JEOL JNM-GX 400. The NMR solvent was Me_2SO-d_6 unless otherwise noted, and chemical shifts are reported in parts per million downfield from internal standard Me_4Si. High resolution Fast Atom Bombardment Mass Spectra (FABMS) and Electron Impact Mass Spectra (EIMS) were obtained from Midwest Center for Mass Spectrometry at the University of Nebraska, at Lincoln. UV visible spectra were recorded on a Cary 219 spectrometer in the base line correction mode. Chromatography was carried out under positive air pressure using EM Science Kiesgel 60 (230-400 mesh). Reagent grade chemicals were used as received except for dimethyl formamide (DMF, Mallinckrodt), which was dried over 4Å molecular sieves. β-Carbonato(trien)Co(III)perchlorate was purchased from Sigma. Non-aqueous reactions were carried out under Argon.

4-Nitropyrrole-2-carboxylic acid ethyl ester (1). 7 g of 4-nitropyrrole-2-carboxylic acid (48 mmol) was prepared by the published method (31) and added to 8 mL H_2SO_4 and 72 ml ethanol in a 250 mL round bottom flask. This solution was then refluxed for 8 h, cooled slowly to 0°C, and filtered. The filtered solid was recrystalized in MeOH. 6 g of ester **1** (32 mmol) was obtained in 60% yield. ^1H NMR (90 MHz) δ 7.76 (s, 1H), 7.23 (s, 1H), 4.33 (q, 2H), 1.40 (t, 3H). EIMS calcd. for $C_7H_8N_2O_4$ (M+) 184.0848. Found 184.0843.

2-bromoethylamine-t-butylcarbamate (2). A solution of 2-bromoethylamine hydrobromide (4.08 g, 20 mmol) and triethylamine (2.02 g, 20 mmol) in 50% aqueous dioxane was stirred at RT for 1 h. The reaction mixture was treated with 0.95 eq. di-t-butyldicarbonate (Aldrich) and

stirred until the solution became clear. After a mixture was stirred for 12 h, the solvent was removed *in vacuo*. The residue was dissolved in ether and washed 3 times with water. The ether solution was dried over $MgSO_4$ and evaporated to give 3.56 g of **2** (9 mmol, Y=75%) as a white solid. ^1H NMR (DMSO, 400 MHz) δ 5.2 (s, 1H), 3.56 (t, 2H), 3.42 (t, 2H), 1.42 (s, 9H). EIMS calcd. for $C_7H_{14}NO_2$ (M+) 224.0114. Found 224.0116

N-(2-t-butylcarbamatoethyl)-4-nitropyrrole-2-carboxylic acid ethylester (3): A solution of **1** (1.72 g, 9.3 mmol), **2** (2.24 g , 10 mmol), 1 eq. NaI and potassium carbonate in 20 mL acetone was refluxed under argon for 48 h. The mixture was then filtered and the solvent was evaporated under reduced pressure. Chromatography on silica gel using 5% acetonitrile in dichloromethane gave 2.7 g of **3** (8.25 mmol) as a white solid. ^1H NMR (DMSO, 400 MHz) δ 8.04 (s, 1H), 7.41 (s, 1H), 6.84 (t, 1H), 4.41 (t, 2H), 4.26 (q, 2H), 3.31 (m, 2H). 1.14 (m, 12H). EIMS calcd. for $C_{14}H_{21}N_3O_6$ (M+) 327.1430. Found 327.1434.

N-(2-t-butylcarbamatoethyl)-4-nitro-2-carboxylic acid (4). A solution of **3** (1.6 g, 4.9 mmol) and NaOH (40 mg, 10 mmol) in aqueous ethanol was refluxed for 3 h then cooled to 0°C and neutralized with 1N HCl solution. The solvent was removed *in vacuo*, and the residue was chromatographed on silica gel using methanol affording 1.2 g of the acid **4** (4.01 mmol) as a solid. ^1H NMR (400 MHz) δ 7.71 (s, 1H), 7.14 (s, 1H), 6.83 (s, 1H), 4.46 (t, 2H), 3.32 (m, 2H), 1.32 (s, 9H). EIMS calcd. for $C_{12}H_{17}N_3O_6$ (M+) 299.1117. Found 299.1123.

N-methyl-4-[N-(2-t-butylcarbamatoethyl)-4-nitropyrrole-2-carboxamide-]-pyrrole-2-carboxamide-N,N'-dimethylpropylamine (6). A solution of N-methyl-4-nitropyrrole-2-(N, N-dimethylpropylamino)-carboxamide (**5**) (300

mg, 1.25 mmol) was prepared by the published method (27), in 10 mL DMF and was hydrogenated at atmospheric pressure and RT for 12 h using 40 mg of Pd/C. The mixture was then filtered and treated with 1-HOBT (270 mg, 2 mmol), DCC (270 mg, 1.3 mmol), and acid **4** (360 mg, 1.25 mmol). The mixture was stirred at RT under argon for 16 h, it was then filtered, and the solvent was distilled *in vacuo*. The residue was chromatographed on silica gel using 1% NH_4OH in MeOH to afford 450 mg of **6** (0.89 mmol) as a light yellow foam. ^1H NMR δ 10.21 (s, 1H), 8.12 (t, 1H), 8.00 (s, 1H), 7.62 (s, 1H), 7.21 (s, 1H), 6.90 (t, 1H), 6.87 (s, 1H), 4.42 (t, 2H), 3.83(s, 3H), 3.37(m, 2H), 3.23(m, 2H), 2.23(t, 2H), 2.19(s, 6H), 1.60(m, 2H), 1.36 (s, 9H). FABMS calcd. for $C_{23}H_{36}N_7O_6$ (M+H+) 506.2727 Found 506.2734.

N-methyl-4-{N-(2-t-butylcabamatoethyl)-4-[N-methyl-4-nitropyrrole-2-carboxamide]pyrrole-2-carboxamide]pyrrole-2-caboxamide-N,N'-dimethyl-propylamine (7): A solution of **6** (260 mg, 0.54 mmol) in 10 mL DMF was hydrogenated using 40 mg of Pd/C under one atmosphere of H_2 at RT for 12 h. The mixture was filtered and treated with 1-HOBT (140 mg,1.04 mmol), DCC (120 mg, 0.58 mmol) and N-methyl-4-nitropyrrole-2-carboxylic acid (100 mg, 0.58 mmol). The mixture was stirred under argon at RT for 16 h. The solvent was distilled *in vacuo*. Chromatography on silica gel using 1% NH_4OH in MeOH afforded 270 mg of **7** (0.44 mmol, Y=81%) as a beige solid. ^1H NMR (400 MHz) δ 10.31 (s, 1H), 9.97 (s, 1H),8.18 (s, 1H), 8.03 (t, 1H), 7.61 (s, 1H), 7.28 (s, 1H), 7.20 (s, 1H), 7.03(s, 1H), 6.85 (t. 1H), 6.83 (s, 1H), 4.36 (t, 2H), 4.91 (s, 3H), 3.81 (s, 3H), 3.27 (m, 2H), 3.21 (m, 2H), 2.24 (t, 2H), 2.17 (s, 6H), 1.61(m, 2H), 1.38 (s, 9H). FABMS calcd. for $C_{31}H_{42}N_9O_6$ (M+H+) 636.3258. Found 636.3246.

N-methyl-4-{N-(2-t-butylcarbamatoethyl)-4-[N-methyl-4-acetamide-pyrrole-2-carboxamide]pyrrole-2-carboxamide}pyrrole-2-carboxamide-N,N'-dimethylpropylamine (8). A solution of **7** (260 mg, 0.41 mmol) in 10 mL DMF was treated with 5% Pd/C (40 mg), and hydrogenated under one atmosphere of H_2 at RT for 20 h. This mixture was filtered and added to a stirred solution of AcOH (102 mg, 1.7 mmol) and carboxydiimidazole (CDI) (278 mg, 1.7 mmol) in 5 mL DMF. After stirring at RT for 16 h, the mixture was filtered, and the solvent was removed *in vacuo.* Chromatography on silica gel using 1% NH_4OH/MeOH afforded 250 mg of **8** (0.39 mmol) as a solid. ^1H NMR (DMSO,400 MHz) δ 9.92 (s, 1H), 9.90 (s, 1H), 9.82 (s, 1H), 8.06 (t, 1H), 7.28 (s, 1H), 7.21 (s, 1H), 7.18 (s, 1H), 7.09 (s, 1H), 6.87 (t, 1H), 6.85 (s, 1H), 6.84 (s, 1H), 4.32 (t, 2H), 3.85 (s, 3H), 3.82 (s, 3H), 3.26 (m, 2H), 2.23 (t, 2H), 2.24 (t, 2H), 2.17 (s, 6H), 2.01 (s, 2H), 1.62 (m, 2H), 1.38 (s, 9H). FABMS calcd. for $C_{31}H_{43}N_9O_6$ (M+H+) 637.3336. Found 637.3339.

N-methyl-4-{N-(2-aminoethyl)-4-[N-methyl-4-acetamidopyrrole-2-carboxamide]-pyrrole-2-carboxamide}pyrrole-2-carboxamide-N,N'-dimethylpropylamine(9). A solution of **8** (220 mg, 0.36 mmol) in dichloromethane (2 ml) was stirred under argon at 0°C. Trifluoroacetic acid (TFA) (1 mL) was added via syringe, and the mixture removed from the cooling bath and stirred at RT for 30 min. The product was precipitated with anhydrous ether (10 mL). The supernatant was decanted. The residue was chromatographed on silica gel using 5% NH_4OH in MeOH to give 170 mg of **9** (0.33 mmol) as a white solid. ^1H NMR (400 MHz) δ 10.10 (s, 1H), 9.94 (s. 1H), 9.80 (s, 1H), 8.04 (t, 1H), 7.33 (s, 1H), 7.21 (s, 1H), 7.18 (s, 1H), 7.04 (s, 1H), 6.82 (s, 1H), 6.80 (s, 1H), 4.25 (t, 2H), 3.82 (s, 3H), 3.78 (s, 3H), 3.20 (m,

2H), 2.82 (t, 2H), 2.27 (t, 2H), 2.21 (s, 6H), 1.99 (s, 3H), 1.62 (m, 2H). FABMS calcd. for $C_{26}H_{38}N_9O_4$ (M+H+) 540.3046. Found 540.3050.

Distamycin-M-histidine (10, P3-M-His). A solution of **9** (110 mg, 0.21 mmol), 1-HOBT (54 mg, 0.4 mmol), DCC (45 mg, 0.22 mmol), and l-t-boc histidine (56 mg, 0.20 mmol) in 10 ml DMF was stirred under argon at RT for 12 h. The solvent was removed *in vacuo*, and the residue was chromatographed on silica gel using 1% NH_4OH in MeOH to afford 120 mg of a white solid product . The solid product was dissolved in dichloromethane (1 mL), cooled in an ice bath under argon, and treated with 0.5 mL TFA. The mixture was removed from the cooling bath and stirred for 1 h at RT. The product was precipitated with ether (4mL) and the supernatant was discarded. The residue was dissolved in 5 mL 7% NH_4OH in MeOH, then concentrated under reduced pressure. Chromatography on silica gel using 7% NH_4OH in MeOH afforded 60 mg of **10** (0.09 mmol). ^1H NMR (400 MHz) δ 9.93 (s, 1H), 9.91 (s, 1H), 9.81 (s, 1H), 8.07 (t, 1H), 7.99 (t, 1H), 7.49 (s, 1H), 7.23 (s, 1H), 7.20 (s, 1H), 7.15 (s, 1H), 7.09 (s, 1H),6.85 (s, 1H), 6.82 (s, 1H), 6.71 (s, 1H), 4.34 (t, 2H), 3.79 (s, 3H), 3.78 (s, 3H), 3.45 (m, 2H), 3.18 (m, 2H), 3.16 (m, 2H), 2.81 (d, 1H), 2.49 (t, 2H), 2.20 (s, 6H), 2.04 (s, 3H), 1.60 (m, 2H). FABMS calcd. for $C_{32}H_{45}N_{12}O_5$ (M+H+) 677.3635. Found: 677.3637.

Distamycin-GABA-histidine (12, P3-Ga-His): The compound **11** was prepared by the published method (32). A solution of **11** (110 mg, 0.2 mmol), DCC (45 mg, 0.22 mmol), HOBT (54 mg, 0.4 mmol), and l-t-boc-histidine (56 mg, 0.2 mmol) in DMF (10 ml) was stirred under argon at RT for 10 h. The solvent was removed *in vacuo*, and the residue was chromatographed on silica gel using 1% NH_4OH in MeOH to afford 110 mg of a light yellow solid.

The above product was dissolved in dichloromethane (1 mL) and stirred at 0 C under argon. TFA (0.5 mL) was added via syringe, the mixture was removed from the cooling bath and stirred at RT for 1 h. The product was precipitated by adding ether (4 mL), and the supernatant decanted. The residue was dissolved in 3 mL 10 % NH_4OH in MeOH, concentrated at reduced pressure and chromatographed on silica gel using the same solvent to afford 60 mg of **12** (0.083 mmol, Y=83%) as a white solid. ^1H NMR (400 MHz) δ 9.90 (s, 1H), 9.87 (s, 1H), 9.84 (s, 1H), 8.32 (t, 1H), 8.06 (t, 1H), 7,92 (s, 1H), 7.52 (s, 1H), 7.22 (s, 1H), 7.17 (s, 1H), 7.15 (s, 1H), 7.01 (s, 1H), 6.85 (s, 1H), 6.78 (s, 1H), 3.83 (s, 3H), 3.81 (s, 3H), 3.78 (s, 3H), 3.24 (m, 2H), 3.17 (m, 2H), 2.84 (m, 1H), 2.50 (m, 2H), 2.24 (m, 4H), 2.19 (s, 6H), 1.67 (m, 2H), 1.60 (m, 2H). FABMS calcd. for $C_{33}H_{47}N_{12}O_5$ (M+H+) 691.3792. Found 691.3789.

6-methylpicolinic acid (13). A solution of 6-methylpyridine-2-carboxyaldehyde (10.2 g, 84 mmol, Aldrich) in water was vigorously stirred and heated to 60°C. The heating bath was removed and 30% hydrogenperoxide (11.2 mL) was added so as to maintain 50° C. The reaction mixture was allowed to sit overnight. The aqueous solution was washed twice with methylene chloride. The solvent was evaporated under reduced pressure and the residue was chromatographed on silica gel using ethylacetate to afford 9 g of **13** (65 mmol, Y=77%). ^1H NMR (D_2O, 90 MHz) δ 8.5 (d, 1H), 8.33 (t, 1H), 8.00 (d, 1H). EIMS calcd. for $C_7H_7NO_2$ (M+) 137.0476 Found 137.0466.

6-methylpicolinic acid methylester (14). A solution of **13** (8 g, 58 mmol) in excess thionyl chloride (20 mL) was refluxed for 2 h. ,Then the thionyl chloride was removed under reduced pressure. The remaining residue was treated with 20 mL of methanol. After 1 h the solvent was removed *in vacuo*

and the residue distilled at 95 C at 0.1 torr to afford 4.6 g of the ester **14** (42 mmol, Y=72%). ^{1}H NMR ($CDCl_3$, 400 MHz) δ 7.81 (d, 1H), 7.67 (t, 1H), 7.26 (d, 1H), 3.94 (s, 3H), 2.61 (s, 3H). FABMS calcd. for $C_8H_9NO_2$ (M+) 151.0633. Found 151.0633.

6-carboxyaldehydepicolinic acid methylester (15). A mixture of **14** (3.3 g, 20 mmol) and I_2 (5.08 g, 20 mmol) was stirred at RT for 3 h. The reaction mixture was added dropwise to DMSO (7 mL) at 130°C (27) . The reaction mixture was cooled to 0°C and neutralized with 3 N sodium bicarbonate solution. The aqueous solution was extracted twice with ether, and the solvent was removed under reduced pressure. The resulting residue was chromatographed on silica gel using dichloromethane to afford 1.70 g of **15** (10.2 mmol). ^{1}H NMR ($CDCl_3$, 400 MHz) δ 10.20 (s, 1H), 8.64 (d, 1H), 8.15 (d, 1H), 8.06 (q, 1H), 4.07 (s, 3H). EIMS calcd. for $C_8H_8NO_3$ (M+) 166.0504. Found 166.0504.

2-aminoethylamine-t-butylcarbamate (16). A solution of 1,2-diaminoethane (2.4 g, 40 mmol, Aldrich) and imidazol-t-butylcarbamate (6.7 g, 40 mmol,Aldrich) in 20 mL of dried THF was stirred with a catalytic amount of NaOH at RT for 2 h. Then the solvent was removed under reduced pressure. The residue was chromatographed on silica gel using 2% NH_4OH in MeOH to afford 1.6 g of **16** (10 mmol) as a beige liquid. ^{1}H NMR (90 MHz) δ 5.7 (t, 1H), 3.14 (m, 2H), 2.74 (m, 2H), 2.43 (s, 2H), 1.38 (s, 9H). EIMS calcd. for $C_7H_{16}N_2O_2$ (M+) 160.1211. Found 160.1214.

6-[N-(2-t-butylcarbamatoethyl)aminomethyl]picolinic acid methylester (17). A solution of **16** (1.66 g, 10 mmol) and **15** (1.6 g, 10 mmol) was stirred overnight in 50 mLof acetonitrile containing 10 g of 4Å sieves. The mixture was filtered, and the solvent was distilled *in vacuo*. The remaining residue

was immediately dissolved in 50 ml of absolute ethanol and hydrogenated with 200 mg of 5% Pd/C at 50 psi overnight. The solution was filtered and the solvent was removed under *vacuo* to give 2.6 g of **17** (8.4 mmol, Y=84%). ^{1}H NMR ($CDCl_3$, 400 MHz) δ 8.04 (d, 1H), 7.80 (m, 1H), 7.53 (d. 1H), 4.07 (s, 3H), 4.03 (s, 2H), 3.21 (m, 2H), 2.81 (m, 2H), 2.12 (s, 1H), 1.42 (s, 9H). FABMS calcd. for $C_{15}H_{24}N_3O_4$ (M+H+) 310.1766. Found 310.1763.

6-[(N-2-t-butylcarbamatoethyl)benzylcarbamatoethyl]picolinic acid (18). The amine **17** (2.0 g, 6.5 mmol) was dissolved in methylene chloride. The solution was added to aqoeous NaOH (0.25 N) and treated at 0°C with benzylchloroformate (1.9 mL, 10.7 mmol, Aldrich) After 1 h methylene chloride layer was dried and the solvent was removed under *vacuo* to give 2.5 g of protected product (5.6 mmol, Y=86%). A solution of above product (1.5 g, 3.35 mmol) in 20 mL MeOH was treated with aqueous sodium hydroxide solution (2 N, 4 mL) and stirred for 3 h. The solution was neutralized with aqoeous 1 N HCl. the solvent was removed under reduced pressure to give the crude residue. The crude acid was passed through silica gel using methanol to afford acid **18** (1.1 g, 2.62 mmol , Y=77%) ^{1}H NMR (DMSO, 400 MHz) δ 12.2 (s, 1H), 9.11 (t, 1H),7.92 (m, 2H), 7.59 (s, 1H), 7.38 (m, 3H), 7.21 (s, 1H), 7.11 (s, 1H), 6.90 (m, 2H), 5.14 (s, 1H), 5.02 (s, 1H), 4.79 (m, 1H), 4.61 (s, 2H), 3.19 (m. 4H), 3.12 (m, 2H), 1.31 (s, 9H). FABMS calcd. for $C_{22}H_{28}N_3O_6$ (M+H+) 430.1978. Found 430.1968

Distamycin-N-PYML(19, P-PYML). A solution of **10** (50 mg, 0.073 mmol), the acid **18** (30 mg, 0.073 mmol), DCC (16 mg, 0.08 mmol), and 1-HOBT (19 mg, 0.14 mmol) was stirred under argon at RT for 12 h. The reaction mixture was distilled *in vacuo*, and the residue was chromatographed on silica gel using 1% NH_4OH in MeOH to afford 52 mg

of a white solid. 40 mg of the above product was dissolved in AcOH (4 mL) and a 32% HBr/AcOH solution (1 mL) was added dropwise. The reaction mixture was stirred under argon at RT for 8 h. The product was precipitated with ether (4 ml) and the supernatant discarded. The solid was dissolved in 15% NH_4OH in MeOH, then concentrated at reduced pressure. Chromatography using 15% NH4OH in MeOH afforded 20 mg of **19** (0.023 mmol, Y=62%). ^1H NMR (400 MHz) δ 9.94 (s, 2H), 9.82 (s, 1H), 8.93 (m, 1H), 8.28 (t, 1H), 8.06 (t, 1H), 7.84 (m, 2H), 7.56 (d, 1H), 7.50 (s, 1H), 7.21 (s, 1H), 7.17 (s, 1H), 7.15 (s, 1H),7.07 (s, 1H), 6.80 (s, 1H), 6.76 (s, 1H), 6.74 (s, 1H), 4.66 (m, 1H), 4.28 (t, 2H), 3.88 (s, 2H), 3.78 (s, 3H), 3.77 (s, 3H), 3.43 (m, 2H), 3.20 (m, 2H), 3.00 (m, 2H), 2.81 (m, 2H), 2.68 (t, 2H), 2.21 (t, 2H), 2.17 (s, 6H), 1.99 (s, 3H), 1.61 (m, 2H).FABMS calcd. for $C_{42}H_{56}N_{15}O_6$ (M+H+) 868.4694. Found 868,4650. UV(H_2O) λ 306(e=34 200)

Distamycin-M-EDTA(20, P3-M-EDTA). A solution of EDTA-triethylester (Group stock, 62 mg, 0.76 mmol) in 5 mL DMF was activated with 1.1 eq. of carboxydiimidazole (CDI) and stirred for 2 h. at RT under argon. The mixture was taken up in a syringe and added to a solution of **9** (40 mg, 0.77 mM) in DMF (3 mL). After stirring for 12 h under argon at RT, the solvent was removed *in vacuo,* and the residue was chromatographed using 1% NH_4OH in MeOH to give 50 mg of triester product as a beige foam. The triester product was dissolved in 60% aqueous methanol containing 10 mg LiOH, and stirred for 12 h under argon at RT. The solvent was evaporated *in vacuo,* and the residue was chromatographed using 2% NH_4OH in MeOH to affored 26 mg of **20** (0.033 mmol) as a solid. ^1H NMR (CF_3OOH/DMSO, 400 MHz) δ 9.94 (s, 2H), 9.80 (s, 1H), 9.20 (s, 1H), 8.52 (t, 1H), 8.20 (t, 1H), 7.25 (s, 1H), 7.20 (s, 1H), 7.17 (s,

1H), 7.06 (s, 1H), 6.86 (s, 1H), 6.83 (s, 1H), 4.38 (t, 2H), 4.01 (s, 2H), 3.80 (s, 2H), 3,79 (s, 5H), 3.76 (s, 3H), 3.50 (s, 2H), 3.26 (s, 4H), 3.20 (s, 2H), 3.05 (m, 2H), 2.81 (d, 6H), 1.98 (s, 3H), 1.84 (m, 2H). FABMS calcd. for $C_{36}H_{51}N_{11}O_{11}$ (M+H+) 814.3836. Found 814.3841. UV(H_2O) λ 308(e=33 000)

Distamycin-M-1,10-phenanthroline(21, P3-M-PH). A solution of **9** (220 mg, 0.42 mmol), 1,10-phenanthroline-2-carboxylic acid (92 mg, 0.39 mmol), 1-HOBT (122 mg, 0.9 mmol), and DCC (93 mg, 0.45 mmol) in 10 mL DMF was stirred under argon at RT for 12 h. The solvent was removed *in vacuo*. The residue was chromatographed on silica gel using 2% NH_4OH in MeOH to afford 290 mg of **21** (0.27 mmol, Y=64%) ^1H NMR (DMSO, 400 MHz) δ 9.91 (s, 2H), 9.79 (s, 1H), 9.13 (s, 1H), 8.93 (d, 1H), 8.69 (d, 1H), 8.60 (d, 1H), 8.33 (d, 1H), 8.12 (m, 2H), 8.01 (t, 1H), 7.83 (t, 1H), 7.90-7.30 (m, 4H), 6.80 (s, 1H), 6.73 (s, 1H), 4.47 (t, 2H), 3.83 (s, 3H), 3.70 (s, 3H), 3.18 (m, 4H), 2.21 (t, 2H), 2.16 (s, 6H), 2.00 (s, 3H), 1.58 (m, 2H). FABMS. calcd. for $C_{39}H_{44}N_{11}O_5$ (M+H+):746.4526. Found: 746.4520.UV (ethanol) λ=302(e= 34 200)

Distamycin-GABA-1,10-phenanthroline-2-carboxamide(22, P3-Ga-PH). A solution of **9** (550 mg, 0.84 mmol), 1,10-phenanthroline-2-carboxylic acid (224 mg, 1 mmol), DCC (202 mg, 1 mmol), and 1-HOBT (270 mg, 2 mmol) in 10 ml DMF was stirred at RT under argon for 12 h. The solvent was removed *in vacuo*, and the residue was chromatographed using 2% NH_4OH in MeOH to afford 400 mg of **22** as a solid. ^1H NMR (400 MHz) δ 9.82 (s, 3H), 9.17 (d, 1H), 8.92 (t, 1H), 8.65 (d, 1H), 8.57 (d, 1H), 8.40 (d, 1H), 8.06 (m, 2H), 7.81 (q, 1H), 7.23 (s, 1H), 7.20 (s, 1H), 7.18 (s, 1H), 7.03 (s, 1H), 6.83 (s, 1H), 6.80 (s, 1H), 3.86 (s, 3H), 3.80 (s, 3H), 3.76 (s, 3H), 3.53 (m, 2H), 3.21 (m, 2H), 2.38 (t, 2H), 2.23 (t, 2H), 2.19 (s, 6H), 1.94 (m, 2H), 1.63 (m, 2H). FABMS

calcd. for $C_{40}H_{45}N_{11}O_5$ (M+H+) 760.3683. Found 760.3689. UV(ethanol) λ 303(ε=34 200)

DNA preparations and reactions. Doubly distilled water was used for all aqueous reactions and dilutions. pBR 322 plasmid DNA, from group stock, was used for reactions. Calf thymus (CT) DNA, from group stock, was purchased originally from Sigma and then sonicated, deproteinized, and dialyzed. Enzymes were purchased from Boehringer Mannheim or New England Biolabs. Gel scanning was performed at 633 nm using LKB Ultrascan densitometer Model XL.

Cleavage of ende-labeled DNA restriction fragments: Preparation of specially end-labeled DNA restriction fragments began by cleaving superhelical pBR322 DNA with restriction endonuclease EcoRI. Linearized pBR322 DNA was labeled on the 3'-ends using 5'-[α-^{32}P]dATP (Amersham, 3000Ci/mmol) in the presence of the Large (Klenow) fragment of DNA polymerase I (41). This procedure also included dTTP and dATP which were purchased from Phamarcia as 100 mM solutions. Removal of 5'-phosphate groups from linearized pBR322 with calf alkaline phosphatase was followed by treatment with 5'-[γ-^{32}P]dATP (New England Nuclear, 7000Ci/m mol) in the presence of polynucleotide kinase which afforded 5'-end-labeled DNA. Digestion of both 3' and 5' end-labeled DNA with restriction endonuclease RsaI yielded 3'-and 5'-end-labeled restriction fragments of 167 and 517 nucleotides in length. These were isolated by preparative gel electrophoresis on a 2 mm thick, 5% 1:20 cross-linked polyacrylamide gel. The bands of DNA were visualized by autoradiograph, and were excised from the gel. The fragments were eluted into 1 ml buffer (500 mmol NH_4OAc, 10 mmol $MgCl_2$, 1 mmol EDTA, 0.25% SDS),

microfiltered, extracted with phenol, dry butanol, and then ethanol precipitated several times before use.

Fe(II) complexes of each compound were made by mixing one equivalent of $Fe(NH_4)_2(SO_4)_2 \cdot 6H_2O$ with **19** and **20.** DNA cleavage reactions with Fe(II) in the presence of DTT and dioxygen were run in a total volume of 15 μl. For each reaction, 6 μL of a solution containing > 10,000cpm of ^{32}P end-labeled restriction fragment, 1.5 μL of a 1mM (bp) CT DNA solution, 1.5 μL of 400 mM Tris/50 mM NaOAC buffer (pH 7.9) (final concentrations; 100 mM CT DNA(bp), 40 mM Tris/5 mM NaOAc). To the reaction mixture was added 3 μL of an appropriately diluted solution of **19** Fe(II) and **20•** Fe(II). After equilibriation for 30 minutes at 37°C, cleavage was initiated by the addition of 3 μL of 20 mM dithiothreitol (DTT, Beohringer Manheim) solution. Final concentrations were: CT DNA, 100 μM bp; Tris base, 40 mM; NaOAc, 5 mM; DTT, 4 mM. The reactions were run for 40 minutes at 37 C, then frozen, lyophilized, and suspended in 5 μL of 10 mM Tris borate, 80% formamide solution. After heat denaturation 4 μL of each sample were loaded onto a 0.4 mm thick, 40 cm long, 8% 1:20 cross-linked polyacrilamide/50% urea gel and electrophoreised at 1200 V. Gels were then transferred to chromatography paper (Whatman 3mm Chr), dried on a Bio-Rad Model 483 slab dryer, and autoradiographed at -78°C using Kodak X-omat AR film with an intensifing screen. The DNA cleavage patterns were quantified by densitometry. The relative peak area for each site was equated to the relative cleavage efficiency at that site.

Sequence-specific cleavage of DNA by P3-M-His (**10**) and P3-Ga-His (**12**) in the presence of $CuSO_4$ (200 μM) was examined using the 167 base pair restriction fragment. DNA cleavage reactions with Cu(II) were run in a

total volume of 30 μL. For each reaction, 12 μL of a solution containing >10,000 cpm of ^{32}P end-labeled restriction fragment, 3 μL of a 1mM(bp) CT DNA solution, 3 μL of 400 mM Tris/50 mM NaOAC buffer (pH 7.5, 8.5, and 9.5) was treated with 12 μL of an appropriately diluted solution of **10** and **12**. Final concentrations were: CT DNA, 100μM bp; Tris base, 40 mM; NaOAc, 5mM; Cu(II), 20 μM. The reactions were run for 72 h at 50° C, then frozen, lyophilized, and suspended in 5 ml of 10 mM Tris borate, 80% formamide solution. After heat denaturation 4 μL of each sample was loaded onto a 0.4 mm thick, 40 cm long, 8% 1:20 cross linked polyacrylamide/50% urea gel and electrophoreised at 1200 V. Gels were then transferred to chromatography paper (Whatman 0.3 mm Chr), dried on a Bio-Rad Model 483 slab Dryer, and autoradiographed at -78 C using Kodak X-omat AR film. The DNA cleavage patterns were quantified by densitometry. The relative peak area for each site was equated to the relative cleavage efficiency at that site. Footprinting of DNA by MPE·Fe(II) for compound **12** in the prescence of DTT and dioxygen was also examined by using the 167 base pair restriction fragment. P3-Ga-His(**12**) was allowed to equilibriate with DNA restriction fragments at RT for 0.5 h before MPE•Fe(II) was added. MPE•Fe(II) was allowed to equilibriate with the DNA-P_3-Ga-His (**12**) mixtures for 15 min at 37°C before the reaction was initiated by addition of DTT. After reaction for 12 min at 37°C, the samples were frozen, lyophilized, suspended in formamide buffer, heat denatured and loaded.

Sequence-specific cleavage of DNA by **21** and **23** in the presence of UV light and β-carbonato(trien)Co(III)perchlorate complex was also examined using the 167 base pair restriction fragment. Photo-induced DNA cleavage reactions were run in a total volume of 30 μL. For each reaction, 15 μL of a

solution containing > 2000 cpm of ^{32}P-end labeled restriction fragments was used. Final concentrations were: 100 μmol CT DNA (bp), 10 mmol sodium cacodalate, appropriately diluted **21** and **23** and 1 equivalent β-carbonato(trien)Co(III)perchlorate. A range of concentrations of each molecule was allowed to equilibrate with the DNA restriction fragment for 0.5 h at room temperature before the reaction was initiated by UV light (366 nm) using a Model UVGI-58 (UVP Inc., 115 volts, 60 Hz, and 0.16 AMPs). The reaction were photolyzed for 3 h at room temperature, then frozen, lyophilized, and resuspended in 5 μL of 100 mmol Tris borate, 80% formamide solution and then the gel run and developed the same as above. The cleavage reactions of DNA by bleomycin·Co(III) were done using the same conditions as above in the absence of β-carbonato(trien)Co(III)perchlorate.

Footprinting of DNA by MPE·Fe(II) for compound **23** in the presence of DTT and dioxygen was also examined by using the 167 base pair restriction fragment. A range of P_3-Ga-PH (**23**) was allowed to equilibriate with DNA restriction fragments at RT for 0.5 h before MPE•Fe(II) was added. MPE ·Fe(II) was allowed to equilibriate with the DNA-P_3-Ga-PH mixtures for 15 min at 37°C. Then the reaction was initiated by addition of DTT. After reaction for 12 min at 37°C, the samples were frozen, lyophilized, suspended in formamide buffer, heat denatured and loaded.

Preparations of oligonucleotides. Oligonucleotides **24** and **25** were synthesized with a Beckman Oligonucleotide Synthesizer. Synthesized oligonucleotides were dried *in vacuo*, transferred to a vial, and 1 ml ammonium hydroxide was added to the vials to remove the oligonucleotides from the solid support. After 2 h, the supernatant was

transfered into a screw capped eppendorf tube, and the solvent was removed with dry argon. Concentrated NH_4OH (1 ml) was added to the eppendorf tube and the tubes allowed to stand at 55°C. 24 h latert the solvent was removed by lyophilization. The remaining solid was suspended in 250 µl of pH 8.3, 100 mM Tris-borate, 80% formamide loading buffer and loaded onto five lanes of a 2 mm thick, 20% 1:20 cross-linked polyacrilamide/40% urea denatured gel and electrophoresed at 550 V for 24 h. The band of desired oligonucleotide was visualized under UV light and excised from the gel. The oligonucleotides were eluted into a solution of 1.5 M NaCl, 1 mM EDTA, microfiltered and dialyzed against doubly distilled water for 72 h.

Preparation of end-labeled 27 base pair oligonucleotide. The two strands were mixed in 20 mM Tris HCl, pH 7.4, 50 mM NaCl, heated to 95° C for 5 minutes, and cooled slowly to RT. The resulting double-stranded oligonucleotide was ethanol precipitated, and labeled on the 3'-end using 5'-α-^{32}P dCTP (Amersham, 3000Ci/mmol) in the presence of the large (Klenow) fragment DNA polymerase I, and 3'-labeled oligonucleotide was isolated by preparative gel electrophoresis on a 2 mm thick, 15% 1:20 cross-linked polyacrylamide gel. The band of labeled DNA was visualized with autoradiography using Kodak X-omat AR film, and was excised from the gel. The oligonucleotide was eluted into 1 mL of buffer (500 mM NH_4OAc, 10 mM $MgCl_2$, 1 mM EDTA, 0.25% SDS), microfiltered, extracted with phenol and butanol, and dialyzed for 24 h before use. For 5' end-labeled 27 base pair oligonucleotide, a single stranded oligonucleotide was labeled on 5'-end using [γ-^{32}P]dATP in the presence of polynucleotide kinase. The labeled strand was hybridized as before. After hybridization, the 3'-end was filled using dATP,dTTP, dGTP, and dCTP in the presence of DNA polymerase I.

Cleavage of 3' and 5' end-labeled 27 base pair DNA. Oligonucleotide cleavage reactions were run in a total volume of 30 μL. Each reaction contained 20,000 cpm of ^{32}P end-labeled oligonucleotide, 100 μM (bp) cold oligonucleotide which has same sequence, 10 mM sodium cocodalate, 25 μM β-carbonato(trien)Co(III)perchlorate complexes, and 5 μM compound **23**. Photocleavage reactions were conducted as described for the 167 base pair fragment. After reaction, the samples were frozen, lyophilized, and resuspended in 5 μLof 100mM tris borate (pH 8.30), 80% formamide solution. After heat denaturation at 90°C, 4 μL of each sample was loaded onto a 0.4 mm thick, 40 cm long, 20% 1:20 cross-linked polyacrylamide/40% urea denatured gel and electrophoresed at 1500 V. The gel was covered with saran wrap and autoradiographed at -78°C using Kodak X-omat AR film.

Analysis of termini by gel electrophoresis. The presence of phosphate groups on the 5'-termini of the cleavage site was tested by using calf intestine alkaline phosphotase (CAP). Degraded DNA was ethanol precipitated, dissolved in 20 μL of 40 mM Tris-HCl (pH 7.8), mM NaOAc and heat denatured at 90°C for 5 min. 1 μL of CAP(12 u/μL) was added and incubated at 37°C for 1 h. The reaction was terminated by ethanol precipitation and taken up in loading buffer for gel electrophoresis. The nature of the 3'-termini was examined by using T_4 polynucleotide kinase to remove 3'-phosphate groups (30). DNA derived from the cleavage reaction was ethanol precipitated. The pellet was dissolved in 20 μL of H_2O, heat denatured at 90°C for five min and chilled on ice. 20 μL of a buffer containing 20 mM Tris-HCl, pH 6.6, 20 mM magnesium chloride, and 10 mM β-mercaptoethanol was added followed by 0.5 μL of T_4 polynucleotide kinase (19 units/μL). The reaction was incubated at 37°C for 1 h and ethanol

precipitated. The DNA derived from the cleavage reaction was suspended in 5 μL of a pH 8.3, 100 mM Tris-Borate, 80% formamide loading buffer and heat denatured at 90°C for 2 min. The samples were loaded onto a 0.4 mm thick, 40 cm long, 20% polyacrilamide, 1:20 cross-linked, 40 % urea gel and electrophoresed at 1500 V until the bromophenol blue tracking dye had moved 30 cm. Autoradiography was carried out at -78°C on Kodak X-omat AR film.

References and notes.

1) Saenger, W.; in " *Principles of Nucleic Acid Structure*", edited by, Cantor, C. R.; Springer-Verlag, New York Inc (**1984**).

2) a) Drew, H. R.; Wing, R. M.; Takano, T.; Broka, C.; Tanaka, S.; Itakura, K.; Dickerson, R. E. *Proc. Natl. Acad. Sci. U. S. A.* **1981**, *78*, 2179. b) Dickerson, R. E.; Drew, H. R. *J. Mol. Biol.* **1981**, *149*, 761.

3) Zimmer, C.; Wahnert, U. *Prog. Biophys. Mol. Biol.* **1986**, *47*, 31.

4) Neidle, S.; Pearl, L. H.; Skelly, J. V. *Biochem. J.* **1987**, *243*,1.

5) Neidle, S. R. *CRC Crit. Rev. Biochem.* **1984**, *17*, 73.

6) Berman, H. M.; Neidle, S.; Zimmer, C.; Thrum, H. *Biochim. Biophys. Acta.* **1979**, *561*, 124.

7) Kopka, M. L.; Yoon, C.; Goodsell, D.; Pjura, P.; Dickerson, R. E. *Proc. Natl. Acad. Sci. U. S. A.* **1985**. *82*, 1376.

8) Kopka, M. L.; Yoon, C.; Goodsell, D.; Pjura, P.; Dickerson, R. E. *J. Mol. Biol.* **1985**, *183*, 553.

9) Coll, M.; Fredrick, C.; Wang, AH.-J.; Rich, A. *Proc. Natl. Acad. Sci. U. S. A.* **1987**, *84*, 8385.

10) Goodsell, D.; Dickerson, R. E.*J. Med. Chem.* **1986**, *29*, 727.

11) Patel, D. J.; Shapiro, L.; Hare, D. *Biopolymers* **1986**, *25*, 693.

12) Patel, D. J.; Shapiro, L. *J Biol. Chem.* **1986**, *261*, 1230.

13) Klevitt, R. E.; Wemmer, D. E.; Reid, B. R. *Biochemistry* **1986**, *25*, 3296.

14) Halford, S. E. *Trends Biochem. Sci.* **1983**, *8*, 455.

15) Stubbe, J.; Kozarich, J. W. *Chem. Rev.* **1987**, *87*, 1107.

16) a) Goldberg, I, H.; "*Free radicals in Biology and Medicine* **1987**, *3*, 41. b) Chin, D. H.; Zeng, C. H.; Costello, C. E.; Goldberg, J. H. *Biochemistry* **1988**, *27*, 8106.

17) Kozarich, J. W.; Worth, L.; Frank, B. L.; Christner, D. F.; Vanderwall, D. E.; Stubbe, J. *Science* **1989**, *245*, 1396.

18) Schultz, P. G.; Dervan, P. B. *Proc. Natl. Acad. Sci. U. S. A.* **1983**, *80*, 6834.

19) Schultz, P. G.; Dervan, P. B. *Tetrahedron* **1984**, *40*, 457.

20) Griffin, J. H.; Dervan, P. B. *J. Amer. Chem. Soc.* **1987**, *109*, 6840.

21) Sluka, J. P.; Horvath, S. J.; Bruist, M. F.; Simon, M. I.; Dervan, P. B. *Science* **1987**, *238*, 1129.

22) Moser, H. E.; Dervan, P. B. *Science* **1987**, *238*, 645.

23) Chen, C-H. B.; Sigman, D. S. *Science* **1987**, *237*, 1197.

24) Muller, B. C.; Raphael, A. L.; Barton, J. K. *Proc. Natl. Acad. Sci. U. S. A* **1987**, *84*, 1764.

25) a) Miller, S. M.; Klinman, J. P. *Biochemistry* **1985**, *24*, 2114. b) Brenner, M. C.; Klinman, J. P. *Biochemistry* **1989**, *28*, 4664.

26) *Org. Syn. Coll.* Vol. IV, p. 944.

27) Sluka, J. P. Ph.D. Thesis, Caltech, Pasadena, California, 1988.

28) Taylor, J. S. unpublished results.

29) Maxam, A. M.; Gilbert, W. *Methods Enzymol.* **1980**, *65*, 499.

30) Hertzberg, R. P., Ph. D. Thesis, Caltech, Pasadena, California, 1984.

31) Sigman, D. S. *Acc. Chem. Res.* **1986**, *19*, 180.

32) Zein, N. Sinha, A. M.; McGahren, W. J.; Ellestad, G. A. *Science* **1988**, *240*, 1198.

33) Sugiyama, H.; Xu, C.; Murugesan, N.; Hecht, S. M. *J. Amer. Cherm. Soc.* **1985**, *107*, 4104.

34) Povirk, L. F.; Houlgrave, C. W.; Han, Y.-H. *J. Biol. Chem.* **1988**, *263*, 19263 and references therein.

35) Chang, C.-H.; Mears, C. F. *Biochemistry* **1982**, *21*, 6332.

36) Klein, F. D.; Moeller, C. W. *Inorg. Chem.* **1965**, *4*, 394.

37) Malone, S. D.; Endicott, J. F. *J. Phys. Chem.* **1973**, *76*, 2223.

38) Kurtz, J. L.; Burce, G. L.; Margerum, D. W. *Inorganic Chemistry* **1978**, *17*, 2454.

39) Reddy, K. V.; Jin, S-J.; Arora, P. K.; Sfeir, D. S.; Malony, S. S. C.; Urbach, F. L.; Sayre, L. M. *J. Amer. Chem. Soc.* **1990**, *112*, 2332.